A Multinuclear Magnetic Resonance Spectroscopy Study of *E*/*Z* Configurational isomers of Unsymmetrical *N*-alkyl-*N*-alkyl(aryl)-*N*'-acylthioureas of Platinum(II) Complexes

Sibusiso Mtongana

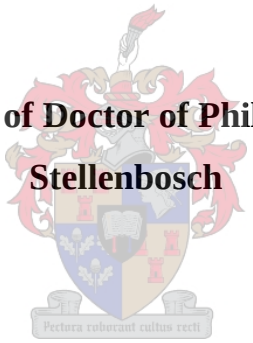

Dissertation for the Degree of Doctor of Philosophy at the University of Stellenbosch

Supervisor: Professor Klaus R. Koch **December 2006**

I, the undersigned, hereby declare that the work contained in this dissertation is my own original work and that I have not previously in its entirety or in part submitted it at any university for a degree.

SIGNATURE:

DATE:

Abstract

The partial double bond character of the carbon-nitrogen bond of the (S)C-NRR' moiety results in unsymmetrical dialkyl-substituted *N*-alkyl-*N*-alkyl(aryl)-*N'*-acylthioureas, R"C(O)NHC(S)NRR' (HL) displaying *E,Z* configurational isomerism in solution. The isomerism manifests itself by the duplication of resonances of the *N*-alkyl groups in the ^{1}H and ^{13}C NMR spectra. In one class of these ligands where R and R' groups are non-equivalent alkyl groups the isomerism is easily observable at 298 K in chloroform. In the other class where R' is still an alkyl group and R is a *para*-substituted phenyl group the isomerism is only observable at much lower temperatures due to a lower barrier to rotation around the (S)C-N(alkyl)(*para*-X-Ph) bond (X = O-CH_3, H and NO_2). The electron-withdrawing nature of the nitro group in *N*-methyl-*N*-(4-nitro-phenyl)-*N'*-*2,2*-dimethylpropanoylthiourea, HL^{3A} and *N*-pentyl-*N*-(4-nitro-phenyl)-*N'*-*2,2*-dimethylpropanoylthiourea, HL^{3D} result in the *E,Z* isomerism of these ligands not observable even at 198 K in dichloromethane. The distribution of *E* and *Z* isomers of the unbound ligands vary depending on these R and R' groups. Several *E* isomers of these ligands have been isolated and structurally characterised and the (S)C-NRR' bond falls in the range [1.343(3) – 1.329(3) Å] which shorter than the average C-N single bond of 1.472(5) Å.

The *E,Z* configurational isomerism in the unbound ligands is passed on to the Pt(II) chelates derived from these ligands. The presence of ***cis*-[Pt(*ZZ*-L-*S,O*)$_2$]**, ***cis*-[Pt(*EZ*-L-*S,O*)$_2$]** and ***cis*-[Pt(*EE*-L-*S,O*)$_2$]** is readily observable by means of ^{195}Pt NMR spectroscopy which shows three well resolved resonances, and this can be confirmed by ^{1}H and ^{13}C NMR spectra of these complexes. The ^{195}Pt nuclei are spatially linked to the ^{13}C nuclei, four bonds away resulting in $^{4}J(^{195}\text{Pt}\text{-}^{13}\text{C})$ couplings with *N*-CH_2- or *N*-CH_3 carbons in a **W** pathway. The ^{195}Pt NMR spectra are also linked to *N*-CH_2- or *N*-CH_3 proton resonances by means of the *ZZ*, *EZ* and *EE* isomer distributions. Assignment of these configurational isomers was then achieved by means of a combination of low magnetic field ^{13}C NMR spectra and high-resolution gHSQC (^{1}H/^{13}C) NMR experiments.

^{1}H NMR rotational dynamics study showed that the barrier to rotation, $\Delta G^{\neq}$, around the (S)C-N(Me)(*para*-X-Ph) bond in *cis*-bis(*N*-methyl-*N*-(4-methoxy-phenyl)-*N'*-*2,2*-dimethylpropanoylthioureato)platinum(II), ***cis*-[Pt(L^{1A}-*S,O*)$_2$]**; *cis*-bis(*N*-methyl-*N*-phenyl-*N'*-*2,2*-dimethylpropanoylthioureato)platinum(II), ***cis*-[Pt(L^{2A}-*S,O*)$_2$]** and *cis*-bis(*N*-methyl-*N*-(4-nitro-phenyl)-*N'*-*2,2*-dimethylpropanoylthioureato)platinum(II), ***cis*-[Pt(L^{3A}-*S,O*)$_2$]** complexes was observed to follow the order: (electron-withdrawing group) NO_2 < H < (electron-donating group) O-CH_3. The *ZZ* isomer was observed to be favoured over the *EZ* and *EE* isomers in this order of the *para*-substituent on the *N*-phenyl group. The ^{1}H dynamic NMR trends about the barrier to rotation, $\Delta G^{\neq}$, around the (S)C-N(Me)(*para*-X-Ph) bond were also complemented by DFT linear transit calculations. The isomer distributions were also influenced by solvent polarity and the temperature at which the distributions are determined apart from the electronic influence of the *para*-substituent of the *N*-phenyl group.

The *ZZ*, *EZ* and *EE* isomers of complexes derived from *N*-alkyl-*N*-(*para*-X-Ph)-*N'*-acylthioureas with varying *N*-alkyl substituent (methyl, isopropyl, cyclohexyl and n-pentyl) were determined from the ^{195}Pt NMR spectra which

were measured under identical conditions. The *ZZ* isomer was observed to be favoured over the *EZ* and *EE* isomers upon methyl group substitution with a bulkier alkyl group in the order: methyl < isopropyl < cyclohexyl < n-pentyl. Qualitatively it has been shown that a bulkier *N*-pentyl group increases the barrier to rotation around the (S)C-N(alkyl)(*para*-X-Ph) bond over the *N*-methyl group and this leads to higher concentrations of the *ZZ* isomer over the *EZ* and *EE* isomers. The combined effects of the electron-donating substituent (X = O-CH_3) on the *N*-(*para*-X-Ph) group and the bulkier *N*-alkyl group (n-pentyl) result in highest *ZZ* concentration (76 %) over *EZ* and *EE* isomers in the complex *cis*-bis(*N*-pentyl-*N*-(4-methoxy-phenyl)-*N'*-*2,2*-dimethylpropanoylthioureato)platinum(II), ***cis*-[Pt(L^{1D}-*S,O*)$_2$]**. The lowest concentration *ZZ* (27 %) is obtained in the complex *cis*-bis(*N*-methyl-*N*-(4-nitro-phenyl)-*N'*-*2,2*-dimethylpropanoylthioureato)platinum(II), ***cis*-[Pt(L^{3A}-*S,O*)$_2$]** when the coordinated ligand has both *N*-methyl group and *N*-(4-nitro-Ph) group which both lower the barrier to rotation around the (S)C-N(alkyl)(*para*-X-Ph) bond.

A crystal of the complex *cis*-bis(*N*-pentyl-*N*-(4-methoxy-phenyl)-*N'*-*2,2*-dimethylpropanoylthioureato)platinum(II), ***cis*-[Pt(L^{1D}-*S,O*)$_2$]** has been isolated and structurally characterised and was shown to be in the *ZZ* configuration, which is the major component (76 %) in chloroform. This is the first example of Pt(II) chelates with asymmetrically disubstituted ligands to be reported.

Opsomming

Die gedeeltelike dubbelbinding karakter van die koolstof-stikstof-binding van die (S)C-NRR'-moieteit lei tot onsimmetriese dialkiel-gesubstitueerde *N*,*N*-dialkiel-*N'*-asieltioureums, R"C(O)NHC(S)NRR' (HL) wat *E*,*Z*-konfigurasionele isomerie in oplossing besit. Die isomerie is sigbaar in die verdubbelling van die seine van die *N*-alkielgroepe in die ^{1}H- en ^{13}C-KMR spektra. In een so klas ligande waar R- en R'-groepe nie-ekwivalente alkielgroepe is, is isomerie duidelik sigbaar by 298 K in chloroform. In die ander klas waar R' steeds 'n alkielgroep is, en R 'n *para*-gesubstitueerde feniel groep, is die isomerie alleenlik sigbaar by baie laer temperature as gevolg van 'n laer rotasieversperring om die (S)C-N(alkiel)(*para*-X-Ph)-binding (X = O-CH_3, H and NO_2). Die elektrononttrekkende aard van die nitrogroep in *N*-metiel-*N*-(4-nitrofeniel)-*N'*-(*2*,*2*-dimetielpropanoïel)tioüreum, HL^{3A} en *N*-(4-nitrofenyl)-*N*-pentiel-*N'*-(*2*,*2*-dimetielpropanoïel)tioüreum, HL^{3D} lei daartoe dat die *E*,*Z*-isomerie van die ligande nie eers by 198 K in dichlorometaan waargeneem word nie. Die verspreiding van die *E* en *Z* isomere verskil na gelang van die R en R' groepe. Verskeie *E*-isomere van hierdie ligande is geïsoleer en struktureel gekarakteriseer en die (S)C-NRR'-bindingslengte is in 'n gebied [1.343(3) – 1.329(3) Å] wat korter is as die gemiddelde C-N-enkelbindingslengte van 1.472(5) Å.

Die Pt(II) chelate wat afgelei is van die ligande is blootgestel aan die *E*,*Z*-konfigurasie isomere van die ongebinde ligande. Die teenwoordigheid van ***cis*-[Pt(*ZZ*-L-*S*,*O*)$_2$]**, ***cis*-[Pt(*EZ*-L-*S*,*O*)$_2$]** en ***cis*-[Pt(*EE*-L-*S*,*O*)$_2$]** is maklik waarneembaar deur middel van ^{195}Pt-KMR-spektroskopy wat drie goed geresolueerde seine toon, en dit kan bevestig word met ^{1}H- en ^{13}C-KMR spectra van hierdie komplekse. Die ^{195}Pt kerne is ruimtelik geskakel met die ^{13}C kerne deur vier bindings wat aanleiding gee tot $^{4}J(^{195}\text{Pt}\text{-}^{13}\text{C})$-koppelings met *N*-$CH_2$- of *N*-$CH_3$-koolstofatome in 'n **W**-konformasie. Die ^{195}Pt KMR spektra word geskakel met die *N*-CH_2- of *N*-CH_3-protonresonansies in al drie die moontlike *ZZ*, *EZ* en *EE* kompleksisomere. Toekenning van die konfigurasionele isomere is dan bewerkstellig deur middel van 'n kombinasie van lae magneetveld ^{13}C-KMR spectra en hoë resolusie gHSQC (^{1}H/^{13}C) KMR experimente.

^{1}H-KMR-rotasiedinamiek studie toon dat die rotasiegrens, $\Delta G^{\neq}$, om die (S)C-N(Me)(*para*-X-Ph)-binding in *cis*-bis(*N*-metiel-*N*-(4-metoksifeniel)-*N'*-2,2-dimetielpropanoïeltioureato)platinum(II), ***cis*-[Pt(L^{1A}-*S*,*O*)$_2$]**; *cis*-bis(*N*-feniel-*N*-metiel-*N'*-2,2-dimetielpropanoïeltioureato)platinum(II), ***cis*-[Pt(L^{2A}-*S*,*O*)$_2$]** en *cis*-bis(*N*-metiel-*N*-(4-nitrofeniel)-*N'*-2,2-dimetielpropanoïeltioureato)platinum(II), ***cis*-[Pt(L^{3A}-*S*,*O*)$_2$]** komplekse was met die volgende orde bepaal: (elektron-ontrekkende groep) NO_2 < H < (elektron-skenkende groep) O-CH_3. Die *ZZ*-isomeer blyk by voorkeur te vorm bo die *EZ*- en *EE*-isomere in dieselfde orde as hierbo wat betref *para*-substituent aan die *N*-fenielgroep. Die ^{1}H dinamiese KMR tendencies ten opsigte van die rotasiegrens, $\Delta G^{\neq}$, om die (S)C-N(Me)(*para*-X-Ph)-binding is gekomplimenteer met DFT-linêre organgs berekeninge. Die isomer verspreidings blyk ook beïnvloed te word deur die oplosmiddel polariteit en die temperatuur waarby die verspreidings bepaal is, buiten die elektroniese invloed van die *para*-substituent aan die *N*-fenielgroep.

Die *ZZ*, *EZ* en *EE* isomeer verspreiding van komplekse wat afgelei is van *N*-alkiel-*N*-(*para*-X-Ph)-*N*'-asieltioureums met veranderlike *N*-alkiel substituente (metiel, isopropyl, sikloheksiel, en n-pentiel) is vasgestel deur middel van die ^{195}Pt KMR wat opgeneem is onder identiese kondisies. Die *ZZ*-isomeer blyk die verkose isomeer te wees bo die *EZ*- en *EE*-isomere waar die metiel substituent vervang word met 'n groter alkiel groep in die orde van: metiel < isopropiel < sikloheksiel < n-pentiel. Dit is kwalitatief getoon dat die groter *N*-pentielgroep die rotasiegrens verhoog vir rotasie om die (S)C-N(alkiel)(*para*-X-Ph)-binding bo dié van die *N*-metielgroep wat aanleiding gee tot hoër konsentrasies van die *ZZ*-isomeer relatief tot die *EZ*- en *EE*-isomere. Die gekombineerde uitwerking van die electron-skenkende substituent (O-CH_3) op die *N*-(*para*-X-Ph)-groep en die groter *N*-alkiel groep (n-pentiel) gee aanleiding tot die hoogste *ZZ*-konsentrasie (76%) bo *EZ*- en *EE*-isomere in die kompleks *cis*-bis(*N*-pentiel-*N*-(4-metoksifeniel)-*N'*-2,2-dimetielpropanoïeltioureato)platinum(II), ***cis*-[Pt(L^{1D}-*S,O*)$_2$]**. Die laagste konsentrasie *ZZ* (27%) is verkry in die kompleks *cis*-bis(*N*-metiel-*N*-(4-nitrofeniel)-*N'*-2,2-dimetielpropanoïel)tioureato)platinum(II), ***cis*-[Pt(L^{3A}-*S,O*)$_2$]** waar die gekoördineerde ligand beide die *N*-metiel- sowel as die *N*-(4-nitro-Ph)-groep, wat albei die rotasiegrens van die (S)C-N(alkiel)(*para*-X-Ph)-binding verlaag.

'n Kristalstruktuur van die kompleks *cis*-bis(*N*-pentiel-*N*-(4-metoksifeniel)-*N'*-2,2-dimetielpropanoïeltio-ureato)platinum(II), ***cis*-[Pt(L^{1D}-*S,O*)$_2$]** wat geïsoleer is, is struktureel gekarakteriseer en is in die *ZZ*-konfigurasie, wat die hoofkomponent (76%) is in chloroform. Hierdie is die eerste voorbeeld van Pt(II) chelate met asimmetriese digesubstitueerde ligande om geraporteer te word.

On the chessboard lies and hypocrisy do not survive long. The creative combination lays bare the presumption of a lie; the merciless fact, culminating in a checkmate, contradicts the hypocrite.

Grandmaster Dr. Emanuel Lasker
1868 – 1941

Acknowledgements

I would like to thank Professor Klaus R. Koch for guidance and support throughout my studies.

Thanks to

Ms Marga Burger for the valuable contribution she made on the theoretical calculations and discussions.

Dr. Jurjen Kramer for the never-ending enthusiasm, support and valuable comments (I don't know where you get all the energy, man).

The ever-patient duo from the NMR Laboratory: Jean McKenzie and Elsa Malhebe for my NMR training and keeping up with me.

The PGM research group members, who helped in many ways for the success of my work.

To parents and siblings for continued support and encouragement that has given me strength when energy reserves were low during my studies.

For financial support I would like to thank Sasol, the National Research Foundation and the University of Stellenbosch.

The work presented in this thesis has been presented in various forms in local and international media:

Paper:

- D. Argyropoulos, E. Hoffmann, S. Mtongana, and K. R. Koch, *Magn. Reson. Chem.*, **2003**, *41*, 102.

Locally:

Oral:

- South African Spectroscopic Society Meeting, IThemba Laboratories, Cape Town, 2003
- Cape Organometallic Symposium I, Morgenoff Wine Estate, Stellenbosch, 2003

Poster:

- SACI Inorganic Conference, Pretoria, 2003
- SACI Inorganic Conference, Pietermaritzburg, 2005
- Cape Organometallic Symposium III, Waterfront, Cape Town, 2005

Internationally:

Poster:

- Small Molecule NMR (SMASH) Conference, Verona, Italy, 2005
- 37th International Conference of Coordination Chemistry, Cape Town, 2006

CONTENTS

Chapter 1: General Introduction

In this thesis we report on the study of the coordination chemistry of chelating asymmetrically disubstituted *N*-alkyl-*N*-alkyl(aryl)-*N'*-acylthiourea ligands towards Pt(II) metal ion. The double bond character of the C-N bond of the (S)C-N(R)(R') moiety of these ligands leads to *E,Z* configurational isomers. This isomerism is then relayed to the resulting platinum(II) chelates derived from these ligands. Variations of R and R' presents a wide variety of these ligands and their respective Pt(II) complexes. We explored these variations and their implications on the nature of ligands that were synthesised and their *E,Z* isomer distributions and how the nature of the ligand impacts on the isomer distribution of the complexes resulting from them. To a large extent the ligands with the general motif described in the thesis have been shown to have high affinity for a variety of transition metals and this has proved valuable to the platinum group metal (PGM) industry.

In this study we briefly describe the synthesis of asymmetric secondary amines, which are important to ligand design followed by the actual ligand synthesis and subsequently the platinum(II) chelates derived from these ligands. We then used multinuclear magnetic resonance spectroscopic techniques for structural elucidation of these complexes in solution, then moved on and explored factors that may influence the isomer distributions of the platinum complexes, also by means of multinuclear magnetic resonance techniques. Besides multinuclear magnetic resonance techniques as means of analysing these mixtures, other techniques such as Reverse Phase High Performance Liquid Chromatography (RP-HPLC) were considered, however with limited success. Since the RP-HPLC results were not as encouraging and compounded with time limitation, this line of analysis was not pursued any further. In **chapter 4**, we have also used Density Function Theory linear transit calculations as a complementary tool to the ^{1}H NMR spectroscopy Rotational Dynamics study.

1.1 General coordination chemistry of *N*-alkyl- and *N,N*-dialkyl-*N'*-acyl(aroyl)thioureas towards transition metals

Ligands of the type *N*-alkyl- and *N,N*-dialkyl-*N'*-acyl(aroyl)thiourea, (H_2L and HL) are easily synthesised in high yield in a two-step procedure[1] and are known to display rich coordination chemistry towards a wide variety of transition metals.[2,3] The *N,N*-dialkyl-*N'*-acyl(aroyl)thiourea ligands readily form stable complexes with transition metals coordinating in a chelating or bidentate fashion through the oxygen and sulphur atoms, in the process the ligands loose their acidic -(O)CNHC(S)- thioamidic protons. It may well be the dual hard donor oxygen/soft donor sulphur property of these ligands that allow them to coordinate to a wide variety of transition metals in different modes. According to Pearson's Hard Soft Acids Bases (HASB) principle,[4,5] a hard donor like oxygen would prefer to bind with hard metal ions like Co(III) and Ni(II), while a soft donor like sulphur would prefer to bind to soft metal ions like Pd(II) and Pt(II). Predominantly, the mode of coordination for the HL towards transition metals is the *cis* chelating fashion and several examples of *cis*-[Pt(L-*S,O*)$_2$] have been fully characterised in the literature[6-8] and only one fully characterised example in which the ligands are in a *trans* chelating fashion.[9] Recently is was discovered that *cis*-[M(L-*S,O*)$_2$] complexes with M = Pd and Pt undergo photochemically induced *cis* to *trans* isomerisation, however this has not lead to isolation of other *trans* complexes since the isomerisation is thermally reversible in the absence of light.[10] In the case of *N*-alkyl-*N'*-acyl(aroyl)thioureas, H_2L, even though they are also known to coordinate to transition metals[2] they usually form complexes with Pt(II) and Pd(II) through their sulphur atom only (e.g. with $[PtX_4]^{2-}$, X = Cl, Br and I, resulting in mixtures of *cis*- and *trans*-[Pt(HL-S)$_2$X$_2$]).[11-13] The hydrogen of the thiourea -(S)CNHR' moiety is usually involved in intra-molecular hydrogen bonding with the carbonyl oxygen atom and therefore rendering it unavailable for coordination. Scheme 1 illustrates the general modes of coordination for the HL and H_2L type of ligands towards Pt(II) metal ion.

The coordination chemistry, in particular that of *N,N*-dialkyl-*N'*-acyl(aroyl)thioureas towards transition metals has received much attention in view of their practical industrial applications.[14] In pH controlled conditions, effectively, these ligands would coordinate to platinum group metals (PGMs) in the presence of other interfering metals.[15] In this regard these ligands have been found to be industrially useful in liquid-liquid extractions, pre-concentration and separation of PGMs.[15-17] Unterreitmaier and Schuster[18] have also modified these ligands with a fluorescent tag for fluorometric detection of heavy metals. Functional polymeric materials such as *N*-benzoylthiourea modified dendrimers, which are also of practical use for selective and recovery of heavy metal ions have recently been reported by Rether and Schuster.[19] In the on-going contribution to this field we have reported an inter-PGM {Pt(II), Pd(II) and Rh(III)} separation using hydrophilic *N*-acylthioureas by means of reverse phase high performance liquid chromatography (RP-HPLC).[6] Efficient and selective liquid membrane transport of Ag(I) in the presence of Co(I), Ni(II), Cu(II), Zn(II), Cd(II) and Pb(II) metal ions is another example that illustrate the versatility and practical uses of these types of ligands.[20]

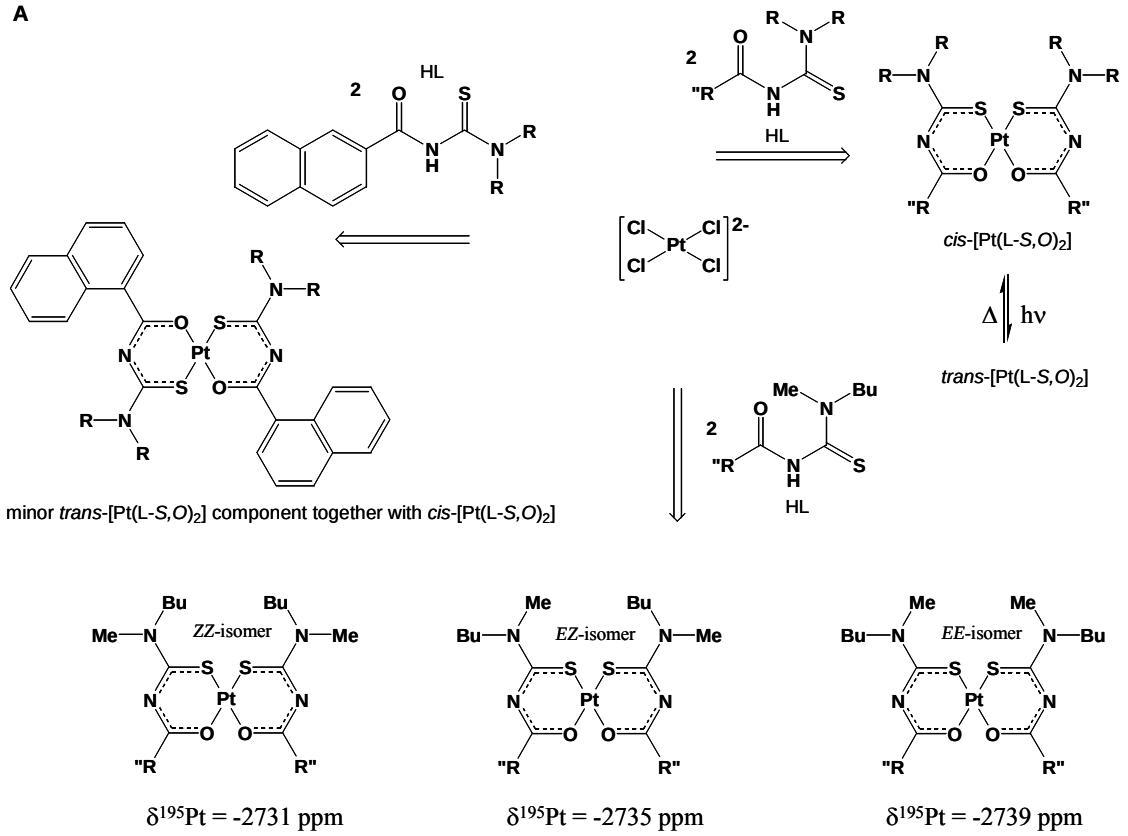

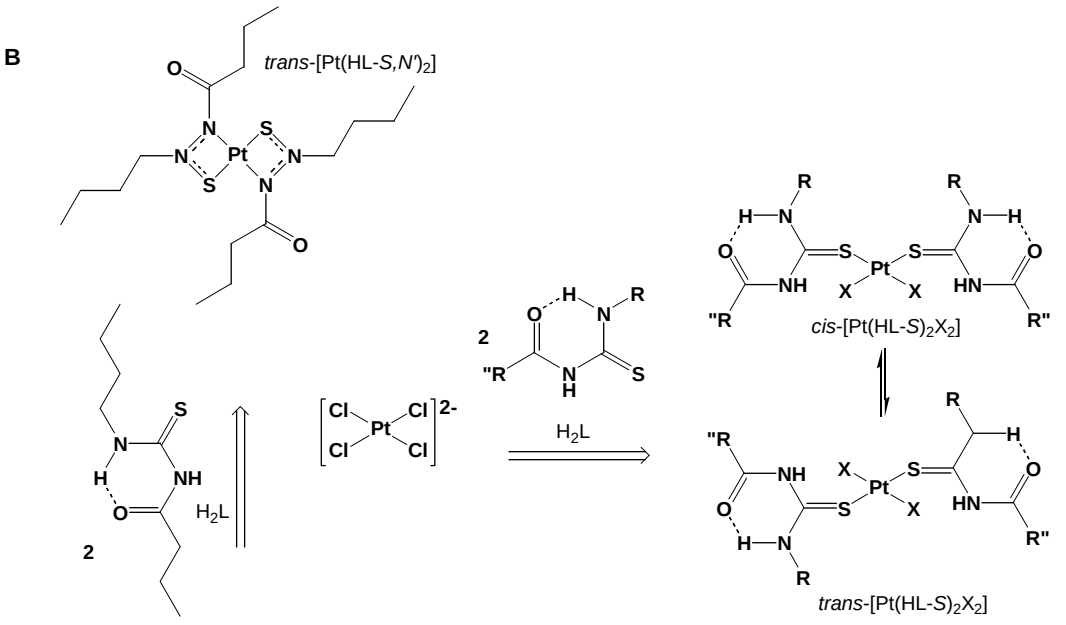

Scheme 1 Coordination modes for HL and H_2L towards Pt(II) used as an example in the figure but in general these coordination modes are applicable to other transition metals.[14] We have *N*-aroylthioureas if R" = aromatic group, *N*-acylthioureas if R" = alkyl group. In (A) R is usually an alkyl group and in (B) one of the alkyl groups, R, has been substituted by a hydrogen atom.

Apart from the applications of these mixed metal-ligand complexes in heavy metal coordination chemistry which has dominated this field, are the biological activity and medicinal properties of such complexes. Sacht *et al.*[7] and Rodger *et al.*[21] reported chiral and achiral mixed platinum(II)-ligand complexes, which are based on thioureas to have encouraging results as potential anti-tumour agents. Egan *et al.*[22] have worked on mixed platinum(II)-ligand complexes that show anti-malaria properties also based on thioureas. Recently we have also reported on intercalation into DNA double helix by water-soluble planar mixed platinum(II)-ligand complexes.[23]

With regard to the coordination chemistry of these deceptively simple ligands, it seems that there is a wide scope of applications that could be explored. To shift the focus from the readily applicable nature of these ligands and their respective metal complexes in this study, the less explored variation on the theme where the R and R' groups of the (S)C-NRR' moiety are not equivalent and none of them is a hydrogen atom, are investigated. We have limited the study to Pt(II) coordination chemistry of these ligands largely because the metal complexes can easily be monitored by means of ^{195}Pt NMR spectroscopy.

1.2 Asymmetrically disubstituted ligands

From the ^{1}H and ^{13}C NMR spectra of the symmetrically disubstituted *N,N*-dialkyl-*N'*-acyl(aroyl)thioureas and their respective metal complexes, it can be noted that the *N*-alkyl groups resonate in different chemical shifts. The principal reason behind this observation is the partial double bond character of the C-N bond of the (S)C-NRR' moiety that results in the *N*-alkyl groups being either coplanar with the sulphur atom or point away from the sulphur atom of the (S)C-NRR' moiety. The chemical and magnetic differences of these positions invariably make them to resonate at different chemical shifts.

Of interest is when the two *N*-alkyl groups are not the same since the restricted rotation around this C-N bond results in *E,Z* configurational isomerism of these ligands. We define an *E* (*entgegen*) isomer (*entgegen* from German meaning opposite) as the isomer that has its *N*-alkyl group of highest priority pointing away from the sulphur atom. The *Z* (*zusammen*) isomer (*zusammen* from German meaning together) as the isomer that has its *N*-alkyl group of highest priority on the same side as the sulphur atom. The priority in the case of alkyl groups is determined by the size of the alkyl group, the larger taking highest priority as exemplified in Figure 1.1 below.

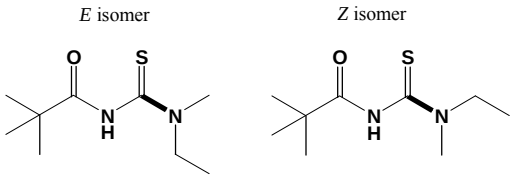

Figure 1.1 *E* and *Z* configurational isomers of *N*-ethyl-*N*-methyl-*N'*-*2,2*-dimethylpropanoylthiourea that result from the partial double bond character of the highlighted C-N bond. Since the ethyl group is larger than the methyl group it takes priority.

The *E,Z* isomerism in the unbound ligand is carried through to the resultant platinum(II) chelates, resulting in *cis*-[Pt(*EE*-L-*S,O*)$_2$], *cis*-[Pt(*EZ*-L-*S,O*)$_2$] and *cis*-[Pt(*ZZ*-L-*S,O*)$_2$] configurational isomers, all of which are easily observable from their ^{195}Pt NMR spectra. Clearly, the *cis*-[Pt(*EE*-L-*S,O*)$_2$] configurational isomer will have both of its ligands orientated in the *E* configuration and the *cis*-[Pt(*ZZ*-L-*S,O*)$_2$] configurational isomers would have its ligands orientated in the *Z* configuration. The *cis*-[Pt(*EZ*-L-*S,O*)$_2$] configurational isomer will then have one ligand orientated in the *E* configuration while the other ligand is orientated in the *Z* configuration (see scheme 1).

The coordination chemistry of these ligands is similar to that of symmetrically substituted ones in that it is dominated by *cis* coordination mode of the ligands and not even trace evidence of the *trans* coordination mode has been reported to date. This is evident from the ^{195}Pt NMR chemical shift range in which these complexes resonate. Normally, the *trans* complexes appear about 300 ppm upfield relative to the *cis* complexes as observed by Miller.[24] As an example the *N*-morpholino-*N'*-naphthoylthioureatoplatinum(II) complex reported by Grimmbacher[25] had the *cis* isomer appearing at -2708 ppm while the *trans* isomer appeared at -3027 ppm. Previously, the unambiguous assignment of the Pt(II) configurational isomers derived from such ligands was achieved by means of triple resonance ^{1}H/^{13}C/^{195}Pt correlation NMR spectroscopy.[26] This technique is not readily available to us and it requires a special NMR probe with three channels with which the correlated nuclei can be tuned. With courtesy of Varian Applications Laboratory in Darmstadt, Germany we were able to employ this technique with remarkable success, as illustrated for *ZZ*, *EZ* and *EE* isomers of *cis*-bis(*N*-ethyl-*N*-methyl-*N'*-*2,2*-dimethylpropanoylthioureato)platinum(II) (Figures 1.2, 1.3 and 1.4).

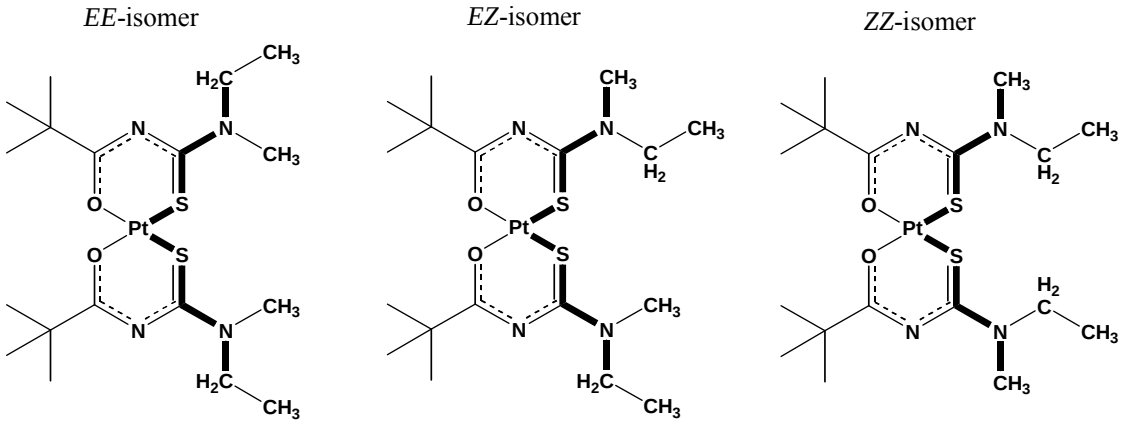

Figure 1.2 *EE*, *EZ* and *ZZ* configurational isomers of the *cis*-bis(*N*-ethyl-*N*-methyl-*N'-2,2*-dimethylpropanoylthioureato)platinum(II) showing a favourable **W** $^{4}J(^{195}Pt\text{-}^{13}C)$ coupling pathway in bold.

Only the *N*-CH_3 and *N*-CH_2- carbons in the favourable **W** pathway couple to the ^{195}Pt isotope as illustrated by ^{13}C NMR spectrum measured at low magnetic field (Figure 1.3).

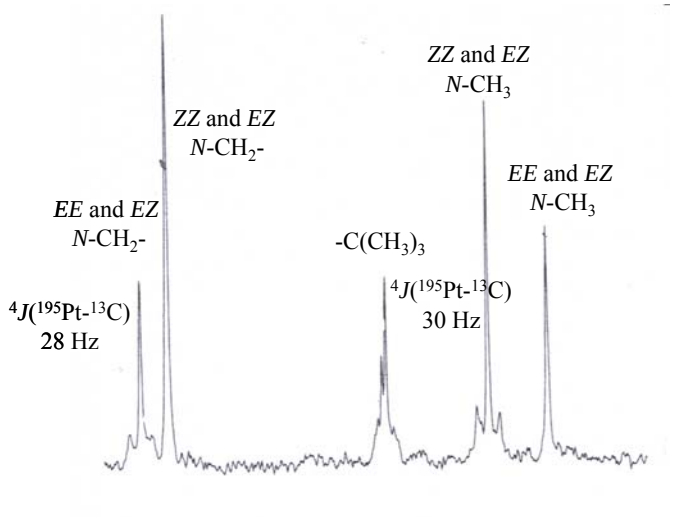

Figure 1.3 Low magnetic field (50 MHz ^{13}C frequency) sections of the ^{13}C NMR spectrum of *cis*-bis(*N*-ethyl-*N*-methyl-*N'-2,2*-dimethylpropanoylthioureato)platinum(II) showing *ZZ*, *EZ* and *EE* isomers $^{4}J(^{195}Pt\text{-}^{13}C)$ couplings to *N*-CH_2- carbons and *N*-CH_3 carbons via a **W** coupling pathway to the ^{195}Pt isotope.

Due to the insensitivity of the carbon nucleus in NMR spectroscopy and the expected broadness of the $^{195}Pt\text{-}^{13}C$ satellites due to chemical anisotropy broadening at high field, the platinum nucleus could not be directly correlated to these carbons even though they are in a favourable pathway. Instead, the highly sensitive protons, attached to these $^{195}Pt\text{-}^{13}C$ coupled carbons were correlated to platinum, achieving a $^{1}H\text{-}(^{13}C)\text{-}^{195}Pt$ NMR correlation spectrum.

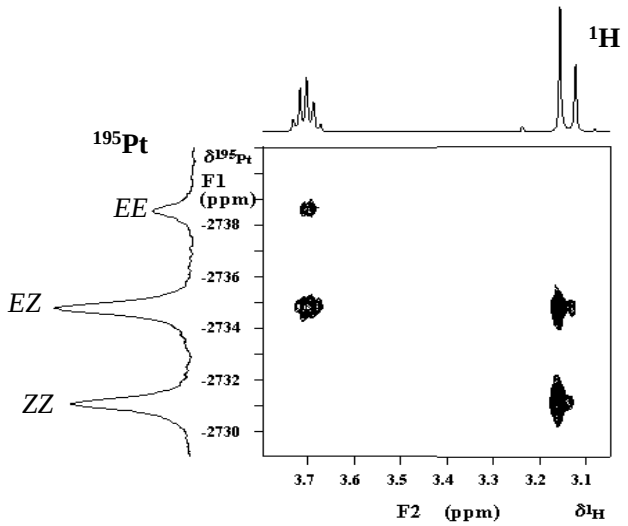

Figure 1.4 $^{1}H/^{13}C/^{195}Pt$ correlation spectrum of *cis*-bis(*N*-ethyl-*N*-methyl-*N'*-*2,2*-dimethylpropanoylthioureato)platinum(II) in $CDCl_3$ at 298 K, results in the assignment of the ^{195}Pt peaks at -2739 ppm, -2735 and -2731 ppm to the *EE*, *ZE* and *ZZ* isomers, respectively.

In the $^{1}H/^{13}C/^{195}Pt$ correlation NMR spectrum a double magnetization transfer experiment is performed in which the magnetization is relayed from the sensitive ^{1}H to ^{13}C to ^{195}Pt and back to ^{13}C and ^{1}H. For the *cis*-bis(*N*-ethyl-*N*-methyl-*N'*-*2,2*-dimethylpropanoylthioureato)platinum(II) complex, the correlation of the (fortuitously overlapping) ^{1}H resonance at *ca* 3.7 ppm of the *N*-CH_2- moiety with the ^{195}Pt peaks at -2739 ppm and -2735 ppm confirm the assignment to *EE* and *EZ* isomers, respectively. The ^{195}Pt peak at -2735 ppm is correlated to both the *N*-CH_3 and the *N*-CH_2- resonances, which can only be for the *EZ* isomer, while the correlation between the ^{195}Pt peak at -2731 ppm and the *N*-CH_3 resonance at 3.17 ppm, confirms the assignment the *ZZ* isomer. Earlier work by Koch *et al.*[27] had observed this kind of isomerism and gave valuable suggestions of how these could be assigned unambiguously by NMR spectroscopy and indeed this preliminary work was confirmed by the $^{1}H/^{13}C/^{195}Pt$ correlation NMR experiment (Figure 1.4). Even though these isomers could be assigned the outstanding question that remained unanswered was regarding the isomer distributions of the complexes obtained. In the two cases previously investigated the statistically predicted distribution for the complexes was never mirrored by the experimentally observed distributions. For example, in the case of *N*-ethyl-*N*-methyl-*N'*-*2,2*-dimethylpropanoylthiourea ligand, the *Z* to *E* isomer distribution was determined to be 75 % to 25 %. The statistically expected isomer distribution of the resultant complexes was determined to be 62.5 %(*ZZ*) to 25 %(*EZ*) to 12.5 %(*EE*). [A one-to-one ratio of *Z* and *E* isomers is expected to result in a one-to-two-to-one ratio of *ZZ* : *EZ* : *EE* complexes and the excess *Z* isomers should react and form exclusively *ZZ* complex, which would then contribute to the overall *ZZ* concentration]. However, the experimentally determined integral ratios from the ^{195}Pt NMR spectrum showed a 40 %(*ZZ*) to 47 %(*EZ*) to 13 %(*EE*) isomer distribution.

In this thesis we shall be looking at new means of assigning these configurational isomers with NMR spectroscopic means that are readily available to us and there after attempt to tackle the question of factors that influence these isomer distributions. At first we take a look at the work done in the literature in related compounds. The nature of the literature survey is by no means comprehensive but only highlights aspects that will be applicable in our study.

1.3 Restricted C-N bond rotation in carbonyl, thiocarbonyl amides and related compounds: A literature survey

In the 1970's Stewart and Siddall III[28] gave an extensive review on the NMR studies of amides which is still very useful with regard to topics like the magnetic anisotropy of amide and thioamide groups; criteria used for making signal assignment; *E,Z* isomerism in unsymmetrical *N,N*-disubstituted amides and hindered rotations in these compounds. For most of the discussion these authors held the traditional view of resonance I and resonance II (Scheme 2) being operative in explaining the restricted rotation about the C-N bond. However, the theoretical study by Wiberg and Rablen[29] challenged this view and claimed that it does not describe satisfactorily the nature of electronic interactions that determine the rotational barrier in amides. These authors find it necessary to include

resonance III (Scheme 2) as well, which involves a charge transfer between carbon and nitrogen as opposed to the charge transfer from the nitrogen atom to the chalcogen.

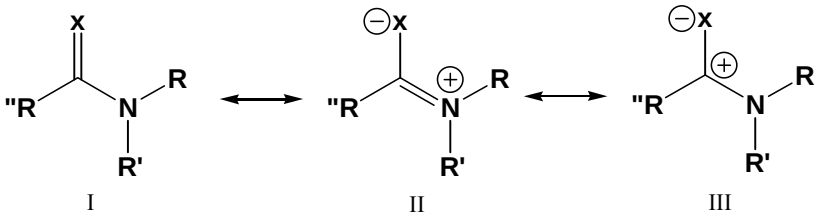

X = any chalcogen O, S or Se
R, R' and R" = H or alkyl group

Scheme 2 Possible resonance structures that result from the partial double bond character of the (X)C-N bond

Their theoretical data showed that thioamides have higher rotation barrier than amides which is a view supported by independent studies by other workers.[30-32] The difference is determined mostly by the charge transfer from nitrogen to sulphur in thioamides opposed to oxygen in amides. Therefore the traditional view is sufficient to explain the high rotation barriers in thioamides[33] and selenoamides.[34] The flow of charge from nitrogen to the chalcogen, X is in the increasing order (X = O < S < Se)[35,36] with electronegativity not being a driving force for electron delocalisation into the π frame work of R"C(X)-NRR'.

It is this traditional view that we will use to explain the observed differences in C-N rotation barriers in the system of compounds that we shall be studying since our ligands resemble the thioamides. Looking at structure II in Scheme 2 the rotation barrier can either be increased or decreased by putting suitable R and R' groups depending on the desired effect. An electron-donating R and R' group should in principle result in higher C-N bond rotation barrier while an electron-withdrawing group should have the opposite effect. The C-N bond rotation barrier is also influenced by changes on the R" substituent[32,37] but this will not form part of the discussion in our system of ligands and complexes. The interest in the factors that affect this C-N bond rotation barrier may be crucial in explaining the *E,Z* configurational isomer distributions we get. To meet the aims of our study we have largely used experimental techniques (NMR spectroscopy) and theoretical techniques were employed to strengthen the experimental observations. In the next section we take a look at the important elements of these tools in connection to the requirements of the study.

1.4 Methods of analysis

1.4.1 Use of different multinuclear NMR spectroscopy in the study of E,Z configurational isomers

As a means of obtaining most reliable information about the populations of *E,Z* isomers it is sometimes essential to use different nuclei for verification. In some cases it has been found that observing one nucleus may not necessarily be sufficient to show all the isomers that are present in solution while the other(s) show the presence of all the isomers. The cause for this discrepancy may be due to insensitivity of one nucleus towards the fast C-N bond rotation compared to the other(s). It was also observed that sometimes the temperature in which the isomerism is investigated is well above coalescence temperature and not all the isomers are observable. Illustrations of these two phenomena are shown in Figure 1.2 and Figure 1.3 for the *ZZ*, *EZ* and *EE* isomers of *cis*-bis(*N*-methyl-*N*-(4-nitro-phenyl)-*N'*-*2,2*-dimethylpropanoylthioureato)platinum(II). In Figure 1.5 the *EZ* isomer is partitioned such that when the ligand is orientated in the E configuration it is labelled *E(EZ)* and labelled *Z(EZ)* when the ligand is in the *Z* orientation.

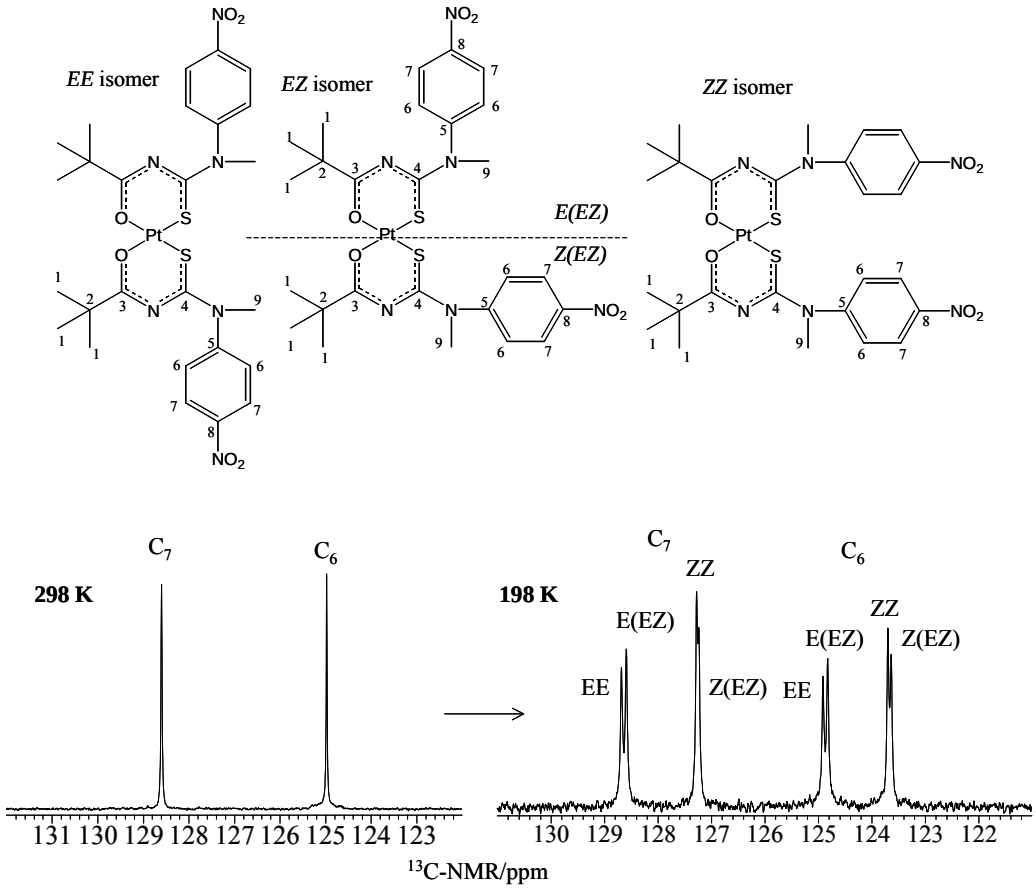

Figure 1.5 Aromatic ^{13}C NMR section of the isomers in the figure measured in deuterated dichloromethane at 298 K shows only two peaks for C6 and C7, and at 198 K each peak C6 and C7 is resolved into four peaks for the three isomers. The *EZ* isomer has two sets of C6 and C7 carbons.

It is easy to be misled at room temperature and assume that the compound exists as one isomer since the ^{13}C NMR peaks are very sharp and not hinting any dynamic process. This is caused by a very low C-N bond rotation barrier in

this compound. It is only at extremely low temperature, can it be seen that in actual fact the compound displays *E,Z* isomerism and therefore exists in three isomeric forms.

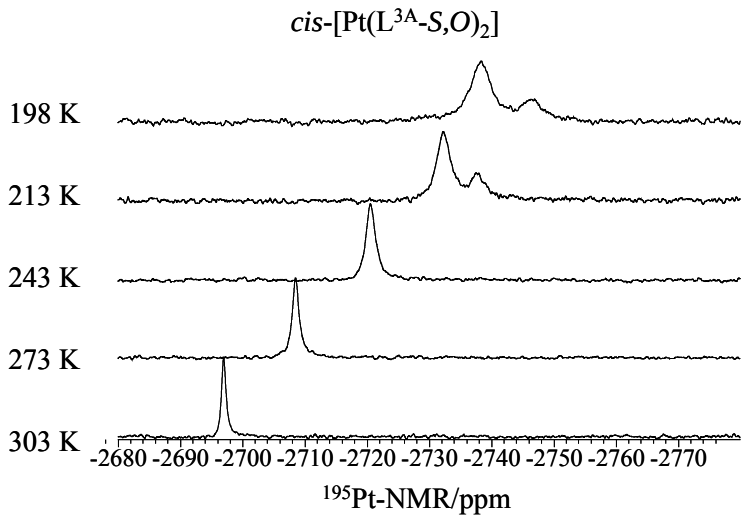

Figure 1.6 A temperature array of the ^{195}Pt NMR spectrum of the same compound as in Figure 1.1. At 303 K a very sharp peak is observed while the temperature is progressively lowered the peak broadens hinting the anticipated dynamics. At 213 K and below only two peaks are observed instead of the three revealed by the ^{13}C NMR spectrum (and ^{1}H NMR spectrum not shown here).

In the case of Figure 1.3 the ^{195}Pt nucleus used as the probe for this *E,Z* isomerism does not reveal all the expected isomers. It is therefore necessary to guard against unsuitable conditions or insufficient information that could be gathered from one nucleus as illustrated in the two figures. The conditions at which the *E,Z* isomerism is investigated must always be optimal and this can be achieved by using multinuclear NMR spectra of the sample. The data that are presented in the thesis are therefore such that whenever one nucleus does not give the anticipated information then the other(s) will be used for maximum information. In most of the cases investigated though, the different nuclei were complementary.

1.4.2 Determination of C-N rotation barrier by means of coalescence temperature determination method

Nuclear magnetic resonance spectroscopy has been used extensively in the literature for the study of amides, thioamides and related compounds. The main subjects of interest in these types of compounds are signal assignment and carbon-nitrogen rotation barrier determination. Pioneering work by Gutowsky and Holm,[38] using a symmetrically disubstituted *N,N*-dimethylformamide, carried out the early work on rotation barrier studies in the 1950's. Many other examples followed and appear in the review by Stewart and Sindall.[28] Most of the restricted rotation studies have been carried out in symmetrically *N,N*-disubstituted amides and only a few examples of unsymmetrical compounds. It is simply an extension of this technique in analysing *E,Z* configurational isomers that

result from the restricted rotation about the C-N bond. NMR is a suitable technique for studying inter-conversion of one isomer to the other if the process is sufficiently slow on the NMR time scale.

The general principle of studying rotation barrier involves observing the *N*-alkyl groups (for example by ^{1}H NMR) at a particular temperature where these *N*-alkyl groups are distinguishable from each other and resonate in different chemical environments. By gradually increasing the temperature these *N*-alkyl resonances are superimposed on each other at a particular temperature called coalescence temperature, T_c. Beyond T_c these signals often sharpen further as a single resonance. It is therefore at a coalesce temperature that thermodynamic parameters can be calculated. Accurate thermodynamic parameters such as the activation energy, E_a, enthalpy of activation, $\Delta H^{\neq}$ and entropy of activation, $\Delta S^{\neq}$ are usually obtained by means of total line shape analysis.[39-41] This technique involves the use of a computer program for an accurate determination of the value of τ, the lifetime of *N*-alkyl protons in a particular site as a function of temperature. The rate constant for exchange of the *N*-alkyl protons between the two sites is defined as:

$$k = 1/\tau \qquad [1.1]$$

A plot of the logarithm of this rate constant vs 1/T, where T is the absolute temperature, is linear. The slope gives the activation energy, E_a, for rotation about the C-N bond of interest, from the Arrhenius equation:

$$k = A\exp(-E_a/RT) \qquad [1.2]$$

where A is frequency factor from the intercept of the Arrhenius plot and R is the gas constant.

The enthalpy of activation, $\Delta H^{\neq}$ can be obtained from the relationship:

$$\Delta H^{\neq} = E_a - RT \qquad [1.3]$$

Both the enthalpy of activation and the entropy of activation, $\Delta S^{\neq}$, can in turn be obtained from the Erying equation:

$$k = 1/\tau = \kappa(k_BT/h)\exp(-\Delta H^{\neq}/RT + \Delta S^{\neq}/R) \qquad [1.4]$$

where κ = transmission coefficient assumed to be equal to 1, k_B = is the Boltzmann constant and h = is the Plank constant.[41]

From linear plots of k vs 1/T thermodynamic parameters $\Delta H^{\neq}$ and $\Delta S^{\neq}$ are easily obtained from the slope and intercept, respectively.

Apart from these heavily involved calculations it is also possible to use approximation methods that agree very well with total line shape analysis method.[42,43] After determining the T_c, particularly in the case of unequal isomeric populations we can calculate the Gibbs energy of activation using the equation developed by Shanin-Atidi and Bar-Eli,[43] which take into account the effect of unequal populations of isomer A and isomer B (**chapter 4**).

$$\Delta G^{\neq}_{(A\text{-}B)} = 4.57Tc[10.62 + \log(X/2\pi(1 - \Delta P)) + \log Tc/\Delta\upsilon] \qquad [1.5]$$

$$\Delta G^{\neq}_{(B\text{-}A)} = 4.57Tc[10.62 + \log(X/2\pi(1 + \Delta P)) + \log Tc/\Delta\upsilon] \qquad [1.6]$$

Where $\Delta G^{\neq}_{(A\text{-}B)}$ and $\Delta G^{\neq}_{(B\text{-}A)}$ are the Gibbs free energy of activation for the conversion of A to B and from B to A, $\Delta\upsilon$ is the frequency separation in Hertz between the B and A peaks, ΔP = difference in populations of B and A isomers and

$$P_B - P_A = \Delta P = [(X^2 - 2)/3]^{3/2} \cdot 1/X \qquad [1.7]$$

We shall be employing these coalescence temperature techniques for the determination of the rotational barriers in the system of ligands and complexes presented in this thesis. Other workers have employed this method successfully where the isomer distributions of the interchanging systems are unequal.[44,45]

The difference in energy of the two isomers can be evaluated by the equation:

$\Delta G_0 = -RT\ln K$ [1.8]

Where K = [isomer 1]/[isomer 2] < 1, the molar concentration of the isomers could be taken from the deconvolution analysis (peak integrals) of the ^{1}H NMR spectra and T = temperature at which the peaks are well separated.

1.5 Objectives and outline of this thesis

The aim of the research presented in this thesis is to account for the factors that affect the isomer distributions obtained when asymmetrically disubstituted *N,N*-dialkyl-*N'*-acylthioureas coordinate to a Pt(II) metal centre. The nature of this research is of academic interest and has no immediate applications. The interest brought about this research is the observation that the isomer distributions of the unbound ligands do not convert statistically to predicted isomers in the resultant Pt(II) chelates.[26] This observation suggested that there must be some underlying driving principle(s) that govern these Pt(II) chelate isomer distributions and we were set to find these out. This meant that a careful ligand design was necessary to evaluate a particular principle that may be operative in steering the isomer distribution in a particular way.

In this regard we have synthesised and fully characterised a series of asymmetrically disubstituted *N,N*-dialkyl-*N'*-acylthioureas in **chapter 2**. In the same chapter we briefly describe their general chemistry in solid-state as well as in solution. Not all the secondary amines with which most of the ligands were synthesised are commercially available therefore we also synthesised these in our laboratories.

In **chapter 3**, using a selected few of these ligand-metal complexes, we illustrate how the ^{195}Pt NMR spectra of the configurational isomers are implicitly assigned unambiguously with a combination of low magnetic field ^{13}C NMR spectra and gHSQC (^{1}H/^{13}C) NMR experiments with equipment readily available to us.

In **chapter 4**, making systematic electronic variations on ligands with the same structural motif, we study the impact these changes have on the C-N rotation barrier and the implications thereof on isomer distributions. Complementary to the solution NMR techniques with which the electronic effects have on the C-N bond restricted rotation Density Functional Theory calculations were employed to verify the experimental methods. Temperature and solvent changes are also discussed here as they also have an influence on the C-N restricted rotation.

The influence the alkyl group variations have on the ligands with the same structural motif is discussed in **chapter 5**.

Chapter 6 is a summary of the findings discussed in preceding chapters and ends with some recommendations for future work on this topic.

References

1 I. B. Douglass and F. B. Dains, *J. Am. Chem. Soc.*, **1934**, *56*, 719.
2 L. Beyer, E. Hoyer, J. Liebscher, and H. Hartmann, *Z. Chem.*, **1981**, *21*, 81.
3 P. Muehl, K. Gloe, F. Dietze, E. Hoyer, and L. Beyer, *Z. Chem.*, **1986**, *26*, 81.
4 R. G. Pearson, *J. Chem. Ed.*, **1968**, *45*, 581.
5 R. G. Pearson, *J. Chem. Ed.*, **1968**, *45*, 643.
6 A. N. Mautjana, J. D. S. Miller, A. Gie, S. A. Bourne, and K. R. Koch, *J. Chem. Soc., Dalton Trans.*, **2003**, 1952.
7 C. Sacht, M. S. Datt, S. Otto, and A. Roodt, *J. Chem. Soc., Dalton Trans.*, **2000**, 727.
8 A. Irving, K. R. Koch, and M. Matoetoe, *Inorg. Chim. Acta*, **1993**, *206*, 193.
9 K. R. Koch, J. du Toit, M. R. Caira, and C. Sacht, *J. Chem. Soc., Dalton Trans.*, **1994**, 785.
10 D. Hanekom, J. M. McKenzie, N. M. Derix, and K. R. Koch, *Chem. Commun.*, **2005**, 767.
11 S. Bourne and K. R. Koch, *J. Chem. Soc., Dalton Trans.*, **1993**, 2071.
12 K. R. Koch, Y. Wang, and A. Coetzee, *J. Chem. Soc., Dalton Trans.*, **1999**, 1013.
13 A. N. Westra, C. Esterhuysen, and K. R. Koch, *Acta Crystallogr., Sect C*, **2004**, *C60*, m395.
14 K. R. Koch, *Coord. Chem. Rev.*, **2001**, *216-217*, 473.
15 K. H. Koenig, M. Schuster, B. Steinbrech, G. Schneeweis, and R. Schlodder, *Fresen. J. Anal. Chem.*, **1985**, *321*, 457.
16 P. Vest, M. Schuster, and K. H. Koenig, *Fresen. J. Anal. Chem.*, **1989**, *335*, 759.
17 M. Schuster, *Frensen. J. Anal. Chem.*, **1992**, *342*, 791.
18 E. Unterreitmaier and M. Schuster, *Anal. Chim. Acta.*, **1995**, *309*, 339.
19 A. Rether and M. Schuster, *React. Funct. Polym.*, **2003**, *57*, 13.
20 H. G. Berhe, S. A. Bourne, M. W. Bredenkamp, C. Esterhuysen, M. M. Habtu, K. R. Koch, and R. C. Luckay, *Inorg. Chem. Commun.*, **2006**, *9*, 99.
21 A. Rodger, K. K. Patel, K. J. Sanders, M. Datt, C. Sacht, and M. J. Hannon, *J. Chem. Soc., Dalton Trans.*, **2002**, 3656.
22 T. J. Egan, K. R. Koch, P. L. Swan, C. Clarkson, D. A. Van Schalkwyk, and P. J. Smith, *J. Med. Chem.*, **2004**, *47*, 2926.
23 Y.-S. Wu, K. R. Koch, V. R. Abratt, and H. H. Klump, *Arch. Biochem. Biophys.*, **2005**, *440*, 28.
24 J. D. S. Miller, *PhD Thesis, University of Cape Town*, **2000**.
25 T. Grimmbacher, *PhD Thesis, University of Cape Town*, **1995**.
26 D. Argyropoulos, E. Hoffmann, S. Mtongana, and K. R. Koch, *Magn. Reson. Chem.*, **2003**, *41*, 102.
27 K. R. Koch, C. Sacht, T. Grimmbacher, and S. Bourne, *S. Afr. J. Chem.*, **1995**, *48*, 71.
28 W. E. Stewart and T. H. Siddall, III, *Chem. Rev.*, **1970**, *70*, 517.
29 K. B. Wiberg, P. R. Rablen, D. J. Rush, and T. A. Keith, *J. Am. Chem. Soc.*, **1995**, *117*, 4261.
30 K. E. Laidig and L. M. Cameron, *J. Am. Chem. Soc.*, **1996**, *118*, 1737.
31 D. Lauvergnat and P. C. Hiberty, *J. Am. Chem. Soc.*, **1997**, *119*, 9478.
32 S. M. N. Crawford, A. N. Taha, N. S. True, and C. B. LeMaster, *J. Phys. Chem. A*, **1997**, *101*, 4699.
33 K. B. Wiberg and D. J. Rush, *J. Am. Chem. Soc.*, **2001**, *123*, 2038.
34 B. V. Prasad, P. Uppal, and P. S. Bassi, *Chem. Phy. Lett.*, **1997**, *276*, 31.
35 E. D. Glendening and J. A. Hrabal, II, *J. Am. Chem. Soc.*, **1997**, *119*, 12940.
36 P. V. Bharatam, R. Moudgil, and D. Kaur, *J. Phys. Chem. A*, **2003**, *107*, 1627.
37 T. Drakenberg, K. I. Dahlqvist, and S. Forsen, *J. Phys. Chem.*, **1972**, *76*, 2178.
38 H. S. Gutowsky and C. H. Holm, *J. Chem. Phys.*, **1956**, *25*, 1228.
39 L. Isbrandt, W. C. T. Tung, and M. T. Rogers, *J. Magn. Reson.*, **1973**, *9*, 461.
40 M. D. Wunderlich, L. K. Leung, J. A. Sandberg, K. D. Meyer, and C. H. Yoder, *J. Am. Chem. Soc.*, **1978**, *100*, 1500.
41 N. K. Wilson, *J. Phys. Chem.*, **1971**, *75*, 1067.

42 M. Raban, D. Kost, and E. H. Carlson, *J. Chem. Soc., Chem. Commun.*, **1971**, 656.
43 H. Shanan-Atidi and K. H. Bar-Eli, *J. Phys. Chem.*, **1970**, *74*, 961.
44 J. E. Haky, J. E. Saavedra, and B. D. Hilton, *Org. Magn. Reson.*, **1983**, *21*, 79.
45 H. G. Bonacorso, M. S. B. Caro, N. Zanatta, M. A. P. Martins, and P. Fischer, *Quim. Nova*, **1992**, *15*, 208.

Chapter 2: Synthesis, characterisation and general properties of asymmetrically disubstituted *N*-alkyl-*N*-alkyl(aryl)-*N'*-acylthioureas

Summary

Asymmetrically disubstituted ligands of the type *N*,-alkyl-*N*-alkyl(aryl)-*N'*-acylthioureas R"C(O)NHC(S)NRR' were synthesised by a well established synthetic route. Systematic variations on these ligands were achieved by altering the R and R' groups of the (S)C-NRR' moiety. The double bond character of the C-N bond of the (S)C-NRR' moiety resulted in *E,Z* configurational isomerism in these ligands. This was easily observable by the doubling of the *N*-alkyl resonances in both ^{1}H and ^{13}C NMR spectra of these ligands. In some cases the isomerism was only observable at low temperature due to fast exchange at room temperature. In all the cases the distributions of the *E,Z* isomers were never equal. In one set of ligands the *Z* isomer was noted to be the major isomer while in the other the *E* was the major isomer. The *E* isomers of several of these ligands were isolated in solid state.

2.1 Introduction

To meet the aims of this thesis, in this chapter the synthesis of a wide range of asymmetrically disubstituted *N,N*-dialkyl-*N'*-acylthioureas is described, with systematic variations on the R and R' groups. This would hopefully allow an evaluation of factors that influence the isomer distributions of the *E,Z* configurational isomers of the ligands and the Pt(II) chelates derived from these ligands and that forms part of **chapters 4** and **5**. For the design of certain ligands with systematic variation it was also necessary to synthesise secondary amines, which were not commercially available. It is shown that for all the ligands the C-N bond restricted rotation result in *E,Z* configurational isomers and these isomers can easily be assigned. Some of the ligands synthesised here were suitable for multinuclear NMR assignments of the complexes resulting from them and these ligands and their complexes are discussed in **chapter 3**. Lastly, some properties of these ligands in solid state as well as in solution are discussed.

2.2 Synthesis and characterisation of asymmetrically disubstituted *N*-alkyl-*N*-alkyl(aryl)-*N'*-acylthioureas

Ligands of the type *N*-alkyl-*N*-alkyl(aryl)-*N'*-acyl(aroyl)thioureas are routinely synthesised via a two step, one pot synthesis using the Douglass and Dains method as shown in the reaction scheme 1 below.[1]

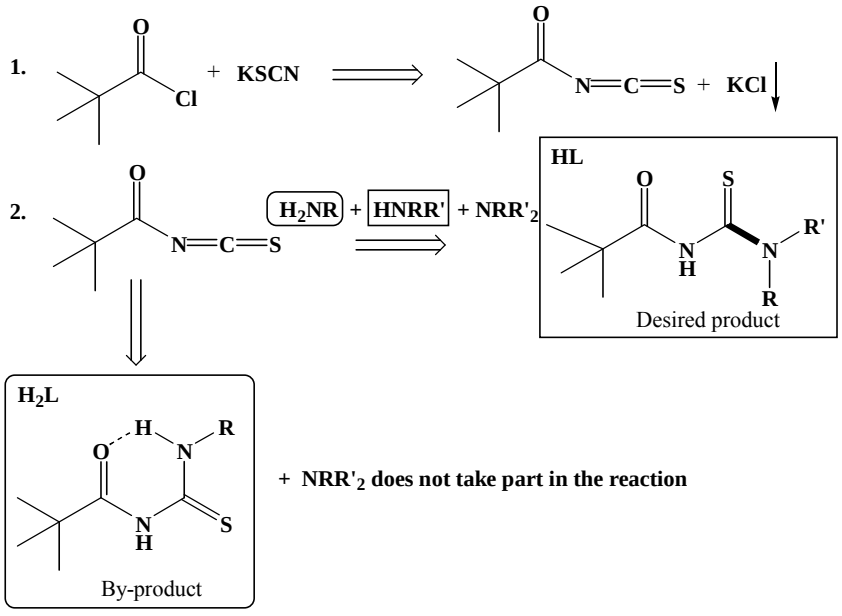

Reaction scheme 1 General synthesis of asymmetrically disubstituted *N*-alkyl-*N*-alkyl(aryl)-*N'*-acylthioureas. The desired product is obtained in pure form when a pure secondary amine is used in the second step of the reaction. The by-product H_2L is formed when primary amine is present in the second step.

All the reactions for the synthesis of the ligands were carried out under inert atmosphere (nitrogen gas). The acetone used as a solvent in the reactions was distilled over molecular sieves under inert atmosphere and the potassium thiocyanate was dried in a vacuum oven at 100 ºC. The typical method of synthesis was as follows: To an amount of about 0.03 moles of potassium thiocyanate dissolved in 75 ml of acetone an equimolar amount of acid chloride (also dissolved in anhydrous acetone) was added drop-wise while stirring. The mixture was refluxed for 45 minutes then allowed to cool to room temperature. An equimolar amount of secondary amine (also dissolved in 75 ml of anhydrous acetone) was added to the stirring mixture. This was heated to reflux for a further 45 minutes then the reaction mixture was allowed to cool to room temperature. The contents were then poured into about 100 ml of water and allowed to stand in the fume hood until all the acetone evaporated. The water has a dual purpose of dissolving the inorganic potassium chloride and precipitating out the desired organic product, which is the ligand. The product was then collected by filtration and washed several times with water. The crude product was then dried under vacuum before it was recrystallised from a water acetone mixture.

All the reagents used in the synthesis of *N,N*-diethyl-*N'*-benzoylthiourea, HL^4, *N*-benzyl-*N*-methyl-*N'-2,2*-dimethylpropanoylthiourea, HL^5, *N*-phenethyl-*N*-methyl-*N'-2,2*-dimethylpropanoylthiourea, HL^6, *N*-anthrocen-9-ylmethyl-*N*-methyl-*N*'-*2,2*-dimethylpropanoylthiourea, HL^7, *N*-(2-methylpyrrolidine)-*N*'-*2,2*-dimethylpropanoylthiourea, HL^8 were commercially available and were used as such.

Before the synthesis of the rest of the ligands ($HL^{1A,1B,1C,1D}$, $HL^{2A,2B,2C,2D}$ and $HL^{3A,3D}$), secondary amines were synthesised by direct alkylation of primary aromatic amine (aniline, 4-methoxyaniline and 4-nitroaniline) by an appropriate alkyl halide (R-X, R = Me, X = I; and R = isopropyl, cyclohexyl and n-butyl, X = Br). Out of the available synthetic routes for the synthesis of secondary amines shown in Scheme 1,[2] the synthetic route shown in bold was chosen.

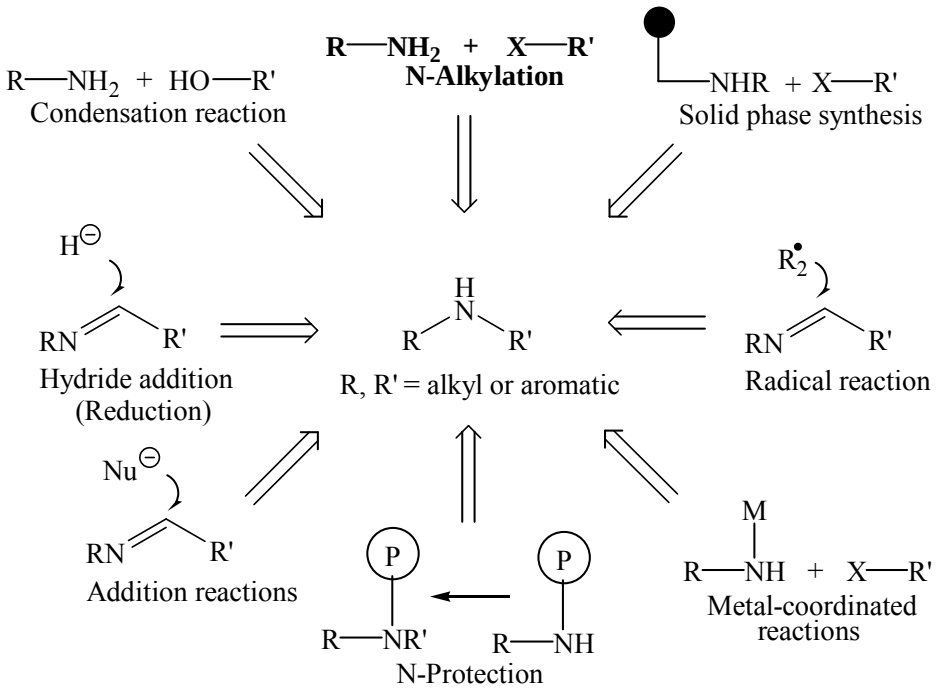

Scheme 1 Various synthetic routes that could be employed for synthesis of secondary amines. The alkylation of primary amines by an appropriate alkyl halide (marked in bold) is the chosen synthetic route.

The method of Srivastava *et al.*,[3] which was very successful for the direct alkylation of aniline and 4-flouroaniline with alkyl bromides of varying chain lengths was employed in our systems. The typical method of synthesis is as follows: To a stirred mixture of 0.04 moles of aniline in 1 ml dimethyl sulfoxide (DMSO) and equimolar amount of potassium carbonate, an equimolar amount of alkyl halide was added and stirred continuously at 80 ºC overnight. The filtrate was poured in water and extracted into chloroform. The extracts were washed with 10% brine solution and dried over sodium sulphate (Na_2SO_4). After evaporating the solvent, the crude product is filtered through a column (silica gel 70-230 mesh, 60 Å) with dichloromethane as an eluent. This proved to be rather inefficient due to formation of tertiary amines while leaving residual starting amines as well. This was particularly so for the methylation of 4-nitroaniline. The progress of the reaction was readily followed by means of TLC using 2% Ninhydrin in ethanol to visualise the developed plates. Ninhydrin is particularly suitable for the identification of primary, secondary and tertiary amines as they have distinct pink, yellow and orange colours, respectively. Due to the difficulty of separating the three amines *viz*: the residual primary amines, the desired secondary amines and the dialkylated tertiary amines, the syntheses of the ligands were carried out using the mixture of amines. With the tertiary amines not taking part in the reaction the primary amines leads to formation of *N*-monoalkyl-*N'*-acylthioureas (H_2L) and the secondary amines yield to the desired products (HL). The two types of ligands are easy to separate by means of column chromatography (silica gel 70-230 mesh, 60 Å) with dichloromethane as the eluent (Reaction scheme 1). The yields of these ligands were not reported since the composition of the primary, secondary

and tertiary amines was not determined and moreover due to losses incurred during the purification steps. However, the isolated amounts were sufficient for full characterisation as well as the synthesis of their platinum(II) complexes.

2.3 Experimental details

2.3.1 General remarks

All the elemental analyses of the ligands, HL, as well as the by-products, H_2L, were performed using a Carlo Erba EA 1108 elemental analyser from the University of Cape Town and showed sufficient purity of the compounds. Scheme 2 below shows the pictorial representation of the series of synthesised and fully characterised ligands and by-products with their abbreviations that are used throughout the thesis.

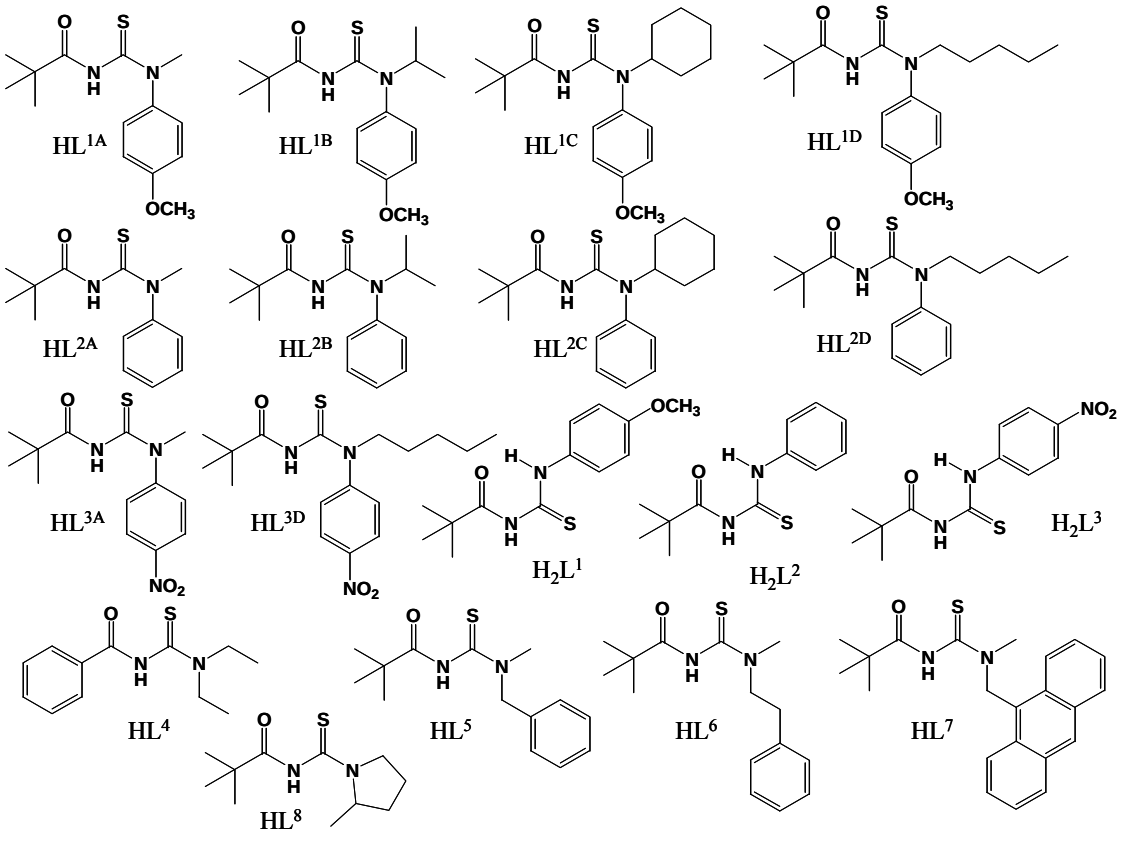

Scheme 2 Naming scheme of all the synthesised and fully characterised ligands and by-products

2.3.2 NMR spectroscopy

Conventional ^{1}H and ^{13}C NMR spectra of relatively high concentrations (*ca* 80 mg.cm^{-3}) of the ligands and H_2L using 5 mm diameter tubes were obtained at 298 K in deuterated chloroform using a Varian Inova 400 spectrometer operating at 400 and 101 MHz for ^{1}H and ^{13}C, respectively. For the set of ligands $HL^{1A,1B,1C,1D}$ and $HL^{2A,2B,2C,2D}$ their ^{1}H and ^{13}C NMR spectra were obtained at various temperatures. All samples were carefully filtered before any spectroscopic measurement was undertaken. ^{1}H chemical shifts are quoted relative to the residual $CHCl_3$ solvent resonance at 7.26 ppm and the ^{13}C chemical shifts are quoted relative to the $CDCl_3$ middle resonance of the triplet at 77.0 ppm. In the case where CD_2Cl_2 is used as the solvent, ^{1}H chemical shifts are quoted relative to the solvent triplet resonance at 5.31 ppm and the ^{13}C chemical shifts are quoted relative solvent quintet resonance at 55.8 ppm.

2.3.3 Synthetic methods and characterisation of compounds

_N_-Methyl-_N_-(4-methoxy-phenyl)-_N'_-(_2,2_-dimethylpropanoyl)thiourea, HL^{1A}

The desired product was isolated from the by-product H_2L^1 by means of column chromatography (silica gel, CH_2Cl_2). Crystals of HL^{1A} were obtained after recrystallisation from water-acetone solvent mixture and analysed. Found C, 60.04; H, 7.71; N, 10.06; S, 11.02. $C_{14}H_{20}N_2SO_2$ required C, 59.97; H, 7.19; N, 9.99; S, 11.44%. δ_H(400 MHz; solvent $CDCl_3$): 8.22 (1H, s, N-H(Z)), 7.95 (1H, s, N-H(E)), 7.23 (2H, d, C_6H_4(Z)), 7.14 (2H, d, C_6H_4(E)), 6.96 (2H, d, C_6H_4(Z)), 6.89 (2H, d, C_6H_4(E)), 3.81 (3H, s, O-CH_3(Z)), 3.80 (3H, s, O-CH_3(E)), 3.68 (3H, s, N-CH_3(E)), 3.40 (3H, s, N-CH_3(Z)), 1.29 (9H, s, 3CH_3(Z)), 0.88 (9H, s, 3CH_3(E)). δ_C(101 MHz, solvent $CDCl_3$): 182.26 (C(S))(Z), 179.35 (C(S))(E), 174.68 (C(O))(Z), 173.26 (C(O))(E), 158.55 – 114.14 (C_6H_4)(E and Z), 55.48 (O-CH_3)(E) 55.34 (O-CH_3)(Z), 45.41 (N-CH_3) (E and Z), 39.74 (C(=O)-$\underline{C}(CH_3)$)(Z), 39.58 (C(=O)-$\underline{C}(CH_3)$)(E), 26.94 (C(=O)-$\underline{C}(\underline{CH_3})$)(Z), 26.64 (C(=O)-$\underline{C}(\underline{CH_3})$)(E).

_N_-(4-Methoxy-phenyl)-_N'_-(_2,2_-dimethylpropanoyl)thiourea, H_2L^1

By-product separated from the synthesis of HL^{1A} by means of column chromatography (silica gel, CH_2Cl_2) and analysed. Found C, 58.49; H, 6.54; N, 10.38; S, 12.40. $C_{13}H_{18}N_2SO_2$ required C, 58.62; H, 6.81; N, 10.52; S, 12.04%. δ_H(400 MHz; solvent $CDCl_3$):12.29 (1H, s, N-H), 8.52 (1H, s, N-H), 7.50 (2H, d, C_6H_4), 6.90 (2H, d, C_6H_4), 3.79 (3H, s, O-CH_3), 1.29 (9H, s, C(=O)-$\underline{C}(\underline{CH_3})_3$). δ_C(101 MHz, solvent $CDCl_3$): 179.21 (C(S)), 178.62 (C(O)), 158.07 – 113.92 (C_6H_4), 55.32 (O-CH_3), 39.86 (C(=O)-$\underline{C}(CH_3)_3$), 26.86 (C(=O)-$\underline{C}(\underline{CH_3})_3$).

_N_-Isopropyl-_N_-(4-methoxy-phenyl)-_N'_-(_2,2_-dimethylpropanoyl)thiourea, HL^{1B}

HL^{1B} was recrystallised in water-acetone solvent mixture and analysed. Found C, 62.02; H, 7.47; N, 9.14; S, 10.83. $C_{16}H_{24}N_2SO_2$ required C, 62.30; H, 7.84; N, 9.08; S, 10.40%. δ_H(400 MHz; solvent $CDCl_3$): 8.88 (1H, s, N-H(Z)), 7.78 (1H, s, N-H(E)), 7.10 (2H, d, C_6H_4(Z)), 7.02 (2H, d, C_6H_4(E)), 6.95 (2H, d, C_6H_4(E)), 5.74 (1H, septet, N-$\underline{C}H(CH_3)_2$, 3.83 (3H, s, O-CH_3(E)), 1.10 (6H, d, N-CH(=O)-$\underline{C}(\underline{CH_3})_2$(E)), 0.82 (9H, s, C(=O)-$\underline{C}(\underline{CH_3})$(E)). δ_C(101 MHz, solvent

$CDCl_3$): 177.96 (C(S))(E), 174.20 (C(O))(E), 129.8 – 114.36 (C_6H_4)(E), 55.52 (O-CH_3)(E), 52.02 (N-$\underline{CH}(CH_3)_2$)(E), 39.87 ($\underline{C}(CH_3)$)(E), 26.52 (C($\underline{CH_3}$))(E), 20.26 (N-CH($\underline{CH_3}$)$_2$)(E).

_N_-Cyclohexyl-_N_-(4-methoxy-phenyl)-_N'_-(_2,2_-dimethylpropanoyl)thiourea, HL^{1C}

Crystals of HL^{1C} were obtained recrystallisation from water-acetone solvent mixture and analysed. Found C, 65.34; H, 10.55; N, 8.18; S, 11.56. $C_{19}H_{28}N_2SO_2$ required C, 65.48; H, 8.10; N, 8.04; S, 9.20%. δ_H(400 MHz; solvent $CDCl_3$): 7.87 (1H, s, N-H(Z)), 7.78 (1H, s, N-H(E)), 7.04 (2H, d, C_6H_4(Z)), 7.01 (2H, d, C_6H_4(E)), 6.95 (2H, d, C_6H_4(E)), 5.30 (1H, tt, N-$\underline{CH}(CH_2)_2(CH_2)_2CH_2$, 3.83 (3H, s, O-$CH_3$(E)), 1.82 (4H, dd, N-CH($\underline{CH_2}$)$_2$(CH_2)$_2CH_2$(E)), 1.38 (4H, m, N-CH(CH_2)$_2$($\underline{CH_2}$)$_2CH_2$(E)), 0.98 (2H, m, N-CH(CH_2)$_2$(CH_2)$_2\underline{CH_2}$(E)), 0.82 (9H, s, C($\underline{CH_3}$)$_3$. δ_C(101 MHz, solvent $CDCl_3$): 177.72 (C(S))(E), 174.19 (C(O))(E), 159.43 – 114.34 (C_6H_4)(E), 59.69 N-$\underline{CH}(CH_2)_2(CH_2)_2CH_2$(E), 55.52 (O-$CH_3$)(E), 39.90 ($\underline{C}(CH_3)$)(E), 30.50 (N-CH($\underline{CH_2}$)$_2$($CH_2$)$_2CH_2$)(E) 26.53 (C($\underline{CH_3}$))(E), 25.26 (N-CH($CH_2$)$_2$($\underline{CH_2}$)$_2CH_2$)(E), 24.96 (N-CH($CH_2$)$_2$($CH_2$)$_2\underline{CH_2}$)(E).

_N_-Pentyl-_N_-(4-methoxy-phenyl)-_N'_-(_2,2_-dimethylpropanoyl)thiourea, HL^{1D}

Crystals of HL^{1D} were obtained recrystallisation from water-acetone solvent mixture and analysed. Found C, 64.78; H, 9.12; N, 8.44; S, 9.27. $C_{18}H_{28}N_2SO_2$ required C, 64.25; H, 8.38; N, 8.33; S, 9.53%. δ_H(400 MHz; solvent $CDCl_3$): 8.10 (1H, s, N-H(Z)), 7.86 (1H, s, N-H(E)), 7.20 (2H, d, C_6H_4(Z)), 7.10 (2H, d, C_6H_4(E)), 6.94 (2H, d, C_6H_4(Z)), 6.90 (2H, d, C_6H_4(E)), 4.10 (2H, m, N-$\underline{CH_2}CH_2CH_2CH_2CH_3$)(E), 3.80 (3H, s, O-$CH_3$(E)), 1.65 (2H, m, N-$CH_2\underline{CH_2}CH_2CH_2CH_3$)(E), 1.23 (4H, m, N-$CH_2CH_2\underline{CH_2CH_2}CH_3$)(E), 0.85 (9H, s, C($\underline{CH_3}$)$_3$, 0.82 (3H, t, N-$CH_2CH_2CH_2\underline{CH_3}$)(E), δ_C(101 MHz, solvent $CDCl_3$): 178.72 (C(S))(E), 173.30 (C(O))(E), 158.57 – 114.14 (C_6H_4)(E), 56.57 N-$\underline{CH_2}CH_2CH_2CH_2CH_3$)(E), 55.48 (O-$CH_3$) 39.58 ($\underline{C}(CH_3)$)(E), 28.56 (N-$CH_2\underline{CH_2}CH_2CH_2CH_3$)(E), 26.61 (C($\underline{CH_3}$))(E), 25.55 (N-$CH_2CH_2\underline{CH_2}CH_2CH_3$)(E), 22.35 (N-$CH_2CH_2CH_2\underline{CH_2}CH_3$)(E), 14.07 (N-$CH_2CH_2CH_2CH_2\underline{CH_3}$)(E).

_N_-Methyl-_N_-phenyl-_N'_-(_2,2_-dimethylpropanoyl)thiourea, HL^{2A}

The desired product was isolated from the by-product H_2L^2 by means of column chromatography (silica gel, CH_2Cl_2). Crystals of HL^{2A} were obtained after recrystallisation from water-acetone solvent mixture and analysed. Found C, 62.81; H, 7.62; N, 11.33; S, 12.29. $C_{13}H_{18}N_2SO$ required C, 62.37; H, 7.25; N, 11.19; S, 12.81%. δ_H(400 MHz; solvent $CDCl_3$): 8.27 (1H, s, N-H)(Z), 7.96 (1H, s, N-H)(E), 7.29 (1H, t, C_6H_5)(E), 7.36 (2H, t, C_6H_5)(E), 7.22 (2H, d, C_6H_5)(E), 3.72 (3H, s, N-CH_3)(E), 3.43 (3H, s, N-CH_3)(Z), 1.30 (9H, s, C($\underline{CH_3}$)$_3$)(Z), 0.85 (9H, s, C($\underline{CH_3}$)$_3$)(E). δ_C(101 MHz, solvent $CDCl_3$): 182.07 (C(S))(Z), 179.68 (C(S))(E), 174.72 (C(O))(Z), 173.06 (C(O))(E), 146.09 – 127.22 (C_6H_4)(E and Z), 45.47 (N-CH_3)(E), 45.20 (N-CH_3)(Z), 39.75 ($\underline{C}(CH_3)_3$)(Z), 39.44 ($\underline{C}(CH_3)_3$)(E), 26.94 (C($\underline{CH_3}$)$_3$)(Z), 26.53 (C($\underline{CH_3}$)$_3$)(E).

_N_-Phenyl-_N'_-(_2,2_-dimethylpropanoyl)thiourea, H_2L^2

By-product separated from the synthesis of HL^{2A} by means of column chromatography (silica gel, CH_2Cl_2) and analysed. Found C, 61.10; H, 7.02; N, 11.92; S, 12.94. $C_{12}H_{16}N_2SO$ required C, 60.98; H, 6.82; N, 11.85; S, 13.57%.

δ_H(400 MHz; solvent $CDCl_3$):12.49 (1H, s, N-H), 8.54 (1H, s, N-H), 7.66 (2H, d, C_6H_5), 7.39 (2H, tt, C_6H_5), 7.26 (1H, tt, C_6H_5) 1.31 (9H, s, C($\underline{CH_3}$)$_3$). δ_C(101 MHz, solvent $CDCl_3$): 179.28 (C(S)), 178.38 (C(O)), 137.51 – 123.89 (C_6H_5), 39.31 ($\underline{C}(CH_3)_3$), 26.88 (C($\underline{CH_3}$)$_3$).

_N_-isoPropyl-_N_-phenyl-_N'_-(_2,2_-dimethylpropanoyl)thiourea, HL^{2B}

HL^{2B} was recrystallised in water-acetone solvent mixture and analysed. Found C, 64.74; H, 8.57; N, 10.17; S, 11.10. $C_{15}H_{22}N_2SO$ required C, 64.71; H, 7.96; N, 10.06; S, 11.52%. δ_H(400 MHz; solvent $CDCl_3$): 7.89 (1H, s, N-H(Z)), 7.68 (1H, s, N-H(E)), 7.45 (3H, m, C_6H_4(E and Z)), 7.12 (2H, d, C_6H_4(E)), 7.01 (2H, d, C_6H_4(Z)), 5.74 (1H, septet, N-$\underline{CH}(CH_3)_2$, 1.12 (6H, d, N-CH($\underline{CH_3}$)$_2$(E)), 0.82 (9H, s, C($\underline{CH_3}$)(Z)), 0.77 (9H, s, C($\underline{CH_3}$)(E)). δ_C(101 MHz, solvent $CDCl_3$): 178.02 (C(S))(E), 174.12 (C(O))(E), 137.31 – 128.67 (C_6H_4)(E), 52.42 (N-$\underline{CH}(CH_3)_2$)(E), 39.73 ($\underline{C}(CH_3)$)(E), 26.39 (C($\underline{CH_3}$))(E), 20.30 (N-CH($\underline{CH_3}$)$_2$)(E).

_N_-cycloHexyl-_N_-phenyl-_N'_-(_2,2_-dimethylpropanoyl)thiourea, HL^{2C}

HL^{2C} was recrystallised in water-acetone solvent mixture and analysed. Found C, 68.35; H, 8.76; N, 8.91; S, 9.55. $C_{18}H_{26}N_2SO$ required C, 67.88; H, 8.23; N, 8.80; S, 10.07%. δ_H(400 MHz; solvent $CDCl_3$): 7.88 (1H, s, N-H(Z)), 7.66 (1H, s, N-H(E)), 7.45 (3H, m, C_6H_4(E and Z)), 7.10 (2H, dd, C_6H_4(E)), 5.30 (1H, tt, N-$\underline{CH}(CH_2)_2(CH_2)_2CH_2$, 1.84 (4H, dd, N-CH($\underline{CH_2}$)$_2$($CH_2$)$_2CH_2$(E)), 1.38 (4H, m, N-CH($CH_2$)$_2$($\underline{CH_2}$)$_2CH_2$(E)), 0.98 (2H, m, N-CH($CH_2$)$_2$($CH_2$)$_2\underline{CH_2}$(E)), 0.77 (9H, s, C($\underline{CH_3}$)$_3$. δ_C(101 MHz, solvent $CDCl_3$): 177.74 (C(S))(E), 174.11 (C(O))(E), 137.96 – 128.61 (C_6H_4)(E), 60.04 N-$\underline{CH}(CH_2)_2(CH_2)_2CH_2$(E), 39.77 ($\underline{C}(CH_3)$)(E), 30.52 (N-CH($\underline{CH_2}$)$_2$($CH_2$)$_2CH_2$)(E) 26.40 (C($\underline{CH_3}$))(E), 25.28 (N-CH($CH_2$)$_2$($\underline{CH_2}$)$_2CH_2$)(E), 24.92 (N-CH($CH_2$)$_2$($CH_2$)$_2\underline{CH_2}$)(E).

_N_-Pentyl-_N_-phenyl-_N'_-(_2,2_-dimethylpropanoyl)thiourea, HL^{2D}

HL^{2D} was recrystallised in water-acetone solvent mixture and analysed. Found C, 66.37; H, 8.57; N, 9.07; S, 9.96. $C_{17}H_{26}N_2SO$ required C, 66.62; H, 8.53; N, 9.14; S, 10.42%. δ_H(400 MHz; solvent $CDCl_3$): 7.83 (1H, s, N-H(E)), 7.39 (2H, t, C_6H_4(E)), 7.31 (1H, tt, C_6H_4(E)), 7.19 (2H, d, C_6H_4(E)), 4.14 (2H, m, N-$\underline{CH_2}CH_2CH_2CH_2CH_3$)(E), 1.67 (2H, m, N-$CH_2\underline{CH_2}CH_2CH_2CH_3$)(E), 1.25 (4H, m, N-$CH_2CH_2\underline{CH_2}\underline{CH_2}CH_3$)(E), 0.83 (9H, s, C($\underline{CH_3}$)$_3$, 0.81 (3H, t, N-$CH_2CH_2CH_2CH_2\underline{CH_3}$)(E), δ_C(101 MHz, solvent $CDCl_3$): 179.01 (C(S))(E), 173.10 (C(O))(E), 142.57 – 126.19 (C_6H_4)(E), 56.81 N-$\underline{CH_2}CH_2CH_2CH_2CH_3$)(E), 39.46 ($\underline{C}(CH_3)$)(E), 28.57 (N-$CH_2\underline{CH_2}CH_2CH_2CH_3$)(E), 26.51 (C($\underline{CH_3}$))(E), 25.56 (N-$CH_2CH_2\underline{CH_2}CH_2CH_3$)(E), 22.34 (N-$CH_2CH_2CH_2\underline{CH_2}CH_3$)(E), 14.08 (N-$CH_2CH_2CH_2CH_2\underline{CH_3}$)(E).

_N_-Methyl-_N_-(4-nitro-phenyl)-_N'_-(_2,2_-dimethylpropanoyl)thiourea, HL^{3A}

The desired product was isolated from the by-product H_2L^3 by means of column chromatography (silica gel, CH_2Cl_2). Found C, 53.13; H, 6.24; N, 14.24; S, 9.57. $C_{13}H_{17}N_3SO_3$ required C, 52.86; H, 5.80; N, 14.23; S, 10.86%. δ_H(400 MHz; solvent CD_2Cl_2): 8.40 (1H, s, N-H(E)), 8.18 (2H, d, C_6H_4(E)), 7.40 (2H, d, C_6H_4(E)), 3.70 (3H, s, N-CH_3(E)), 0.80 (9H, s, 3CH_3(E)). δ_C(101 MHz, solvent CD_2Cl_2): 180.78 (C(S))(E), 172.44 (C(O))(E), 150.45 – 124.02 (C_6H_4)(E), 46.09 (N-CH_3) (E), 39.07 ($\underline{C}(CH_3)$)(E), 26.09 (C($\underline{CH_3}$))(E).

_N_-(4-Nitro-phenyl)-_N'_-(_2,2_-dimethylpropanoyl)thiourea, H_2L^3

By-product separated from the synthesis of HL^{3A} by means of column chromatography (silica gel, CH_2Cl_2) and analysed. Found C, 51.41; H, 5.69; N, 14.90; S, 10.73. $C_{12}H_{15}N_3SO_3$ required C, 51.23; H, 5.37; N, 14.94; S, 11.40%. δ_H(400 MHz; solvent $CDCl_3$):12.98 (1H, s, N-H), 8.60 (1H, s, N-H), 8.24 (2H, d, C_6H_4), 7.99 (2H, d, C_6H_4), 1.32 (9H, s, C($\underline{CH_3}$)$_3$). δ_C(101 MHz, solvent $CDCl_3$): 179.76 (C(S)), 178.26 (C(O)), 145.02 – 122.95 (C_6H_4), 40.08 ($\underline{C}(CH_3)_3$), 26.85 (C($\underline{CH_3}$)$_3$).

_N_-Pentyl-_N_-(4-nitro-phenyl)-_N'_-(_2,2_-dimethylpropanoyl)thiourea, HL^{3D}

Found C, 58.16; H, 7.95; N, 11.92; S, 10.12. $C_{17}H_{25}N_3SO_3$ required C, 58.09; H, 7.17; N, 11.96; S, 9.12%. δ_H(400 MHz; solvent $CDCl_3$): 8.20 (2H, d, C_6H_4(E)), 7.93 (1H, s, N-H(E)), 7.39 (2H, d, C_6H_4(E)), 4.17 (2H, m, N-$\underline{CH_2}CH_2CH_2CH_2CH_3$)(E), 1.71 (2H, m, N-$CH_2\underline{CH_2}CH_2CH_2CH_3$)(E), 1.29 (4H, m, N-$CH_2CH_2\underline{CH_2}\underline{CH_2}CH_3$)(E), 0.93 (9H, s, C($\underline{CH_3}$)$_3$, 0.85 (3H, t, N-$CH_2CH_2CH_2CH_2\underline{CH_3}$)(E), δ_C(101 MHz, solvent $CDCl_3$): 181.28 (C(S))(E), 172.52 (C(O))(E), 149.75 – 124.07 (C_6H_4)(E), 57.74 N-$\underline{CH_2}CH_2CH_2CH_2CH_3$)(E), 39.34 ($\underline{C}(CH_3)$)(E), 28.70 (N-$CH_2\underline{CH_2}CH_2CH_2CH_3$)(E), 26.62 (C($\underline{CH_3}$))(E), 26.11 (N-$CH_2CH_2\underline{CH_2}CH_2CH_3$)(E), 22.16 (N-$CH_2CH_2CH_2\underline{CH_2}CH_3$)(E), 13.84 (N-$CH_2CH_2CH_2CH_2\underline{CH_3}$)(E).

_N,N_-Diethyl-_N'_-benzoylthiourea {_ca_ 50% ^{13}C enriched at C(S)}, HL^4

A yield of 73% was collected and analysed. Found C, 60.91; H, 6.81; N, 11.79; S, 13.34. $C_{12}H_{16}N_2SO$ required C, 60.98; H, 6.82; N, 11.85; S, 13.57%. δ_H(400 MHz; solvent $CDCl_3$): 8.52 (1H, s, N-H), 7.81 (2H, d, C_6H_5), 7.54 (1H, tt, C_6H_5), 7.34 (2H, tt, C_6H_5), 3.99 (2H, s(br), N-$\underline{CH_2}CH_3$), 3.58 (2H, s(br), N-$\underline{CH_2}CH_3$), 1.34 (3H, t, N-$CH_2\underline{CH_3}$), 1.27 (3H, t, N-$CH_2\underline{CH_3}$). δ_C(101 MHz, solvent $CDCl_3$): 179.27 (C(S)), 163.76 (C(O)), 132.74-127.77 (C_6H_5), 47.81 (N-$\underline{CH_2}CH_3$), 47.57 (N-$\underline{CH_2}CH_3$), 13.15 (N-$CH_2\underline{CH_3}$), 11.39 (N-$CH_2\underline{CH_3}$).

_N_-Benzyl-_N_-methyl-_N'-2,2_-dimethylpropanoylthiourea, HL^5

A yield of 74% was collected and analysed. Found C, 65.24; H, 8.38; N, 10.23; S, 11.17. $C_{14}H_{20}N_2SO$ required C, 63.60; H, 7.62; N, 10.60; S, 12.13%. δ_H(400 MHz; solvent $CDCl_3$): 7.98 (1H, s, N-H(Z)), 7.94 (1H, s, N-H(E)), 7.39-7.16 (5H, m, C_6H_5(E and Z)), 5.21 (2H, s, N-CH_2(E)), 4.62 (2H, s, N-CH_2(Z)), 3.23 (3H, s, N-CH_3(Z)), 3.03 (3H, s, N-CH_3(E)), 1.27 (9H, s, C($\underline{CH_3}$)$_3$(E and Z)). δ_C(101 MHz, solvent $CDCl_3$): 181.64 (C(S))(E), 180.76 (C(S)(Z), 174.80 (C(CO))(Z), 174.48(C(CO))(E), 135.21-127.68 (C_6H_5)(E and Z), 59.57 (N-CH_2(E)), 59.03 (N-CH_2(Z)), 42.00 (N-CH_3(Z)),40.07 (N-CH_3(E)), 39.68 ($\underline{C}(CH_3)_3$(E and Z)), 27.05 (C($\underline{CH_3}$)$_3$(E and Z)).

_N_-Phenethyl-_N_-methyl-_N'-2,2_-dimethylpropanoylthiourea, HL^6

A yield of 88% was collected and analysed. Found C, 64.23; H, 7.65; N, 10.74; S, 11.75. $C_{15}H_{22}N_2SO$ required C, 64.71; H, 7.96; N, 10.06; S, 11.52%. δ_H(400 MHz; solvent $CDCl_3$): 7.85 (1H, s, N-H(Z)), 7.52 (1H, s, N-H(E)), 7.29-7.13 (5H, m, C_6H_5(E and Z)), 4.06 (2H, t, N-CH_2(E)), 3.65 (2H, t, N-CH_2(Z)), 3.43 (3H, s, N-CH_3(Z)), 3.09 (2H, t, N-CH_2(E)), 3.08 (3H, s, N-CH_3(E)), 2.93 (2H, t, N-CH_2(E)), 1.26 (9H, s, C($\underline{CH_3}$)$_3$(E)), 1.19 (9H, s, C($\underline{CH_3}$)$_3$(Z)). δ_C(101 MHz, solvent $CDCl_3$): 180.49 (C(S))(Z), 180.17 (C(S)(E), 174.39 (C(CO))(E and Z), 138.15-126.49 (C_6H_5)(E

and Z), 57.96 (N-$\underline{CH_2}CH_2Ph$(E)), 56.99 (N-$\underline{CH_2}CH_2Ph$(Z)), 42.07 (N-CH_3)(Z), 41.07 (N-CH_3(E)), 39.60 ($\underline{C}(CH_3)_3$(E)), 39.45 ($\underline{C}(CH_3)_3$(Z)), 34.10 (N-$CH_2\underline{CH_2}Ph$(E)), 31.88 (N-$CH_2\underline{CH_2}Ph$(Z)), 27.03 (C($\underline{CH_3}$)$_3$(E)), 26.94 (C($\underline{CH_3}$)$_3$(Z)).

_N_-Anthrocen-9-ylmethyl-_N_-methyl-_N'_-_2,2_-dimethylpropanoylthiourea, HL[7]

A yield of 95% was collected and analysed. Found C, 72.34; H, 6.71; N, 7.48; S, 7.85. $C_{22}H_{24}N_2SO$ required C, 72.49; H, 6.64; N, 7.69; S, 8.80%. δ_H(400 MHz; solvent $CDCl_3$): 8.81 (1H, s, N-H(E)), 8.40 (1H, s, N-H(Z)), 8.35-7.35 (9H, ($C_{14}H_9$)(E and Z)) 6.09 (2H, s, N-CH_2- (E)), 5.64 (2H, s, N-CH_2- (Z)), 2.98 (3H, s, N-CH_3 (Z)), 2.65 (3H, s, N-CH_3 (E)), 1.38 (9H, s, C($\underline{CH_3}$)$_3$ (Z)), 1.25 (9H, s, C($\underline{CH_3}$)$_3$ (E)). δ_C(101 MHz, solvent $CDCl_3$): 181.00 (C(S))(E), 180.85, (C(S))(Z), 175.55 (C(O))(Z), 174.52 (C(O))(E), 134.55-123.02 ($C_{14}H_9$)(E and Z), 51.98 (N-CH_2-)(E), 50.55 (N-CH_2-)(Z), 40.02 (N-CH_3)(Z), 39.97 ($\underline{C}(CH_3)_3$)(E) and Z), 38.51 (N-CH_3)(E), 27.22 (C($\underline{CH_3}$)$_3$) (Z), 27.20 (C($\underline{CH_3}$)$_3$) (E).

_N_-(2-Methylpyrrolidine)-_N'_-_2,2_-dimethylpropanoylthiourea, HL[8]

A yield of 95% was collected and analysed. Found C, 58.45; H, 9.14; N, 12.30; S, 13.85. $C_{11}H_{20}N_2SO$ required C, 57.86; H, 8.83; N, 12.27; S, 14.04%. δ_H(400 MHz; solvent $CDCl_3$): 7.82 (1H, s, N-H(E)), 4.61 (1H, ses, N-$\underline{CH}(CH_3)CH_2$-)(E)), 4.21 (1H, ses, N-$\underline{CH}(CH_3)CH_2$-)(Z)), 3.83 (2H, m, N-$\underline{CH_2}CH_2$-)(E), 3.49 (2H, m, N-$\underline{CH_2}CH_2$-)(Z), 2.16 (2H, m, N-$CH_2\underline{CH_2}$-)(E), 1.90 (2H, m, N-$CH_2\underline{CH_2}$-)(Z), 1.76 (2H, m, CH(CH_3)$\underline{CH_2}$-)(E)), 1.62 (2H, m, CH(CH_3)$\underline{CH_2}$-)(Z)), 1.34 (3H, d, CH($\underline{CH_3}$)CH_2-)(Z)), 1.13 (3H, d, CH($\underline{CH_3}$)CH_2-)(E)), 1.18 (9H, s, C($\underline{CH_3}$)$_3$)(Z and E). δ_C(101 MHz, solvent $CDCl_3$): 176.79 (C(S))(Z), 176.64, (C(S))(E), 174.72 (C(O))(Z), 174.60 (C(O))(E), 60.12 (N-$\underline{CH}(CH_3)CH_2$-)(E), 58.71 (N-$\underline{CH}(CH_3)CH_2$-)(Z), 54.74 (N-$\underline{CH_2}CH_2$-)(Z), 52.45 (N-$\underline{CH_2}CH_2$-)(E), 39.42 ($\underline{C}(CH_3)_3$)(E and Z), 33.60 (N-CH(CH_3)$\underline{CH_2}$-)(Z), 32.17 (N-CH(CH_3)$\underline{CH_2}$-)(E), 26.87 (C($\underline{CH_3}$)$_3$)(E and Z), 24.11 (N-$CH_2\underline{CH_2}$-)(E), 21.98 (N-$CH_2\underline{CH_2}$-)(Z), 19.02 (N-CH($\underline{CH_3}$)CH_2-)(Z), 17.91 (N-CH($\underline{CH_3}$)CH_2-)(Z).

2.3.4 Crystallography and structure refinement

Suitable crystals of ligands $HL^{1A,1C,1D}$, HL^{2A}, H_2L and HL^7 were obtained by recrystallisation of these compounds in a water/acetone mixed solvent system. Methyl-(4-nitro-phenyl)-amine is a decomposition fragment that crystallised in a recrystalisation vessel of HL^{3A}. The data for crystal and molecular structure determination of HL^{2A} were collected on a Nonius Kappa CCD diffractometer using 1.5 kW graphite-monochromater Mo-Kα radiation (λ = 0.7107 Å) at 173(2) K. For all the other compounds the data were collected on a Brucker SMART Apex diffractomer also using a graphite-monochromater Mo-Kα radiation (λ = 0.7107 Å) at 100(2) K. The structure was solved using SHELX-97 and refined using SHELXL-97[4] with the aid of the interface program X-SEED.[5] All non-hydrogen atoms were modelled anisotropically. Hydrogen atoms were placed in geometrically calculated positions, with C-H = 0.99 (for -CH_2-), 0.98 (for -CH_3), or 0.95 Å (for phenyl). Hydrogen atoms were placed in geometrically calculated positions and the N-H hydrogen in HL^{1A} was obtained from difference Fourier maps. The relevant crystallographic data is shown in Tables 2.1 and 2.2 and selected bond lengths are shown in Table 2.3.

2.4 Results and Discussion

2.4.1 Molecular structures of isolated unsymmetrical N-alkyl-N-aryl-N'-acylthioureas.

All the ligands shown here were crystallised from water/acetone solvent system. In an attempt to crystallise *N*-methyl-*N*-(4-nitro-phenyl)-*N'-2,2*-dimethylpropanoylthiourea, HL^{3A} in the same manner only a fragment of the starting methyl-(4-nitro-phenyl)-amine was isolated. This was as a result of decomposition of the HL^{3A} ligand in solution. The ^{1}H and ^{13}C NMR spectra of a fresh solution of HL^{3A} showed no presence of the isolated compound, however, after a few days peaks due to this amine appeared and increased in intensity at the expense of the peaks of HL^{3A}. The crystallographic data of all the isolated compounds is shown in Tables 2.1 and 2.2 and Figures 2.1, 2.2 and 2.3 show the molecular structures of the ligands, showing their atomic numbering system. Relevant bond lengths and angles are shown in Table 2.3.

Table 2.1 Crystallographic data of the isolated ligands *N*-alkyl-*N*-aryl-*N'*-acylthioureas, HL^{1A}, HL^{1C} and HL^{1D}.

Compound	HL^{1A}	HL^{1C}	HL^{1D}
Molecular formula	$C_{14}H_{20}N_2O_2S_1$	$C_{19}H_{27}N_2O_2S_1$	$C_{18}H_{28}N_2O_2S_1$
Formula weight/g.mol^{-1}	280.38	347.49	336.48
Crystal system	Monoclinic	Monoclinic	Monoclinic
Space group	C2/c	P2(1)/c	C2/c
a/Å	26.146(4)	12.2859(12)	29.296(3)
b/Å	7.5750(13)	9.3039(9)	9.6257(10)
c/Å	17.819(3)	16.4290(15)	28.334(3)
α/°	90.00	90.00	90.00
β/°	123.495(3)	99.137(2)	102.784(2)
γ/°	90.000	90.00	90.00
V/Å^3	2943.1(9)	1854.1(3)	7792.2(1)
Z	8	4	16
Calculated density/g.cm^{-3}	1.266	1.245	1.147
μ/mm^{-1}	0.22	0.188	0.177
F(000)	1200	748	2912
θ Range scanned/°	1.87 – 28.31	1.68 – 28.28	1.81 – 28.28
Reflections collected/unique	3404/2457	4292/3204	9010/5941
Goodness of fit on F^2	0.962	1.035	1.019
Final R indices [I > 2σI]	R1 = 0.0644	R1 = 0.0665	R1 = 0.0659
R indices [all data]	wR2 = 0.0941	wR2 = 0.0944	wR2 = 0.1053,
Largest difference peak and hole/e Å^{-3}	0.40/-0.41	0.430/-0.309	0.397/-0.283

Table 2.2 Crystallographic data for the isolated ligands HL^{2A} and HL^{7}. The by-product, H_2L^{2}, resulting from the synthesis of HL^{2A} is also listed together with the decomposition fragment (methyl-(4-nitro-phenyl)-amine) resulting from recrystallisation of HL^{3A}.

Compound	HL^{2A}	H_2L^{2}	HL^{7}	Methyl-(4-nitro-phenyl)-amine
Molecular formula	$C_{13}H_{18}N_2S_1O_1$	$C_{12}H_{16}N_2O_1S_1$	$C_{22}H_{24}N_2O_1S_1$	$C_7H_8N_2O_2$
Formula weight/g.mol^{-1}	250.35	236.33	364.49	152.15
Crystal system	Orthorhombic	Monoclinic	Triclinic	Monoclinic
Space group	P2(1)2(1)2(1)	P2(1)/c	P-1	P2(1)/n
a/Å	16.4683(1)	10.8166(14)	12.3683(9)	9.9277(10)
b/Å	9.5803(2)	6.3696(8)	17.1448(12)	6.8418(7)
c/Å	17.4589(2)	18.397(2)	18.4128(13)	10.7476(11)
α/°	90.00	90.00	94.124(1)	90.00
β/°	90.00	104.375(2)	90.907(1)	103.732(2)
γ/°	90.00	90.00	103.730(1)	90.00
V/Å^3	2754.51(7)	1227.8(3)	3708.9(5)	709.15(13)
Z	9	4	8	4
Calculated density/g.cm^{-3}	1.358	1.278	1.281	1.425
μ/mm^{-1}	0.25	0.245	0.184	0.107
F(000)	1206	504	1552	320
θ Range scanned/°	1.70 - 27.10	1.94 – 28.24	1.11 – 28.28	2.51 – 28.21
Reflections collected/unique	6058/5293	2837/2306	17338/10335	1664/1451
Goodness of fit on F^2	1.619	0.963	0.932	1.068
Final R indices [I > 2σI]	R1 = 0.0627	R1 = 0.0455	R1 = 0.0561	R1 = 0.0472
R indices [all data]	wR2 = 0.0772	wR2 = 0.0584	wR2 = 0.0994	wR2 = 0.0547
Largest difference peak and hole/e Å^{-3}	1.304/-0.214	0.429/-0.241	0.636/-0.625	0.429/-0.265

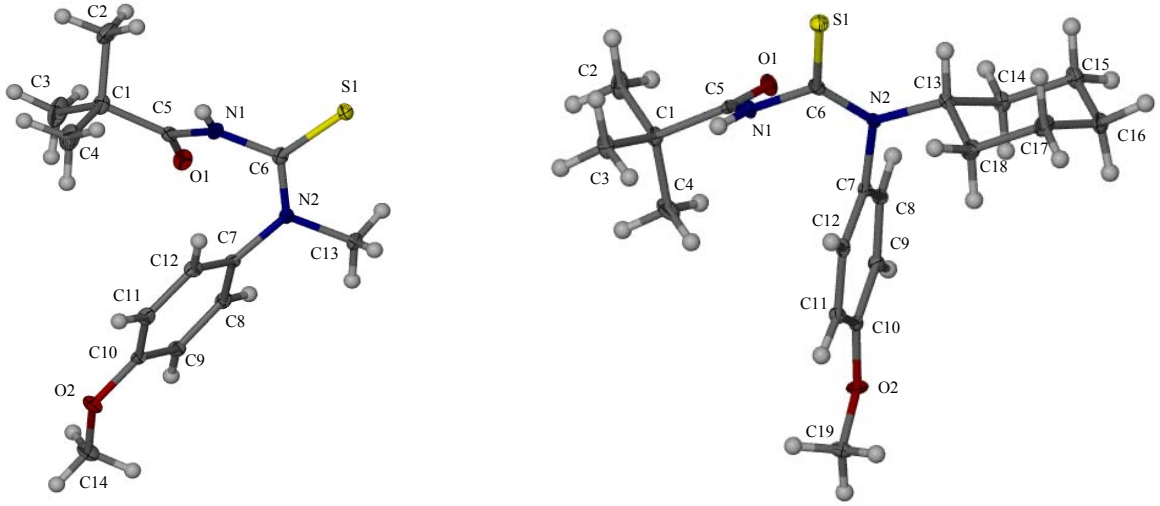

Figure 2.1 The molecular structure of **HL^{1A}** and **HL^{1C}** with atomic numbering scheme. Displacement ellipsoids are drawn at the 50% probability level. The hydrogen atoms have been placed in geometrically calculated positions.

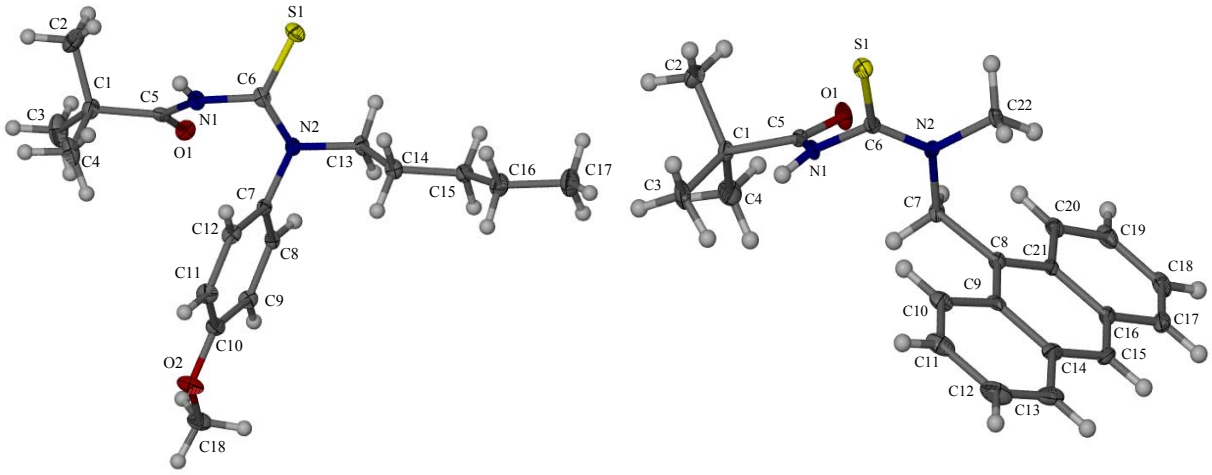

Figure 2.2 The molecular structure of **HL^{1D}** and **HL^{7}** with atomic numbering scheme. Displacement ellipsoids are drawn at the 50% probability level. The hydrogen atoms have been placed in geometrically calculated positions.

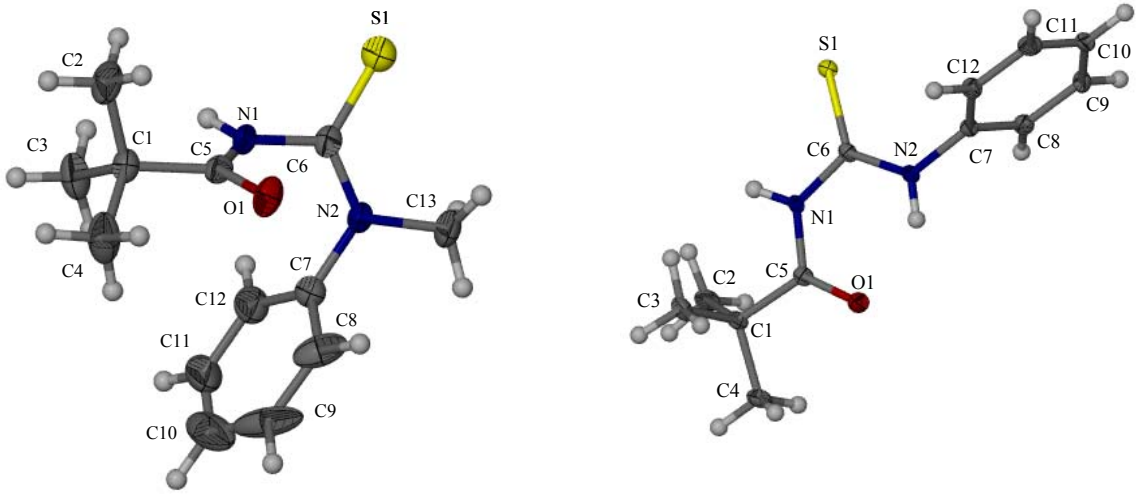

Figure 2.3 The molecular structure of **HL^{2A}** in the *E* configuration and its by-product **H$_2$L^{2}** in the *Z* configuration, with atomic numbering scheme. Displacement ellipsoids are drawn at the 50% probability level. The hydrogen atoms have been placed in geometrically calculated positions

All the ligands isolated have the *E* stereochemistry in that the large *N*-alkyl (for HL^{7}) and *N*-aryl (HL^{1A,1C,1D} and HL^{2A}) are opposite the sulphur atom. The exception to this observation is H$_2$L^{2}, which is slightly different from the other ligands and the reasons for this to be so will be clarified shortly. In the crystal structure this ligand adopts a conformation in which the carbonyl group and thiocarbonyl group do not lie in the same plane, but are approximately

opposite in direction. The hydrogen bonding between the carbonyl oxygen and the N-H hydrogen in the mono alkyl substituted ligand H_2L^2 further enhances this conformation (see Reaction scheme 1).

All the bonds in Table 3 are within the expected range and are similar to other thioureas.[6-8] Of interest is when we compare the **N2-C6** bond lengths it is noticed that this bond is the shortest of the C-N bonds and it is also significantly shorter than a carbon-nitrogen single bond of 1.472(5) Å (source: CRC Handbook of Chemistry and Physics 64th Ed, 1983, Lide D. R. Ed in Chief, CRC Press Inc. Boca Raton Florida 1983). The partial double bond character of this particular C-N bond in principle results in *E,Z* configurational isomers. In solid state however only the *E* isomers were isolated while in solution both the *E* and *Z* isomers exist in varying distributions depending on the ligand. In this chapter it is shown that both isomers exist in solution with the *Z* or the *E* being favoured depending on the type of ligand in question and that these isomers can systematically assigned.

Table 2.3 Comparison of selected bond lengths (Å) for $HL^{1A,1C,1D}$, HL^{2A}, HL^7 and H_2L^2.

Bond length	HL^{1A}	HL^{1C}	HL^{1D}	HL^{2A}	HL^7	H_2L^2
S1-C6	1.675(3)	1.674(3)	1.678(2)	1.661(3)	1.673(2)	1.6736(17)
O1-C5	1.209(3)	1.210(3)	1.213(3)	1.229(4)	1.219(2)	1.219(2)
N2-C6	1.343(3)	1.338(3)	1.332(3)	1.340(4)	1.329(3)	1.330(2)
N1-C6	1.396(3)	1.407(3)	1.404(3)	1.413(4)	1.404(3)	1.394(2)
N1-C5	1.395(3)	1.386(3)	1.367(3)	1.370(4)	1.383(3)	1.384(2)

From Table 2.3 it is noted that in all the ligands the bond lengths of carbon-nitrogen bonds are in the order: N1-C6 > N1-C5 > N2-C6. As mentioned earlier the relative shortness of N2-C6 results in *E,Z* configurational isomers, which are manifested by magnetic inequivalence of the *N*-alkyl moieties in the ^1H and ^{13}C NMR spectra of these ligands. In the series of ligands that has been isolated it can be noted that HL^7 (with only alkyl groups on the *N*-(alkyl)(alkyl) moiety) has the shortest of all the N2-C6 bonds with 1.329(3) Å. The ligands with *N*-(alkyl)(*para*-Ph) groups have the N2-C6 bond in the range [1.332(3) – 1.343(3) Å] which is much sorter than 1.329(3) Å. The differences in the N2-C6 bond lengths are a qualitative measure of the bond strength or ease of rotation around this bond. This has remarkable consequences with reference to the temperature at the *E,Z* isomerism is observable by ^1H and ^{13}C NMR of these ligands and this is discussed in the next section.

2.4.2 E,Z configurational isomerism in asymmetrically disubstituted N-alkyl-alkyl(aryl)-N'-acylthioureas: A solution NMR study.

The ligands have been classified into two separate categories, those for which *E,Z* isomerism is observable at room temperature (298 K) in solution, and those that necessitate lowering the temperature of the sample to observe the isomerism.

2.4.2.1 E,Z isomerism observed at room temperature for symmetrically disubstituted N-alkyl-N-alkyl(aryl)-N'-acylthioureas ligands HL[5], HL[6], HL[7] and HL[8]

At room temperature (298 K) ligands HL^5, HL^6, HL^7 and HL^8 readily display *E,Z* configurational isomerism in solution and this is evident from both their ^1H and ^{13}C NMR spectra. In Figure 2.4 sections of their ^1H NMR spectra illustrate the isomerism as for each ligand for the *N*-alkyl groups R and R' appear in two distinct resonances for *E* and *Z* isomers. In all the cases the *Z* isomer (with larger *N*-alkyl group coplanar with the sulphur atom of the thiocarbonyl group) is favoured. This assignment of the peaks is based on the expected magnetic anisotropy of the adjacent thiocarbonyl group, which is likely to deshield the closest nuclei coplanar to it, as has been observed for compounds with a thione group as well as thioamides derivatives.[9,10] As an example, in compounds HL^5, HL^6 and HL^7 the singlet resonances due to the *N*-CH_3 groups of the *E* isomers are relatively downfield (due to the above mentioned deshielding effect) to the *N*-CH_3 groups of the *Z* isomers and are the minor component. This is consistent with the chemical shift trends of the respective resonances of the *N*-CH_2- groups. The *N*-CH_2- groups of the *Z* isomer are relatively deshielded with respect to the *N*-CH_2- groups of the *E* isomer and in all the cases the relatively deshielded *N*-CH_2- belong to the major isomer. The same argument holds for the determination of the major isomer for HL^8 and is self-consistent with respect to the *N*-CH- and *N*-CH_2- groups. In support of this argument the N-H protons that is coplanar to the oxygen atoms in H_2L^1, H_2L^2 and H_2L^3 (see Figure 2.3 as an example) are deshielded and appear at 12.29 ppm, 12.49 ppm and 12.98 ppm respectively, while the N-H protons pointing away from the oxygen atoms appear at 8.52 ppm, 8.54 ppm and 8.60 ppm, respectively.

Table 2.4 shows the results of the deconvolution analysis (digital integration) of the spectra and the relative populations of the *E* and *Z* isomers.

Table 2.4 Relative distributions of the *E,Z* configurational isomers of asymmetrically disubstituted ligands determined from the ^1H NMR spectra at room temperature. The reported percentage distributions are estimated to have an error of ± 1%.

Ligand	*Z*-isomer (%)	*E*-isomer (%)
HL^5	71	29
HL^6	75	25
HL^7	70	30
HL^8	80	20

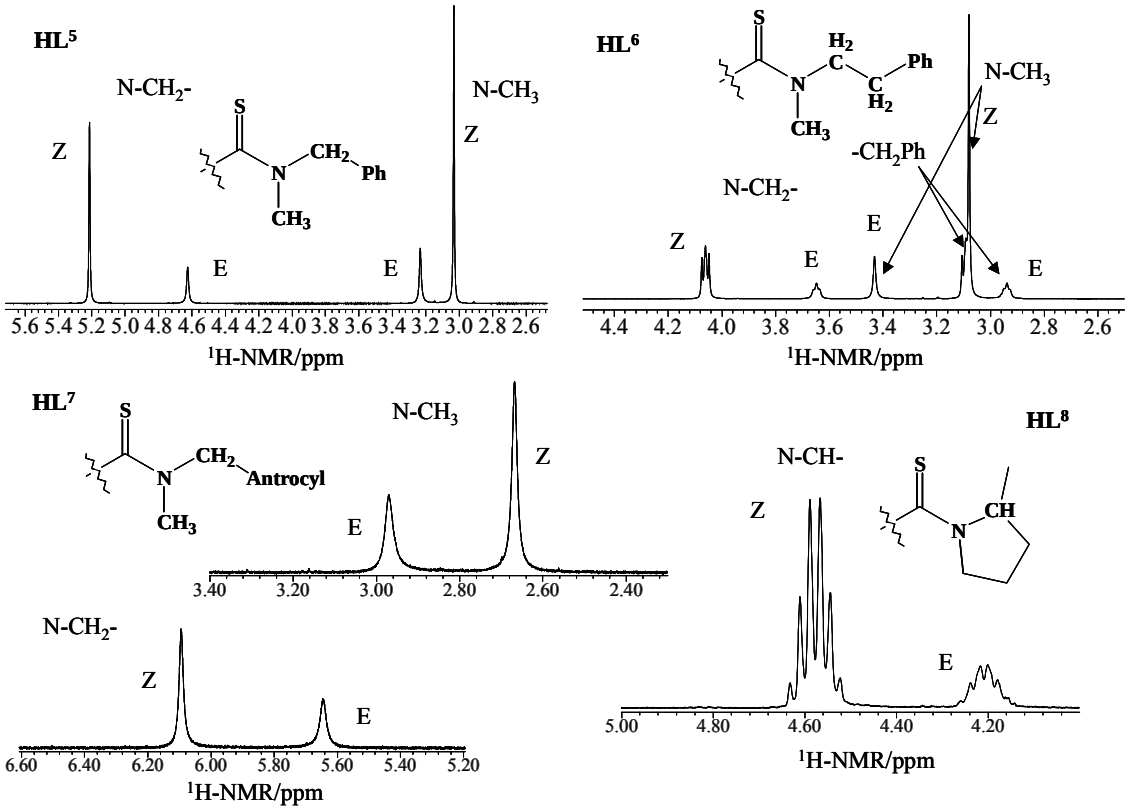

Figure 2.4 The *N*-alkyl section of ^{1}H NMR spectra of HL[5], HL[6], HL[7] and HL[8] showing the *E,Z* configurational isomers at 298 K in chloroform. In all the cases the *Z* isomer shown pictorially is the major component of the isomer.

In an attempt to confirm this assignment a benzene titration method was under taken. The principle behind this method is that when the ^{1}H NMR spectrum of *N*-alkyl groups (in amides and related compound) in benzene is compared with the spectrum of the *N*-alkyl groups in non-aromatic solvent, the resonances of the *N*-alkyl groups should appear upfield in benzene.[11] However, one of the *N*-alkyl groups would be expected to exhibit a greater upfield shift than the other, since the benzene π electrons could be expected to interact with the 'positively charged' (thio)amide nitrogen atom, with the 'negatively' charged chalcogen being as "far away" from the centre of the benzene ring as possible. The *N*-alkyl group coplanar to the chalcogen should then exhibit this upfield shift to a lesser extent than the *N*-alkyl group which is pointing away from the chalcogen. Table 2.5 shows such a benzene titration experiment with HL[6] as an example and Figure 2.5 is the actual ^{1}H NMR spectrum.

Table 2.5 298 K measurements of chemical shifts of *N*-**CH$_2$**-CH$_2$-Ph and *N*-**CH$_3$** proton resonances of *E* and *Z* isomers of HL^6 in chloroform as the benzene concentration increases. In parentheses are downfield shifts of each resonance per indicated volume of benzene added to the sample.

Amount of benzene added (μL)	δ(*N*-**CH$_2$**-CH$_2$-Ph) ppm		δ(*N*-**CH$_3$**) ppm	
	Z	*E*	*Z*	*E*
0	4.056	3.642	3.075	3.428
60	4.114(0.058)	3.694(0.052)	3.114(0.039)	3.474(0.046)
120	4.176(0.062)	3.749(0.055)	3.156(0.042)	3.522(0.048)
240	4.284(0.108)	3.845(0.094)	3.228(0.072)	3.607(0.085)

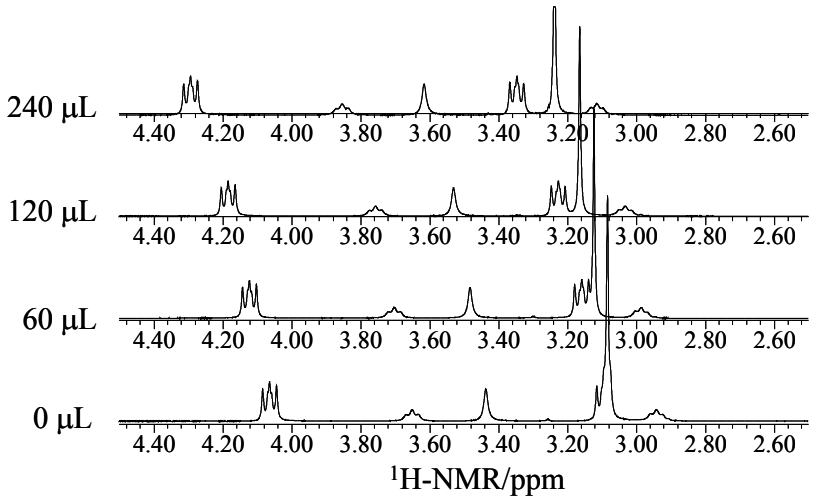

Figure 2.5 A section of ^{1}H NMR spectrum of HL^6 showing the *N*-CH$_3$ and *N*-CH$_2$CH$_2$- proton resonances in chloroform as the benzene titration of the sample is carried out with indicated amounts. All the resonances experience a downfield shift as the concentration of benzene increases.

From the data in Table 2.5 only the *N*-**CH$_2$**-CH$_2$-Ph and *N*-**CH$_3$** proton resonances are shown but consistent trends were also observed for the second *N*-CH$_2$-**CH$_2$**-Ph resonance. This experiment was also performed to other compounds with the same out come and here HL^6 is used as an illustration of our results. From both Table 2.5 and Figure 2.5 it is clear that there is a downfield shift of all the peaks as the concentration of the benzene increases. This is contrary to the expected upfield shift reported in the literature[11,12] for *N*-methyl-, *N*-ethyl-, *N*-*iso*-propyl- and *N*-*tert*-butylformamide. This way of assigning could not be extended to the system ligands studied here, however there are positive aspects that could be drawn from this experiment. Firstly, all the *N*-alkyl resonances that belong to the *Z* isomer 'recognise' each other in that the *N*-**CH$_2$**-**CH$_2$**-Ph proton resonances coplanar to the sulphur atom exhibit a greater degree of downfield shift while the *N*-CH$_3$ proton resonances in the same molecule have a lesser downfield

shift. The reverse holds for the *N*-alkyl groups that belong to the *E* isomer. This implies that a genuine benzene effect (deshielding in this case) on the *N*-alkyl groups is observed to be more pronounced on a particular side of the molecule as predicted by other workers. Secondly, what is particularly advantageous about this spectrum is that after titrating with 240 μL of benzene the triplet resonance due to *N*-CH_2-**CH_2**-Ph protons is well resolved from the *N*-CH_3 signal, while in pure chloroform it is overlapping with this *N*-CH_3 single resonance. This is achievable again by the fact that these *N*-**CH_2**-CH_2-Ph protons of the *Z* isomer exhibit a greater degree of downfield shift than the *N*-CH_3 protons of the same molecule.

2.4.2.2 E,Z isomerism observed at low temperature for symmetrically disubstituted N-alkyl-N-aryl-N'-acylthioureas ligands: $HL^{1A,1B,1C,1D}$ and $HL^{2A,2B,2C,2D}$

At room temperature the ^{1}H and ^{13}C NMR spectra of the ligands only show one set of *N*-alkyl and *N*-aryl resonances. Compounded by the fact that some of these were also isolated as crystals in one configuration only, which was the *E* configuration, one would falsely assume that these ligands are in one configuration. It became apparent later that these ligands also display the *E,Z* isomerism as well. However, due to the significantly lower barrier to rotation around the C-N bond of the (S)C-N(alkyl)(aryl) moiety the *N*-alkyl and *N*-aryl resonances are in fast exchange on the NMR time scale at room temperature, hence they are observed as one set instead of two. In the literature it has been known for some time that the N-aromatic groups lower the C-N rotation barrier.[13] The reason being that the nitrogen lone pair of electron may either contribute to the C-N bond or be pulled towards the aromatic system. To observe the *E,Z* isomerism in the new set of ligands their ^{1}H and ^{13}C NMR spectra had to acquired at low temperature and Figure 2.6 is an example of a temperature array of ^{1}H NMR spectra of *N*-methyl-*N*-(4-methoxy-phenyl)-*N'*-(*2,2*-dimethylpropanoyl)thiourea, HL^{1A} in deuterated chloroform.

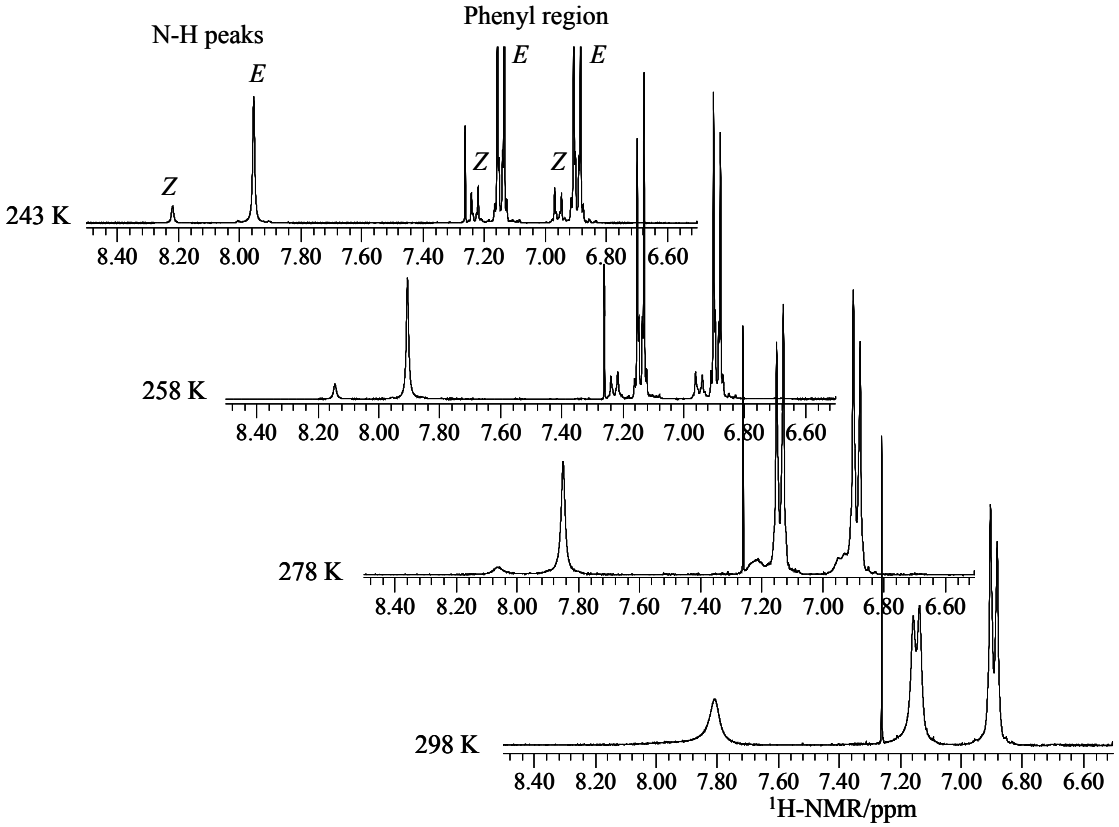

Figure 2.6 A section of a temperature array ^{1}H NMR spectrum of HL^{1A} in $CDCl_3$, showing one set of resonances at room temperature (298 K), however as the temperature is lowered it is clear that the compound displays *E,Z* isomerism in chloroform.

The way the assignment of the new set of ligands is done is similar to the set of ligands described above and the difference being that the *E* isomer in these ligands is the major isomer. Detailed assignments are shown in chapters 4 and 5. This is consistent with numerous examples of related N-alkylacetanilides that exist predominantly as *E*.[14-16] Interestingly, as the temperature is lowered the N-H resonances experience a downfield shift. The observed deshielding effect of the N-H proton may be attributed to strengthening of intermolecular hydrogen bonding as the temperature is decreased. The hydrogen bonding of the N-H protons in the solid state is shown in Figure 2.7. In the literature it has been reported that breaking of intermolecular hydrogen bonding of hydroxy protons as temperature increases results in increasing shielding effect in enol tautomer of β-dicarbonyls.[17] In solution ($CDCl_3$), it is thought that these hydrogen bond interactions become favoured and as the temperature is systematically lowered hence explaining the downfield shift trends seen for these N-H resonances.

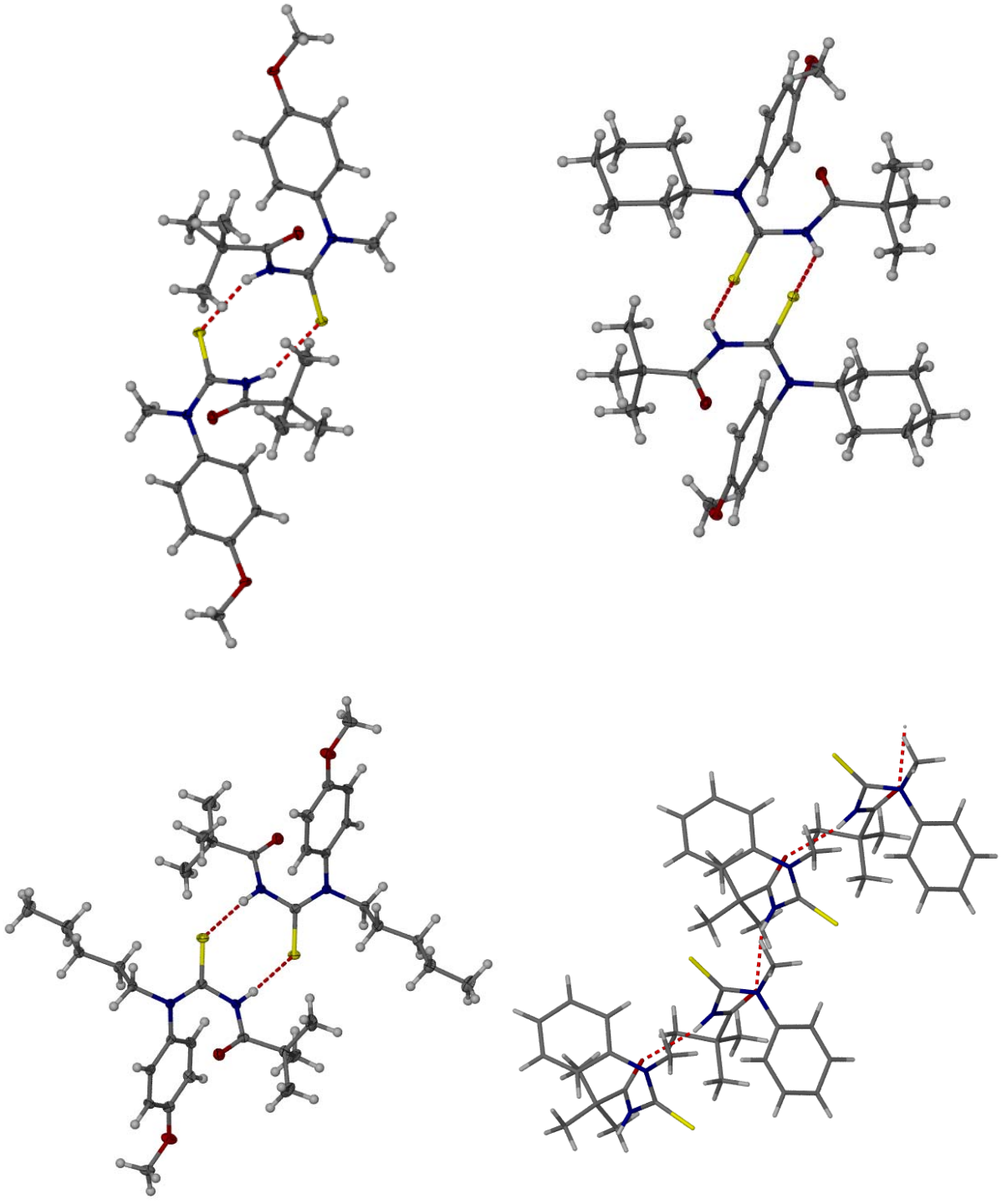

Figure 2.7 Hydrogen bonding of the N-H in $HL^{1A,1C,1D}$ and HL^{2A}. In $HL^{1A,1C,1D}$ these form dimers with the adjacent molecule while in HL^{2A} the hydrogen bonding network results in chains.

Table 3.2 Hydrogen-bonding geometry (Å, °) for *N*-methyl-*N*-(4-methoxy-phenyl)-*N'*-(*2,2*-dimethylpropanoyl)thiourea, HL^{1A}, *N*-cyclohexyl-*N*-(4-methoxy-phenyl)-*N'*-(*2,2*-dimethylpropanoyl)thiourea, HL^{1C}, *N*-pentyl-*N*-(4-methoxy-phenyl)-*N'*-(*2,2*-dimethylpropanoyl)thiourea, HL^{1D} and *N*-methyl-*N*-phenyl-*N'*-(*2,2*-dimethylpropanoyl)thiourea, HL^{2A}.

Ligand	Donor-H···Acceptor	Donor-H	H···Acceptor	Donor···Acceptor	Donor-H···Acceptor
HL^{1A}	N(1)-H(1)···O(2)^{i}	0.88	2.525	3.357	157.95
HL^{1C}	N(1)-H(1)···O(2)^{ii}	0.88	2.788	3.485	137.14
HL^{1D}	N(1)-H(1)···O(2)^{iii}	0.88	2.756	3.493	153
HL^{2A}	N(1)-H(1)···S(2)^{iv}	0.88	2.235	3.092	166.22

Symmetry code: (i) -x, y, ½-z; (ii) 1-x, 1-y, -z; (iii) ½-x, ½-y, 1-z; (iv) x, y-1, z

2.4.3 Spontaneous decomposition of N-methyl-N-(4-nitro-phenyl)-N'-(2,2-dimethylpropanoyl)thiourea, HL^{3A} in solution

Several attempts of growing suitable crystals of *N*-methyl-*N*-(4-nitro-phenyl)-*N'*-(*2,2*-dimethylpropanoyl)thiourea, HL^{3A} failed and all the time the crystals that grew were solved to be N-methyl-(4-nitro-phenyl)-amine (Figure 2.8). We were interested in this particular crystal for comparing of relevant bond lengths with the other ligands, as the ligand with an electron-withdrawing group would complete the series. Decomposition took place even when the possibility of contamination was excluded since the ^{1}H and ^{13}C NMR spectra of a fresh sample of this ligand showed no residual peaks of the starting material. This suggested that decomposition of this ligand in solution is taking place.

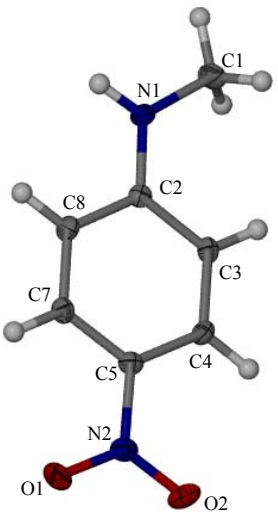

Figure 2.8 The molecular structure of N-methyl-(4-nitro-phenyl)-amine, which is a decomposition fragment of HL^{3A}.

To investigate the spontaneous decomposition of this ligand in solution, ^{1}H NMR spectrum of this compound was measured several days apart. It was noticed that in a few days extra peaks appear in the spectrum and these grow at the expense of the parent peaks over time. This observation was also noted with a similar ligand *N*-pentyl-*N*-(4-nitro-phenyl)-*N'*-(*2,2*-dimethylpropanoyl)thiourea, HL^{3D}, however no attempts were made to isolate the *N*-pentyl-(4-nitro-phenyl)-amine as we did with N-methyl-(4-nitro-phenyl)-amine. Figure 2.9 shows the ^{1}H NMR spectrum of HL^{3A} over time.

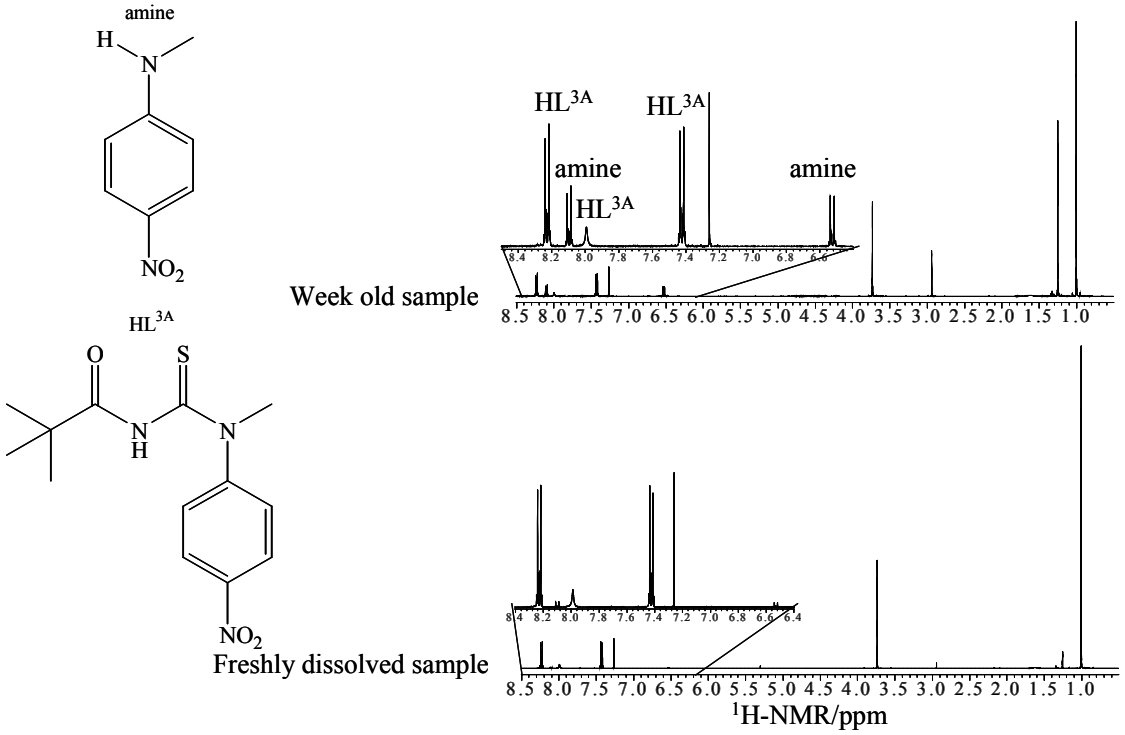

Figure 2.9 Full ^{1}H NMR spectrum and expansion of the phenyl region of HL^{3A}. The peaks of N-methyl-(4-nitro-phenyl)-amine grow at the expense of the HL^{3A} parent peaks, over time. This illustrates the spontaneous decomposition of HL^{3A} in solution.

Formation of the amine from HL^{3A} takes place via the cleaving of the C-N bond of the (S)C-N(methyl)(4-methyl-phenyl) moiety. This means that the remote nitro-substituent has notable effect on the C-N bond, which is several bonds away. The weakening of this very bond is also verified by the fact that the *E,Z* isomers of HL^{3A} and HL^{3D} are not observable even at 198 K in dichloromethane. Even at this low temperature the two isomers are still in fast exchange and this can only be explained by the influence of the nitro-substituent.

2.5 Concluding remarks

In conclusion we can say that the synthesis of the new series of ligands was successfully carried out using well-established method. The magnetic anisotropy of the thiocarbonyl group was used to assign the configurational isomers of all the ligands. The ligands with *N*-aryl substituents showed no presence of two isomers at room temperature, however on lowering the temperature it was verified that these ligands also display *E,Z* isomerism as well. It is the barrier lowering nature of the aromatic substituent that has lead to fast exchange at room temperature. The low C-N rotation barrier proved to be particularly influenced by electron withdrawing group even if they are much remote from this C-N bond. In the next chapters we look at the coordination chemistry of these ligands on platinum(II) metal ion.

References

1 I. B. Douglass and F. B. Dains, *J. Am. Chem. Soc.*, **1934**, *56*, 719.
2 R. N. Salvatore, C. H. Yoon, and K. W. Jung, *Tetrahedron*, **2001**, *57*, 7785.
3 S. K. Srivastava, P. M. S. Chauhan, and A. P. Bhaduri, *Synthetic. Commun.*, **1999**, *29*, 2085.
4 G. M. Sheldrick, *SHELXS-97 and SHELXL-97, Programs for the Solution and Refinement of Crystal Structures, University of Göttingen, Germany*, **1997**.
5 L. J. Barbour, *J. Supramol. Chem.*, **2003**, *1*, 189.
6 A. Dago, Y. Shepelev, F. Fajardo, F. Alvarez, and R. Pomes, *Acta Crystallogr. C*, **1989**, *C45*, 1192.
7 K. R. Koch, C. Sacht, T. Grimmbacher, and S. Bourne, *S. Afr. J. Chem.*, **1995**, *48*, 71.
8 J. D. S. Miller, *PhD Thesis, University of Cape Town*, **2000**.
9 S. N. Balasubrahmanyam, S. N. Bharathi, and G. Usha, *Org. Magn. Reson.*, **1983**, *21*, 474.
10 H. O. Kalinowski, W. Lubosch, and D. Seebach, *Chem. Ber.*, **1977**, *110*, 3733.
11 L. A. LaPlanche and M. T. Rogers, *J. Ame. Chem. Soc.*, **1964**, *86*, 337.
12 T. H. Siddall, III, W. E. Stewart, and F. D. Knight, *J. Phys. Chem.*, **1970**, *74*, 3580.
13 A. Liden and J. Sandstrom, *Acta. Chem. Scand.*, **1973**, *27*, 2567.
14 J. P. Perdew, J. A. Chevary, S. H. Vosko, K. A. Jackson, M. R. Pederson, D. J. Singh, and C. Fiolhais, *Phys. Rev. B*, **1992**, *46*, 6671.
15 J. A. Weil, A. Blum, A. H. Heiss, and J. K. Kinnaird, *J. Chem. Phys.*, **1967**, *46*, 3132.
16 J. P. Chupp and J. F. Olin, *J. Org. Chem.*, **1967**, *32*, 2297.
17 J. L. Burdett and M. T. Rogers, *J. Phys. Chem.*, **1966**, *70*, 939.

Chapter 3: Coordination chemistry of asymmetrically disubstituted *N*-alkyl-*N*-alkyl(aryl)-*N'*-acylthioureas to platinum(II)

Part 1: A multinuclear NMR spectroscopic assignment of *E,Z* configurational isomers of platinum(II) complexes of *N*-alkyl-*N*-alkyl(aryl)-*N'*-acylthioureas

Summary

Unsymmetrically dialkyl-substituted *N*-alkyl-*N*-alkyl(aryl)-*N'*-acylthioureas display *E,Z* configurational isomerism at room temperature in chloroform, which is readily observable by means of ^{1}H and ^{13}C NMR spectroscopy. The *Z* isomer was found to be favourably formed in solution ($CDCl_3$) for all investigated ligands of this type. The isomerism is relayed to the platinum(II) chelates derived from these ligands. The presence of the isomers ***cis*-[Pt(*ZZ*-L-*S,O*)$_2$]**, ***cis*-[Pt(*EZ*-L-*S,O*)$_2$]** and ***cis*-[Pt(*EE*-L-*S,O*)$_2$]** is directly observed from the ^{195}Pt NMR spectra of these complexes. These isomers were assigned by means of a combination of low magnetic field (7.05 T) ^{13}C NMR spectra and high-resolution **g**radient **H**eteronuclear **S**ingle **Q**uantum **C**orrelation (gHSQC) (^{1}H/^{13}C) NMR experiments. The platinum nuclei are spatially linked to *N*-CH_3 and *N*-CH_2- carbons in a **W** coupling pathway with $^{4}J(^{195}\text{Pt}\text{-}^{13}\text{C})$ coupling constants of about 20 Hz observed with low magnetic field ^{13}C NMR experiments. The gHSQC (^{1}H/^{13}C) NMR experiment indirectly links the platinum nuclei to the protons attached to the *N*-CH_3 and *N*-CH_2- carbons, achieving the assignment of the *EE*, *EZ* and *ZZ* platinum(II) chelates. A rotation of the N-C bond of the (S)C-NRR' moiety during complexation results in isomer distributions which favour the *ZZ* isomer (53%, 57% and 65%) followed by the *EZ* isomer (39%, 35% and 30%) then the *EE* isomer (8%, 8% and 5%) for *cis*-bis(*N*-phenethyl-*N*-methyl-*N'*-*2,2*-dimethylpropanoylthioureato)platinum(II), ***cis*-[Pt(L^6-*S,O*)$_2$]**, *cis*-bis(*N*-benzyl-*N*-methyl-*N'*-*2,2*-dimethylpropanoylthioureato)platinum(II), ***cis*-[Pt(L^5-*S,O*)$_2$]** and *cis*-bis(*N*-anthrocen-9-ylmethyl-*N*-methyl- *N'*-*2,2*-dimethylpropanoylthioureato)platinum(II), ***cis*-[Pt(L^7-*S,O*)$_2$]** complexes, respectively. The three ^{195}Pt NMR

resonances for the *EE*, *EZ* and *ZZ* isomers of *cis*-bis(*N*-(2-methylpyrrolidine)-*N'*-*2,2*-dimethylpropanoylthioureato)platinum(II) complex, ***cis*-[Pt(L^8-*S,O*)$_2$]** can only be observed at low temperature.

3.1 Introduction

Ligands of the type *N,N*-dialkyl-*N'*-acyl(aroyl)thioureas (HL) display rich coordination chemistry towards the platinum group metal (PGM) ions and other transition metal ions as shown in general introduction.[1,2] Of interest here is the configurational isomerism that arises in asymmetrically dialkyl-substituted *N*-alkyl-*N*-alkyl(aryl)-*N'*-acylthioureas and corresponding *N-alkyl-N*-aryl-*N'*-acylthioureas. Similar to the well-documented double bond character of thioamides,[3-5] the (S)C-NRR' moiety shows restricted rotation around the C-N bond resulting in *E,Z* configurational isomers in solution when R and R' differ. This is reflected in the appearance of two sets of *N*-alkyl resonances in both the ^{1}H and ^{13}C NMR spectra at room temperature (Chapter 3). This configurational isomerism is relayed to the corresponding platinum(II) complexes. Shown in Scheme 1 are the *EE*, *EZ* and *ZZ* isomers of some of these complexes with a similar structural motif.

cis-[Pt(*EE*-L-*S,O*)$_2$] *cis*-[Pt(*ZZ*-L-*S,O*)$_2$]

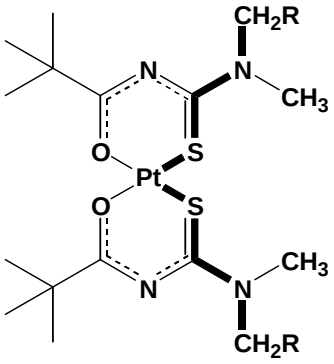

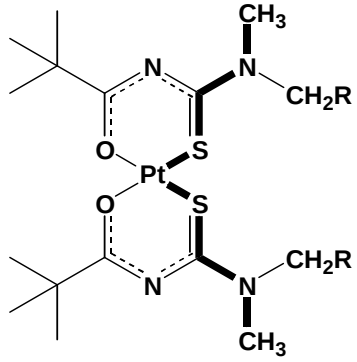

R = for HL[5]

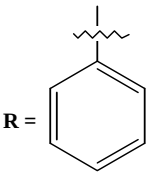

R = for HL[6]

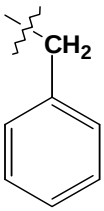

cis-[Pt(*EZ*-L-*S,O*)$_2$]

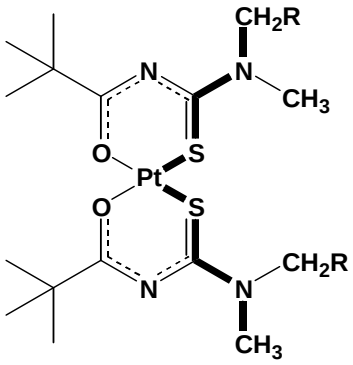

R = for HL[7]

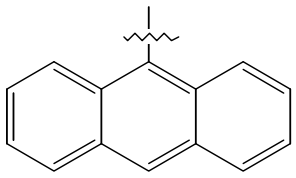

Scheme 1: *EE*, *EZ* and *ZZ* configurational isomers of the platinum(II) chelates, ***cis*-[Pt(L^5-*S,O*)$_2$]**, ***cis*-[Pt(L^6-*S,O*)$_2$]** and ***cis*-[Pt(L^7-*S,O*)$_2$]** showing a favourable **W** $^{4}J(^{195}Pt\text{-}^{13}C)$ coupling pathway in bold.

The ^{195}Pt NMR spectra of *cis*-bis(*N*-benzyl-*N*-methyl-*N'*-*2,2*-dimethylpropanoylthioureato)platinum(II); ***cis*-[Pt(L^5-*S,O*)$_2$]**, *cis*-bis(*N*-phenethyl-*N*-methyl-*N'*-*2,2*-dimethylpropanoylthioureato)platinum(II); ***cis*-[Pt(L^6-*S,O*)$_2$]** and *cis*-bis(*N*-anthrocen-9-ylmethyl-*N*-methyl- *N'*-*2,2*-dimethylpropanoylthioureato)platinum(II); ***cis*-[Pt(L^7-*S,O*)$_2$]** at room temperature clearly show well resolved peaks for the three isomers. However, to observe all the isomers for the *cis*-bis(*N*-(2-methylpyrrolidine)-*N'*-*2,2*-dimethylpropanoylthioureato)platinum(II); ***cis*-[Pt(L^8-*S,O*)$_2$]** complex the ^{195}Pt NMR spectrum had to be recorded at low temperature (228 K). Similarities between the *N*-CH(CH$_3$)- and *N*-CH$_2$-groups of the 2-methylperrilidyl moiety are thought to result the ^{195}Pt NMR resonances of three isomers not being well resolved even at low temperature (Figure 3.3)

Unambiguous assignment of the ^{195}Pt NMR resonances directly from either the ^{1}H NMR or ^{13}C NMR spectra is not entirely straightforward. Certainly by determining the relative integrals of the complexes from the ^{1}H NMR spectra, the central resonances in the ^{195}Pt NMR spectra are easily assigned to the *EZ* isomers. However, the ambiguity is not resolved for the most downfield and the most upfield resonances. Moreover the chemical shift of the *EZ* isomer might intuitively be expected to resonate between the chemical shifts of the *EE* and *ZZ* isomers. This is indeed the case for all the complexes evaluated by comparing the relative integrals in the ^{195}Pt NMR spectra with those in the ^{1}H NMR spectra (as will be shown in the discussion).

Previously, the assignment of similar complexes was achieved by means of ^{1}H/^{13}C/^{195}Pt correlation NMR spectroscopy.[6] This technique requires a triple resonance probe tunable for ^{1}H, ^{13}C and ^{195}Pt nuclei and it was not readily available to us hence it was necessary to devise 'in-house' means of examining these types of complexes with the equipment at our disposal. In the ^{1}H NMR spectra of the complexes the expected long range $^5J(^{195}\text{Pt-}^1\text{H})$ couplings between the platinum nuclei and the *N*-alkyl protons are not observed, due to the field-dependent chemical shift anisotropy (CSA) broadening characteristic of square planar Pt(II) complexes.[7] Besides such long range $^5J(^{195}\text{Pt-}^1\text{H})$ couplings would be expected to be very small. Therefore indirect detection techniques (^{1}H-X, X being ^{195}Pt in this particular case) could not be exploited for the unambiguous assignment of the ^{195}Pt resonances. In the ^{1}H NMR spectra of these complexes the *EZ* isomer is observed to have two resonances for its *N*-CH$_3$ protons as well as for its *N*-CH$_2$- protons. This is because one set of each *N*-alkyl group is coplanar with the sulphur atom while the other set is pointing away from the sulphur atom. The *N*-alkyl set pointing away from the sulphur atom is in a favourable **W** coupling pathway to the platinum atom (see Scheme 1), and is therefore expected to have a characteristic $^5J(^{195}\text{Pt-}^1\text{H})$ coupling satellites. Sequential irradiating of either the two *N*-CH$_3$ proton resonances or the two *N*-CH$_2$- proton resonances of the *EZ* complex with the ^{195}Pt frequency of the *EZ* isomer as a decoupler (readily obtained from the ^{195}Pt NMR spectra) did not result in any of the resonances growing although this was expected to occur since the associated $^5J(^{195}\text{Pt-}^1\text{H})$ couplings should collapse leading to growth of the *N*-alkyl proton resonance in a favourable **W** coupling pathway. The success of this Heteronuclear **S**elective **P**opulation **T**ransfer (SPT) experiment is entirely dependent on whether the particular *N*-CH$_2$- protons or *N*-CH$_3$ protons are spin-coupled to the ^{195}Pt nucleus in question (in this case the *EZ* isomer). The failure of this experiment in this case may again be explained by the expected small $^5J(^{195}\text{Pt-}^1\text{H})$ coupling constant of the platinum nuclei to the *N*-alkyl protons. Ideally this technique should be adequate to unambiguously assign the platinum resonances, should the $^5J(^{195}\text{Pt-}^1\text{H})$ be sufficiently large.

In this chapter we primarily illustrate by means of a combination of low magnetic field ^{13}C NMR and high-resolution 2D gHSQC NMR spectroscopy how the ^{195}Pt resonances of the (*EE*, *EZ* and *ZZ*) isomers can be unambiguously assigned. We also note that the statistically predicted (*EE*, *EZ* and *ZZ*) isomer distributions of the complexes are never mirrored with the observed populations determined either from the ^{1}H or ^{195}Pt NMR spectra, however we probe the factors affecting these distributions in chapters 4 and 5.

3.2 Experimental

3.2.1 General remarks

The synthesis and characterisation of the asymmetrically dialkyl-substituted ligands has already been described in detail in chapter 2 and will not form part of the discussion here. It will only be where necessary comparisons to the complexes are made that the ligands will form part of the discussion. The complex *cis*-bis(*N*,*N*-diethyl-*N*'-benzoylthioureato)platinum(II); ***cis*-[Pt(L^4-*S*,*O*)$_2$]** is not asymmetrically disubstituted, however it forms part of the discussion since it has some important structural features which are extrapolated to other complexes.

3.2.2 NMR spectroscopy

Conventional ^{1}H and ^{13}C NMR spectra of relatively high concentrations (*ca* 80 mg.cm^{-3}) of the ligands and their respective platinum(II) complexes using 5 mm diameter tubes were obtained at 25 °C in deuterated chloroform using a Varian Inova 400 spectrometer operating at 400 and 101 MHz for ^{1}H and ^{13}C, respectively. The gHSQC NMR experiments for selected complexes were also acquired on the Varian Inova 400 spectrometer. For selected complexes ^{13}C NMR spectra were also recorded on a Varian VXR 300 spectrometer operating at 76 MHz for ^{13}C. All samples were carefully filtered before any spectroscopic measurement was undertaken. ^{1}H chemical shifts are quoted relative to the residual $CDCl_3$ solvent resonance at 7.26 ppm and the ^{13}C chemical shifts are quoted relative to the $CDCl_3$ middle resonance of the triplet at 77.0 ppm. The ^{195}Pt NMR spectra of the complexes were recorded at 30 °C (***cis*-[Pt(L^8-*S*,*O*)$_2$]** was also measured at various temperatures) using the Varian Inova 400 spectrometer operating at 86 MHz for ^{195}Pt [external reference material: 500 mg.cm^{-3} H_2PtCl_6 in 30% (v/v) D_2O-1M HCl; $\delta(^{195}Pt) = 0$ ppm at 30 °C].

3.2.3 Synthesis of platinum complexes

Platinum(II) complexes were prepared and characterised according to a previously published method,[1] which entails drop-wise addition of a K_2PtCl_4 solution (in a one to one volume of acetonitrile to water) to a solution of ligand and sodium acetate (also in a one to one volume of acetonitrile to water). All the reagents were commercially available and were used without any prior purification. The reactions were generally conducted at 50 ºC for two hours. After the reaction solutions had cooled to room temperature, excess water was added and the reaction mixtures were

refrigerated before the products were collected by means of centrifugation and dried under vacuum. Elemental analyses were performed using a Carlo Erba EA 1108 elemental analyser courtesy of the University of Cape Town.

cis-bis(_N,N_-Diethyl-_N'_-benzoylthioureato)platinum(II), _cis_-[Pt(L^4-_S,O_)$_2$]

A yield of 74% of the product was collected and analysed. Found: C, 43.27; H, 4.34; N, 8.35; S, 9.39 $PtC_{24}H_{30}N_4S_2O_2$ required C, 43.30; H, 4.54; N, 8.42; S, 9.63%. δ_H(400 MHz; solvent $CDCl_3$): 8.27 (2H, d, C_6H_5), 7.52 (1H, tt, C_6H_5), 7.42 (2H, tt, C_6H_5), 3.78 (4H, broad, 2N-$\underline{CH_2}CH_3$), 1.27 (6H, broad, 2N-$CH_2\underline{CH_3}$). δ_C(101 MHz, solvent $CDCl_3$): 168.74 (C(O)), 167.31 (C(S)), 137.78-128.22 (C_6H_5), 46.87 (N-$\underline{CH_2}CH_3$), 45.79 (N-$\underline{CH_2}CH_3$), 12.89 (N-$CH_2\underline{CH_3}$), 12.21 (N-$CH_2\underline{CH_3}$).

cis-bis(_N_-Benzyl-_N_-methyl-_N'-2,2_-dimethylpropanoylthioureato)platinum(II), _cis_-[Pt(L^5-_S,O_)$_2$]

A yield of 73% of the product was collected and analysed. Found: C, 46.70; H, 5.18; N, 7.46; S, 8.47 $PtC_{28}H_{38}N_4S_2O_2$ required C, 46.59; H, 5.31; N, 7.76; S, 8.88%. δ_H(400 MHz; solvent $CDCl_3$): 7.36-7.15 (5H, m, C_6H_5)(ZZ, EZ and EE), 5.01 (2H, s, N-CH_2-)(ZZ), 5.00 (2H, s, N-CH_2-)(Z(EZ)), 4.98 (2H, s, N-CH_2-)(E(EZ)), 4.94 (2H, s, N-CH_2-)(EE), 3.16 (3H, s, N-CH_3)(ZZ), 3.14 (3H, s, N-CH_3)(E(EZ)), 3.12 (3H, s, N-CH_3)(Z(EZ)), 1.25 (9H, s, C($\underline{CH_3}$)$_3$)(EE and E(EZ)), 1.17 (9H, s, C($\underline{CH_3}$)$_3$)(ZZ and Z(EZ)). δ_C(101 MHz, solvent $CDCl_3$): 184.04 (C(O))(E(EZ)), 183.92(C(O))(EE), 183.62 (C(O))(ZZ), 183.51 (C(O))(Z(EZ)), 168.56 (C(S))(ZZ, EZ and ZZ), 136.44-127.31 (C_6H_5)(ZZ, EZ and ZZ), 57.02 (N-CH_2-)(EE and E(EZ)), 55.17 (N-CH_2-)(ZZ and Z(EZ)), 42.40 ($\underline{C}(CH_3)_3$)(EE and E(EZ)), 42.24 ($\underline{C}(CH_3)_3$)(ZZ and Z(EZ)), 39.37 (N-CH_3)(ZZ and Z(EZ)), 38.08 (N-CH_3)(EE and E(EZ)), 28.34 (C($\underline{CH_3}$)$_3$)(EE and E(EZ)), 28.17 (C($\underline{CH_3}$)$_3$)(ZZ and Z(EZ)).

cis-bis(_N_-Phenethyl-_N_-methyl-_N'-2,2_-dimethylpropanoylthioureato)platinum(II), _cis_-[Pt(L^6-_S,O_)$_2$]

A yield of 83% of the product was collected and analysed. Found: C, 48.17; H, 5.51; N, 7.23; S, 8.11 $PtC_{38}H_{42}N_4S_2O_2$ required C, 48.05; H, 5.65; N, 7.47; S, 8.55%. δ_H(400 MHz; solvent $CDCl_3$): 7.31-7.16 (5H, m, C_6H_5)(ZZ, EZ and EE), 3.92 (2H, t, N-$\underline{CH_2}CH_2Ph$)(ZZ and Z(EZ)), 3.88 (2H, t, N-$\underline{CH_2}CH_2Ph$)(EE and E(EZ)), 3.11 (3H, s, N-CH_3)(E(EZ)), 3.10 (3H, s, N-CH_3)(EE), 3.09 (3H, s, N-CH_3)(Z(EZ)), 3.08 (3H, s, N-CH_3)(ZZ), 3.04 (2H, t, N-$CH_2\underline{CH_2}Ph$)(EE and E(EZ)), 2.90 (2H, t, N-$CH_2\underline{CH_2}Ph$)(ZZ and Z(EZ)), 1.26 (9H, s, C($\underline{CH_3}$)$_3$)(ZZ and Z(EZ)), 1.23 (9H, s, C($\underline{CH_3}$)$_3$)(EE and E(EZ)). δ_C(101 MHz, solvent $CDCl_3$): 183.57 (C(O))(E(EZ)), 183.19 (C(O))(ZZ), 183.12 (C(O))(Z(EZ)), 167.67 (C(S))(Z(EZ)), 167.61 (C(S))(ZZ), 167.35 (C(S))(EE), 167.25 (C(S))(E(EZ)), 138.64-126.48 (C_6H_5)(ZZ, EZ and EE), 55.70 (N-$\underline{CH_2}CH_2Ph$)(EE and E(EZ)), 54.94 (N-$\underline{CH_2}CH_2Ph$)(ZZ and Z(EZ)), 42.29 ($\underline{C}(CH_3)_3$)(ZZ, EZ and EE), 40.78 (N-CH_3)(ZZ and Z(EZ)), 39.38 (N-CH_3)(EE and E(EZ)), 33.95 (N-CH_2CH_2Ph)(ZZ and Z(EZ)), 33.07 (N-$CH_2\underline{CH_2}Ph$)(EE and E(EZ)), 28.32 (C($\underline{CH_3}$)$_3$)(ZZ, EZ and EE).

cis-bis(_N_-Anthrocen-9-ylmethyl-_N_-methyl-_N'-2,2_-dimethylpropanoylthioureato)platinum(II), _cis_-[Pt(L^7-_S,O_)$_2$]

A yield of 91% of the product was collected and analysed. Found: C, 57.20; H, 4.57; N, 6.28; S, 6.93 $PtC_{44}H_{46}N_4S_2O_2$ required C, 57.31; H, 5.03; N, 6.08; S, 6.96%. δ_H(400 MHz; solvent $CDCl_3$): 8.49 – 7.47 (9H, ($C_{14}H_9$) EE, EZ and ZZ), 6.11 (2H, s, N-CH_2-)(Z(EZ)), 6.07 (2H, s, N-CH_2-)(ZZ)), 5.89 (2H, s, N-CH_2-)(EE)), 5.82

(2H, s, N-CH_2-)(E(EZ)), 2.85 (3H, s, N-CH_3)(Z(EZ)), 2.79 (3H, s, N-CH_3)(ZZ)), 2.76 (3H, s, N-CH_3)(EE)), 2.73 (3H, s, N-CH_3)(E(EZ)), 1.45 (9H, s, C($\underline{CH_3}$)$_3$(ZZ and Z(EZ)), 1.26 (9H, s, C($\underline{CH_3}$)$_3$(EE and E(EZ)). δ_C(101 MHz, solvent $CDCl_3$): 183.80 (C(O))(ZZ and Z(EZ)), 183.11 (C(O))(EE and E(EZ), 167.95 (C(S))(EE and E(EZ)) 167.86 (ZZ and Z(EZ)), 134.07-123.76 ($C_{14}H_9$), 48.42 (N-CH_2-)(EE and E(EZ)), 45.98 (N-CH_2-)(ZZ and Z(EZ)), 42.80 ($\underline{C}(CH_3)_3$)(ZZ and Z(EZ)), 42.49 ($\underline{C}(CH_3)_3$)(EE and E(EZ)), 36.69 (N-CH_3)(ZZ and Z(EZ)), 34.98 (N-CH_3)(EE and E(EZ)), 28.57 (C($\underline{CH_3}$)$_3$)(ZZ and Z(EZ)), 28.38 (C($\underline{CH_3}$)$_3$)(EE and E(EZ)).

***cis*-bis(*N*-(2-Methylpyrrolidine)-*N'*-*2,2*-dimethylpropanoylthioureato)platinum(II), *cis*-[Pt(L^8-*S,O*)$_2$]**

A yield of 79% of the product was collected and analysed. Found: C, 40.06; H, 5.99; N, 8.48; S, 9.30 $PtC_{22}H_{38}N_4S_2O_2$ required C, 40.79; H, 5.66; N, 8.65; S, 9.90%. δ_H(400 MHz; solvent $CDCl_3$): 4.53-4.36 (1H, m, N-$\underline{CH}(CH_3)CH_2$-)(ZZ, EZ and EE), 3.64-3.44 (2H, m, N-$\underline{CH_2}CH_2$-)(ZZ, EZ and EE), 1.98 (2H, m, N-CH(CH_3)$\underline{CH_2}$-)(ZZ, EZ and EE), 1.64 (2H, m, N-$CH_2\underline{CH_2}$-)(ZZ, EZ and EE), 1.25 (3H, d, N-CH(CH_3)$\underline{CH_2}$-)(ZZ, EZ and ZZ), 1.17-1.15 (9H, s, C($\underline{CH_3}$)$_3$)(ZZ, EZ and EE). δ_C(101 MHz; solvent $CDCl_3$): 183.24-182.84 (C(O))(ZZ, EZ and EE), 164.59-164.20 (C(S))(ZZ, EZ and EE), 56.88-56.44 (N-$\underline{CH}(CH_3)CH_2$-)(ZZ, EZ and EE), 50.04-49.95 (N-$\underline{CH_2}CH_2$-)(ZZ, EZ and EE), 41.92 ($\underline{C}(CH_3)_3$)(ZZ, EZ and EE), 32.09-31.54 (N-CH(CH_3)$\underline{CH_2}$-)(ZZ, EZ and EE), 28.18-28.05 (C($\underline{CH_3}$)$_3$)(ZZ, EZ and EE), 22.65-21.87 (N-$CH_2\underline{CH_2}$-)(ZZ, EZ and EE), 18.97-18.21 (N-CH($\underline{CH_3}$)CH_2-)(ZZ, EZ and EE).

3.3 Results and Discussion

The series of asymmetrically disubstituted *N*-alkyl-*N*-alkyl(aryl)-*N'*-acylthioureas was synthesised and subsequently reacted with K_2PtCl_4 to form chelates that carry through the isomerism, with clear objective to assign the platinum(II) chelates that are derived from them by means of various NMR spectroscopic techniques. We have also synthesised a symmetrically substituted ligand *N,N*-diethyl-*N'*-benzoylthiourea and its corresponding Pt(II) chelate. The thiocarbonyl carbon of this ligand was *ca* 50% ^{13}C isotopically enriched. The motivation for the inclusion of this ligand and its complex in the discussion is that there are certain parallels that we wish to infer with the other complexes without necessarily having to label them due to the high cost of isotopically enriched reagents

3.3.1 E,Z configurational isomerism in uncoordinated asymmetrically disubstituted N-alkyl-N-alkyl(aryl)-N'-acylthioureas, ligands; HL^5, HL^6, HL^7 and HL^8

The *E,Z* configurational isomerism of the titled ligands has already been discussed in chapter 2, Section *2.4.2.1*, however we bring them to a discussion here since the complexes discussed in this chapter are derived from them. It was clearly shown that all these ligands display *E,Z* configurational isomerism at room temperature in chloroform. In all the cases the major isomer was assigned to be the *Z* isomer. The relative distributions of the *E,Z* isomers were determined by digital integration of the *N*-CH_3 and *N*-CH_2- proton resonances are shown in Table 3.1.

Table 3.1 Relative distributions of the *E,Z* configurational isomers of asymmetrically disubstituted ligands determined from the ^{1}H NMR spectra at room temperature. The reported percentage distributions are estimated to have an error of ± 1%.

Ligand	*Z*-isomer (%)	*E*-isomer (%)
HL^{5}	71	29
HL^{6}	75	25
HL^{7}	70	30
HL^{8}	80	20

3.3.2 Platinum(II) chelates derived from $HL^{4,5,6,7,8}$

3.3.2.1 cis-[Pt(L^{4}-(S,O)$_2$]

Using ^{13}C enriched sodium thiocyanate the synthesis resulted in symmetrically disubstituted *N,N*-diethyl-*N'*-benzoylthiourea which was *ca* 50% ^{13}C labelled at the thiocarbonyl carbon. The primary purpose of this was to unambiguously establish which of the two (thio)carbonyl peaks can be attributed to C=O and which to C=S. Figure 3.1 shows that upon complexation the thiocarbonyl carbon shifts upfield while the carbonyl carbon does the opposite i.e. shifts downfield. Hereafter this is assumed to be the case for all the ligands as it would be too expensive to prepare enriched ligands for all the compounds presented in the thesis. Figure 3.1 together with Table 3.2 show where the carbonyl carbon and thiocarbonyl carbon resonate before and after complexation to the platinum(II) centre.

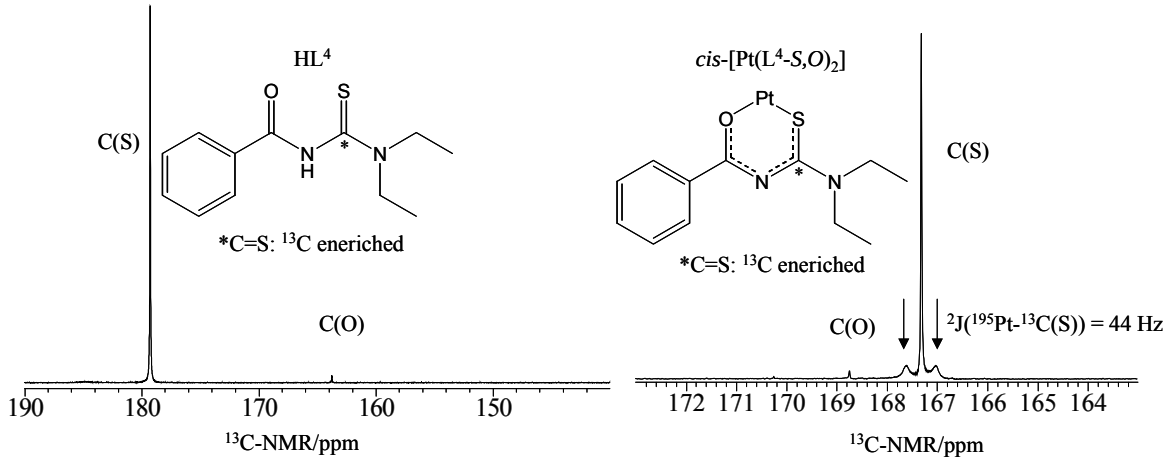

Figure 3.1 Sections of ^{13}C NMR spectra of thiocarbonyl ^{13}C enriched *N,N*-diethyl-*N'*-benzoylthiourea, HL^{4} and its corresponding Pt(II) complex, illustrating the upfield shift of the thiocarbonyl carbon and the downfield shift of the carbonyl carbon upon complexation.

Table 3.2 Comparisons of the ^{13}C chemical shifts (ppm) of the carbonyl and thiocarbonyl resonances of unbound ligands $HL^{4,5,6,7,8}$ and coordinated ligands in ***cis*-[Pt($L^{4,5,6,7,8}$-(*S,O*)$_2$]** complexes

Ligand	Ligand $\delta^{13}C$: C(O)	Complex $\delta^{13}C$: C(O)	$\Delta(\delta^{13}C)$	Ligand $\delta^{13}C$: C(S)	Complex $\delta^{13}C$: C(S)	$\Delta(\delta^{13}C)$
HL^4	163.76	168.74	+4.98	179.27	167.31	-11.96
HL^5	174.48 (*E*)	183.92 (*EE*)	+9.44	181.64 (*E*)	168.56 (*EE*)	-13.08
	174.80 (*Z*)	183.62 (*ZZ*)	+8.82	180.76 (*Z*)	168.56 (*ZZ*)	-12.20
HL^6	174.39 (*E*)	Not observed		180.17 (*E*)	167.35 (*EE*)	-12.82
	174.39 (*Z*)	183.19 (*ZZ*)	+8.80	180.49 (*Z*)	167.61 (*ZZ*)	-12.88
HL^7	174.52 (*E*)	183.11 (*EE*)	+8.59	181.00 (*E*)	167.95 (*EE*)	-13.39
	175.55 (*Z*)	183.80 (*ZZ*)	+8.25	180.85 (*Z*)	167.86 (*ZZ*)	-12.90
HL^8	174.60 (*E*)	183.24 (*EE*)	+8.67	176.64 (*E*)	164.59 (*EE*)	-12.05
	174.72 (*Z*)	182.84 (*ZZ*)	+8.12	176.79 (*Z*)	164.26 (*ZZ*)	-12.53

The upfield shift of the thiocarbonyl carbons and the downfield shift of the carbonyl carbons are also tabulated in Table 3.2 and these observations are in accordance with previous work on similar ligands.[8,9] From the table we see that there is nearly a $\Delta(\delta^{13}C) = \delta^{13}C(O)_{complex} - \delta^{13}C(O)_{ligand}$ = 5 to 9 ppm downfield shift for the carbonyl carbons and nearly a $\Delta(\delta^{13}C) = \delta^{13}C(S)_{complex} - \delta^{13}C(S)_{ligand}$ = 12 to 13 ppm upfield shift for the thiocarbonyl carbons. The assignments for the carbonyl and thiocarbonyl peaks of all other ligands $HL^{5,6,7,8}$ and the complexes, ***cis*-[Pt($L^{5,6,7,8}$-(*S,O*)$_2$]** derived from them are based on the illustration in Figure 3.1 for HL4 and its complex ***cis*-[Pt(L^4-(*S,O*)$_2$]** without necessarily confirming with ^{13}C enrichment for each case. Since the thiocarbonyl carbon is ^{13}C enriched it is also easy to see $^2J(^{195}Pt\text{-}^{13}C)$ coupling satellites of about 44 Hz (Figure 3.1).

Another important observation in the ^{13}C NMR spectrum of the ***cis*-[Pt(L^4-(*S,O*)$_2$]** complex is that the downfield resonance (46.87 ppm) due to the *N*-CH_2- carbons pointing away from the sulphur atom has lower intensity with respect to the upfield *N*-CH_2- resonance at 45.79 ppm (on the same side as the sulphur atom) (Figure 3.2). The low intensity of this particular carbon is as a result of being in a favourable **W** coupling pathway (Pt-S-C-N-CH_2-) to the platinum atom. The associated $^4J(^{195}Pt\text{-}^{13}C)$ coupling satellites are marginally observed flanking the parent peak at 46.87 ppm, with a value of about 20 Hz. No such phenomenon is observed in any of the *N*-CH_2-**CH_3** resonances in the ^{13}C NMR spectrum and they are of equal intensity. This is expected since they are much further away from the platinum atom so that the $^5J(^{195}Pt\text{-}^{13}C)$ coupling is too small to see. Both the chemical shift of the *N*-alkyl group in this favourable **W** pathway to the platinum atom together with the associated $^4J(^{195}Pt\text{-}^{13}C)$ coupling satellites are found to be most important for spectral analysis when the alkyl groups R and R' of the (S)CN-NRR' moiety are not equal. This forms a basis for assigning unambiguously the *E,Z* configurational isomers of platinum(II) chelates resulting from asymmetrically disubstituted ligands, as we shall see in the next section.

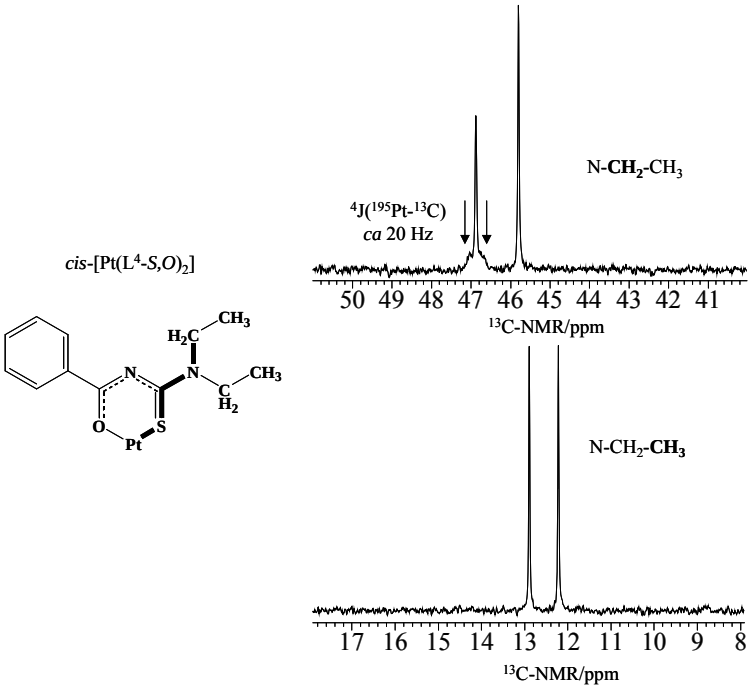

Figure 3.2 Low magnetic field (7 MHz on ^{13}C) sections of ^{13}C NMR spectrum of *cis*-bis(*N,N*-diethyl-*N*'-benzoylthioureato)platinum(II), showing the *N*-$\mathbf{CH_2}$-CH_3 resonances. One resonance (in a favourable **W** pathway to the Pt atom, shown in bold) couples to the platinum atom while the other does not. The *N*-CH_2-$\mathbf{CH_3}$ resonances, since being much further away from the platinum atom do not show this difference and hence resonate with equal intensity.

3.3.2.2 Complexes derived from asymmetrically disubstituted N-alkyl-N-alkyl(aryl)-N'-acylthioureas, ligands; HL^5, HL^6, HL^7 and HL^8

On coordination to the platinum(II) centre the asymmetrically disubstituted ligands carry through their *E,Z* configurational isomerism resulting in *ZZ*, *EZ* and *EE* isomers of the platinum(II) chelates (Figure 3.3). The presence of such isomers is illustrated by well-resolved ^{195}Pt NMR resonances at room temperature for ***cis*-[Pt($L^{5,6,7}$-*S,O*)$_2$]**. However, for ***cis*-[Pt(L^8-*S,O*)$_2$]** it was necessary to lower the temperatures significantly to verify the presence of the three isomers. At room temperature the ^{195}Pt NMR spectrum of this particular complex is rather deceptive as it shows only one peak (Figure 3.3(d)). Still from ^1H and ^{13}C NMR spectra it was concluded that there ought to be more than one isomer present. Moreover the ligand (HL^8) with which the complex had been synthesised does clearly display *E,Z* isomerism at room temperature. Therefore, it would have been unexpected for the resultant complex to adopt *only* one configuration. Indeed, upon lowering of the temperature significantly the three isomers became visible, something which is beautifully displayed in Fig.3.3(d). Figure 3.3 together with Table 3.3 summarise where the isomers of all the complexes resonate and also show their various *ZZ*, *EZ* and *EE* isomer populations. In both Figure 3.3 and Table 3.3 the *ZZ*, *EZ* and *EE* isomers have been assigned, however, the actual assignments of these isomers is discussed in the following Section 3.3.2.3.

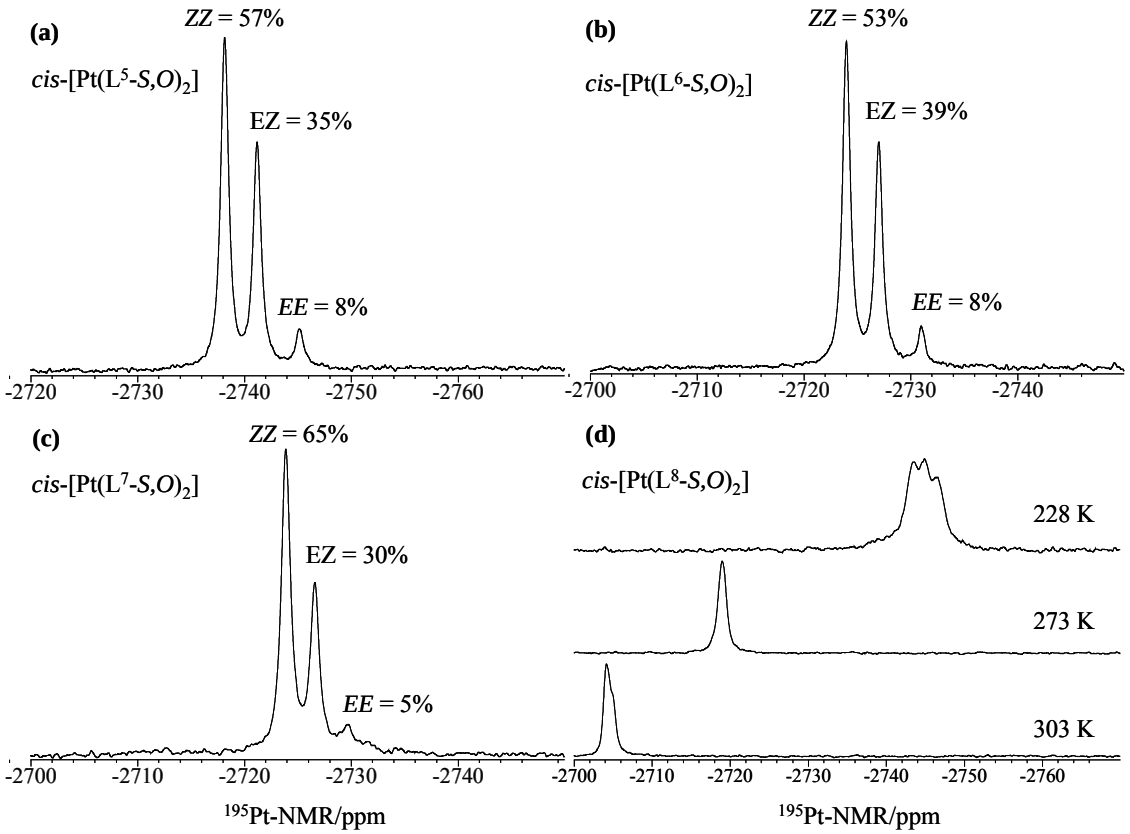

Figure 3.3: The 86 MHz ^{195}Pt NMR spectra of ***cis*-[Pt(L^{5,6,7,8}-*S,O*)$_2$]** showing their isomer distribution with the exception of ***cis*-[Pt(L^{8}-*S,O*)$_2$]** for which deconvolution analysis could not be performed. All the measurements were carried out in deuterated chloroform (at 303 K for ***cis*-[Pt(L^{5,6,7,8}-*S,O*)$_2$]** and at various temperatures for ***cis*-[Pt(L^{8}-*S,O*)$_2$]**)

Table 3.3 Assignments of δ(^{195}Pt) (ppm) and the relative distributions (taken from ^{195}Pt NMR deconvolution analysis) of configurational isomers of ***cis*-[Pt(L^{5,6,7,8}-*S,O*)$_2$]** complexes. ^{195}Pt NMR measurements were carried out in $CDCl_3$ at 298 K except for ***cis*-[Pt(L^8-*S,O*)$_2$]**, which was at 228 K. In parenthesis are the ^{1}H NMR integrals.

Complex	*ZZ*	*EZ*	*EE*
δ(^{195}Pt) ***cis*-[Pt(L^5-*S,O*)$_2$]**	-2738	-2741	-2745
[b]Statistical (%)	57	29	14
[a] Relative integrals (%)	57 (56)	35 (38)	8 (6)
δ(^{195}Pt) ***cis*-[Pt(L^6-*S,O*)$_2$]**	-2731	-2733	-2738
[b]Statistical (%)	63	25	12
[a] Relative integrals (%)	53 (54)	39 (39)	8 (7)
δ(^{195}Pt) ***cis*-[Pt(L^7-*S,O*)$_2$]**	-2724	-2727	-2730
[b]Statistical (%)	55	30	15
[a] Relative integrals (%)	65 (65)	30 (31)	5 (4)
δ(^{195}Pt) ***cis*-[Pt(L^8-*S,O*)$_2$]**	-2744	-2745	-2747
[b]Statistical (%)	10	20	70
[c]Relative integrals (%)	-	-	-

[a] The observed relative ^{195}Pt NMR integrals are estimated to have an error of ± 1%.
[b] Calculated from the *E,Z* distributions of the ligands assuming that they retain their configuration during and after complexation to the platinum(II) centre.
[c] Could not be measured reliably since these peaks are not well resolved even at 228 K.

3.3.2.3 Assignment of E,Z configurational isomer of platinum(II) chelates by multinuclear magnetic resonance spectroscopy

Thus far, the ^{195}Pt NMR spectra are presented such that the most downfield resonance is assigned to the *ZZ* isomer followed by the *EZ* isomer being further upfield, followed by the *EE* isomer. This assignment is not necessarily straightforward as the ambiguity being that the *EE* and *ZZ* assignments could be reversed. In the unbound ligands the argument of the magnetic anisotropy of the thiocarbonyl group deshielded the *N*-alkyl protons coplanar to it, was used. Due to an expected electronic delocalisation on the thiocarbonyl moiety upon ligand coordination to the Pt(II) metal centre it is uncertain that this thiocarbonyl group would display the same magnetic anisotropy. Since the deshielding effect of the thiocarbonyl moiety on the coplanar *N*-alkyl protons is in doubt, we cannot rely on this way of assigning the complexes.

Hence an alternative multinuclear NMR spectroscopic technique has been used for the assignment of these complexes. Only ***cis*-[Pt(L^{5,6,7}-*S,O*)$_2$]** complexes will be used as an illustration as to how these complexes are assigned. With the ***cis*-[Pt(L^8-*S,O*)$_2$]** complex we were limited by severe overlapping of the resonances in both the ^{1}H and ^{13}C NMR spectra as well as the low temperature necessity to observe the ^{195}Pt NMR resonances of the three

isomers (Figure 3.3), which are important for assigning of the isomers, however it is assumed that the assignments of its isomers follow the same trend as the other complexes.

In this context it is not necessary to show the full ^{1}H and ^{13}C NMR spectra of these complexes; only key sections of the spectra that lead to the assignments of these isomers are discussed. At room temperature for ***cis*-[Pt(L^{5}-*S,O*)$_2$]** and ***cis*-[Pt(L^{7}-*S,O*)$_2$]** complexes the ^{1}H NMR spectra show four singlet resonances for both *N*-CH_3 and *N*-CH_2- protons for the three isomers. Two resonances are of equal intensity within experimental error and are clearly due to the *EZ* isomer since this isomer has two slightly magnetically different 'halves' (on one side the ligand is orientated in the *Z* configuration and on the side the ligand is orientated in the *E* configuration). Having assigned the central resonance in the ^{195}Pt NMR spectra to the *EZ* isomer by comparing its relative integrated peak intensity to the resonances of equal intensity in the ^{1}H NMR spectra for both *N*-CH_3 and *N*-CH_2- regions, we are only left with the *ZZ* and *EE* isomers to assign. In the case of ***cis*-[Pt(L^{6}-*S,O*)$_2$]** only the *N*-CH_3 resonances have the described feature (i.e. four resonances are observed for the three isomers) so the same arguments hold for the assignment of the *EZ* isomer. Only two sets of the *N*-CH_2- triplet resonances are observed for the three isomers implying some overlapping of resonances. It is assumed that the *ZZ* and '*Z* half' of the *EZ* isomer (alternatively labelled as *Z(EZ)*) *N*-CH_2- protons overlap and contribute to one triplet resonance and that the *EE* and the '*E* half' of the *EZ* isomer (alternatively labelled as *E(EZ)*) *N*-CH_2- protons overlap and contribute to the second triplet resonance. This overlapping does not necessarily hamper the attempts of assigning the isomers of this particular complex, as the singlet *N*-CH_3 proton resonances suffice for the purpose of assignment. Figure 3.4 shows the *N*-CH_2- proton resonances of ***cis*-[Pt(L^{5}-*S,O*)$_2$]** and ***cis*-[Pt(L^{7}-*S,O*)$_2$]** and *N*-CH_3 proton resonances of ***cis*-[Pt(L^{6}-*S,O*)$_2$]**.

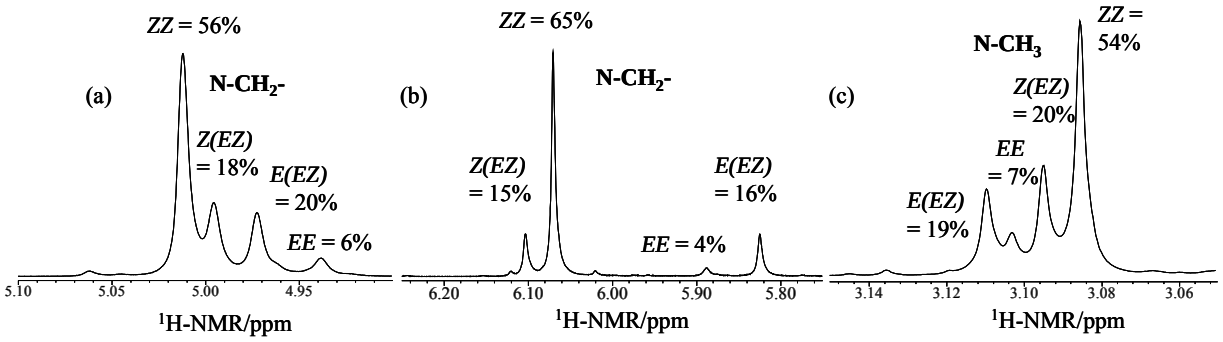

Figure 3.4 Sections of ^{1}H NMR spectra for (a) ***cis*-[Pt(L^{5}-*S,O*)$_2$]**, (b) ***cis*-[Pt(L^{7}-*S,O*)$_2$]** and (c) ***cis*-[Pt(L^{6}-*S,O*)$_2$]**, respectively. Deconvolution analyses show the relative populations of each isomer.

The relative populations of *ZZ*, *EZ* (combination of *Z(EZ)* and *E(EZ)*) and *EE* in the ^{1}H NMR spectra mirror the observed integrals of these isomers in the ^{195}Pt NMR spectra within experimental error.

In the ^{13}C NMR spectra of all the complexes, ***cis*-[Pt(L^{5,6,7}-*S,O*)$_2$]**, only two sets of *N*-CH_3 carbons and *N*-CH_2- carbons are observed, namely those in a favourable **W** coupling pathway. This implies that for *N*-CH_3 and *N*-CH_2- carbons the *ZZ* and *Z(EZ)* isomers overlap as one resonance while the *EE* and *E(EZ)* isomers overlap as the second resonance. Even though $^2J(^{195}Pt\text{-}^{13}C)$ couplings are not observable for the C(O) and C(S) carbons in the chelate ring, relatively broad $^4J(^{195}Pt\text{-}^{13}C)$ *ca* 20 Hz satellites are observed for *only* one set of *N*-CH_3 carbons as well as to *only* one set of the *N*-CH_2- carbons. These satellites were observed on an NMR spectrometer with a magnetic strength of 7.05 T (300 MHz ^{1}H frequency or 76 MHz ^{13}C frequency). Ideally for well-resolved satellites to be attained, the spectra should be run at even lower magnetic field spectrometer, however this was unfortunately not available. At higher magnetic field the $^4J(^{195}Pt\text{-}^{13}C)$ coupling satellites are lost due to field dependent chemical shift anisotropy broadening, which is characteristic of Pt(II) square planar complexes.[7] The set of *N*-CH_3 carbons and *N*-CH_2- carbons that show these $^4J(^{195}Pt\text{-}^{13}C)$ coupling satellites described above are orientated in a favourable **W** coupling pathway to the ^{195}Pt isotope (depicted by the bold lines in Scheme 1 and exemplified for ***cis*-[Pt(L^5-*S,O*)$_2$]** in Figure 3.5). Secondly, the *N*-alkyl groups that couple to the ^{195}Pt isotope appear relatively downfield relative to the *N*-alkyl groups that do not couple to the ^{195}Pt isotope (Figure 3.5). These findings are consistent with our observations described in the case of ***cis*-[Pt(L^4-*S,O*)$_2$]** with a symmetrically disubstituted ligand (Figure 3.2).

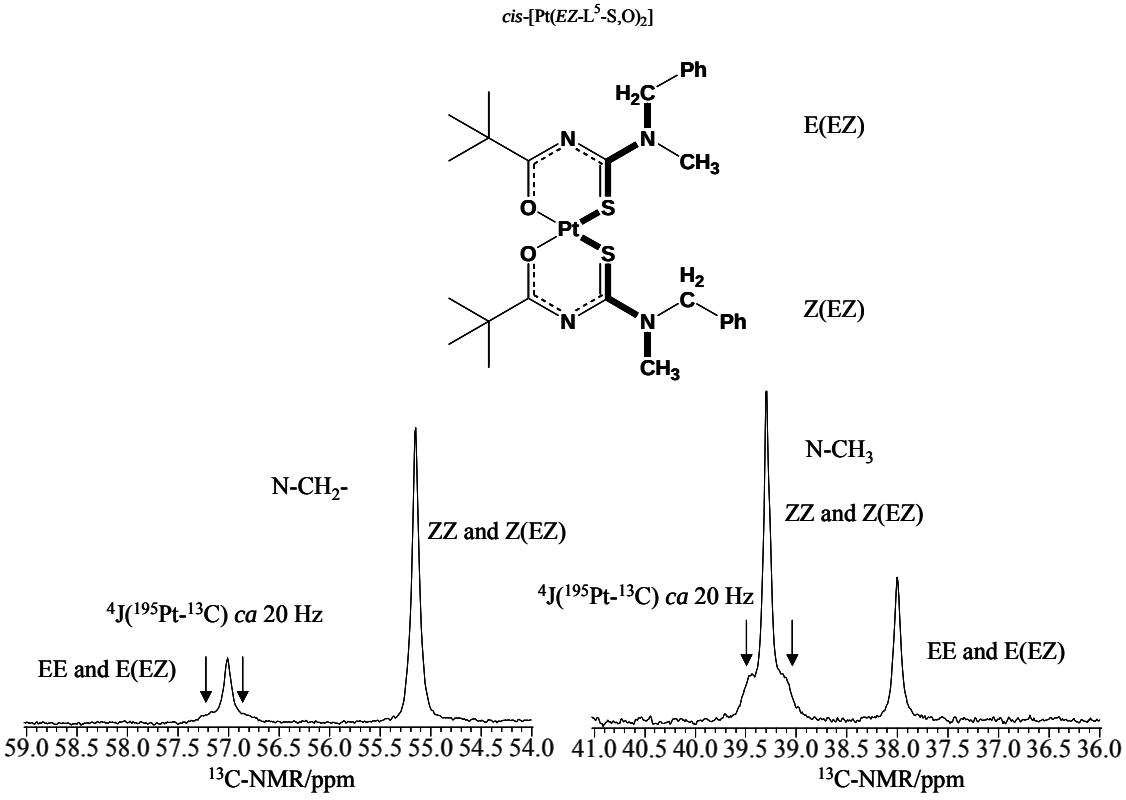

Figure 3.5 76 MHz ^{13}C frequency sections of the ^{13}C NMR spectrum of ***cis*-[Pt(L^5-*S,O*)$_2$]** showing *ZZ, EZ* and *EE* isomers $^4J(^{195}Pt\text{-}^{13}C)$ couplings to *N*-CH_2- carbons and *N*-CH_3 carbons via a **W** coupling pathway to the ^{195}Pt isotope.

In Figure 3.5 the ***cis*-[Pt(L^5-*S,O*)$_2$]** complex is used as an example to illustrate the $^4J(^{195}Pt\text{-}^{13}C)$ couplings, which are observed only for one set of *N*-CH_2- carbons and one set of *N*-CH_3 carbons. The *EZ* isomer is used in the figure since it has both components i.e. where the ligand is orientated in both the *E* and *Z* configurations.

The combined observations from the ^{1}H NMR spectra and low magnetic field ^{13}C NMR spectra allow for a combination of low magnetic field ^{13}C NMR spectra and high-resolution gHSQC ($^1H/^{13}C$) correlation 2D NMR spectra which consequently assigned the three ^{195}Pt NMR resonances of the resultant complexes. This should be possible since the platinum nuclei are linked spatially to specific *N*-alkyl carbons (via the **W** coupling pathway described above) and the gHSQC ($^1H/^{13}C$) experiment can in turn be used to link the *N*-alkyl carbons with the protons directly attached to them. The relative populations of the *ZZ*, *EZ* and *EE* isomers link the ^{1}H resonances with the ^{195}Pt resonances. The combination of the two techniques should in principle result in the same assignments as would be achieved by means of triple resonance $^1H\text{-}(^{13}C)\text{-}^{195}Pt$ correlation NMR spectroscopy that was described by us[6] for complexes with same structural motif.

From the sections of the ^{13}C NMR spectrum presented in Figure 3.5 for ***cis*-[Pt(L^5-*S,O*)$_2$]** it seems that the *EE* isomer is the minor isomer relative to the *ZZ* isomer since the *EE* and the *E(EZ)* isomers give rise to the lower intensity *N*-CH_2- and *N*-CH_3 carbon resonances. By looking at the *N*-CH_2- carbon resonance, for example, the *EE* isomer is thought to be the minor isomer, however, there are two opposing factors that contribute to the intensity of this resonance. First and far most the NMR active 33.8 % natural abundance ^{195}Pt nuclei to which this *N*-CH_2- carbon is coupled diminishes the intensity of this resonance. Secondly this resonance is a contribution of two isomers, the *EE* and *E(EZ)*, which should intensify the *N*-CH_2- carbon resonance. These two effects make it complicated to assign the ^{195}Pt resonance from ^{13}C NMR spectrum alone. In order to draw unambiguous conclusions, a gHSQC ($^1H/^{13}C$) spectrum was recorded confirming that the *EE* isomer is indeed the minor isomer (with respect to the *ZZ* isomer).(Figure 3.6).

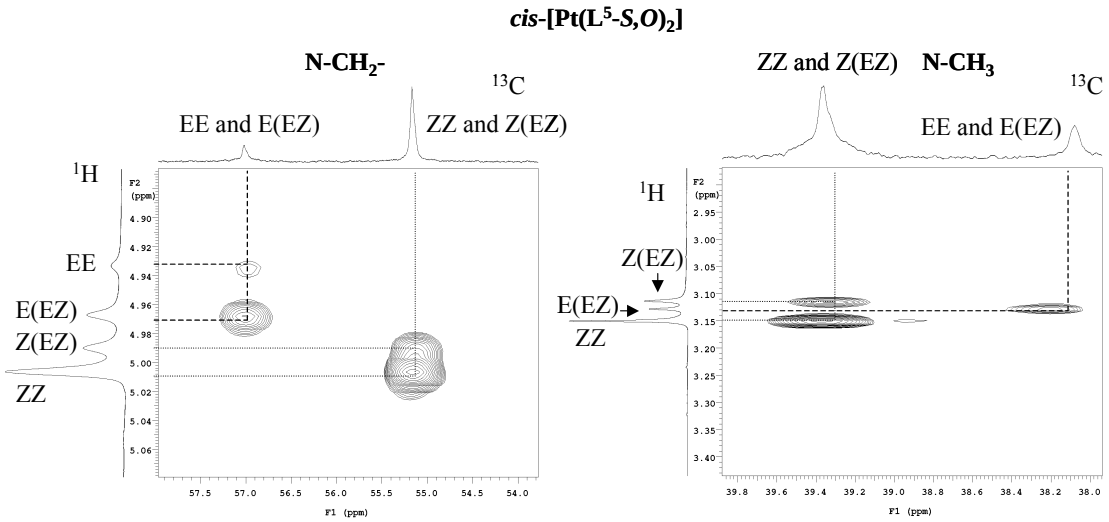

Figure 3.6 A section of a gHSQC ($^{1}H/^{13}C$) NMR spectrum for ***cis*-[Pt(L^5-*S,O*)$_2$]** complex, showing the connection between the *N*-CH_2- protons and the *N*-CH_2- carbons and the connection between the *N*-CH_3 protons and the *N*-CH_3 carbons to which they are attached.

The ^{1}H resonance of smallest intensity at 4.94 ppm shows a cross peak to the *N*-CH_2- ^{13}C resonance in which the ligand is orientated in the *E* configuration. The ^{1}H resonance of highest intensity at 5.01 ppm on the other hand has a cross peak with the *N*-CH_2- carbon in which the ligand is orientated in the *Z* configuration. Clearly, this assignment should be the same in the *EE*, *EZ* and *ZZ* resonances observed in the ^{195}Pt NMR spectrum (Figure 3.3), therefore assigning the most upfield ^{195}Pt resonance to the *ZZ* isomer and the most downfield resonance to the *EE* isomer in the ^{195}Pt NMR spectrum. As a means of confirming the above assignments, the same analysis is done for the *N*-CH_3 (^{1}H and ^{13}C) resonances. From the ^{1}H NMR spectrum, unfortunately, the resonance due to the minor isomer is not observable as a result of unexpected overlapping. However, it can be argued that if one *N*-CH_3 proton resonance at 3.16 ppm (the major isomer in this case) has a cross peak with the *N*-CH_3 carbon in the **W** pathway to the ^{195}Pt isotope then the other *N*-CH_3 proton resonance due to the minor isomer should in principle have a cross peak with the other *N*-CH_3 carbon. This should be the case since they lie in different orientations, one in the *E* orientation in the *EE* isomer and the other in the *Z* orientation in the *ZZ* isomer. This claim is well illustrated by the *Z(EZ)* and *E(EZ)* ^{1}H resonances for both *N*-CH_2- and *N*-CH_3 in Figure 3.6. For example, the *E(EZ)* proton resonance at 4.97 ppm for the *N*-CH_2- protons is correlated to the *EE* and *E(EZ)* *N*-CH_2- carbon resonance. On the other had the Z(EZ) proton resonance at 4.99 ppm for *N*-CH_2- protons is correlated to the *ZZ* and *Z(EZ)* *N*-CH_2- carbon resonance.

As already stated, in the ***cis*-[Pt(L^6-*S,O*)$_2$]** complex there is an overlap of the *N*-CH_2- proton resonances and only the *N*-CH_3 (^{1}H and ^{13}C) resonances can be used in the gHSQC ($^{1}H/^{13}C$) NMR spectrum for the assignment of *EE* and *ZZ* isomers (Figure 3.7). The ^{1}H *N*-CH_3 resonance at 3.08 ppm (due to the major isomer) has a cross peak with the

downfield *N*-CH_3 carbon, implying that it is in the *Z* configuration. Unfortunately, the cross peak for the ^{1}H *N*-CH_3 resonance at 3.10 ppm is not clearly observable but is expected to be correlated with the upfield *N*-CH_3 carbon.

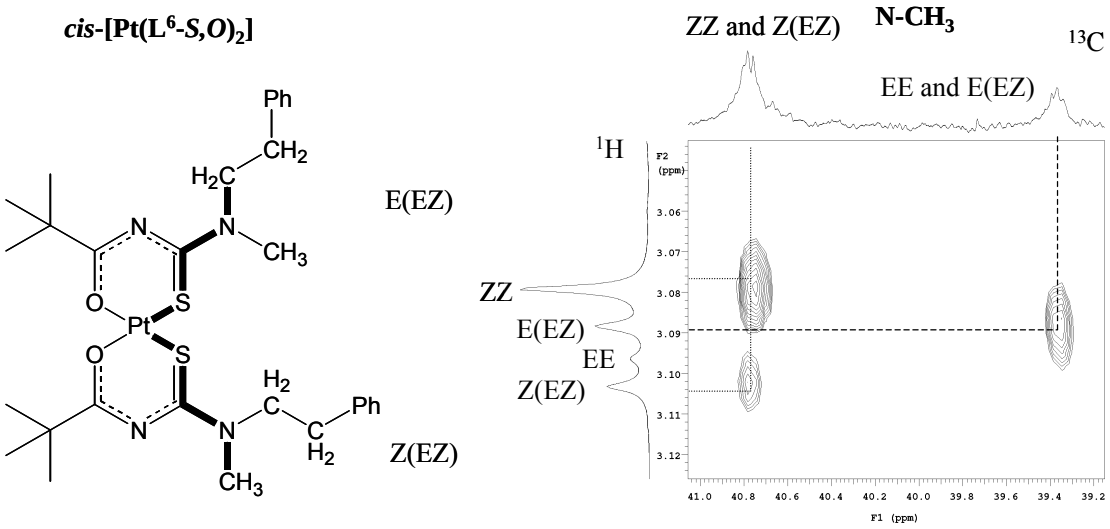

Figure 3.7 A section of a gHSQC (^{1}H/^{13}C) NMR spectrum for ***cis*-[Pt(L^6-*S,O*)$_2$]** complex, showing the connection between the *N*-CH_3 protons and the *N*-CH_3 carbons to which they are attached.

In the case of the ***cis*-[Pt(L^7-*S,O*)$_2$]** complex which is very similar to the ***cis*-[Pt(L^5-*S,O*)$_2$]** complex results in a clearer assignment since all the expected cross peaks in the gHSQC (^{1}H/^{13}C) spectrum for both *N*-CH_2- and *N*-CH_3 resonances are observed with no overlapping (Figure 3.8). Once again the *ZZ* isomer is the major component while the *EE* isomer is in the minor component for the same reasons presented for the ***cis*-[Pt(L^5-*S,O*)$_2$]** complex and therefore the downfield resonance at -2724 ppm in the ^{195}Pt NMR spectrum must be due to the *ZZ* isomer while the most upfield resonance at -2730 ppm is due to the *EE* isomer.

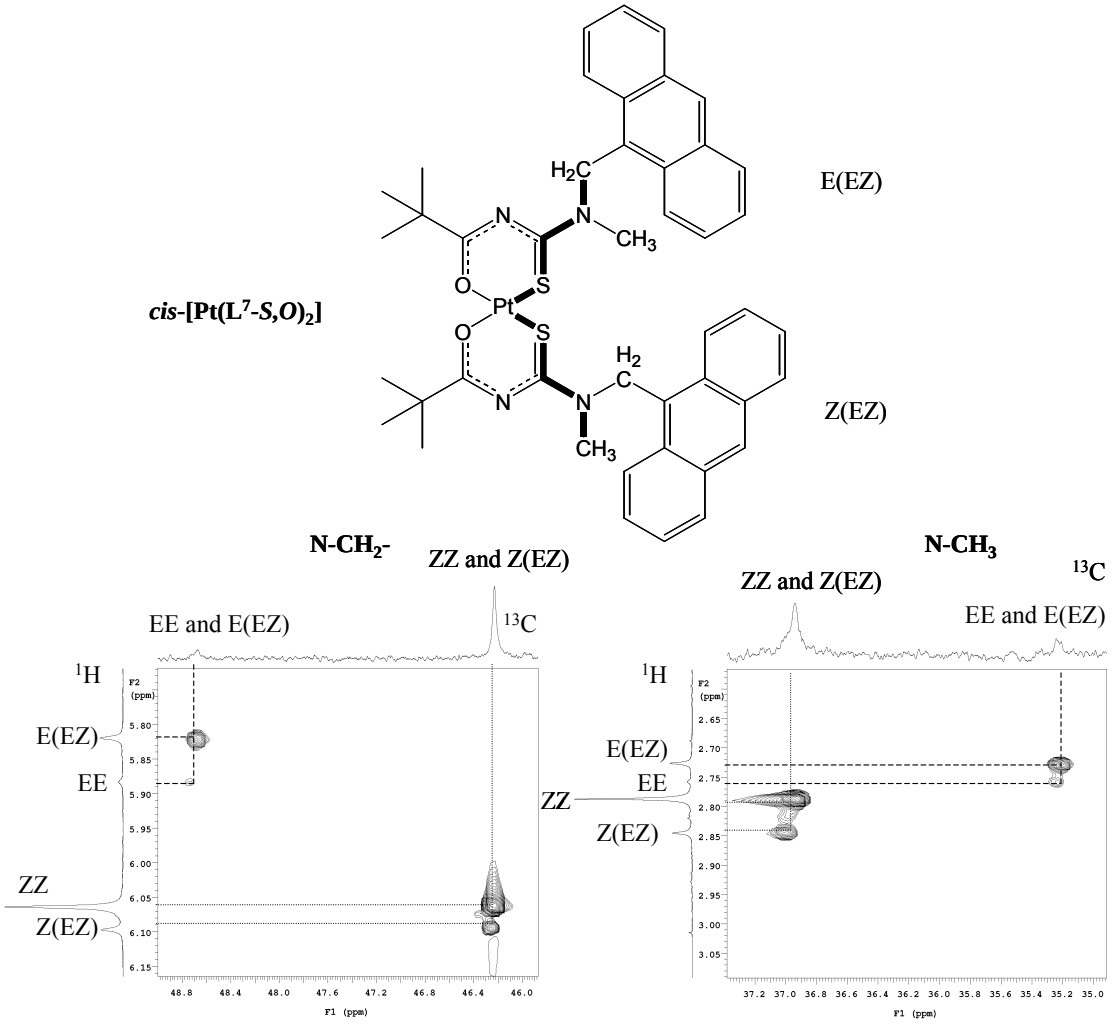

Figure 3.8 A section of a gHSQC ($^{1}H/^{13}C$) NMR spectrum for ***cis*-[Pt(L^{7}-*S,O*)$_2$]** complex, showing the correlation between the *N*-CH_2- protons and the *N*-CH_2- carbons and the correlation between the *N*-CH_3 protons and the *N*-CH_3 carbons to which they are attached.

Since the ligands were assigned by arguing that the magnetic anisotropy of the thiocarbonyl group deshields the *N*-alkyl groups coplanar to it, it is tempting to assign the isomers of the *ZZ*, *EZ* and *EE* Pt(II) configurational isomers in the same manner. This method seems to work if it is employed to the *N*-CH_2- protons (in both Figure 3.6 and 3.8) since the most downfield resonance (as it would be deshielded by the thiocarbonyl group) belong to the major component. However this way of assigning should also be consistent in that the *N*-CH_3 protons of the major component should be upfield relative to those of the minor component. That should be the case since the *N*-CH_3 protons are now coplanar to the thiocarbonyl group and therefore should be more deshielded and resonate downfield. This consistency was observed throughout when the unbound ligands were assigned by this method. In the case of the complexes particularly the much clearer gHSQC ($^{1}H/^{13}C$) NMR spectrum of ***cis*-[Pt(L^{7}-*S,O*)$_2$]** complex illustrates

discrepancy in the chemical shift positions of the *N*-CH_3 protons. It is not so easy to show this discrepancy in the case of ***cis*-[Pt(L^5-*S,O*)$_2$]** since the *N*-CH_3 proton resonance of the minor component is not observed due to overlapping. It seems therefore that the magnetic anisotropy of the thiocarbonyl group in the coordinated ligand is not entirely the same as that of the unbound ligand and cannot be used reliably for assigning the complexes.

3.3.3.4 Comment on isomer distributions

It only remains to make some comments about the isomer distributions observed for the resultant chelates. In Table 3.3 the first thing to note is that the isomer distributions attained are not the same as the statistically predicted ones. The second observation is that deviations from the statistically predicted distributions also occur among ligands with nearly the same *E,Z* isomer distributions (e.g. HL^5 and HL^7). Comparing the distributions of the complexes derived from *N*-phenethyl-*N*-methyl-*N'-2,2*-dimethylpropanoylthiourea, HL^6 with those obtained from a ligand with the same 75% *Z* : 25% *E* isomer ratio, *N*-ethyl-*N*-methyl-*N'-2,2*-dimethylpropanoylthiourea,[6] we find that the differences are even more pronounced. The isomer ratio for a complex derived from this particular ligand was such that the *EZ* isomer was favoured (47%) followed by the *ZZ* isomer (40%) then the *EE* isomer with (13%). It seems that the isomer ratio of the ligand itself may not be the factor that directs isomer distribution that is attained in the resultant complexes. In this chapter we do not attempt to resolve this question and that is left for the following two chapters.

3.4 Concluding remarks

In a series of unsymmetrical dialkyl-substituted ligands that display *E,Z* configurational isomerism at room temperature, it was easily illustrated from ^{1}H and ^{195}Pt NMR spectroscopy that these ligands carry through this isomerism to the resultant platinum(II) chelates derived from them; the *ZZ* configurational isomer is favoured in all the complexes described in this chapter. By means of a low magnetic field ^{13}C NMR spectroscopy, long range $^4J(^{195}\text{Pt}\text{-}^{13}\text{C})$ coupling could be observed between the ^{195}Pt nucleus and *N*-alkyl carbons that are only orientated in a **W** pathway to the ^{195}Pt nucleus itself. This factor together with the good dispersion of the *N*-alkyl protons allowed us to indirectly link the ^{195}Pt resonances with the *N*-alkyl protons via 2D gHSQC (^{1}H/^{13}C) experiments, therefore assigning the ***cis*-[Pt(*ZZ*-$L^{5,6,7}$-*S,O*)$_2$]**, ***cis*-[Pt(*EZ*-$L^{5,6,7}$-*S,O*)$_2$]** and ***cis*-[Pt(*EE*-$L^{5,6,7}$-*S,O*)$_2$]** configurational isomer in all of the ^{1}H, ^{13}C and ^{195}Pt NMR spectra. This technique could not be employed in the case of ***cis*-[Pt(*ZZ*-L^8-*S,O*)$_2$]** due to severe overlapping in both ^{1}H and ^{13}C NMR spectra but it is assumed that the assignments of the ^{195}Pt resonances (which were only observable at 228 K) of this complex are similar to the others i.e. the most downfield resonance is due to the *ZZ* isomer followed by the *EZ* isomer then by the *EE* isomer. We observed that the *E,Z* isomer distributions of the unbound ligands may not necessarily be the factor that determines the *ZZ*, *EZ* and *EE* isomer distributions of the resultant complexes. A detailed probe into the factors that affect these isomer distributions is evaluated in the next two chapters.

References

1 K. R. Koch, C. Sacht, T. Grimmbacher, and S. Bourne, *S. Afr. J. Chem.*, **1995**, *48*, 71.
2 K. R. Koch, *Coord. Chem. Rev.*, **2001**, *216-217*, 473.
3 B. T. Brown and G. F. Katekar, *Tetrahedron Lett.*, **1969**, 2343.
4 K. E. Laidig and L. M. Cameron, *J. Am. Chem. Soc.*, **1996**, *118*, 1737.
5 D. Lauvergnat and P. C. Hiberty, *J. Am. Chem. Soc.*, **1997**, *119*, 9478.
6 D. Argyropoulos, E. Hoffmann, S. Mtongana, and K. R. Koch, *Magn. Reson. Chem.*, **2003**, *41*, 102.
7 J. Y. Lallemand, J. Soulie, and J. C. Chottard, *J. Chem. Soc., Chem. Comm.*, **1980**, 436.
8 K. R. Koch and M. C. Matoetoe, *Magn. Reson. Chem.*, **1991**, *29*, 1158.
9 J. D. S. Miller, *PhD Thesis, University of Cape Town*, **2000**.

Chapter 4: Coordination chemistry of asymmetrically disubstituted *N*-alkyl-*N*-aryl-*N'*-acylthioureas to platinum(II)

Part 2: The electronic influence of the *para*-substituent, X (X = O-CH_3, H and NO_2) of the *N*-(*para*-X-Ph) group on the isomer distribution of *E,Z* configurational isomers of platinum(II) complexes of *N*-methyl-*N*-(*para*-X-Ph)-*N'*-acylthioureas

Summary

In a series of asymmetrically disubstituted ligands of the type *N*-alkyl-*N*-aryl-*N'*-*2,2*-dimethylpropanoylthiourea, the degree of double bond character observed for the thiourea (S)C-N(Me)(*para*-X-Ph) bond (X = O-CH_3, H and NO_2) results in the formation of two possible configurational (*E* and *Z*) isomers of the ligand, reflecting the relative orientation of the aryl moiety with respect to the thiocarbonyl moiety. In solid state, it appears that the *E* orientation is favoured for *N*-methyl-*N*-(4-methoxy-phenyl)-*N'*-(*2,2*-dimethylpropanoyl)thiourea, HL^{1A} and *N*-methyl-*N*-phenyl-*N'*-(*2,2*-dimethylpropanoyl)thiourea, HL^{2A} while in solution at low temperature both of these ligands display *E*/*Z* configurational isomerism. The relative amounts of *E* and *Z* isomers are roughly 90% : 10% for both HL^{1A} and HL^{2A} based on deconvolution analysis of their respective ^{1}H NMR spectra measured at 243 K. The *E* and *Z* isomers of a similar ligand *N*-methyl-*N*-(4-nitro-phenyl)-*N'*-(*2,2*-dimethylpropanoyl)thiourea, HL^{3A} could not separate to individual resonances even at 198 K. The platinum chelates derived from these ligands adopt *EE*, *EZ* and *ZZ* orientations with varying isomer distributions depending on the *para*-substituent X of the *N*-(*para*-X-Ph) group.

Dynamic NMR complemented by DFT linear transit calculations reveal that the barrier to rotation around the (S)C-N(Me)(*para*-X-Ph) bond of ligands and complexes follows the order: X = O-CH_3 > H > NO_2 with X being the *para*-substituent on the aromatic ring. The *ZZ* isomer was observed to be favoured over the *EZ* and *EE* isomers increasingly so in the same order. Importantly therefore, the predominantly configuration has consistently changed going from the ligands to the corresponding Pt(II) complexes. Calculations of the Gibbs free energies of activation, $G^{\neq}_c$, using the coalescence temperatures of these complexes appear to support our findings that the *ZZ* is the energetically favoured isomer, although the energy difference between the *ZZ* and *EE* complexes was found to be only small (*ca* 2 kcal/mol).

4.1 Introduction

In the previous chapter it was shown by means of multinuclear NMR spectroscopy how the ^{195}Pt NMR spectra of the *ZZ*, *EZ* and *EE* configurational isomers of platinum(II) chelates derived from asymmetrically disubstituted *N,N*-dialkyl-*N'*-acylthioureas could be assigned. In turned out generally that the most downfield ^{195}Pt resonance was due to the *ZZ* isomer followed by the *EZ* isomer while the most upfield ^{195}Pt resonance was due to the *EE* isomer. The isomer distributions were also skewed towards the *ZZ* isomer and the *EE* isomer was the least favoured. Having managed to assign the isomers of the Pt(II) chelates discussed in chapter 3, the question of what determines these isomer distributions was next to be undertaken.

This question arose since it was observed that the *E,Z* isomer distributions of the unbound ligands seemed to pay little role in distribution of the *ZZ*, *EZ* and *EE* of the resultant complexes. The question of factors that influence the isomer distributions has been dealt with in two chapters. In this chapter the primary focus was the effect of electronic factors of the R and R' groups of the (S)C-NRR' moiety. For this purpose a new range of ligands was synthesised in which one *N*-alkyl group was fixed while systematic 'electronic' variations on *N*-aryl group were made. In this new repertoire of unsymmetrical *N*-alkyl-*N*-aryl-*N'*-acylthioureas there is no alkyl spacer between the nitrogen atom and the aromatic ring in the -(S)C-N(R)(*para*-X-Ph) moiety with (X = O-CH_3, H and NO_2), as it was the case in some the ligands discussed in the previous chapter (Figure 4.1).

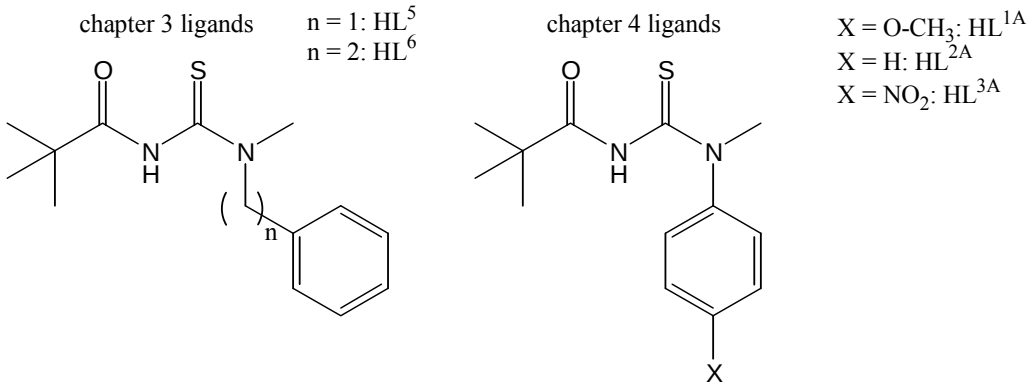

Figure 4.1 Structural differences between the new range of ligands discussed in this chapter and those discussed in chapter 3.

Removal of the alkyl spacer appears to reduce the barrier to rotational around the (S)C-N(Me)(Ar) bond significantly compared to the system of ligands with an alkyl spacer; on the basis that the two sets of *N*-CH_3 resonances due to the *E*/*Z* configurational isomers are only observed at low temperatures unlike the ligands in the previous chapter where these resonances were clear at room temperature. Lowering of the rotational barrier due to aromatic substituents in

N-arylthiocarbamates and N-aryldithiocarbamates[1] and vinyl substituents in N-vinyl substituted amides[2] is a known phenomenon in the literature. It is generally thought that there is a 'cross conjugation' competition for the lone pair electrons on the nitrogen atom as they may either contribute towards the (S)C-N(R)(*para*-X-Ph) bond or be pulled towards the aromatic ring.[1] If the lone pair is pulled towards the aromatic ring one can picture that electron donating/electron pulling substituents on the aromatic ring will have an effect on the rotation barrier of the (S)C-N(R)(*para*-X-Ph) bond. In this regard we have synthesised ligands bearing three different *para*-substituents on the *N*-aryl group of the ligands *viz*: a methoxy group (which is electron-donating), a nitro group (which is electron-withdrawing) and no substituent (which is an intermediate of the two extremes).

Low temperature (278 K to 243 K) ^{1}H and ^{13}C NMR spectra of the ligands in discussion (HL^{1A}, HL^{2A} and HL^{3A}) clearly demonstrate the existence of two isomers while at room temperature (298 K) this is not as apparent. Not understanding the subtleties of the lowered (S)C-N(R)(*para*-X-Ph) bond rotation barrier present in HL^{1A}, HL^{2A} and HL^{3A} at the time, their initial characterisation in solution, at room temperature, together with their crystal structures, initially suggested that the ligands are only oriented in the *E* conformation. It remained a puzzle as to why, on complexation to the platinum(II) centre all three isomers ***cis*-[Pt(*EE*-$L^{1A,2A}$-*S,O*)$_2$]**, ***cis*-[Pt(*EZ*-$L^{1A,2A}$-*S,O*)$_2$]** and ***cis*-[Pt(*ZZ*-$L^{1A,2A}$-*S,O*)$_2$]** were formed (see Scheme 1).

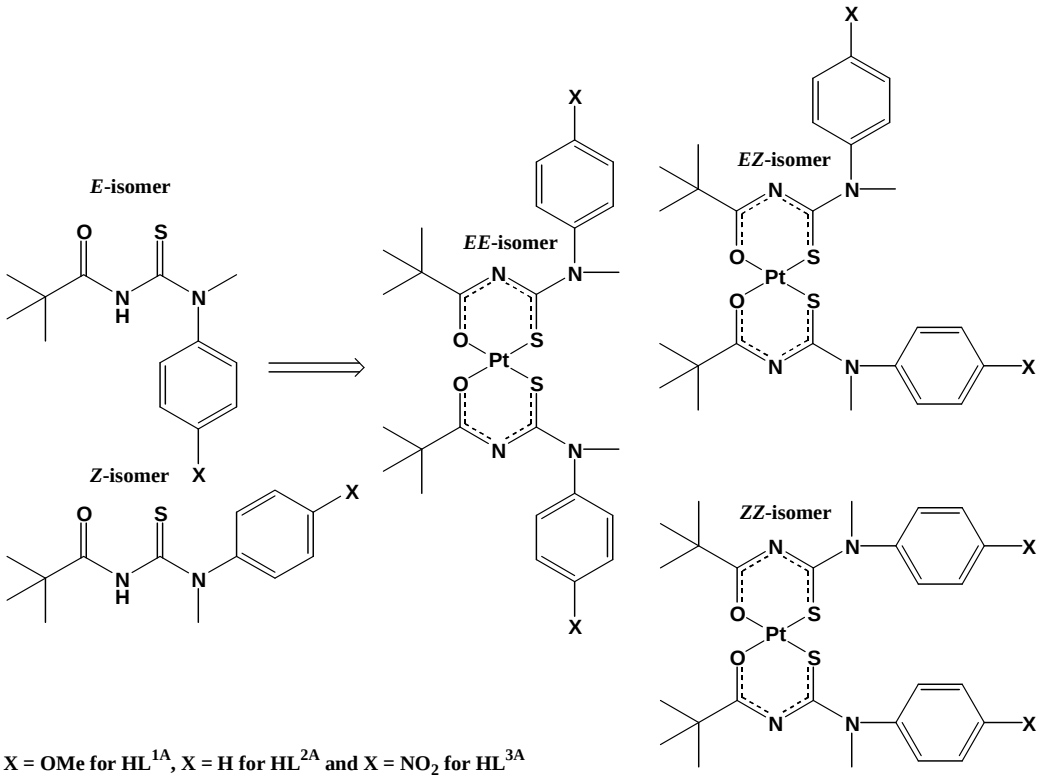

Scheme1 On complexation to $[PtCl_4]^{2-}$ the *E/Z* isomerism in the uncoordinated ligands is relayed to their platinum chelates ***cis*-[*EE*-Pt($L^{1A,2A,3A}$-*S,O*)$_2$]**, ***cis*-[*EZ*-Pt($L^{1A,2A,3A}$-*S,O*)$_2$]** and ***cis*-[*ZZ*-Pt($L^{1A,2A,3A}$-*S,O*)$_2$]**.

The presence of three isomers was evident from the distinct chemical environment the ^{195}Pt nuclei of these configurational isomers which led to separate resonances in the ^{195}Pt NMR spectra. However, the presence of two isomers as reflected by duplication peaks in ^{1}H and ^{13}C NMR spectra of the ligands (HL^{1A} and HL^{2A}) *only* to be revealed at low temperature logically explained this puzzle. Low temperature ^{1}H NMR also assisted in the determination of the *E*/*Z* isomer ratios in the unbound ligands. However, under identical conditions HL^{3A} displays no evidence of the second isomer, which presents an interesting conundrum since this ligand is structurally similar to the other two (HL^{1A} and HL^{2A}) the only difference being the nitro group at the *para* position of the *N*-aryl group. The two isomers could not be observed as separate signals despite the solvent change from chloroform to dichloromethane, a solvent with a lower freezing point. On complexation though, ^{1}H and ^{13}C NMR spectra of the complex reveal the characteristic 'pattern' when three isomers are present (i.e. two peaks due to two isomers, *EE* and *ZZ* and two other peaks due to the *EZ* isomer). The ^{195}Pt NMR spectrum in dichloromethane was nevertheless not well resolved even at 198 K.

In this chapter we primarily analyse electronic effects of remote substituents transferred through an aromatic ring on the rotational barrier of the (S)C-N(R)(*para*-X-Ph) bond and the effects thereof on the configurational isomer distributions of the platinum(II) chelates derived from the *N*-methyl-*N*-(*para*-X-phenyl)-*N'*-acylthiourea ligands. As it happened unintended for this chapter the role of solvent and temperature at which the configurational isomers are measured are also discussed for reasons that will be clear later.

4.2 Experimental

4.2.1 General remarks

The synthesis and characterisation of ligands has already been described in detail in **chapter 2**, however, for comparison with the platinum(II) chelates derived from these ligands their NMR assignments will be discussed.

4.2.2 NMR spectroscopy

Conventional ^{1}H and ^{13}C NMR spectra of relatively high concentrations (*ca* 80 mg.cm^{-3}) of the ligands and their respective platinum(II) complexes using 5 mm diameter tubes were obtained at various temperatures in deuterated chloroform using a Varian Inova 400 spectrometer operating at 400 and 101 MHz for ^{1}H and ^{13}C, respectively. Additionally, an alternative solvent (deuterated dichloromethane) was used to enable analysis to be carried out at even lower temperatures. This was necessary so since HL^{3A} and the platinum complex derived from this ligand could not be adequately analysed at the temperatures at which other compounds were analysed. The coalescence temperature, T_c reported in this chapter is the minimum temperature at which the signals arising from *N*-CH_3 proton signals of all the isomers are no longer distinguishable. The precision of the T_c determinations was estimated by recording the ^{1}H NMR spectra in 1 °C increments over a 5 °C range around each of the T_c's. All samples were

carefully filtered before any spectroscopic measurement was undertaken. ^{1}H chemical shifts are quoted relative to the residual $CDCl_3$ solvent resonance at 7.26 ppm and the ^{13}C chemical shifts are quoted relative to the $CDCl_3$ middle resonance of the triplet at 77.0 ppm. In the case where CD_2Cl_2 is used as the solvent, ^{1}H chemical shifts are quoted relative to the solvent triplet resonance at 5.31 ppm and the ^{13}C chemical shifts are quoted relative solvent quintet resonance at 55.8 ppm. The ^{195}Pt NMR spectra of the complexes were also recorded at various temperatures using the Varian Inova 400 spectrometer operating at 86 MHz [reference material: 500 mg.cm^{-3} H_2PtCl_6 in 30% (v/v) D_2O-1M HCl at $\delta(^{195}Pt) = 0$ ppm at 30 °C].

4.2.3 Density Functional Theory calculations: Computational details

In order to model the influence of the *para*-substituents on the barrier to rotation around the C-N bond, model Pt(II) complexes were chosen over the ligands. The main reason is that the unbound ligands have many degrees of freedom with regard to C-N bond rotations and this would lead to a complex energy surface that is computationally time consuming to workout. For the determination of the relative barriers to rotation around the (S)C-N(Me)(*para*-X-Ph) bond of the Pt(II) complexes as the *para*-substituent is altered from a methoxy group to hydrogen atom to a nitro group, we chose two model systems. In **model 1** the *cis*-bis Pt(II) complex is coordinated with two different ligands *N,N*-dimethyl-*N'*-methylthiourea and *N*-methyl-*N*-(*para*-X-phenyl)-*N'*-methylthiourea. Geometrical optimisation of this complex was performed before the rotation around the C-N bond of interest was done from where the ligand is initially orientated in an *E* position to a final *Z* position (Scheme 2(a)). In **model 2** the *cis*-bis Pt(II) complex is coordinated with two identical ligands of the type *N*-methyl-*N*-(*para*-X-phenyl)-*N'*-methylthiourea. Again geometrical optimisation of this complex was performed with the both ligands in an *E* orientation (i.e. the complex is the *EE* configurational isomer). The rotation about the C-N bond of interest was done on one of the ligands such that after nearly 180-degree rotation an *EZ* complex is obtained. Continuing the increment rotations of this C-N bond for a further *ca* 180-degree rotation the complex is found in the initial *EE* configuration (Scheme 2(b)).

All calculations were performed with the ADF (Amsterdam Density Functional) suite of programs,[3] release 2004.01 and 2005.01. For the restricted ground-state calculations, which included geometry optimisations, and linear conformational scans, we selected the following procedures. We made use of the local density approximation (LDA) functional of Vosko-Wilk-Nusair (VWN),[4] augmented with the non-local gradient correction PW91 from Perdew *et al.*[5] Relativistic effects have been taken into account using the scalar relativistic (SR) zero-order regular approximation (ZORA).[6] The ZORA basis sets used were of triple ζ plus polarization Slater type function (STO) quality (basis TZP in ADF).

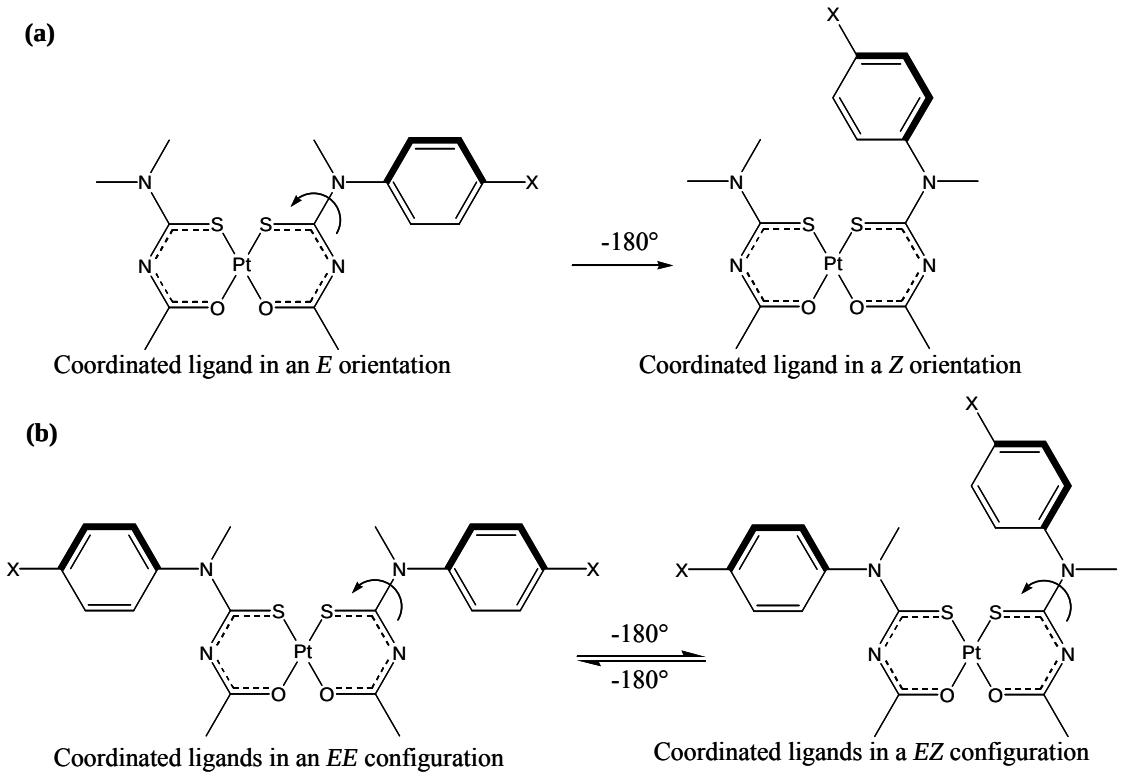

Scheme 2 (a) **Model 1** allows the estimation of the barrier to rotation around the (S)C-N(Me)(*para*-X-Ph) bond of the Pt(II) complexes for *para*-substituent, X = O-CH_3, H and NO_2 as the ligand rotates through 180º angle from the *E* orientation to the *Z* orientation. (b) **Model 2** achieves the same result and is much better model to the actual platinum(II) chelates in Scheme 1.

4.2.4 Synthesis of platinum complexes

Platinum(II) complexes were prepared and characterised according to our previously published method,[7] which entails drop-wise addition a platinum(II) solution (in a one to one volume of acetonitrile to water) to a solution of ligand and sodium acetate (also in a one to one volume of acetonitrile to water). All the reagents were commercially available and were used without any prior purification. The reactions were generally conducted at 50 ºC for two hours. After the reaction solutions had cooled to room temperature, excess water was added and reaction mixtures were refrigerated before the products were collected by means of centrifugation and dried under vacuum. Elemental analyses were performed using a Carlo Erba EA 1108 elemental analyser courtesy of the University of Cape Town. Detailed ^{1}H and ^{13}C NMR spectroscopic data for the new complexes follows the numbering scheme indicated Scheme 3. For the ^{1}H NMR assignments the carbon to which the protons are attached will be indicated.

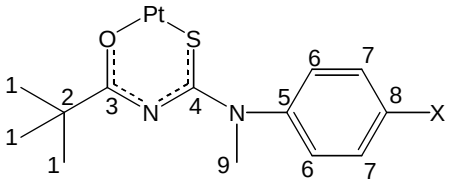

Scheme 3 Numbering scheme for ^{1}H and ^{13}C NMR assignments of the new complexes. The coordinated ligand is only drawn in a *Z* orientation.

***cis*-bis(*N*-Methyl-*N*-(4-methoxy-phenyl)-*N'*-*2,2*-dimethylpropanoylthioureato)platinum(II), *cis*-[Pt(L^{1A}-*S,O*)$_2$]**: A yield of 81% was collected and analysed. Found C 44.85, H 5.11, N 7.65 and S 8.54 $C_{30}H_{40}N_2O_2PtS_2$ required C 44.61, H 5.08, N 7.43 and S 8.51%. δ_H(400 MHz; solvent $CDCl_3$): 7.21 (2H, d, C_6 EZ), 7.10 (2H, d, C_6 ZZ), 7.03 (2H, d, C_6 EE), 6.92 (2H, d, C_7 EZ), 6.84 (2H, d, C_7 ZZ), 3.50 (1H, s, C_9 EE), 3.43 (1H, s, C_9 E(EZ)), 3.37 (1H, s, C_9 ZZ), 3.36 (1H, s, C_9 Z(EZ)), 3.82 (3H, s, O-CH_3 EE), 3.81 (3H, s, O-CH_3 E(EZ)), 3.80 (3H, s, O-CH_3 Z(EZ)), 3.76 (3H, s, O-CH_3 EE), 1.24 (9H, s, C_1 Z(EZ)), 1.22 (9H, s, C_1 ZZ), 0.87 (9H, s, C_1 EE), 0.85 (9H, s, C_1 E(EZ)). δ_C(101 MHz, solvent $CDCl_3$): 183.89 C_3 Z(EZ), 183.68 C_3 ZZ, 182.79 C_3 (EE), 182.65 C_3 E(EZ), 168.08 C_4 ZZ, 168.00 C_4 Z(EZ), 167.83 C_4 E(EZ), 158.42 C_8 Z(EZ), 158.24 C_8 ZZ, 157.32 C_8 EE, 157.23 C_8 E(EZ), 138.74 C_5 E(EZ), 137.94 C_5 Z(EZ), 137.90 C_5 ZZ, 128.24 C_6 Z(EZ), 128.15 C_6 ZZ, 126.99 C_6 E(EZ), 114.46 C_7 Z(EZ), 114.36 C_7 ZZ, 113.24 C_7 EE, 113.17 C_7 E(EZ), 54.40 (O-CH_3) ZZ, EZ and EE, 42.29 C_9 Z(EZ), 42.23 C_9 ZZ, 41.86 C_9 EE, 41.79 C_9 E(EZ), 42.79 C_2 EE, 42.61 C_2 E(EZ), 42.42 C_2 Z(EZ), 42.35 C_2 ZZ, 28.13 C_1 ZZ and Z(EZ), 27.50 C_1 EE and E(EZ).

***cis*-bis(*N*-Methyl-*N*-phenyl-*N'*-*2,2*-dimethylpropanoylthioureato)platinum(II), *cis*-[Pt(L^{2A}-*S,O*)$_2$]**: A yield of 91% was collected and analysed. Found C 45.20, H 4.94, N 8.00 and S 9.08 $C_{28}H_{36}N_2O_2PtS_2$ required C 45.01, H 4.94, N 8.08 and S 9.24%. δ_H(400 MHz; solvent $CDCl_3$): 7.45 (2H, t, C_7 EE and E(EZ)), 7.38 (2H, t, C_8 EE and E(EZ)), 7.35 (2H, m, C_7 ZZ and Z(EZ)), 7.31 (2H, t, C_8 ZZ and Z(EZ)), 7.24 (1H, d, C_6 Z(EZ)), 7.19 (1H, d, C_6 ZZ), 7.04 (1H, d, C_6 EE), 3.53 (1H, s, C_9 EE), 3.46 (1H, s, C_9 E(EZ)), 3.39 (1H, s, C_9 ZZ), 3.38 (1H, s, C_9 Z(EZ)), 1.26 (9H, s, C_1 Z(EZ)), 1.24 (9H, s, C_1 ZZ), 0.85 (9H, s, C_1 EE), 0.84 (9H, s, C_1 E(EZ)). δ_C(101 MHz, solvent $CDCl_3$): 184.12 C_3 Z(EZ), 183.90 C_3 (ZZ), 182.94 C_3 (EE), 182.80 C_3 E(EZ), 168.1 C_4 ZZ, EZ and EE, 145.87 C_5 E(EZ), 145.13 C_5 Z(EZ), 145.07 C_5 ZZ, 129.58 C_7 Z(EZ), 129.47 C_7 ZZ, 128.49 C_7 EE, 128.41 C_7 E(EZ), 127.99 C_8 EE and E(EZ), 127.80 C_8 ZZ and Z(EZ), 127.17 C_6 Z(EZ), 127.06 C_6 ZZ, 126.51 C_6 EE, 126.02 C_6 E(EZ), 42.27 C_9 Z(EZ), 42.14 C_9 ZZ, 41.87 C_9 EE, 41.81 C_9 E(EZ), 42.45 C_2 EE and E(EZ), 42.39 C_2 ZZ and Z(EZ), 28.17 C_1 ZZ and Z(EZ), 27.44 C_1 EE and E(EZ).

***cis*-bis(*N*-Methyl-*N*-(4-nitro-phenyl)-*N'*-*2,2*-dimethylpropanoylthioureato)platinum(II), *cis*-[Pt(L^{3A}-*S,O*)$_2$]**: A yield of 79% was collected and analysed. Found C 53.12, H 6.24, N 14.23 and S 9.57 $C_{28}H_{34}N_4O_6PtS_2$ required C 52.86, H 5.80, N 14.23 and S 10.86%. δ_H(400 MHz; solvent $CDCl_3$): 8.32 (2H, d, C_7 Z(EZ)), 8.22 (2H, d, C_7 ZZ and EE), 8.19 (2H, d, C_7 E(EZ)), 7.56 (2H, d, C_6 Z(EZ)), 7.43 (2H, d, C_6 ZZ), 7.38 (2H, d, C_6 EE), 7.32 (2H, d, C_6

E(EZ)), 3.51 (1H, s, C_9 EE), 3.44 (1H, s, C_9 E(EZ)), 3.38 (1H, s, C_9 ZZ), 3.36 (1H, s, C_9 Z(EZ)), 1.19 (9H, s, C_1 Z(EZ)), 1.18 (9H, s, C_1 ZZ), 0.81 (9H, s, C_1 EE), 0.80 (9H, s, C_1 E(EZ)). δ_C(101 MHz, solvent $CDCl_3$): 184.40 C_3 Z(EZ), 184.34 C_3 (ZZ), 182.86 C_3 (EE), 182.75 C_3 E(EZ), 167.64 C_4 Z(EZ), 167.55 C_4 ZZ, 166.62 C_4 EE, 166.43 C_4 E(EZ), 146.35 C_8 Z(EZ), 146.24 C_8 ZZ, 144.92 C_8 EE, 144.85 C_8 E(EZ), 151.9 C_5 Z(EZ), 151.04 C_5 ZZ, 150.36 C_5 EE, 150.20 C_5 E(EZ), 125.11 C_6 Z(EZ), 125.02 C_6 ZZ, 123.90 C_6 EE, 123.83 C_6 E(EZ), 128.88 C_7 Z(EZ), 128.79 C_7 ZZ, 127.48 C_7 EE, 127.43 C_7 E(EZ), 42.06 C_9 Z(EZ), 42.01 C_9 ZZ, 41.69 C_9 EE, 41.34 C_9 E(EZ), 42.50 C_2 EE and E(EZ), 42.21 C_2 ZZ and Z(EZ), 27.68 C_1 ZZ and Z(EZ), 27.04 C_1 EE and E(EZ).

4.3 Results and Discussion

Ligands with a general motif *N*-methyl-*N*-(*para*-X-phenyl)-*N'-2,2*-dimethylpropanoylthiourea (X = O-CH_3, H and NO_2) have been synthesised, and the electron donating and electron withdrawing properties of the *para*-substituent have been systematically altered. It was envisaged that these ligands would have different rotational barriers of the (S)C-N(Me)(*para*-X-Ph) bond and that would impact on their respective coordination properties towards platinum(II). The series of ligands investigated present a suitable model for examining the possible electronic effects since the altered substituents are six bonds away from the thiocarbonyl C-N bond of interest therefore excluding any possible steric interactions.

4.3.1 E,Z configurational isomerism in asymmetrically disubstituted N-methyl-N-(para-X-phenyl)-N'-acylthiourea ligands, HL^{1A}, HL^{2A} and HL^{3A}

The restricted rotation about the carbon-nitrogen bond of the (S)C-N(Me)(*para*-X-Ph) moiety allows these ligands to adopt two possible configurational isomers but only at sufficiently low temperatures is this revealed by means of ^{1}H and ^{13}C NMR spectroscopy (Figure 4.2). Deconvolution analysis of the *N*-CH_3 proton resonances in the ^{1}H NMR spectra revealed nearly the same isomer ratio for both ligands; in the case of HL^{1A} the isomer distribution is such that the *E* to *Z* isomer distribution is 87% to 13% and HL^{2A} reveals a 90% to 10% ratio in favour of the *E* isomer. In CD_2Cl_2 the *E* to *Z* ratio is very similar to that determined in chloroform; HL^{1A} being 87% to 13% and 88% to 12% for HL^{2A}. It appears that the solvent does not play any role in the isomer distribution of these ligands. The observed ratios fall in a similar range to those determined by Bourn *et al.*[8] for *N*-methyl and *N*-ethylformanilide with the exo (phenyl group pointing away from the oxygen) product favoured 95% to 5%. The observed ratios fall in the general literature survey of N-alkylacetanilides that appear to exist predominantly as the exo isomer.[9-12]

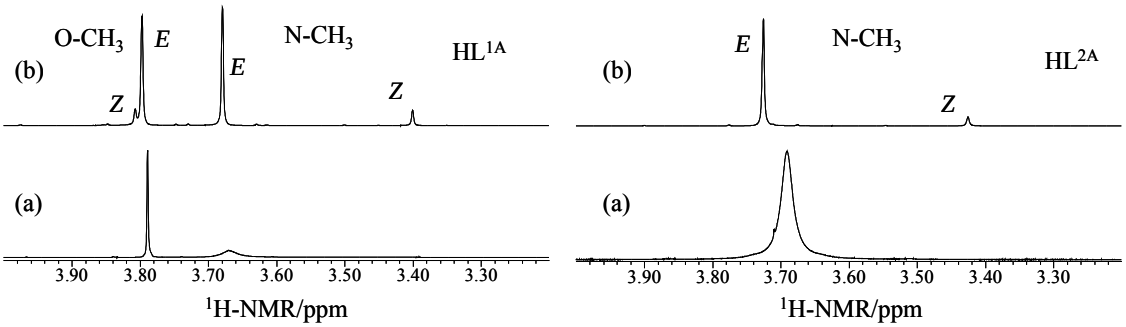

Figure 4.2 Sections of ^{1}H NMR spectra of HL^{1A} and HL^{2A} showing the O-CH_3 and *N*-CH_3 regions in HL^{1A} and only the *N*-CH_3 region for HL^{2A} measured (a) at 298 K seemingly displaying one isomer (present) and (b) at 243 K in $CDCl_3$ clearly showing the presence of two isomers, the *E* isomer being the dominant species.

At low temperature 243 K in chloroform (Figure 4.3) and at 198 K in dichloromethane the *N*-CH_3 peaks for *E* and *Z* isomers of HL^{3A} could not be observed as separate signals, hence it was not possible to assess the *E/Z* ratios for this ligand.

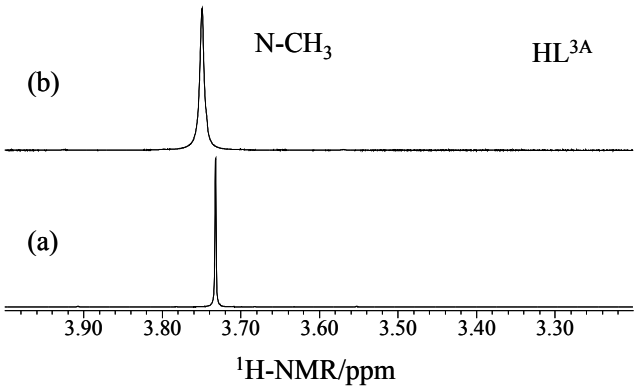

Figure 4.3 A section of ^{1}H NMR spectrum of freshly dissolved HL^{3A} showing the *N*-CH_3 measured (a) at 298 K displaying one isomer and (b) at 243 K seemingly retaining the same stereochemistry.

This could either mean this particular ligand exists exclusively as one isomer or at the low temperatures (243 K in chloroform down to 198 in dichloromethane) at which the *E*/*Z* isomers are investigated are well above the coalescence temperature, hence the second isomer is not observable. The first proposal does not seem likely because if the ligand is in one conformation then it would mean that the (S)C-N(Me)(*para*-X-Ph) bond is stronger as the nitro group is introduced in the *para* position. This would be contrary to the expected trend of the weakening of the (S)C-N(Me)(*para*-X-Ph) bond with a *para* substituent change: **OMe** ~ OEt > Me ~**H** > Cl > COOH >> **NO_2**.[13,14] Of the three ligands (HL^{1A}, HL^{2A} and HL^{3A}), HL^{3A} is expected to have the weakest (S)C-N(Me)(*para*-X-Ph) bond due to the

electron-withdrawing nitro substituent followed by HL^{2A} with no substituent at the *para* position then HL^{1A} with the electron-donating group having the strongest N-C bond. As been discussed in chapter 2 Section 2.4.3, attempts of growing crystals of HL^{3A}, which would support the hypothesis, were not successful. The ligand HL^{3A} unexpectedly decomposed in recrystallisation solvents and only the starting material methyl-(4-nitro-phenyl)-amine was isolated. The decomposition of this ligand was also followed by means of ^{1}H and ^{13}C NMR in chloroform and indeed the ligand decomposes in a few days and the peaks due to methyl-(4-nitro-phenyl)-amine grow at the expense of the ligand peaks (Figure 2.9). Although the decomposition prevented isolation of the desired compound which would have allowed for the appropriate bond length comparisons, it supports of the hypothesis that HL^{3A} has such a weak (S)C-N(Me)(*para*-X-Ph) bond caused by the electron withdrawing properties of the nitro group attached at the *para* position. It is therefore a reasonable assumption that HL^{3A} also displays *E*/*Z* isomerism. The temperature at which the *E*/*Z* isomers are investigated the compound is still in very fast exchange on the NMR time scale. In other words we are operating well above the coalescence temperature. This implies that the rotation barrier about the C-N bond of the (S)C-N(Me)(*para*-X-Ph) moiety in this ligand is low in comparison to the other two ligands (HL^{1A} and HL^{2A}). Looking carefully at the *N*-CH_3 resonance it is observed that this peak is broader at 243 K compared to 298 K, instead of sharpening on lowering the temperature. This is an opposite trend to the one observed for the other two ligands. This could be an indication that in fact both isomers of the ligand are formed, but that they are still in fast exchange on an NMR time scale even at this temperature (243 K).

4.3.2 Platinum(II) chelates derived from ligands HL^{1A}, HL^{2A} and HL^{3A}

The presence of three configurational isomers in the complexes ***cis*-[Pt($L^{1A,2A}$-*S,O*)$_2$]** is clearly shown by ^{195}Pt NMR spectra (see Figure 4.4). The ^{195}Pt NMR spectra of the complexes derived from HL^{1A} and HL^{2A} were measured at low temperature (243 K) since at this temperature the peaks are sharper than the extremes of room temperature and lower temperatures. Moreover, the signal to noise is improved and for this reason give rise to more reliable deconvolution analysis of the peaks which could be compared to the proton spectra deconvolutions at this temperature.

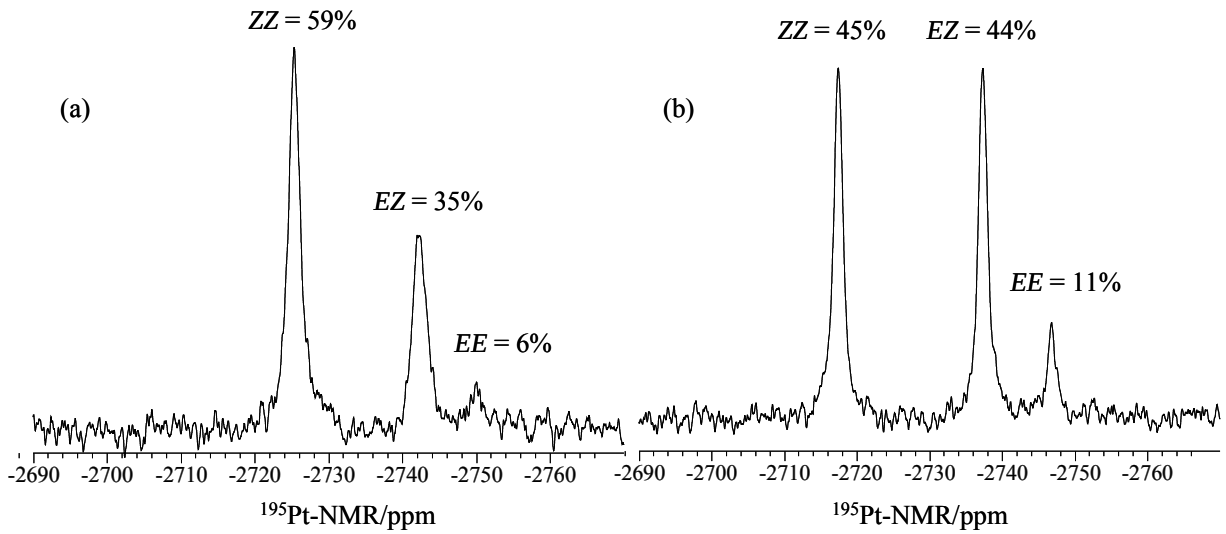

Figure 4.4 The 86 MHz ^{195}Pt NMR spectra of (a) ***cis*-[*ZZ*-Pt(L^{1A}-*S,O*)$_2$]** at δ(^{195}Pt) = -2725 ppm, ***cis*-[*EZ*-Pt(L^{1A}-*S,O*)$_2$]** at δ(^{195}Pt) = -2742 ppm and ***cis*-[*EE*-Pt(L^{1A}-*S,O*)$_2$]** at δ(^{195}Pt) = -2750 ppm and (b) ***cis*-[*ZZ*-Pt(L^{2A}-*S,O*)$_2$]** at δ(^{195}Pt) = -2717 ppm, ***cis*-[*EZ*-Pt(L^{2A}-*S,O*)$_2$]** at δ(^{195}Pt) = -2737 ppm and ***cis*-[*EE*-Pt(L^{2A}-*S,O*)$_2$]** at δ(^{195}Pt) = -2746 ppm measured in deuterated chloroform at 243 K.

In Figure 4.4 (a) and (b), the middle peak has been assigned to the *EZ* complex as this, intuitively, should be positioned between the *ZZ* and *EE* chemical shift extremes. This assignment is in agreement with both the ^{1}H and the ^{13}C NMR spectra of these complexes in that the ratio of the *EZ* (both *E*(*EZ*) and *Z*(*EZ*)) component to *EE* or *ZZ* components reflects what is observed in the platinum spectra (see Figure 4.5).

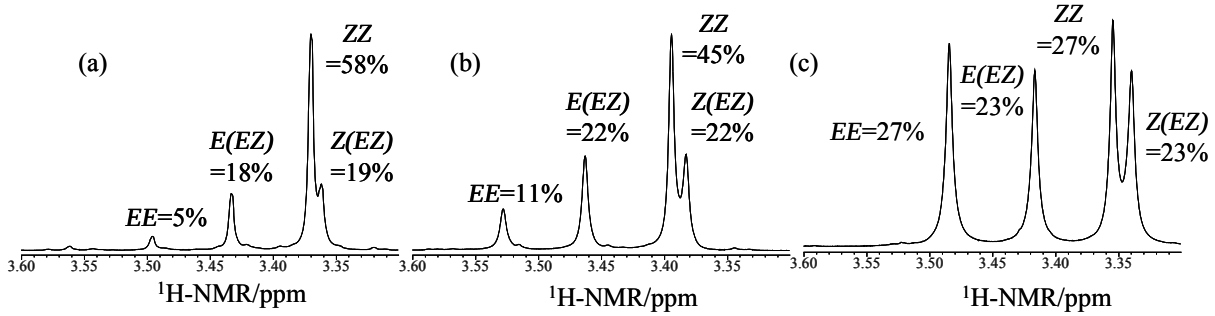

Figure 4.5 ^{1}H NMR spectra showing *N*-CH$_3$ peaks for ***cis*-[Pt(L^{1A}-*S,O*)$_2$]**, ***cis*-[Pt(L^{2A}-*S,O*)$_2$]** measured in $CDCl_3$ at 228 K and 243 K, respectively and *cis*-[Pt(L^{3A}-*S,O*)$_2$] measured in CD_2Cl_2 at 198 K. The deconvolution analyses show percentages of each isomer. In all cases the two peaks of equal intensity undoubtedly belong (*E* of the (*EZ*) and *Z* of the (*EZ*) complexes), while the most downfield peaks (of lowest intensity in (a) and (b)) correspond to the *EE* complexes and the most intense peaks are then due to the *ZZ* complexes.

The assignment of *EE* and *ZZ* isomers here also follows from the arguments presented in the previous chapter, the most downfield resonance assigned to the *ZZ* isomer while the most upfield resonance is assigned to the *EE* isomer. Remarkably, although an E to Z relative distribution of 90:10 in the unbound ligands is observed, the ZZ isomer is the configuration that appears to be (strongly) favoured again upon complexation. Ideally these assignments should be confirmed by means of $^{1}H/^{13}C/^{195}Pt$ correlation NMR spectroscopy at low temperature (243 K for ***cis*-[Pt(L^{2A}-*S,O*)$_2$]** and at 228 K for ***cis*-[Pt(L^{1A}-*S,O*)$_2$]**) where the *N*-CH_3 protons are no longer in fast exchange. The ^{195}Pt resonance assignments were nevertheless assigned as in chapter 3, without being biased by the isomer distributions of the unbound ligands. We have already shown that the *E/Z* isomer distributions of the unbound ligands are not a determining factor of the isomer distributions of the resultant complexes.

At room temperature it is rather misleading that the ^{195}Pt NMR spectrum of the configurational isomers derived from HL^3 shows only one peak, however on lowering the temperature to 228 K in chloroform it was observed that this peak was broadening (Figure 4.6). This might be an indication that this complex may well display *E/Z* configurational isomerism as well, however the minimum temperature attainable using chloroform is not low enough to explicitly demonstrate that.

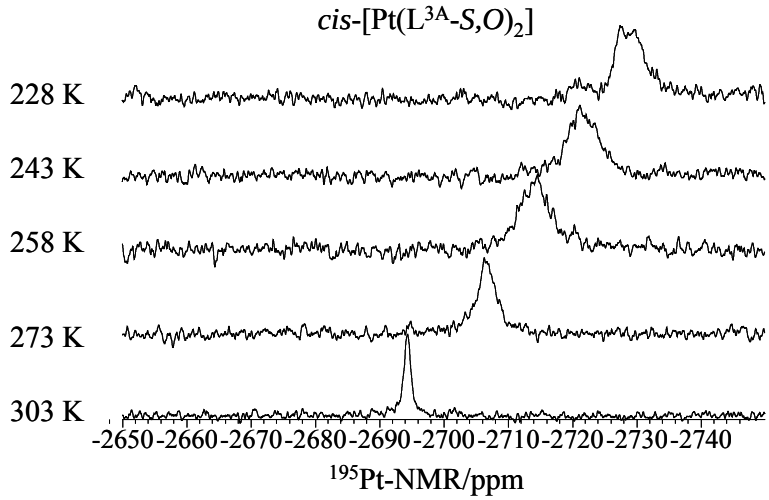

Figure 4.6 ^{195}Pt NMR spectrum of ***cis*-[Pt(L^{3A}-*S,O*)$_2$]** measured in $CDCl_3$ as the temperature is lowered from 303 K to 228 K. As the temperature is lowered there is a hint of existence of more than one peak, however 228 K is not sufficiently low to show all the three isomers.

Due to the limitation of the freezing point of chloroform 209 K (-64 °C) a change of solvent of similar properties but with lower freezing point 176 K (-97 °C) had to be used. For this purpose dichloromethane was chosen and at low temperatures (down to 198 K) the ^{195}Pt NMR spectrum did not reveal all the three isomers and only two peaks were observed (Figure 4.7).

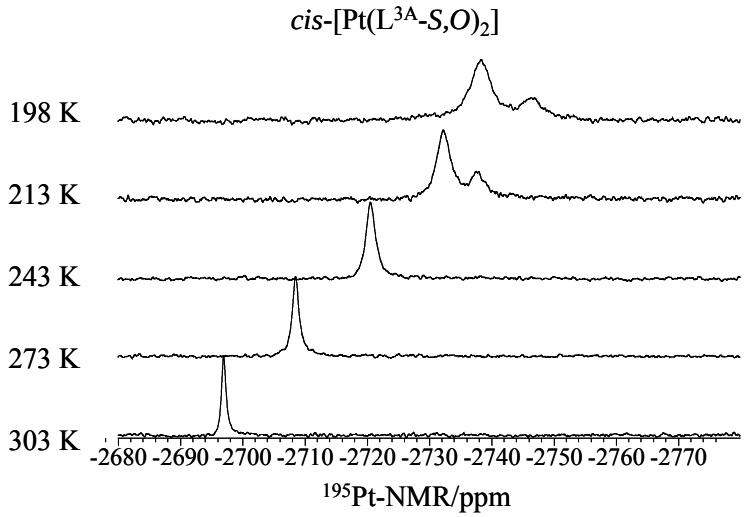

Figure 4.7 ^{195}Pt NMR spectrum of ***cis*-[Pt(L^{3A}-*S,O*)$_2$]** measured in CD_2Cl_2 as the temperature is lowered from 303 K to 198 K. At 303 K a very sharp peak is observed while the temperature is progressively lowered the peak broadens hinting the anticipated dynamics. From 213 K and below only two peaks are observed instead of the expected three according to ^{1}H NMR spectrum of this compound.

Thus, the ^{195}Pt NMR spectra in dichloromethane could not be relied upon for the purpose of determining the isomer distributions because for all the cases ***cis*-[Pt(L^{1A,2A,3A}-*S,O*)$_2$]** as the temperature is lowered to 198 K, not all the peaks due to the three isomers could be observed and hence the isomer distributions were then taken from the deconvolution analysis of the ^{1}H NMR signals of the *N*-CH_3 groups (shown in Figure 4.5 (c)) which show all the peaks due to the three isomers. It is reasonable to rely on the ^{1}H NMR as reflecting the distribution of the isomers since the ^{1}H NMR and ^{195}Pt NMR deconvolution analysis in chloroform were complementing each other very well in the case of ***cis*-[Pt(L^{1A,2A}-*S,O*)$_2$]**.

Apart from the broadening of the peak in Figure 4.6 in $CDCl_3$ and Figure 4.7 in CD_2Cl_2 as the temperature is lowered it is also evident that there is a linear upfield shift of the ^{195}Pt peak. This effect was also observed for ***cis*-[Pt(L^{1A}-*S,O*)$_2$]** and ***cis*-[Pt(L^{2A}-*S,O*)$_2$]** and a plot of $\delta(^{195}Pt)$ versus temperature Figure 4.8 clearly shows the sensitivity of the $\delta(^{195}Pt)$ chemical shift to the temperature change. Cohen and Brown[15] studied various platinum(II) complexes at various temperatures and observed a similar $\delta(^{195}Pt)$ chemical shift dependence on temperature.

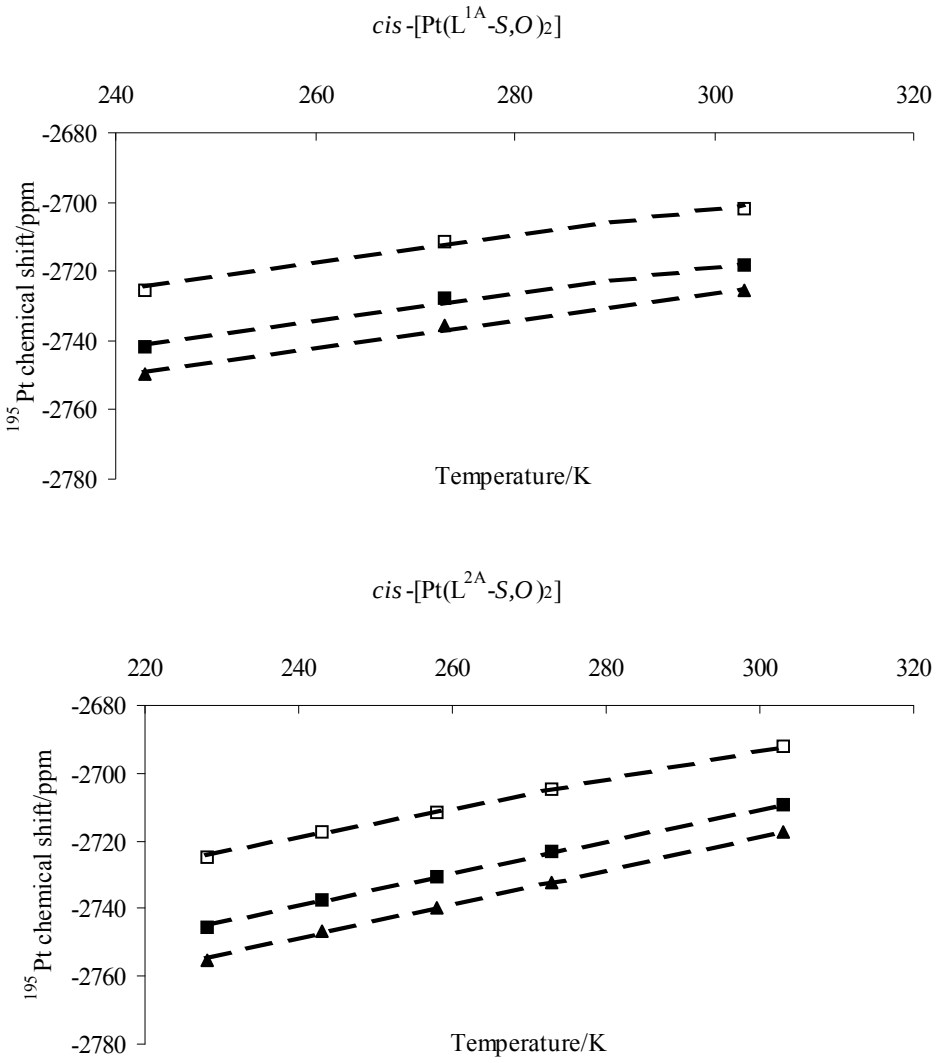

Figure 4.8 Temperature dependence of δ(^{195}Pt) chemical shifts of ***cis*-[Pt(L^{1A}-*S,O*)$_2$]** and ***cis*-[Pt(L^{2A}-*S,O*)$_2$]** complexes with □ *ZZ* ■ *EZ* and ▲ *EE* configurational isomer respectively.

4.3.3 Solvent and temperature effects on the isomer distributions of unbound ligands and their complexes

As discussed in the previous section for ***cis*-[Pt(L^{3A}-*S,O*)$_2$]** it was necessary to change the solvent from chloroform to dichloromethane in order to reach lower temperatures without the sample freezing. It was necessary to determine what impact the change of solvent might have on the isomer distributions of the other two complexes, ***cis*-[Pt(L^{1A,2A}-*S,O*)$_2$]**. This would allow a more accurate comparison of the isomer distributions if the conditions were identical for all the complexes. For completeness this study was carried out for the uncoordinated ligands as well. In deuterated dichloromethane at 243 K, the uncoordinated ligands displayed a similar *E/Z* isomer distribution as found in

chloroform, 87% *E* : 13% *Z* for HL^{1A} and 88% *E* : 12% *Z* for HL^{2A}. The isomer distribution in the complexes however showed a significant change upon moving from $CDCl_3$ to CD_2Cl_2. Figure 4.9 shows the *N*-CH_3 section of the ^{1}H NMR spectra of all the complexes at 198 K.

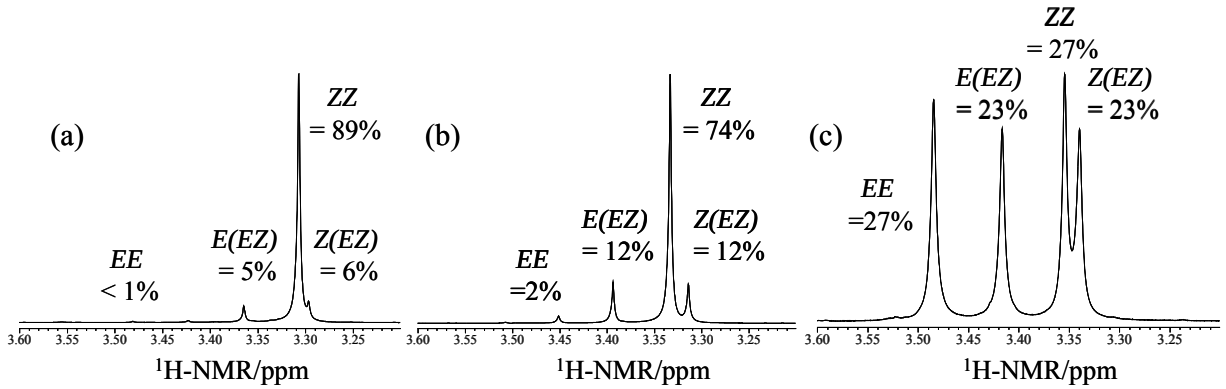

Figure 4.9 ^{1}H NMR spectra showing *N*-CH_3 peaks for (a) ***cis*-[Pt(L^{1A}-*S,O*)$_2$]**, (b) ***cis*-[Pt(L^{2A}-*S,O*)$_2$]** and (c) ***cis*-[Pt(L^{3A}-*S,O*)$_2$]**, measured in CD_2Cl_2 at 198 K. The relative percentages of each isomer are indicated on top of the peaks.

By comparison of spectra (a) and (b) pairs in Figure 4.5 and Figure 4.9 it is clear that there is a significant change in the distribution of isomers as the solvent is changed from chloroform to dichloromethane. Since the temperature is an additional variable for these spectra and their distribution comparisons, it was necessary to measure the distributions in the two solvents at the same temperature. Figure 4.10 illustrates the influence of the solvent on these distributions for ***cis*-[Pt(L^{1A}-*S,O*)$_2$]** and ***cis*-[Pt(L^{2A}-*S,O*)$_2$]** complexes. This confirms that at the same temperature in the two solvents that the solvent has a significant effect on the isomer distributions. It is clear in both complexes ***cis*-[Pt(L^{1A}-*S,O*)$_2$]** and ***cis*-[Pt(L^{2A}-*S,O*)$_2$]** that the *ZZ* isomer appears to grow at the expense of both the *EZ* and *EE* isomers. It has been reported in the literature that amide bond rotation is generally retarded by polar solvents as been shown in numerous experimental and computational studies.[16-24] The dielectric constant of chloroform at 293.2 K is 4.81 while that of dichloromethane at 298.0 K is 8.93 (source: CRC Handbook of Chemistry and Physics 84th Ed, 2003 2004, Lide D. R. Ed in Chief, CRC Press Inc. Boca Raton Florida 2003). This difference in polarity of the two solvents may well account for different rotation barriers of the C-N bond of the (S)C-N(Me)(*para*-X-Ph) moiety and hence the observed differences in the isomer distributions but the solvent effect on isomer distributions needs further investigation to confirm this. Such a study was not undertaken.

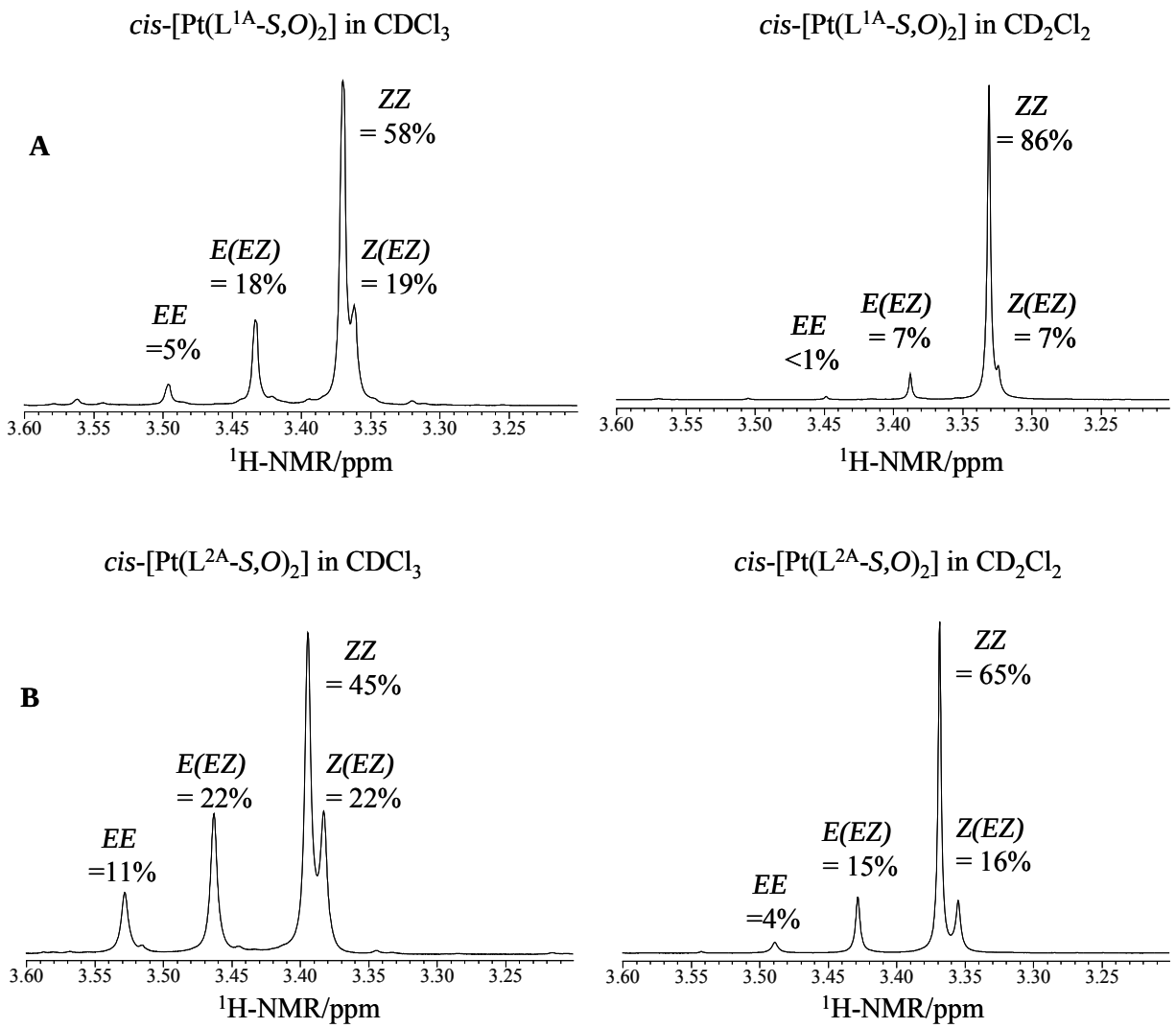

Figure 4.10 ^{1}H NMR spectra measured in $CDCl_3$ and CD_2Cl_2 measured at (**A**) 228 K for ***cis*-[Pt(L^{1A}-*S,O*)$_2$]** and at (**B**) 243 K for ***cis*-[Pt(L^{1A}-*S,O*)$_2$]**. The percentage distributions of the isomers illustrated on each peak are obtained after deconvolution analysis of the spectra in question.

As the temperature is lowered there a systematic increase of the *ZZ* isomer at the expense of both the *EZ* and *EE* isomers for both ***cis*-[Pt(L^{1A}-*S,O*)$_2$]** and ***cis*-[Pt(L^{2A}-*S,O*)$_2$]** regardless of the solvent used. In CD_2Cl_2 the data that demonstrate the temperature effect is readily available by merely comparing Figures 4.9 (a) and 4.10 A for ***cis*-[Pt(L^{1A}-*S,O*)$_2$]** and Figures 4.9 (b) and 4.10 B for ***cis*-[Pt(L^{2A}-*S,O*)$_2$]**. The ^{1}H NMR spectra for ***cis*-[Pt(L^{1A}-*S,O*)$_2$]** and ***cis*-[Pt(L^{2A}-*S,O*)$_2$]** in Figure 4.9 are both measured at 198 K while the ^{1}H NMR spectra in Figure 4.10 are measured at 228 K and 243 K respectively. The effect of a systematic temperature decrease on the isomer distributions in CD_2Cl_2 is shown in Figure 4.11 for the complexes ***cis*-[Pt(L^{1A}-*S,O*)$_2$]** and ***cis*-[Pt(L^{2A}-*S,O*)$_2$]**. Similar

data for ***cis*-[Pt(L^{3A}-*S,O*)$_2$]** is not available since this complex only shows the existence of all the three isomers at 198 K.

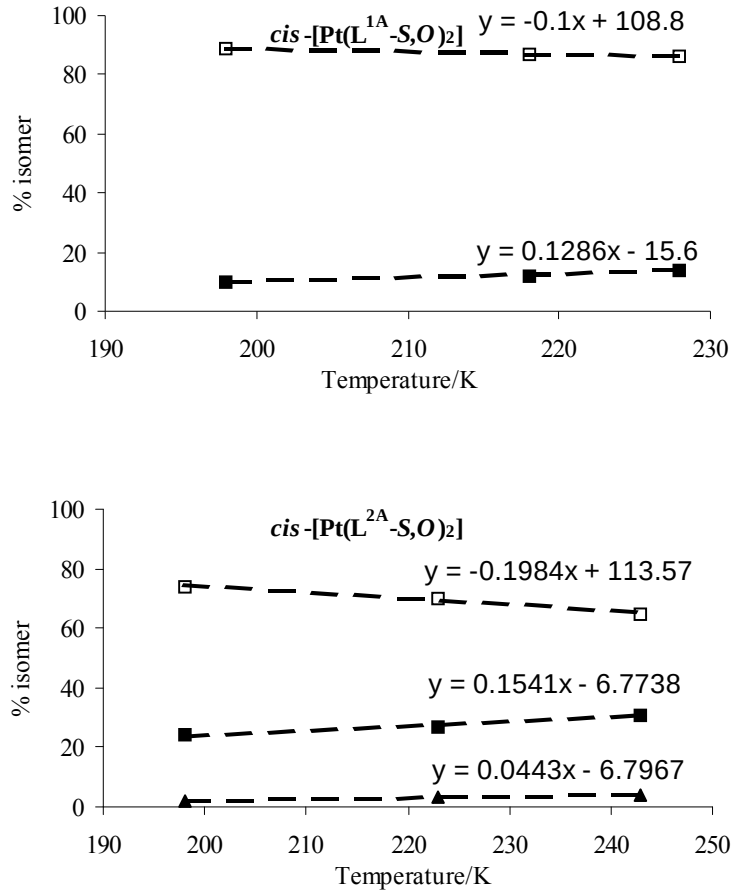

Figure 4.11 Isomer distribution as a function of temperature for ***cis*-[Pt(L^{1A}-*S,O*)$_2$]** and ***cis*-[Pt(L^{2A}-*S,O*)$_2$]** in CD_2Cl_2 with □ *ZZ* ■ *EZ* and ▲ *EE* isomers. The data for the *EE* isomer of ***cis*-[Pt(L^{1A}-*S,O*)$_2$]** is not shown since the percentages are very small for this scale.

These data indicate that the *ZZ* isomer is favoured over the *EZ* and *EE* isomers upon cooling in both complexes. Judging from the slopes it seems that ***cis*-[Pt(L^{2A}-*S,O*)$_2$]** is more temperature sensitive than ***cis*-[Pt(L^{1A}-*S,O*)$_2$]**. The conversion of the *ZZ* isomer to the other isomers (*EZ* and *EE*) as a function of temperature is more pronounced in the case of ***cis*-[Pt(L^{2A}-*S,O*)$_2$]** than for ***cis*-[Pt(L^{1A}-*S,O*)$_2$]**. It becomes clearer to account for the observed different sensitivities towards temperature change after discussing the barrier to rotation around the (S)C-N(Me)(*para*-X-Ph) bond of the two complexes. Hence we can conclude that temperature will have impact less on the distribution changes of the complex which has a higher barrier to rotation around the (S)C-N(Me)(*para*-X-Ph) bond. That happens to be the case for ***cis*-[Pt(L^{1A}-*S,O*)$_2$]** over ***cis*-[Pt(L^{2A}-*S,O*)$_2$]**. These findings also suggest a significant

temperature influence and when making comparisons of the isomer distribution, the temperature has to be fixed. Overall, what we can say now is that for any sensible comparison to be made on these complexes the temperature and the solvent should be fixed since the distributions are sensitive to both these parameters.

4.3.4 Rationalisation of the configurational isomer distributions in terms of the electronic effects

In our previous publication[25] and in the previous chapter the following interesting phenomenon that the relative amounts of the resultant ***cis*-[*ZZ*-Pt(L-*S,O*)$_2$]**, ***cis*-[*ZE*-Pt(L-*S,O*)$_2$]** and ***cis*-[*EE*-Pt(L-*S,O*)$_2$]** complexes were significantly different to the amounts statistically predicted from the observed *E*/*Z* ratios of the ligands in solution as used in the reaction synthesis. In simple terms we can say that if the ligands in *ZZ*, *EZ* and *EE* isomer of one complex were to be removed from the metal centre while retaining the stereochemistry adopted in the complex, the ratio of the *E* to *Z* of the unbound ligands would not be the same as the one before coordination occurred. There would be an apparent increase in one of the configurational isomers (namely: the *Z* isomer in the cases discussed here) of the unbound ligand. In Table 4.2 below we show the relative amounts of these configurational isomers and the statistically predicted amounts.

Table 4.2 Assignments of δ(^{195}Pt) (ppm) and the relative distributions (taken from ^{1}H NMR deconvolution analysis) of configurational isomers of ***cis*-[Pt(L^{1A,2A}-*S,O*)$_2$]** complexes. Measurements were done in $CDCl_3$ at 243 K and all ^{1}H NMR spectra were measured again in CD_2Cl_2 at 198 K for all the ***cis*-[Pt(L^{1A,2A,3A}-*S,O*)$_2$]** complexes.

Complex	*ZZ*	*EZ*	*EE*
δ(^{195}Pt) ***cis*-[Pt(L^{1A}-*S,O*)$_2$]**	-2725	-2742	-2750
Statistical (%)	6	13	81
[a] Relative integrals (%) ($CDCl_3$)	59	35	6
[a] Relative integrals (%) (CD_2Cl_2)	89	11	<1
δ(^{195}Pt) ***cis*-[Pt(L^{2A}-*S,O*)$_2$]**	-2717	-2737	-2746
Statistical (%)	5	10	85
[a] Relative integrals (%) ($CDCl_3$)	45	44	11
[a] Relative intensity (%) (CD_2Cl_2)	74	24	2
δ(^{195}Pt) ***cis*-[Pt(L^{3A}-*S,O*)$_2$]**	-2723	-2723	-2729
[b]Statistical (%)	-	-	-
[c]Relative integrals (%)	27	46	27

[a] The observed relative integrals are estimated to have an error of ± 1%.

[b] Since *E*/*Z* isomers of HL^{3A} could not observed as separate signals (*i.e.* their distribution is unknown) therefore the distribution of resultant complexes could not be predicted.

[c] Based on the deconvolution analysis of the ^{1}H NMR signals of *N*-CH_3 measured at 198 K.

The relative integral values are based on deconvolution analysis of the observed ^{195}Pt NMR spectra in $CDCl_3$ at 243 K for ***cis*-[Pt(L^{1A}-*S,O*)$_2$]** and ***cis*-[Pt(L^{2A}-*S,O*)$_2$]**, which is in good agreement with the ^{1}H NMR spectra deconvolution analysis. The statistically predicted values shown are based on the assumption that the unbound ligands have a fixed *E* : *Z* ratio which does not change during complex formation process. Intuitively, starting with predominantly *E* isomer (90%) over the *Z* isomer (10%) to form the *ZZ, EZ* and *EE* chelate, the *EE* isomer is statistically favoured. The relative integral values reveal the direct opposite of what is statistically predicted in that it is the *ZZ* isomer that it most favoured and *not* the *EE* isomer for ***cis*-[Pt(L^{1A}-*S,O*)$_2$]** and ***cis*-[Pt(L^{2A}-*S,O*)$_2$]**. The isomer distribution of ***cis*-[Pt(L^{3A}-*S,O*)$_2$]** could not be statistically predicted since the estimate of *E* : *Z* isomers of the unbound ligand could not be determined even at 198 K and its isomer distributions were also measured at 198 K in CD_2Cl_2. As mentioned before, for any sensible comparisons to be made on the distributions identical solvent and temperature should be used. For this reason the ^{1}H NMR spectra of all the complexes were measured in CD_2Cl_2 at 198 K, which also resulted in well-separated ^{1}H NMR spectra in which the integrals of the isomers are determined.

We have speculated on various factors such as solvent effects, steric factors and electronic factors that could make the isomer distribution deviate from the statistically predicted one. Even though solvent effects were not extensively studied, our initial approach was to use two different solvent systems in which the complexes are synthesised. Extracting the platinum salt (K_2PtCl_4) with HL^{2A} from aqueous solution into chloroform, the isomer distribution is identical to the one attained by the normal synthetic route, which is carried out in an acetonitrile/water mixture. Initially we thought the solvent does not play any role in the isomer distributions, however, as we have just discussed in Section 4.3.3 dissolving the complexes in different solvents has a notable influence on the isomer distributions. Different alkyl groups of the (S)C-NRR' moiety were shown previously to be playing some role in yielding different distributions, but this was not a systematic study in that changes were done not only on the alkyl groups of the (S)C-NRR' moiety but also on the R" group of the R"C(O)- moiety.[25] We investigate the alkyl substituent influence on the isomer distributions in a much more thorough way in the next chapter.

Chelating ligands with restricted rotation of carbon-nitrogen bond are not uncommon such as the *EE*, *EZ*, *ZZ*-*N*,*N'*-dibenzyl-*N*,*N'*-diethyldithioxamides, Bz_2Et_2DTO reported by Lanza *et al*.[26] These authors, having isolated any of the three configurationally isomer (*EE* or *EZ* or *ZZ*) of the unbound ligand, observed that these ligands isomerise readily in solution to produce an equimolar mixture of all the uncoordinated ligands before complexation to *cis*-$[Pt(Me_2SO)_2Cl_2]$ took place. It is this *E*/*Z* isomerisation of the ligands in solution prior to complexation to the metal centre which allowed for the statistical prediction of the resulting [*EE*-, *EZ*-, *ZZ*-$(Bz_2Et_2DTO)PtCl_2$] complexes. However, the ligands reported in this work seem to retain their *E*/*Z* distribution before complexation takes place evidently by retaining the same distribution even at any temperature from 258 K to 198 K. Hence it is thought that the observed distributions of the complexes differ from the statistically predicted one because the restricted rotation about the (S)C-NRAr bond is lifted during the complex formation process thereby leading to the observed distribution. In related compounds (N-arylthiocarbamates and N-aryldithiocarbamates), the aryl substituent is known to be C-N barrier lowering according to Lidén *et al*[1] since the thiocarbonyl and the aryl substituent compete for conjugation with the lone pair on the nitrogen atom of the (S)C-NRAr moiety. This is also supported by the fact that

the coalescence temperatures of these complexes are very low. It may then be expected that ligands with low barrier to rotation may easily inter-isomerise during complex formation.

*4.3.5 Rotational dynamics: ^{1}H NMR study of restricted rotation around the (S)C-N(Me)(para-X-Ph) bond (X = O-CH_3, H and NO_2) in unbound ligands HL^{1A} and HL^{2A} and the Pt complexes, **cis-[Pt($L^{1A,2A,3A}$-S,O)$_2$]***

The ^{1}H and ^{13}C spectra of HL^{1A} and HL^{2A} as well as their respective complexes, ***cis*-[Pt($L^{1A,2A}$-*S,O*)$_2$]** obtained at room temperature revealed broad peaks while at low temperatures (228 K for ***cis*-[Pt(L^{1A}-*S,O*)$_2$]** and 243 K for ***cis*-[Pt(L^{2A}-*S,O*)$_2$]**) the spectra were well resolved. In order to gain more insight into the rotation dynamics of these compounds from the NMR spectra, a variable temperature NMR study was undertaken.

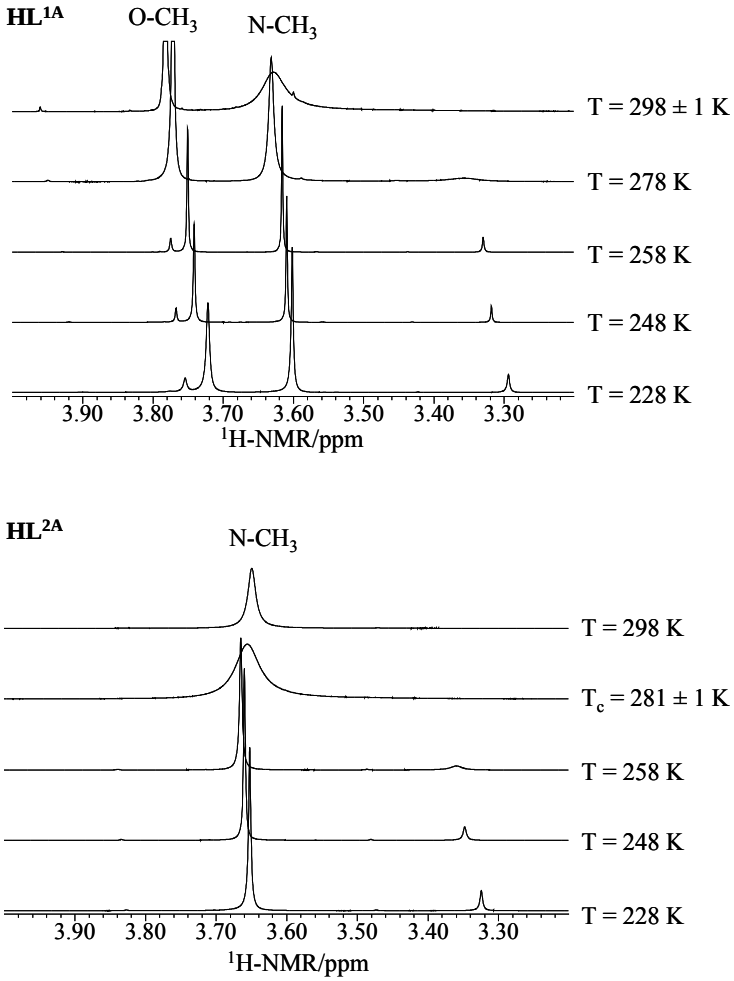

Figure 4.12 In deuterated dichloromethane the coalescence temperature determinations of HL^{1A} and HL^{2A} around the (S)C-N(Me)(*para*-X-Ph) bond (X = O-CH_3 for HL^{1A} and H for HL^{2A}) were found to be 281 ± 1 K and 298 ± 1 K, respectively. The coalescence temperature for HL^{3A} could not be determined even at 198 K due to fast rotation.

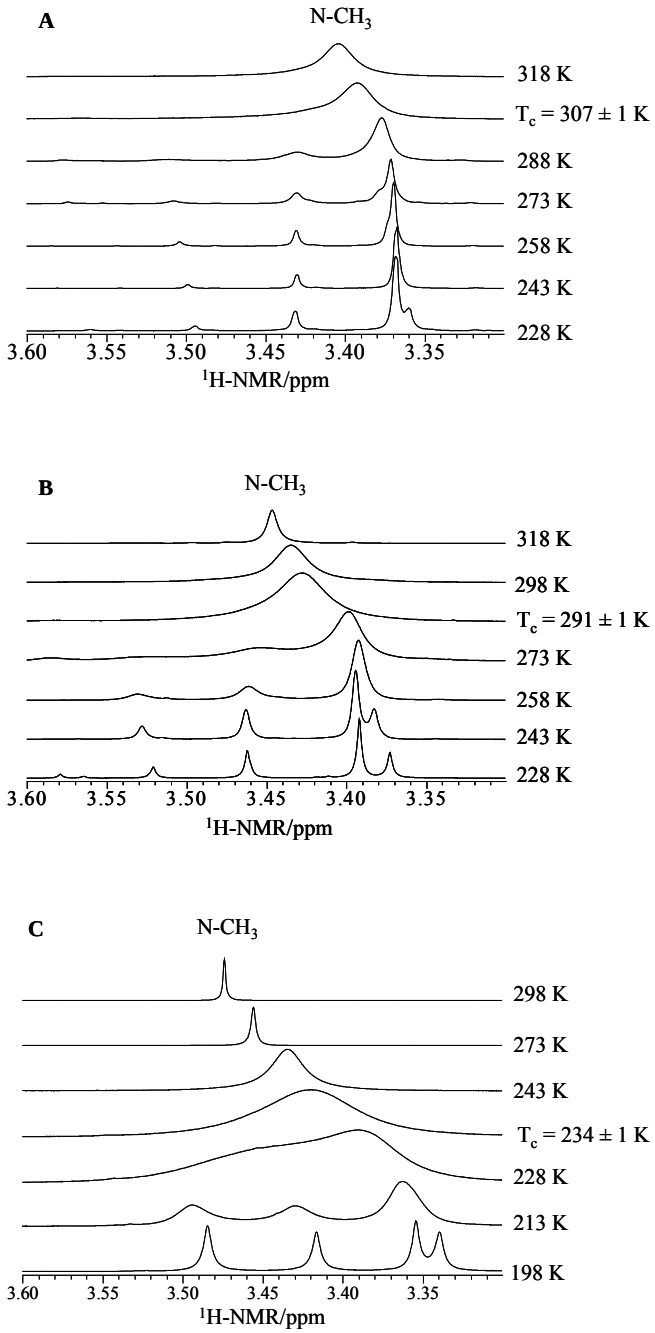

Figure 4.13 Coalescence temperature determinations of (a) ***cis*-[Pt(L^{1A}-*S,O*)$_2$]**, (b) ***cis*-[Pt(L^{2A}-*S,O*)$_2$]** and (c) ***cis*-[Pt(L^{3A}-*S,O*)$_2$]** around the (S)C-N(Me)(*para*-X-Ph) bond were found to be 307 ± 1 K, 291 ± 1 K and 234 ± 1 K, respectively.

The coalescence temperature, T_c determinations were evaluated for the unbound ligands HL^{1A} and HL^{2A} as well as the complexes ***cis*-[Pt(L^{1A}-*S,O*)$_2$]**, ***cis*-[Pt(L^{2A}-*S,O*)$_2$]** and ***cis*-[Pt(L^{3A}-*S,O*)$_2$]** as shown in Figures 4.12 and 4.13,

respectively. Fig. 4.13 beautifully demonstrates the dramatic changes both in peaks shapes and chemical shifts of the complexes upon changing the temperature. In general more accurate T_c values were obtained for the complexes, as it was difficult to accurately measure the T_c's for the ligands since the peaks due to the minor component (*Z*-isomer) broadens into the noise before coalescence is clearly observed. The values obtained for the ligands were measured in dichloromethane and were roughly 10 K lower in temperature than their respective complexes. This implies that the rotational barrier in the unbound ligands is significantly lower than when the ligands are in the metal chelates. Whatever conclusions we arrive at from studying the complexes we could still qualitatively extrapolate information into the respective unbound ligands since it is known in the literature in related *N*,*N*-diethyl-*N'*-benzoylthiourea complexes of Ni(II), Zn(II), Pb(II) and Pd(II) studied by Behrendt *et al*.[27] that chelates have higher rotation barriers than the unbound ligands. In the current study moreover, the unstable of HL^{3A} in solution (due to (S)C-N(Me)(4-nitro-Ph) bond cleavage) remains intact upon coordination to the Pt(II) centre, which is further support for the increased strength of the C-N bond upon coordination to Pt(II).

Having determined the approximate coalescence temperatures of the three complexes ***cis*-[Pt(L^{1A}-*S,O*)$_2$]**, ***cis*-[Pt(L^{2A}-*S,O*)$_2$]** and ***cis*-[Pt(L^{3A}-*S,O*)$_2$]** as well as the unbound ligands HL^{1A} and HL^{2A}, we are now in a position to estimate the Gibbs free energy of activation, $\Delta G^{\neq}_c$ derived from the Eyring equation [4.1]. However, it is more appropriate to calculate the $\Delta G^{\neq}_c$ value for ***cis*-[Pt(L^{3A}-*S,O*)$_2$]** since the *ZZ* and *EE* are of equal population in this case.

$$k = \chi(k_B T/h)\cdot e^{-\Delta G\neq/RT} \quad [4.1]$$

$$\Delta G^{\neq}_c = 4.58Tc\,(10.32 + \log (T_c/K_c)) \text{ where } T_c = \text{coalescence temperature} \quad [4.2]$$

$$K_c = 2.22\Delta\upsilon \quad [4.3]$$

where $\Delta\upsilon$ = difference between the *EE* and the *ZZ* isomer peaks measured in Hertz taken at the temperature at which these peaks are well separated, which is 228 K for ***cis*-[Pt(L^{1A}-*S,O*)$_2$]** and ***cis*-[Pt(L^{2A}-*S,O*)$_2$]** and 198 K for ***cis*-[Pt(L^{3A}-*S,O*)$_2$]**.

The determination of K_c is valid only if the following three conditions are fulfilled:

- the dynamic process occurring is first order kinetically,
- the two singlets have equal intensities, and
- the exchanging nuclei are not coupling to each other.

The first and the last conditions in our systems are satisfied, but the second is not. However, even though not all the conditions have been fulfilled exactly, equation [4.3] remains a good approximation for estimating K_c. For simplicity the calculations of the thermodynamic parameters for the complexes have been limited to those that relate the extreme *ZZ* and *EE* isomers only. The simplification results from the fact that from the ^{1}H NMR perspective both the *ZZ* and the *EE* isomers are represented by a single peak while the *EZ* complex has two peaks. This in principle should give an estimate of the largest rotational barriers between the three isomers, *i.e.* the forward and the reverse reaction between *EE* and *EZ* isomers; *EZ* and *ZZ* isomers and *EE* and *ZZ* isomers. The actual rotational dynamics for

the complexes involves three distinct isomers *ZZ, EZ* and *EE* in different concentrations. This makes the application of the rotational dynamics analysis much more complicated since more than two NMR chemical shift environments are involved. The K_c values that are calculated are therefore only an approximation and represent an average of the various interchanges possible.

For ***cis*-[Pt(L^{1A}-*S,O*)$_2$]** and ***cis*-[Pt(L^{2A}-*S,O*)$_2$]** with unequal populations of *EE* and the *ZZ* isomers, the equilibrium constant K can be calculated from equation [4.4], the relative concentrations of *ZZ* and *EE* isomers are readily determined from the integrations or the corresponding NMR signals. One can then determine the difference between the energies of the two isomers, ΔG_0, by using equation [4.5].

$K = [Z]/[E]$ for HL^{1A} and HL^{2A} and $K = [EE]/[ZZ]$ for the complexes ***cis*-[Pt($L^{1A,2A,3A}$-*S,O*)$_2$]** [4.4]

$\Delta G_0 = -RT\ln K$ [4.5]

The molar concentrations of the isomers for determination of K are taken from the deconvolution analysis (peak integrals) of the ^{1}H NMR spectra.

T = temperature at which the peaks are well separated.

R = 1.9872 cal.K^{-1}.mol^{-1}

Table 4.3 Thermodynamic data for the barrier to rotation around the (S)C-N(Me)(*para*-X-Ph) bond in the unbound ligands HL^{1A} and HL^{2A} and coordinated ligands in ***cis*-[Pt($L^{1A,2A,3A}$-*S,O*)$_2$]** complexes. The values in parenthesis were obtained in chloroform and the rest in dichloromethane.

Complex	T_c/K	Δυ/Hz	K	$\Delta G^{\neq}_c$ [a] kcal/mol	$\Delta G_{0(ZZ\text{-}EZ)}$ kcal/mol	$\Delta G_{0(EZ\text{-}EE)}$ kcal/mol	$\Delta G_{0(ZZ\text{-}EE)}$ kcal/mol
HL^{1A}	298 ± 1	141	0.11	14.1			0.75
***cis*-[Pt(L^{1A})$_2$]**	307 ± 1	45.99	0.01	15.2	0.82	1.37	2.19
***cis*-[Pt(L^{1A})$_2$]**	(307 ± 1)	(50.40)	(0.10)	(15.1)	(0.20)	(0.91)	(1.11)
HL^{2A}	281 ± 1	131	0.11	13.3			0.78
***cis*-[Pt(L^{2A})$_2$]**	291 ± 1	47.19	0.03	14.4	0.45	0.96	1.41
***cis*-[Pt(L^{2A})$_2$]**	(291 ± 1)	(51.50)	(0.24)	(14.3)	(0.01)	(0.63)	(0.64)
***cis*-[Pt(L^{3A})$_2$]**	234 ± 1	52.03	1	11.4	-0.21	0.21	0

[a] The standard deviations do not exceed 0.2 kcal/mol

To facilitate understanding of the $\Delta G^{\neq}_c$ and ΔG_0 values in Table 4.3 calculated from the equations [4.2] and [4.3] respectively, energy diagrams can been used. Figure 4.14 can be regarded as the general energy profile that describes the C-N barrier heights for ***cis*-[Pt(L^{1A}-*S,O*)$_2$]** and ***cis*-[Pt(L^{2A}-*S,O*)$_2$]** with unequal populations of *EE* and *ZZ* isomers while Figure 4.15 is an energy profile specific to the case of ***cis*-[Pt(L^{3A}-*S,O*)$_2$]** with equal populations of *EE* and *ZZ* isomers. In Figure 4.14 ***cis*-[*ZZ*-Pt($L^{1A,2A}$-*S,O*)$_2$]** isomers are lowest in energy followed by ***cis*-[*EZ*-Pt($L^{1A,2A}$-*S,O*)$_2$]** isomers and ***cis*-[*EE*-Pt($L^{1A,2A}$-*S,O*)$_2$]** isomers are highest in energy. The energy diagram in Figure 4.15 is slightly

different and symmetrical since the ***cis*-[*EE*-Pt(L^{3A}-*S,O*)$_2$]** isomer and the ***cis*-[*ZZ*-Pt(L^{3A}-*S,O*)$_2$]** isomer are at an equal energy level, which is slightly higher than that of the most favoured ***cis*-[*EZ*-Pt(L^{3A}-*S,O*)$_2$]** isomer. Furthermore, the ΔG values are increased when going from the ligand to the complex. In both Figures 4.14 and 4.15, TS(*ZZ*-*EZ*) and TS(*EZ*-*EE*) are transition states from the *ZZ* isomer to *EZ* isomer and from the *EZ* isomer to the *EE* isomer, respectively. From Figure 4.14, it is easy to calculate the barrier height from *EZ* to *EE*, which is the same as energy height from *EZ* to TS(*EZ*-*EE*), by taking the difference between $\Delta G^{\neq}_{c}$ and $\Delta G_{0(ZZ\text{-}EZ)}$. It was not possible to calculate the barrier height from *ZZ* to *EZ* since the energy height from *ZZ* to TS(*ZZ*-*EZ*) is unknown. This problem is not encountered in the symmetric energy profile since the heights from *ZZ* to TS(*ZZ*-*EZ*) and from *EZ* to TS(*EZ*-*EE*) are equal. For general comparison of energy barriers we therefore focus on comparing the $\Delta G^{\neq}_{c}$ values, which are available for the two cases.

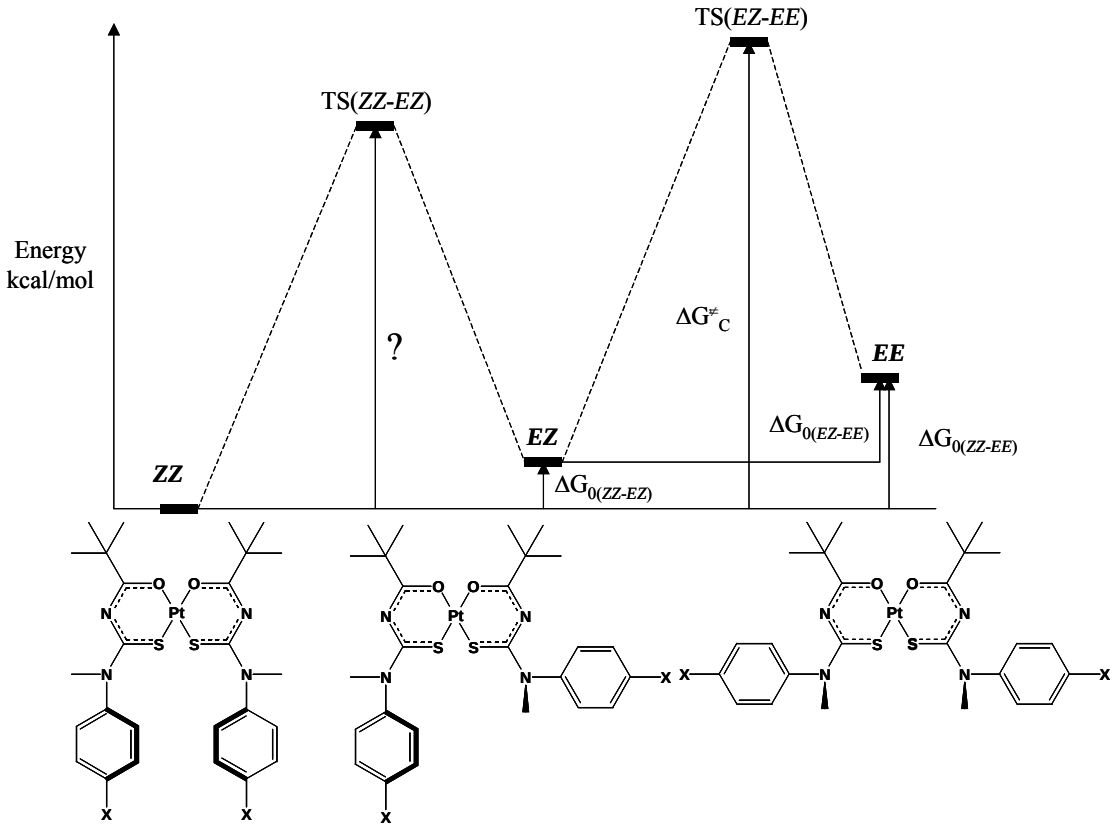

Figure 4.14 General energy diagram showing the inter-conversion of *EE*, *EZ* and *ZZ* isomers for ***cis*-[Pt(L^{1A}-*S,O*)$_2$]** with X = O-CH_3 and ***cis*-[Pt(L^{2A}-*S,O*)$_2$]** with X = H with unequal populations of *EE* and *ZZ* isomers.

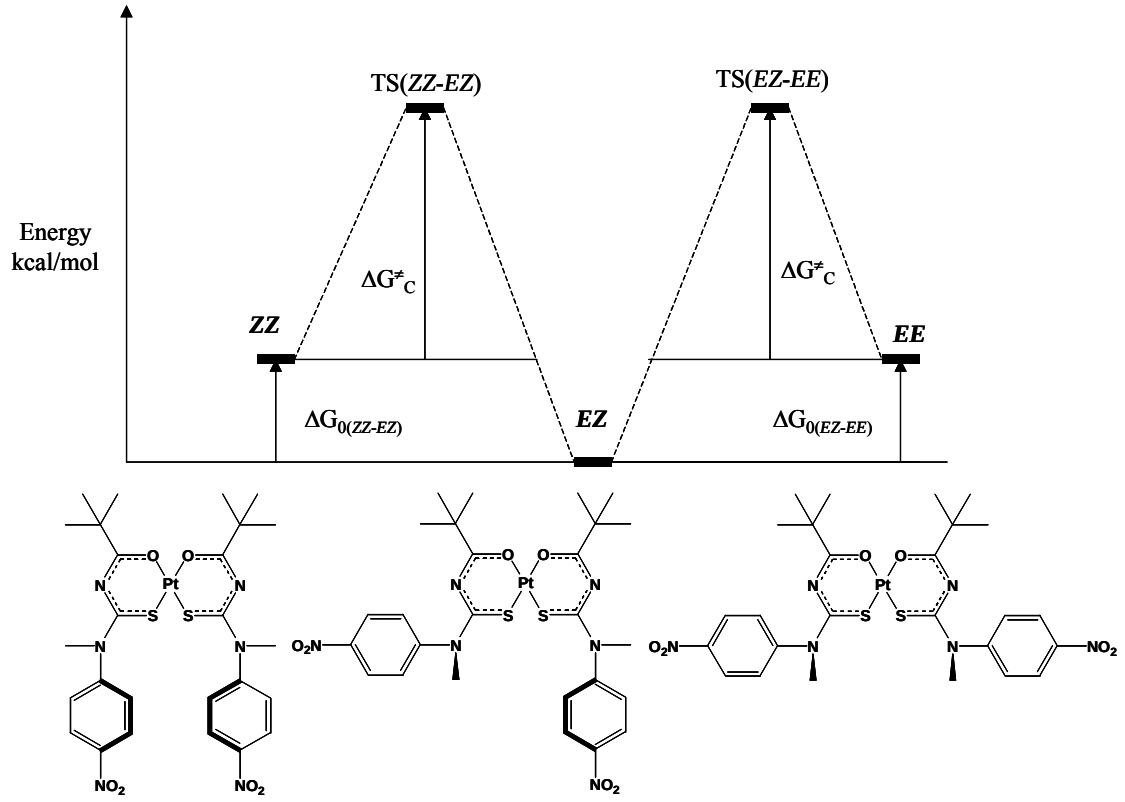

Figure 4.15 Energy diagram showing the inter-conversion of *EE*, *EZ* and *ZZ* isomers for ***cis*-[Pt(L^{3A}-*S,O*)$_2$]**.

A rather convenient method for obtaining the free energies of activation $\Delta G^{\neq}_{(EE\text{-}ZZ)}$ and $\Delta G^{\neq}_{(ZZ\text{-}EE)}$ by means of coalescence temperature of unequal populations can be calculated from the Shanan-Atidi and Bar-Eli[28] method; equations [4.6] and [4.7] respectively. These equations are specifically derived to take into account that the populations of the two isomers are not equal in concentration, which is exactly the case for ***cis*-[Pt(L^{1A}-*S,O*)$_2$]** and ***cis*-[Pt(L^{2A}-*S,O*)$_2$]**. Since these equations are for the general case, they are readily applicable for calculating the enthalpies of activation ($\Delta G^{\neq}_{(EE\text{-}ZZ)}$ and $\Delta G^{\neq}_{(ZZ\text{-}EE)}$) for ***cis*-[Pt(L^{3A}-*S,O*)$_2$]** with equal populations of *EE* and *ZZ* isomer.

$$\Delta G^{\neq}_{(ZZ\text{-}EE)} = 4.57Tc[10.62 + \log(X/2\pi(1 - \Delta P)) + \log Tc/\Delta\upsilon] \qquad [4.6]$$

$$\Delta G^{\neq}_{(EE\text{-}ZZ)} = 4.57Tc[10.62 + \log(X/2\pi(1 + \Delta P)) + \log Tc/\Delta\upsilon] \qquad [4.7]$$

Tc = Coalescence temperature

$\Delta\upsilon$ = frequency separation in Hertz between the *ZZ* and *EE* peaks

ΔP = difference in populations of *ZZ* and *EE* isomers and $P_{ZZ} - P_{EE} = \Delta P = [(X^2 - 2)/3]^{3/2} \cdot 1/X$

The equations [4.6] and [4.7] are readily applicable for their uncoordinated ligands since the *E* and *Z* isomers are of unequal populations. We can also calculate the parameters $\Delta G^{\neq}_{(E\text{-}Z)}$, $\Delta G^{\neq}_{(Z\text{-}E)}$ and $\Delta G_{0(E\text{-}Z)}$ instead of $\Delta G^{\neq}_{(EE\text{-}ZZ)}$, $\Delta G^{\neq}_{(ZZ\text{-}EE)}$ and $\Delta G_{0(ZZ\text{-}EE)}$.

Since the $\Delta G^{\neq}_{(EE\text{-}ZZ)}$ and $\Delta G^{\neq}_{(ZZ\text{-}EE)}$ for the complexes or the $\Delta G^{\neq}_{(E\text{-}Z)}$ and $\Delta G^{\neq}_{(Z\text{-}E)}$ for the unbound ligands are the differences between the ground-state energies and the energies of activation barrier of the isomer conversion, a comparison of these parameters for compounds with different isomer populations cannot indicate the relative heights of inter-conversion barrier. However, an indication of the relative barrier heights can be obtained by comparing the average barrier of rotation, $\Delta G^{\neq}_{(ave)}$ defined to be equal to the sum of $\Delta G^{\neq}_{(EE\text{-}ZZ)}$ and $\Delta G^{\neq}_{(ZZ\text{-}EE)}$ divided by 2 in the case of the complexes while this average, $\Delta G^{\neq}_{(ave)}$ = ($\Delta G^{\neq}_{(E\text{-}Z)}$ and $\Delta G^{\neq}_{(Z\text{-}E)}$)/2 for the unbound ligands. The use of such average barrier, $\Delta G^{\neq}_{(ave)}$ compensates for any raising or lowering of the ground state energies due to the unequal population of isomers, and thus presupposes all the barrier heights to a common ground state.

Table 4.4 Thermodynamic data for the barrier to rotation around the (S)C-N(Me)(*para*-X-Ph) bond in unbound ligands HL^{1A} and HL^{2A} and coordinated ligands in ***cis*-[Pt($L^{1A,2A,3A}$-*S,O*)$_2$]** complexes.

Complex	T_c/K	Δυ/Hz	$\Delta G^{\neq}_{(ZZ\text{-}EE)}$ [a] kcal/mol	$\Delta G^{\neq}_{(EE\text{-}ZZ)}$ [a] kcal/mol	$\Delta G^{\neq}_{(ave)}$ [a] kcal/mol
HL^{1A}	298 ± 1	141	14.1	15.4	14.7
***cis*-[Pt(L^{1A})$_2$]**	307 ± 1	45.99	16.9	15.2	16.1
***cis*-[Pt(L^{1A})$_2$]**	(307 ± 1)	(50.40)	(15.9)	(15.1)	(15.5)
HL^{2A}	281 ± 1	131	13.3	14.4	13.9
***cis*-[Pt(L^{2A})$_2$]**	291 ± 1	47.19	15.4	14.3	14.9
***cis*-[Pt(L^{2A})$_2$]**	(291 ± 1)	(51.50)	(14.7)	(14.3)	(14.5)
***cis*-[Pt(L^{3A})$_2$]**	234 ± 1	52.03	11.4	11.4	11.4

[a] The standard deviations of the ΔG values do not exceed 0.2 kcal/mol

Again for the sake of interpreting the thermodynamic data in Table 4.4 we make use of an energy diagram, Figure 4.16. Here $\Delta G^{\neq}_{(ZZ\text{-}EE)}$ describes the energy barrier from *ZZ* to *EE* and $\Delta G^{\neq}_{(EE\text{-}ZZ)}$ describes the reverse process that is from *EE* to *ZZ* and TS is the transition state. It must be said that this is a simplification for the complexes since this does not take into account of the *EZ* isomer, which is also a stable compound and not a transition state. This energy profile is however, most suitable to describe the energy barriers of the unbound ligands.

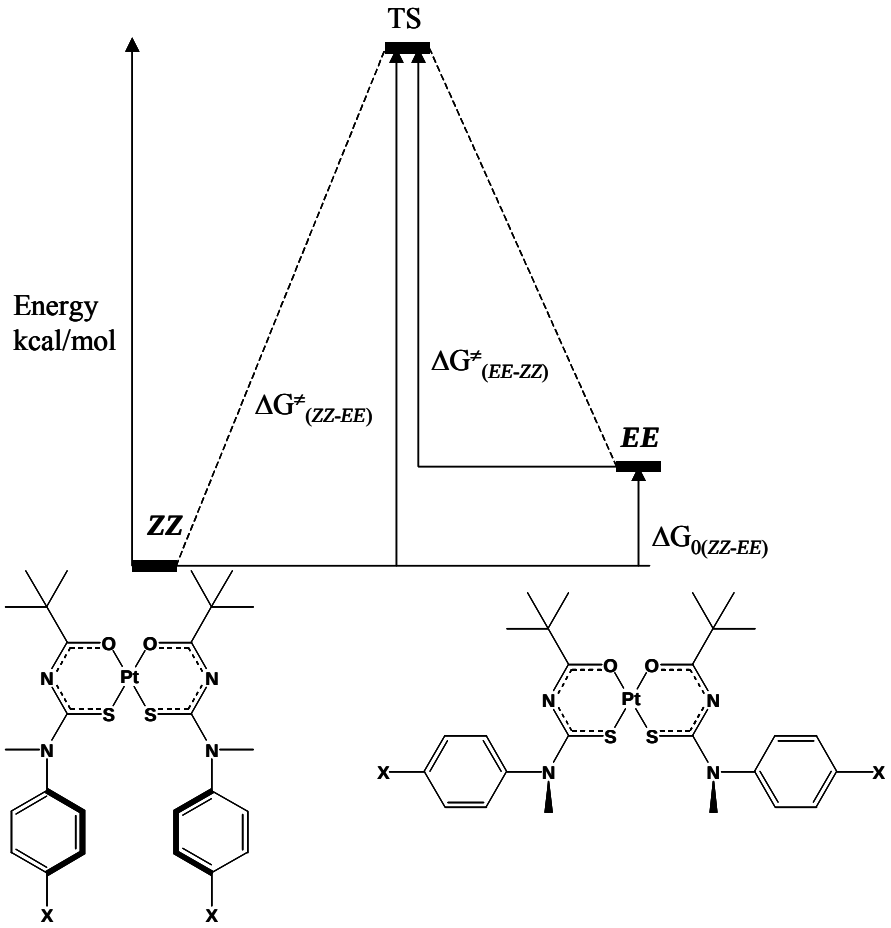

Figure 4.16 A simplified energy diagram that follows from equations [4.6] and [4.7], showing the inter-conversion of *ZZ* and *EE* isomers for ***cis*-[Pt(L^{1A}-*S,O*)$_2$]** when X = O-CH_3 and ***cis*-[Pt(L^{2A}-*S,O*)$_2$]** when X = H. This is more suitable for describing the inter conversion of *E* and *Z* isomers of the unbound ligands but with the *E* isomer being the major component.

4.3.5.1 Rotational energy interpretation of the ligands.

From the estimations of the C-N bond rotation barriers, it can be observed that the ligand with the electron donating group *i.e.* with the methoxy substituent, HL^{1A}, gives rise to the largest $\Delta G^{\neq}$ values (14.1 kcal/mol in Table and 14.7 kcal/mol in Table 4.4), followed by the unsubstituted ligand, HL^{2A} (13.3 kcal/mol in Table 4.3 and 13.8 kcal.mol in Table 4.4). No data is available regarding HL^{3A} (with the electron withdrawing nitro group) since the *Z* isomer could not be observed at low temperature; however it is reasonable to assume that this ligand would give rise to the lowest C-N bond rotation barrier. This assumption is well supported by the comparisons of the free energies of activation of the Pt(II) complexes derived from these ligands. This is indeed expected since an electron-withdrawing substituent, X = NO_2, should in principle weaken the (S)C-N(Me)(*para*-X-Ph) bond the most in the series X = O-CH_3, H and NO_2 and the electronic donating group X = O-CH_3 strengthens this C-N bond. The unsubstituted ligand, HL^{2A} with

substituent X = H, lie between the electronic withdrawing and electronic donating extremes. This trend is seen in the coalescence temperatures of these ligands (Tc = 298 K for HL^{1A} and 281 K for HL^{2A}), again assuming that the coalescence temperature of HL^{3A} is well below 198 K. These findings are contrary to Carter's[29] observations that in *N,N*-dimethyl-*N'*-phenylthioureas with the phenyl substituted in the *para* position, the electron-donating substituent lowered the barrier while the electron withdrawing substituent had the opposite effect. Density functional theory (DFT) calculations by Ilieva *et al*[14] on *para*-substituted acetanilides with the substituent being **H**, CH_3, OH, **OCH_3**, OCH_2CH_3, NH_2, Cl, COOH, **NO_2** and SO_2NH_2 (the substituents shown in bold were investigated in the series of ligands discussed in this thesis) showed that the electron donating groups increase the rotation barrier of the C-N bond while the electron withdrawing groups lower the C-N bond rotation barrier. The observations in the studied series HL^{1A} and HL^{2A} with X = O-CH_3 and H, respectively, are in agreement with this study and the study of substituent effect on carbamate C-N bond rotation barrier done by Smith.[30] Interestingly, the overall difference in thermodynamic stabilities between the *E* and the *Z* isomers regardless of the ligand is marginal, being less than 1 kcal.mol^{-1}. One might expect the *E* isomer to be much more stable than the *Z* isomer in $CDCl_3$ or CD_2Cl_2 solution for both ligands, the ^{1}H NMR spectra suggest an *E* : *Z* ratio of *ca* 9:1.

4.3.5.2 Rotational energy interpretation of the Pt(II) chelates

Regardless of the solvent, the enthalpies of activation of the chelates are larger than those of the uncoordinated ligands, but the difference is no more than 2 kcal.mol^{-1}. Complex formation in principal increases the rotational barrier compared with the unbound ligand since the electrophilic metal centre pulls electrons from the thiocarbonyl C-N bond via the sulphur atom which has formed a dative bond with the metal, according to Behrendt *et al*.[27] The trends observed in the unbound ligands are mirrored in the complexes with no exceptions. These data clearly demonstrate how significant the electronic contribution can be on the C-N rotation barrier no matter how remote (in this case six bonds away) the substituent is.

In the complex, ***cis*-[Pt(L^{1A}-*S,O*)$_2$]**, with the largest barrier to rotation around the (S)C-N(Me)(*para*-X-Ph) bond ($\Delta G^{\neq}_c$ in CD_2Cl_2 = 15.2 kcal/mol in Table 4.3 and 16.0 kcal./mol in Table 4.4) results in formation of the complexes in which the *ZZ* isomer is favoured regardless of the unbound ligand *E*/*Z* isomer distribution. In other words the *ZZ* isomer is stabilised by a high barrier to rotation around the (S)C-N(Me)(*para*-X-Ph) bond. Now it is clear to explain why more of the *ZZ* isomer is formed in a more polar solvent since a polar solvent increases the C-N bond rotation barrier (Section 4.3.3). On the other extreme for the ***cis*-[Pt(L^{3A}-*S,O*)$_2$]** case, when the barrier to rotation around the (S)C-N(Me)(*para*-X-Ph) bond is lowest ($\Delta G^{\neq}_c$ in CD_2Cl_2 = 11.4 kcal/mol in both Table 4.3 and Table 4.4), the driving force that stabilises the *ZZ* isomer is weaker and apparently the *EE* isomer is equally stabilised, hence equal populations are observed. As this happens the *EZ* isomer becomes dominant and this seems to be intuitively sound since this is similar to a 1 : 1 mixture of pure *EE* and *ZZ* isomers resulting in a roughly 1 : 2 : 1 statistical *EE* : *EZ* : *ZZ* isomer distribution. Between these two extremes lies the ***cis*-[Pt(L^{2A}-*S,O*)$_2$]** complex where it seems that the barrier to rotation around the (S)C-N(Me)(*para*-X-Ph) bond ($\Delta G^{\neq}_c$ in CD_2Cl_2 = 14.4 kcal/mol in Table 4.3 and 14.9 kcal./mol in Table 4.4) is still sufficiently high for the *ZZ* isomer to be favoured over the *EE* isomer, and

approximately equally stable to the *EZ* isomer. For this hypothesis to be generally acceptable however, it needs further testing with a wider range of *para*-substituents.

Again as it was noted for the ligands the energy differences between the individual configurational isomers of the complexes are very small, at most being about 2.2 kcal.mol^{-1}. Still, the *ZZ* isomer has been calculated to have the lower energy, it is however remarkable and even surprising that this small energy difference could result in such a strong preference for the *ZZ* Pt-complex. Additionally, upon solvent change from chloroform to dichloromethane we observe a notable change in these energies and that may be an indication that a solvent may play significant role in stabilising a particular configurational isomer rather than a thermodynamic driving force towards one isomer.

4.3.6 A gas phase study of the barrier to rotation around the C-N bond by means of Density Functional Theory (DFT) linear transit calculation: A complementary theoretical method to the solution NMR experimental method.

Model 1 (Figure 4.17): Here unlike the complexes investigated in solution (with two equal ligands), the complex is coordinated with one symmetrically disubstituted ligand and one asymmetrically disubstituted ligand and the C-N bond rotation is performed on the latter. **Model 2** (Figure 4.18): Both ligands on the complex are asymmetrically disubstituted much like the solution experiments. In both models, full geometrical optimisation of the complex in which the ligand(s) is orientated in the *E* position resulted in the *N*-(*para*-X-Ph) moiety nearly orthogonal to the chelate ring for all the coordinated *para*-substituted ligands. The same applies when the ligand is in the *Z* orientation the *N*-(*para*-X-Ph) moiety is once again nearly orthogonal to the chelate ring instead of being flat and collinear. The most structural parameter that can be linked to the stability of one configuration over the other is the (S)C-N(Me)(*para*-X-Ph) bond length and these are all included in both Figures 4.17 and 4.18. In general, upon rotation from *E* to *Z* configuration there is a marginal but noticeable shortening of this C-N bond implying that the *Z* configuration is preferred over the *E* configuration. What is slightly divergent between the calculated trends and those obtained by solution NMR experiments is the relative energy of the *Z* configuration to that of the *E* configuration when the *para*-substituent is the nitro group. These small differences in gas phase may, however, drastically change in solution and cannot be relied on for predicting a favoured configuration. We have already shown how drastic the relative population (hence energies) can shift upon solvent change.

Model 1: Figure 4.17 together with Table 4.5 clearly show the barrier heights as the *para*-substituent is changed and this trend is in accord with the experiment results that an electron-donating substituent (O-CH_3) should give rise to a higher rotation barrier than an electron-withdrawing substituent (NO_2). The electron-donating substituent facilitates resonance between the nitrogen lone pair and the thiocarbonyl sulphur, resulting in an increased barrier of rotation. The reverse holds when the electron-withdrawing substituent is in place since the nitrogen lone pair is drawn into the aromatic ring. The calculated barrier height when the *para*-substituent is the hydrogen atom lies between the two extremes as observed in solution. In support of this analysis when we take a look at the calculated C-N bond lengths whether it be comparing the *E* configurations or the *Z* configurations, there is a shortening of this bond in the order NO_2 > H > O-CH_3. Only a marginal difference is observed between the latter two *para*-substituents.

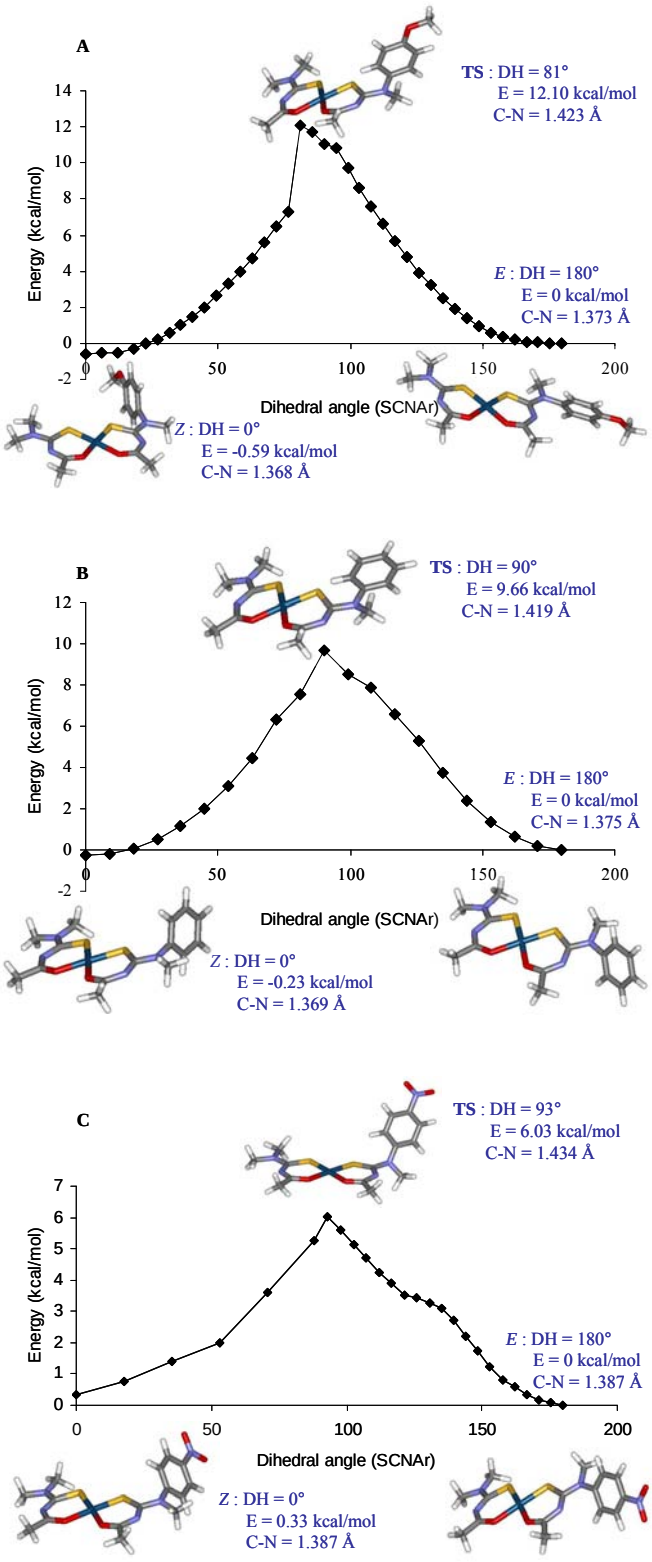

Figure 4.17 Energy diagram for the rotation around the C-N bond in Pt(II) coordinated *para*-substituted model *N*-methyl-*N*-(*para*-X-phenyl)-*N'*-methylthioureas. In (**A**) the *para*-substituent is a methoxy group, in (**B**) the *para*-substituent is a hydrogen atom and in (**C**) the *para*-substituent is a nitro group.

Table 4.5 Theoretical energy barriers to rotation around the (S)C-N(Me)(*para*-X-Ph) bond in Pt(II) coordinated *para*-substituted model *N*-methyl-*N*-(*para*-X-phenyl)-*N'*-methylthioureas as determined by DFT calculation.

para-substituent	E_{TS}^{rel} [a] kcal/mol	E_Z kcal/mol	$\Delta E = E_{TS} - E_Z$ [b] kcal/mol
O-CH_3	12.10	-0.59	12.69
H	9.66	-0.23	9.89
NO_2	6.03	0.33	5.70

[a] E_{TS}^{rel} is the energy of the transition state relative to the *E* isomer (set at 0 kcal/mol).
[b] ΔE is the energy barrier for the *Z* to *E* rotation through the TS transition state (Figure 4.17).

Model 2: Figure 4.18 is a much closer model to the complexes investigated in solution the only difference being the methyl group attached to the carbonyl carbon instead of a tertiary butyl. This small difference, in principle should have no bearing on the aim of the study, which is to evaluate the barrier to rotation around the C-N bond of the (S)C-N(Me)(*para*-X-Ph) moiety as the *para*-substituent is altered. This model thus far is incomplete in two ways: firstly, the energy diagram with the O-CH_3 *para*-substituent did not converge but from **model 1** we can predict where this should be relative to the others. Secondly, due to time constraints modelling of *ZZ* to *EZ* was not performed and the energy diagram only shows rotation of *EE* configuration to *EZ* configuration. In both energy diagrams in Figure 4.18 there are two transition states through which the *EZ* configuration can be reached from the *EE* configuration. This is an indication that in the geometrically optimised *EE* complex, the topside is not identical to the bottom side. After a 360-degree rotation from the *EE* configuration we arrive in the same configuration, which is at a slightly different energy level. For all practical purposes these are indistinguishable from each other. Important parameters that include dihedral angles (DH), C-N bond length and energies are included in the energy diagrams. Table 4.6 summarises the calculated energy barriers for the transition from *EE* to *EZ* configuration. The expected transition state through which the *EZ* configuration is attained is probably the one that is slightly lower in energy, which is TS2. The analysis of Figure 4.18 is no different to that of Figure 4.17 in terms of trends of energy barriers as the *para*-substituent is altered. Comparing the two models it seems that the nature of the ligand to which no rotation is performed is not really relevant for the calculations of the relative rotation barriers. ΔE = 9.89 kcal/mol (**model 1**) and ΔE_2 = 9.53 kcal/mol (**model 2**) when the *para*-substituent is a hydrogen atom while ΔE = 5.70 kcal/mol (**model 1**) and ΔE_2 = 5.73 kcal/mol (**model 2**) when the *para*-substituent is a nitro group. This may mean that the *N*-(*para*-X-Ph) group of the ligand that is not being rotated is far enough for steric factors not to play any significant role in the calculations of these relative energies. It should be interesting to see whether this would hold in *ZZ* to *EZ* modelling, although it could be that the one of the transition states would be forbidden due to possible steric factors.

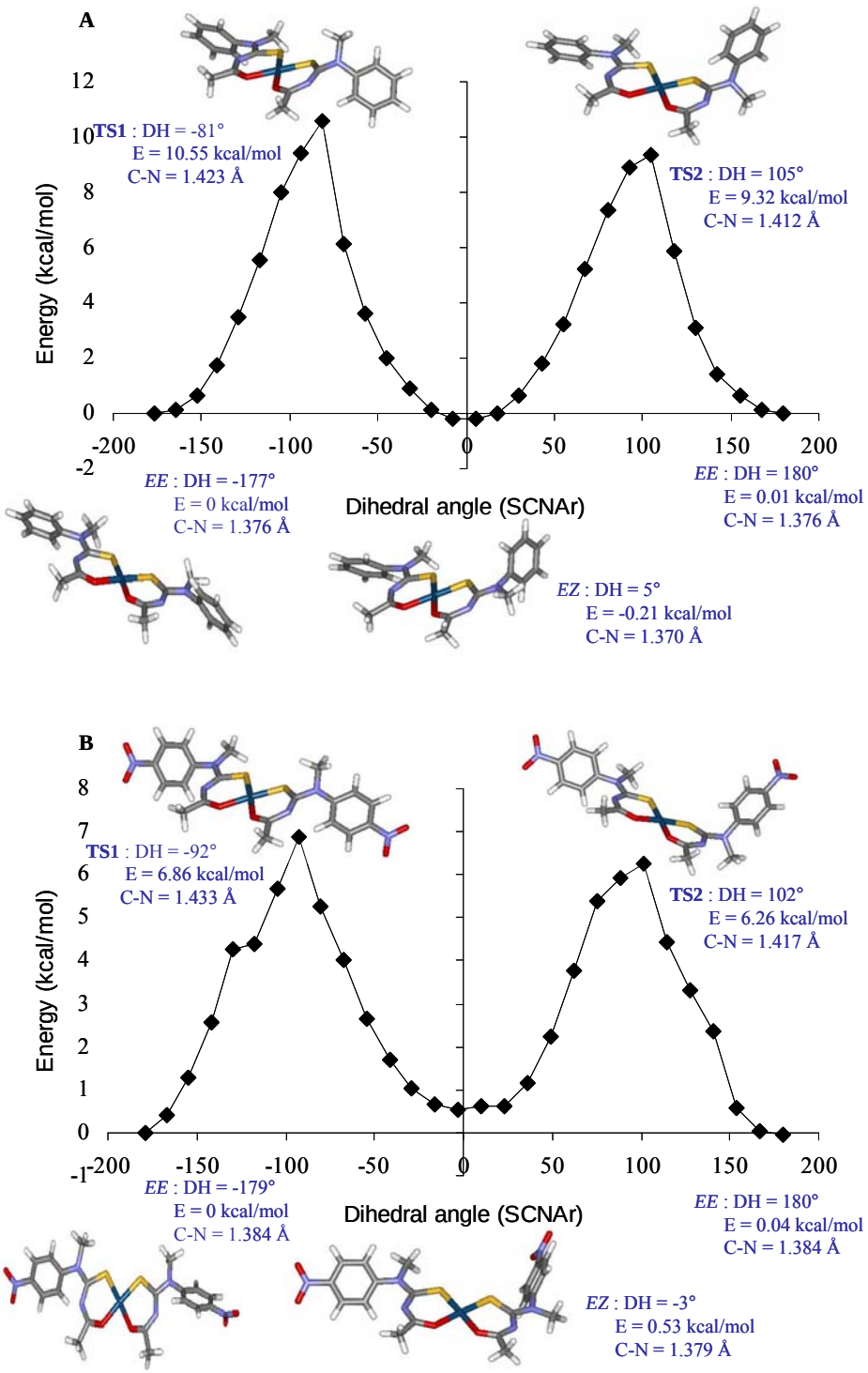

Figure 4.18 Energy diagram for the rotation around the C-N bond in coordinated *para*-substituted *N*-methyl-*N*-(*para*-X-phenyl)-*N'*-methylthioureas of model *cis*-bis Pt(II) chelates. In (**A**) the *para*-substituent is a hydrogen atom and in (**B**) the *para*-substituent is a nitro group.

Table 4.6 Theoretical energy barriers to rotation around the (S)C-N(Me)(*para*-X-Ph) bond in Pt(II) coordinated *para*-substituted model *N*-methyl-*N*-(*para*-X-phenyl)-*N'*-methylthioureas as determined by DFT calculation.

para-substituent	E_{TS1}[rel] [a] kcal/mol	E_{TS2}[rel] [a] kcal/mol	$\Delta E_1 = E_{TS1} - E_{EZ}$ [b] kcal/mol	$\Delta E_2 = E_{TS2} - E_{EZ}$ [b] kcal/mol
H	10.55	9.32	10.76	9.53
NO_2	6.86	6.26	6.33	5.73

[a] E_{TS1}^{rel} and E_{TS2}^{rel} are the energies of the first and second transition state, respectively, relative to the *EE* isomer (set at 0 kcal/mol).

[b] ΔE_1 and ΔE_2 are the energy barriers for the *EZ* to *EE* rotation through TS1 and TS2 transition states, respectively (Figure 4.18).

4.4 Concluding remarks

Low temperature NMR proved to be a valuable tool for full characterisation of the ligands as well as the complexes derived from them by slowing down the fast dynamics of these systems at ambient temperature. The remote substituent effect on *N*-methyl-*N*-(*para*-X-phenyl)-*N'*-acylthioureas has been shown to have significant consequences on the partial double C-N bond character of the (S)C-N(Me)(*para*-X-Ph) moiety and this impacts on the resultant *EE*/*EZ*/*ZZ* isomer distributions of the Pt(II) complexes. We arrive at this conclusion since it seems that the *ZZ* isomer is stabilised by a higher C-N bond rotation barrier and more of this isomer is observed the higher this barrier is. We can therefore conclude that electronic effects play an important role in the distribution of configurational isomers of platinum derived from these ligands. The calculations of the thermodynamic parameters followed the expected trend in the strengthening of the partial double (S)C-NR(*para*-X-Ph) bond; the nitro substituent resulting in the weakest bond followed by the unsubstituted moiety and the methoxy substituent resulting in the strongest C-N bond. In addition to electronic effects of the substituent, X, the influence of the solvent proved to be quite significant in the rotational barrier of thiocarbonyl C-N bond and subsequently the isomer distribution. Thus far it can be speculated that the different polarities of the solvent do lead to these differences, but two these solvents are by no means a comprehensive study to say this with more certainty, hence a thorough study needs to be undertaken with regard to solvent effect. Principally it has been shown that in as much as the electronic effects play a significant role in steering the isomer distributions, so does the solvent polarity in which the complexes are dissolved. In addition to these two factors it has also been shown that the temperature at which the NMR measurements are made are critical to the results obtained for these complexes. It was therefore essential to measure and quote the distributions in identical conditions. Complementary to the solution NMR results are the DFT theoretical calculations of the energy barriers as a function of the *para*-substituent in these complexes. The trends that are obtained theoretical in this study are rather qualitative in their manner and agree well with our experimental data (and theoretical studies of others), which lends confidence to our results.

References

1 A. Liden and J. Sandstrom, *Acta. Chem. Scand.*, **1973**, *27*, 2567.
2 D. G. Gehring, W. A. Mosher, and G. S. Reddy, *J. Org. Chem.*, **1966**, *31*, 3436.
3 E. J. Baerends, Autschbach, J.,Bérces, A.,Bo, C. *et al.*, <http://www.scm.com>. **2004**.
4 S. H. Vosko, L. Wilk, and M. Nusair, *Can. J. Phys.*, **1980**, *58*, 1200.
5 J. P. Perdew, J. A. Chevary, S. H. Vosko, K. A. Jackson, M. R. Pederson, D. J. Singh, and C. Fiolhais, *Phys. Rev. B*, **1992**, *46*, 6671.
6 E. van Lenthe, J. G. Snijders, and E. J. Baerends, *J. Chem. Phys.*, **1996**, *105*, 6505.
7 K. R. Koch, C. Sacht, T. Grimmbacher, and S. Bourne, *S. Afr. J. Chem.*, **1995**, *48*, 71.
8 A. J. R. Bourn, D. G. Gillies, and E. W. Randall, *Tetrahedron*, **1966**, *22*, 1825.
9 B. F. Pedersen and B. Pedersen, *Tetrahedron Lett.*, **1965**, 2995.
10 J. A. Weil, A. Blum, A. H. Heiss, and J. K. Kinnaird, *J. Chem. Phys.*, **1967**, *46*, 3132.
11 R. E. Carter, *Acta Chem. Scand.*, **1967**, *21*, 75.
12 J. P. Chupp and J. F. Olin, *J. Org. Chem.*, **1967**, *32*, 2297.
13 B. Galabov, S. Ilieva, B. Hadjieva, and E. Dinchova, *J. Phys. Chem. A*, **2003**, *107*, 5854.
14 S. Ilieva, B. Hadjieva, and B. Galabov, *J. Org. Chem.*, **2002**, *67*, 6210.
15 S. M. Cohen and T. H. Brown, *J. Chem. Phys.*, **1974**, *61*, 2985.
16 W. E. Stewart and T. H. Siddall, III, *Chem. Rev.*, **1970**, *70*, 517.
17 T. Drakenberg, K. I. Dahlqvist, and S. Forsen, *J. Phys. Chem.*, **1972**, *76*, 2178.
18 S. M. N. Crawford, A. N. Taha, N. S. True, and C. B. LeMaster, *J. Phys. Chem. A*, **1997**, *101*, 4699.
19 C. Suarez, C. B. LeMaster, C. L. LeMaster, M. Tafazzoli, and N. S. True, *J. Phys. Chem.*, **1990**, *94*, 6679.
20 E. M. Duffy, D. L. Severance, and W. L. Jorgensen, *J. Am. Chem. Soc.*, **1992**, *114*, 7535.
21 C. L. Perrin, J. D. Thoburn, and A. J. Kresge, *J. Am. Chem. Soc.*, **1992**, *114*, 8800.
22 K. B. Wiberg and D. J. Rush, *J. Am. Chem. Soc.*, **2001**, *123*, 2038.
23 K. B. Wiberg, P. R. Rablen, D. J. Rush, and T. A. Keith, *J. Am. Chem. Soc.*, **1995**, *117*, 4261.
24 P. R. Rablen, *J. Org. Chem.*, **2000**, *65*, 7930.
25 D. Argyropoulos, E. Hoffmann, S. Mtongana, and K. R. Koch, *Magn. Reson. Chem.*, **2003**, *41*, 102.
26 S. Lanza, F. Nicolo, and G. Tresoldi, *Eur. J. Inorg. Chem.*, **2002**, 1049.
27 S. Behrendt, L. Beyer, F. Dietze, E. Kleinpeter, E. Hoyer, E. Ludwig, and E. Uhlemann, *Inorg. Chim. Acta*, **1980**, *43*, 141.
28 H. Shanan-Atidi and K. H. Bar-Eli, *J. Phys. Chem.*, **1970**, *74*, 961.
29 R. E. Carter, *Acta. Chem. Scand.*, **1968**, *22*, 2643.
30 B. D. Smith, D. M. Goodenough-Lashua, C. J. E. D'Souza, K. J. Norton, L. M. Schmidt, and J. C. Tung, *Tetrahedron Lett.*, **2004**, *45*, 2747.

Chapter 5: Coordination chemistry of asymmetrically disubstituted *N*-alkyl-*N*-aryl-*N'*-acylthioureas to platinum(II)

Part 3: The influence of the alkyl substituent on the isomer distribution of *E,Z* configurational isomers of platinum(II) complexes of *N*-alkyl-*N*-aryl-*N'*-acylthioureas

Summary

The influence of the alkyl substituent change has been investigated on the distributions of *ZZ*, *EZ* and *EE* configurational isomer of platinum(II) chelates derived from unsymmetrical *N*-alkyl-*N*-aryl-*N'*-acylthiourea ligands. The ^{195}Pt NMR spectra of these complexes have been measured under identical conditions with *N*-alkyl groups changing from methyl, *iso*-propyl, cyclohexyl to *n*-pentyl and the *N*-aryl group is either substituted at the *para*-position with a methoxy or nitro group or has no para-substituent at all. Parallel to the ligands described in the previous chapter, even though the *E* isomer is hugely favoured over the *Z* isomer in the unbound ligands, on complexation to the platinum(II) metal centre the *ZZ* isomer interestingly is most favoured over the *EZ* isomer and more so over the *EE* isomer. The *ZZ* isomer is observed to be increasingly favoured in the following sequence as the *N*-alkyl group is changed: n-pentyl > cyclohexyl > iso-propyl > methyl in the cases where the *N*-aryl group has been fixed as either 4-methoxy substituted or unsubstituted. Even the incomplete series of the case where the *N*-aryl group has a nitro substituent the *ZZ* isomer is favoured when the *N*-alkyl group is n-pentyl over the methyl. A few examples of these ligands in the *E* configuration in solid state have been isolated and for the very first time a platinum(II) chelate with unsymmetrical ligands of this type in a *ZZ* configuration has also been isolated.

5.1 Introduction

In the previous chapter it was clearly demonstrated in detail that the relative increase or decrease of the double bond character of the C-N bond of the (S)C-N(R)(*para*-X-Ph) (X = O-CH_3, H and NO_2) moiety in *N*-methyl-*N*-(*para*-X-phenyl)-*N'*-acylthioureas is dependent on the electron donating/electron withdrawing properties of the *para*-substituent, more especially upon ligand complexation to platinum(II) metal ion. When the complexes are dissolved in chloroform the *ZZ* isomer is energetically favoured over both the *EZ* and the *EE* isomers for the complex with highest rotation barrier of the C-N bond of the (S)C-N(R)(*para*-X-Ph) moiety. It was also noted that in a more polar solvent, dichloromethane, the C-N bond rotation barrier increases slightly, favouring the *ZZ* isomer even more. In this regard a solvent in which these compounds are dissolved is an important factor in the determination of these configurational isomers. Another significant factor is the temperature at which the measurement of the distributions is carried out; the lower the temperature is, there more of the *ZZ* isomer is observed. Hence the overall factors which have remarkable consequences on the *EE*/*EZ*/*ZZ* distributions of the platinum(II) complexes derived from these ligands are electronic, solvent polarity and temperature. To arrive fairly to any conclusions about the nature of the *N*-alkyl group influence on these isomer distributions, it is clearly necessary to keep the other factors unchanged. For comparisons of the isomer distributions of these complexes (listed in Scheme 1) all their ^{195}Pt NMR spectra were carried out in deuterated chloroform at 243 K. The exception to these conditions is the determination of isomer populations of ***cis*-[Pt(L^{3A}-*S,O*)$_2$]**, which were measured in deuterated dichloromethane at 198 K for the reasons already discussed in the previous chapter.

In this chapter the influence that a change in the *N*-alkyl group, R, has on the rotational barrier of the (S)C-N(R)(*para*-X-Ph) bond and the effects on the configurational isomer distributions of the platinum(II) chelates derived from two sets of *N*-alkyl-*N*-(*para*-X-phenyl)-*N'*-acylthiourea ligands is examined. For the purpose of achieving these aims a new series of ligands with the same structural motif as the ligands studied in the previous chapter was synthesised. The variation of the *N*-CH_3 group by substituting with a variety of alkyl groups: isopropyl, cyclohexyl and pentyl groups were studied. For each series of *N*-alkyl groups, the *N*-(*para*-X-phenyl) moiety was kept unchanged with the *para*-substituent being either a hydrogen atom or a methoxy group or a nitro group (see Scheme 1). This would hopefully allow the determination of the influence the *N*-alkyl group has on the isomer distributions in three different systems. As observed in the previous chapter the *N*-(*para*-X-phenyl) group is barrier lowering on the (S)C-N(R)(*para*-X-Ph) bond most so when the *para*-substituent X is a nitro group, which is electron withdrawing. Low temperature ^{195}Pt NMR experiments were employed to monitor qualitatively what effect a change in the *N*-alkyl group has on the C-N bond rotation barrier on two complexes with an *N*-(4-nitro-phenyl) group. Even though the low temperature experiments could only be carried out for two compounds, ***cis*-[Pt(L^{3A}-*S,O*)$_2$]** and ***cis*-[Pt(L^{3D}-*S,O*)$_2$]** with methyl and pentyl groups, respectively, important inferences about the effect an *N*-alkyl group change has on the isomer distributions were drawn.

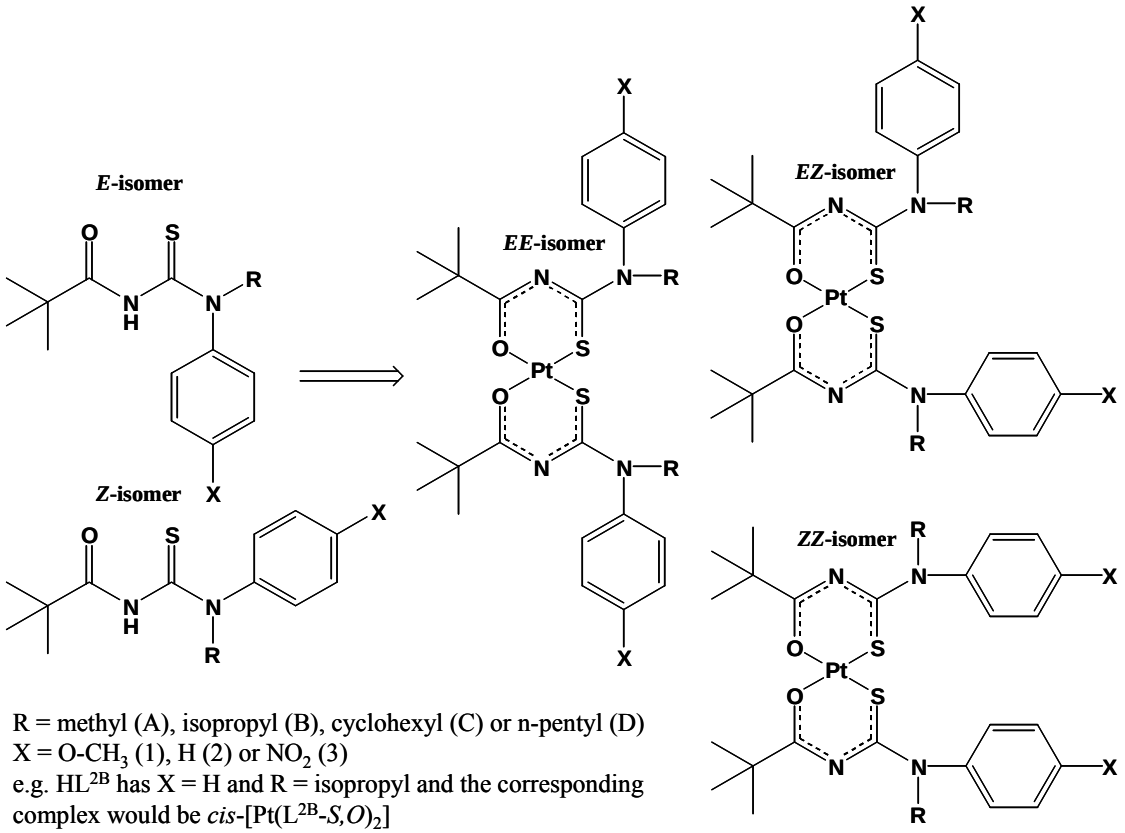

Scheme 1 A series of new ligands and their corresponding platinum(II) chelates with systematic electronic variations on the *para*-substituent, X and *N*-alkyl substituent, R. The nitro series has two sets of ligands, one with R = methyl and pentyl group. The methoxy and the H series are complete with all the *N*-alkyl substituents.

Here it is also demonstrated that the general isomer distribution trends obtained in the previous chapter for the complexes derived from the *N*-methyl-*N*-(*para*-X-Ph)-*N'*-acylthioureas are retained for each of the three additional *alkyl* substituent changes. In the complexes studied here the population of the *ZZ* isomer, though dominant, as determined by ^{195}Pt NMR spectroscopy progressively gets smaller for the *para*-substituent of the *N*-(*para*-X-phenyl) moiety in the order: O-CH_3 > H > NO_2. Therefore these observations support the findings of the previous chapter.

5.2 Experimental

5.2.1 General remarks

The synthesis and characterisation of ligands has already been described in detail in **chapter 2**, however, for comparison with the platinum(II) chelates derived from these ligands their NMR assignments will be discussed.

5.2.2 NMR spectroscopy

Conventional ^{1}H and ^{13}C NMR spectra of relatively high concentrations (*ca* 80 mg.cm^{-3}) of the ligands and their respective platinum(II) complexes using 5 mm diameter tubes were obtained at various temperatures in deuterated chloroform using a Varian Inova 400 spectrometer operating at 400 and 101 MHz for ^{1}H and ^{13}C, respectively. The calibration curve for the broadband probe was defined as: Actual temperature (°C) = 0.9892 x Set temperature (°C) + 0.0859 (°C). All samples were carefully filtered before any spectroscopic measurement was undertaken. The ^{195}Pt NMR spectra of the complexes were also recorded at various temperatures using the Varian Inova 400 spectrometer operating at 86 MHz [reference material: 500 mg.cm^{-3} H_2PtCl_6 in 30% (v/v) D_2O-1M HCl at $\delta(^{195}Pt)$ = 0 ppm at 30 °C].

5.2.3 Synthesis of platinum complexes

The new series of Pt(II) complexes were prepared and characterised according to our previously published method,[1] which entails drop-wise addition a platinum(II) solution (in a one to one volume of acetonitrile to water) to a solution of ligand and sodium acetate (also in a one to one volume of acetonitrile to water). All the reagents were commercially available and were used without any prior purification. The reactions were generally conducted at 50 ºC for two hours. After the reaction solutions had cooled to room temperature, excess water was added and reaction mixtures were refrigerated before the products were collected by means of centrifugation and dried under vacuum. Elemental analyses were performed using a Carlo Erba EA 1108 elemental analyser courtesy of the University of Cape Town. Detailed ^{1}H and ^{13}C NMR spectroscopic data for the new complexes follows the numbering scheme indicated Scheme 2. For the ^{1}H NMR assignments the carbon to which the protons are attached will be indicated.

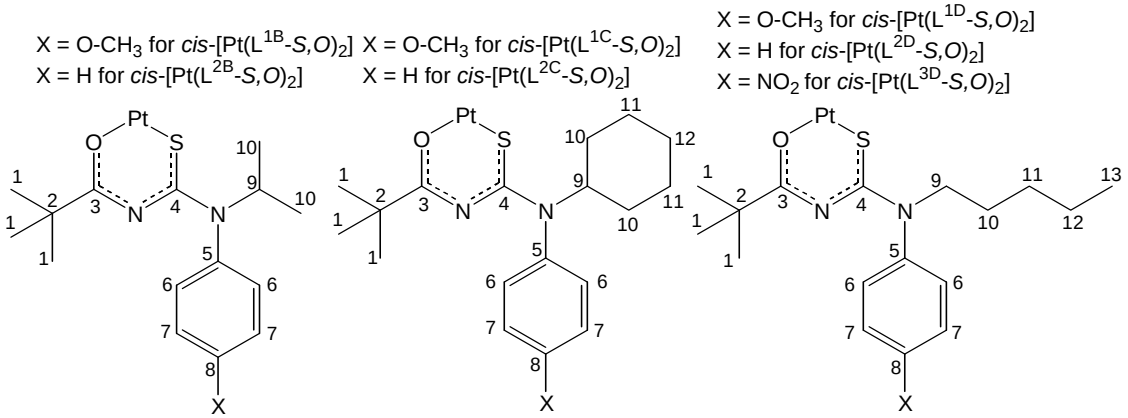

Scheme 2 Numbering scheme for ^{1}H and ^{13}C NMR assignments of the new complexes. The coordinated ligand is only drawn in an *E* orientation.

***cis*-bis(*N*-Isopropyl-*N*-(4-methoxy-phenyl)-*N'*-*2,2*-dimethylpropanoylthioureato)platinum(II), *cis*-[Pt(L^{1B}-*S,O*)$_2$]**: A yield of 93% collected and analysed. Found C, 47.42; H, 5.66; N, 6.90; S, 7.60 $C_{32}H_{42}N_4O_2PtS_2$ required C, 47.45; H, 5.72; N, 6.92; S, 7.92%. δ_H(400 MHz; solvent $CDCl_3$): 7.05 (2H, d, C_6 (EZ)), 6.93 (2H, d, C_6 (ZZ)), 6.79 (2H, d, C_7 (ZZ)), 5.45 (1H, ses, C_9 Z(EZ)), 5.40 (1H, ses, C_9 ZZ), 5.18 (1H, ses, C_9 EE), 5.00 (1H, ses, C_9 E(EZ)), 3.81 (3H, s, O-CH_3 E(EZ)), 3.79 (3H, s, O-CH_3 Z(EZ)), 3.72 (3H, s, O-CH_3 ZZ), 1.23 (9H, s, C_1 Z(EZ)), 1.22 (9H, s, C_1 ZZ), 0.76 (9H, s, C_1 EE), 0.75 (9H, s, C_1 E(EZ)), 0.96 (6H, d C_{10} ZZ). δ_C(101 MHz, solvent $CDCl_3$): 183.47 C_3 Z(EZ), 183.31 C_3 (ZZ), 182.65 C_3 E(EZ), 168.54 C_4 ZZ, EZ and EE, 158.78 C_8 Z(EZ), 158.59 C_8 ZZ, 157.82 C_8 E(EZ), 132.79 C_5 E(EZ), 132.32 C_5 Z(EZ), 132.16 C_5 ZZ, 130.77 C_6 Z(EZ), 130.61 C_6 ZZ, 129.64 C_6 E(EZ), 114.04 C_7 Z(EZ), 113.95 C_7 ZZ, 114.04 C_7 E(EZ), 55.33 (O-CH_3) ZZ, EZ and EE, 50.26 C_9 ZZ, EZ and EE, 42.31 C_2 Z(EZ), 42.28 C_2 ZZ, 42.28 C_2 E(EZ), 28.05 C_1 ZZ and Z(EZ), 27.47 C_1 EE and E(EZ), 21.03 C_{10} EE and E(EZ), 20.77 C_{10} ZZ and E(EZ).

***cis*-bis(*N*-Cyclohexyl-*N*-(4-methoxy-phenyl)-*N'*-*2,2*-dimethylpropanoylthioureato)platinum(II), *cis*-[Pt(L^{1C}-*S,O*)$_2$]**: A yield 85% collected and analysed. Found C, 51.31; H, 6.46; N, 6.34; S, 7.25 $PtC_{38}H_{54}N_4S_2O_4$ required C, 51.28; H, 6.12; N, 6.29; S, 7.21%. δ_H(400 MHz; solvent $CDCl_3$): 7.06 (2H, d, C_6 (EZ)), 6.93 (2H, d, C_6 (ZZ)), 6.79 (2H, d, C_7 (ZZ)), 6.75 (2H, d, C_6 (EZ)), 5.01 (1H, ses, C_9 Z(EZ)), 4.95 (1H, ses, C_9 ZZ), 4.54 (1H, ses, C_9 E(EZ)), 3.83 (3H, s, O-CH_3 E(EZ)), 3.79 (3H, s, O-CH_3 Z(EZ)), 3.76 (3H, s, O-CH_3 ZZ), 1.74 (4H, br, C_{10} ZZ, EZ and EE) 1.23 (9H, s, C_1 Z(EZ)), 1.22 (9H, s, C_1 ZZ), 0.76 (9H, s, C_1 EE), 1.01 (4H, m, C_{11} ZZ, EZ and EE), 0.85 (2H, m, C_{12} ZZ, EZ and EE), 0.75 (9H, s, C_1 E(EZ)). δ_C(101 MHz, solvent $CDCl_3$): 183.28 C_3 Z(EZ), 183.12 C_3 (ZZ), 182.51 C_3 E(EZ), 168.45 C_4 ZZ, EZ and EE, 158.72 C_8 Z(EZ), 158.56 C_8 ZZ, 157.76 C_8 E(EZ), 133.69 C_5 E(EZ), 133.10 C_5 Z(EZ), 132.29 C_5 ZZ, 130.59 C_6 Z(EZ), 130.44 C_6 ZZ, 129.49 C_6 E(EZ), 114.04 C_7 Z(EZ), 113.89 C_7 ZZ, 113.03 C_7 E(EZ), 55.73 (O-CH_3) ZZ, EZ and EE, 55.45 C_9 E(EZ), 55.39 C_9 Z(EZ), 55.31 C_9 ZZ, 42.36 C_2 Z(EZ), 42.24 C_2 ZZ, 41.59 C_2 E(EZ), 31.17 C_{10} ZZ, EZ and EE 28.22 C_1 ZZ and Z(EZ), 27.47 C_1 EE and E(EZ), 25.67 C_{11} ZZ, EZ and EE, 25.07 C_{12} ZZ, EZ and EE.

***cis*-bis(*N*-Pentyl-*N*-(4-methoxy-phenyl)-*N'*-*2,2*-dimethylpropanoylthioureato)platinum(II), *cis*-[Pt(L^{1D}-*S,O*)$_2$]**: A yield of 81% was collected and analysed. Found C, 50.24; H, 6.64; N, 6.54; S, 7.24 $C_{36}H_{54}N_4O_4PtS_2$ required C, 49.93; H, 6.28; N, 6.47; S, 7.41%. δ_H(400 MHz; solvent $CDCl_3$): 7.18 (2H, d, C_6 (EZ)), 7.05 (2H, d, C_6 (ZZ)), 6.94 (2H, d, C_7 E(EZ)), 6.90 (2H, d, C_7 E(EZ)), 6.82 (2H, d, C_7 (ZZ)), 3.79 (2H, m, C_9 ZZ, EZ and EE), 3.74 (3H, s, O-CH_3 ZZ, EZ and EE), 1.54 (4H, br, C_{10} and C_{11} ZZ, EZ and EE), 1.23 (9H, s, C_1 Z(EZ)), 1.22 (9H, s, C_1 ZZ), 0.81 (9H, s, C_1 E(EZ)),1.17 (2H, br, C_{12} ZZ, EZ and EE), 0.82 (3H, t, C_{13} ZZ, EZ and EE). δ_C(101 MHz, solvent $CDCl_3$): 183.62 C_3 Z(EZ), 183.47 C_3 (ZZ), 182.72 C_3 E(EZ), 168.27 C_4 ZZ, EZ and EE, 158.55 C_8 Z(EZ), 158.40 C_8 ZZ, 157.52 C_8 E(EZ), 137.53 C_5 E(EZ), 136.89 C_5 Z(EZ), 136.77 C_5 ZZ, 129.07 C_6 Z(EZ), 128.93 C_6 ZZ, 127.87 C_6 E(EZ), 114.51 C_7 Z(EZ), 114.41 C_7 ZZ, 113.44 C_7 E(EZ), 55.24 (O-CH_3) ZZ, EZ and EE, 55.39 C_9 ZZ, EZ and EE, 42.27 C_2 Z(EZ), 42.21 C_2 ZZ, 41.72 C_2 E(EZ), 28.74 C_{10} ZZ, EZ and EE, 28.04 C_1 ZZ and Z(EZ), 27.53 C_1 EE and E(EZ), 26.96 C_{11} ZZ, EZ and EE, 22.45 C_{12} ZZ, EZ and EE, 14.13 C_{13} ZZ, EZ and EE.

***cis*-bis(*N*-Isopropyl-*N*-phenyl-*N'*-*2,2*-dimethylpropanoylthioureato)platinum(II), *cis*-[Pt(L^{2B}-*S,O*)$_2$]**: A yield of 91% was collected and analysed. Found C, 47.61; H, 5.61; N, 7.42; S, 8.40 $C_{30}H_{42}N_4O_2PtS_2$ required C, 48.05; H, 5.65; N, 7.47; S, 8.55%. δ_H(400 MHz; solvent $CDCl_3$): 7.43 (2H, dd, C_7 EE and E(EZ)), 7.34 (2H, dd, C_7 ZZ and Z(EZ)), 7.16 (2H, dd, C_6 EE and E(EZ)), 7.03 (2H, dd, C_6 ZZ and Z(EZ)), 6.94 (1H, dd, C_8 EE and E(EZ)), 6.87 (1H, dd, C_8 ZZ and Z(EZ)), 5.05 (1H, ses, C_9 Z(EZ)), 5.44 (1H, ses, C_9 ZZ), 5.20 (1H, ses, C_9 EE), 5.01 (1H, ses, C_9 E(EZ)), 1.24 (9H, s, C_1 Z(EZ)), 1.23 (9H, s, C_1 ZZ), 0.73 (9H, s, C_1 EE), 0.72 (9H, s, C_1 E(EZ)), 1.05 (6H, d C_{10} E(EZ)), 1.04 (6H, d C_{10} Z(EZ)), 0.97 (6H, d C_{10} ZZ). δ_C(101 MHz, solvent $CDCl_3$): 183.56 C_3 Z(EZ), 183.39 C_3 (ZZ), 182.60 C_3 E(EZ), 168.09 C_4 ZZ, EZ and EE, 140.13 C_5 EE and E(EZ), 139.41 C_5 ZZ and Z(EZ), 129.85 C_7 EE and E(EZ), 129.70 C_7 ZZ and Z(EZ), 129.10 C_6 Z(EZ), 129.01 C_6 ZZ, 128.80 C_6 E(EZ), 128.31 C_8 E(EZ), 128.23 C_8 Z(EZ), 128.16 C_8 E(EZ), 50.34 C_9 ZZ, EZ and EE, 42.34 C_2 Z(EZ), 42.26 C_2 ZZ, 41.58 C_2 E(EZ), 28.06 C_1 ZZ and Z(EZ), 27.34 C_1 EE and E(EZ), 21.06 C_{10} EE and E(EZ) 20.87 C_{10} E(EZ), 20.82 C_{10} ZZ.

***cis*-bis(*N*-Cyclohexyl-*N*-phenyl-*N'*-*2,2*-dimethylpropanoylthioureato)platinum(II), *cis*-[Pt(L^{2C}-*S,O*)$_2$]**: A yield of 91% was collected and analysed. Found C, 51.10; H, 6.00; N, 6.68; S, 7.28 $C_{36}H_{50}N_4O_2PtS_2$ required C, 52.09; H, 6.07; N, 6.75; S, 7.73%. δ_H(400 MHz; solvent $CDCl_3$): 7.43 (2H, br, C_7 EE and E(EZ)), 7.31 (2H, dd, C_7 ZZ and Z(EZ)), 7.16 (2H, dd, C_6 EE and E(EZ)), 7.03 (2H, dd, C_6 ZZ and Z(EZ)), 6.92 (1H, br, C_8 EE and E(EZ)), 6.85 (1H, br, C_8 ZZ and Z(EZ)), 5.05 (1H, tt, C_9 Z(EZ)), 4.99 (1H, tt, C_9 ZZ), 4.72 (1H, tt, C_9 EE), 4.54 (1H, tt, C_9 E(EZ)), 1.79 (4H, br, C_{10} ZZ, EZ and EE) 1.24 (9H, s, C_1 Z(EZ)), 1.23 (9H, s, C_1 ZZ), 0.73 (9H, s, C_1 EE), 0.72 (9H, s, C_1 E(EZ)), 1.51 (4H, m, C_{11} ZZ, EZ and EE), 0.89 (2H, m, C_{12} ZZ, EZ and EE). δ_C(101 MHz, solvent $CDCl_3$): 183.43 C_3 Z(EZ), 183.29 C_3 (ZZ), 182.54 C_3 E(EZ), 168.06 C_4 ZZ and Z(EZ), 167.90 C_4 EE and E(EZ), 141.06 C_5 E(EZ), 140.32 C_5 Z(EZ), 140.16 C_5 ZZ, 129.76 C_7 EE and E(EZ), 129.62 C_7 ZZ and Z(EZ), 129.21 C_6 Z(EZ), 129.06 C_6 ZZ, 128.77 C_6 E(EZ), 128.27 C_8 EE and E(EZ), 128.19 C_8 ZZ and Z(EZ), 59.89 C_9 EE and E(EZ), 58.85 C_9 ZZ and Z(EZ), 42.47 C_2 Z(EZ), 42.34 C_2 ZZ, 41.65 C_2 E(EZ), 31.42 C_{10} E(EZ), 31.36 C_{10} Z(EZ), 31.30 C_{10} ZZ, 28.25 C_1 ZZ and Z(EZ), 27.44 C_1 EE and E(EZ), 25.87 C_{11} ZZ and E(EZ), 25.37 C_{11} EE and E(EZ), 25.13 C_{12} ZZ, 25.05 C_{12} Z(EZ), 24.98 C_{12} E(EZ).

***cis*-bis(*N*-Pentyl-*N*-phenyl-*N'*-*2,2*-dimethylpropanoylthioureato)platinum(II), *cis*-[Pt(L^{2D}-*S,O*)$_2$]**: A yield of 91% was collected and analysed. Found C, 49.76; H, 6.90; N, 6.86; S, 8.79 $C_{34}H_{50}N_4O_2PtS_2$ required C, 50.67; H, 6.25; N, 6.95; S, 7.96%. δ_H(400 MHz; solvent $CDCl_3$): 7.47 (2H, t, C_7 EE and E(EZ)), 7.43 (2H, t, C_8 EE and E(EZ)), 7.34 (2H, m, C_7 ZZ and Z(EZ)), 7.30 (2H, m, C_8 ZZ and Z(EZ)), 7.14 (1H, d, C_6 ZZ and Z(EZ)), 6.98 (1H, d, C_6 EE and E(EZ)), 3.89 (2H, t, C_9 E(EZ)), 3.82 (2H, t, C_9 ZZ), 3.76 (2H, t, C_9 Z(EZ)), 1.56 (4H, br, C_{10} and C_{11} ZZ, EZ and EE), 1.24 (9H, s, C_1 Z(EZ)), 1.22 (9H, s, C_1 ZZ), 0.78 (9H, s, C_1 E(EZ)), 1.18 (2H, br, C_{12} ZZ, EZ and EE), 0.81 (3H, t, C_{13} ZZ, EZ and EE). δ_C(101 MHz, solvent $CDCl_3$): 183.72 C_3 Z(EZ), 183.56 C_3 (ZZ), 182.76 C_3 E(EZ), 167.88 C_4 ZZ, EZ and EE, 144.71 C_5 E(EZ), 144.04 C_5 Z(EZ), 143.92 C_5 ZZ, 129.64 C_7 EE and E(EZ), 129.53 C_7 ZZ and Z(EZ), 128.64 C_6 E(EZ), 128.10 C_6 Z(EZ), 127.93 C_6 ZZ, 126.99 C_8 ZZ and Z(EZ), 126.69 C_8 EE and E(EZ), 55.69 C_9 ZZ, EZ and EE, 42.29 C_2 Z(EZ), 42.22 C_2 ZZ, 41.70 C_2 E(EZ), 28.77 C_{10} ZZ, EZ and EE, 28.13 C_1

ZZ and Z(EZ), 27.41 C_1 EE and E(EZ), 26.98 C_{11} ZZ, EZ and EE, 22.41 C_{12} ZZ, EZ and EE, 14.13 C_{13} ZZ, EZ and EE.

***cis*-bis(*N*-Pentyl-*N*-(4-nitro-phenyl)-*N'*-*2,2*-dimethylpropanoylthioureato)platinum(II), *cis*-[Pt(L^{3D}-*S,O*)$_2$]**: A yield of 87% was collected and analysed. Found C, 45.34; H, 5.66; N, 9.27; S, 7.69 $C_{34}H_{48}N_6O_6PtS_2$ required C, 45.58; H, 5.40; N, 9.38; S, 7.16%. δ_H(400 MHz; solvent $CDCl_3$): 8.25 (2H, d, C_7 ZZ, EZ and EE), 7.35 (2H, d, C_6 ZZ, EZ and EE), 3.89 (2H, t, C_9 ZZ, EZ and EE), 1.55 (2H, br, C_{10} ZZ, EZ and EE), 1.21 (4H, br, C_{11} and C_{12} ZZ, EZ and EE) 1.07 (9H, s, C_1 ZZ, EZ and EE), 0.80 (3H, t, C_{13} ZZ, EZ and EE). δ_C(101 MHz, solvent $CDCl_3$): 185.11 C_3 ZZ, EZ and EE, 169.29 C_4 ZZ, EZ and EE, 150.40 C_5 ZZ, EZ and EE, 146.88 C_8 ZZ, EZ and EE 129.32 C_7 ZZ, EZ and EE, 124.98 C_6 ZZ, EZ and EE, 54.24 C_9 ZZ, EZ and EE, 42.27 C_2 ZZ, EZ and EE, 28.65 C_{10} ZZ, EZ and EE, 27.71 C_1 ZZ, EZ and EE, 27.06 C_{11} ZZ, EZ and EE, 22.11 C_{12} ZZ, EZ and EE, 13.68 C_{13} ZZ, EZ and EE.

We have already reported on the synthesis and characterisation of ***cis*-[Pt(L^{1A}-*S,O*)$_2$]**, ***cis*-[Pt(L^{2A}-*S,O*)$_2$]** and ***cis*-[Pt(L^{3A}-*S,O*)$_2$]** in the previous chapter. These form part of the discussion here for the sake of comparison since all these complexes are similar to the new complexes.

5.2.4 Crystallography and structure refinement of cis-bis(*N*-pentyl-*N*-(4-methoxy-phenyl)-*N'-2,2*-dimethylpropanoylthioureato)platinum(II), ***cis*-[Pt(L^{1D}-*S,O*)$_2$]**

The ***cis*-[Pt(L^{1D}-*S,O*)$_2$]** complex crystallised in chloroform at low temperature to produce suitable single crystals for X-ray structure analysis. The crystals were first covered with paratone oil before they were mounted on a thin glass fibre and data were collected on a Bruker-Nonius SMART Apex diffractometer using monochromated Mo-Kα radiation (λ = 0.7107 Å). The structure was solved using SHELX-97 and refined using SHELXL-97[2] with the aid of the interface program X-SEED.[3] All non-hydrogen atoms were modelled anisotropically. Hydrogen atoms were placed in geometrically calculated positions, with C-H = 0.99 (for -CH_2-), 0.98 (for -CH_3), or 0.95 Å (for phenyl). The relevant crystallographic data is shown in Table 5.5 and selected bond lengths and angles are shown in Table 5.6.

5.3 Results and Discussion

5.3.1 *E,Z configurational isomerism in asymmetrically disubstituted N-alkyl-N-(para-X-phenyl)-N'-acylthiourea ligands, $HL^{1B,1C,1D}$, $HL^{2B,2C,2D}$ and HL^{3D}*

All the unbound ligands with the general structure *N*-alkyl-*N*-(*para*-X-phenyl)-*N'*-acylthiourea of relevance in this chapter (listed in Scheme 1) display *E,Z* isomerism that is observed at sufficiently low temperatures. Again it is attributable to the barrier lowering nature of the aryl substituent[4] that the *E,Z* isomerism is not observable at room temperature in chloroform. The ligands with a *N*-(4-nitro-phenyl) group have such a low C-N bond rotation barrier, that the *E,Z* isomers are in fast exchange on the NMR time scale and therefore appear as one signal even at much

lower temperatures (198 K) in dichloromethane. This is attributed to the electron withdrawing nitro group that can be assumed to draw the (S)C-N(alkyl)(*para*-X-phenyl) nitrogen lone pair electrons into the aromatic ring so lowering the rotation barrier of the C-N bond. For the other ligands the *E,Z* configurational isomers are readily observed by duplication of peaks in the ^{1}H and ^{13}C NMR spectra at 243 K. Here we shall not show the sections of either the ^{1}H or ^{13}C NMR spectra for all the ligands as they are similar to those discussed in the previous two chapters.

For quantitative determination of the relative populations of the *E* and the *Z* isomers in the new ligands the N-H proton singlet resonances were integrated. This region of the spectrum is less complicated than the *N*-CH-/*N*-CH_2-proton region with $^{3}J(^{1}H\text{-}^{1}H)$ couplings or the phenyl region. Even more complicated region is the rest of the *N*-alkyl group. Figure 5.1 illustrates the $^{3}J(^{1}H\text{-}^{1}H)$ coupling involved in *N*-CH- protons of the *N*-isopropyl group of HL^{2B} together with much simple N-H singlet resonances.

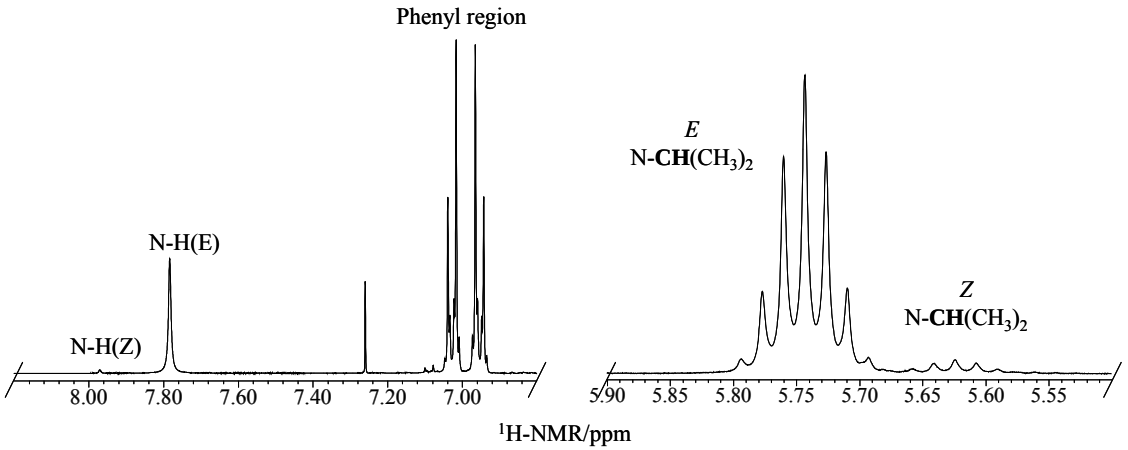

Figure 5.1 Sections of ^{1}H NMR spectrum showing the $^{3}J(^{1}H\text{-}^{1}H)$ couplings on the *N*-CH- protons of the *E,Z* isomers of HL^{2B}, the phenyl region and the N-H resonances. The spectrum was acquired at 243 K in deuterated chloroform.

The assignment of *E* and *Z* isomers is similar to that discussed previously and will not again be discussed here. In Figure 5.1 the upfield resonance of the *N*-**CH**$(CH_3)_2$ proton at 5.62 ppm due to the *Z* isomer is suppose to be identical to the downfield septet resonance of the *N*-**CH**$(CH_3)_2$ proton at 5.75 ppm of the *E* isomer. Due to the relatively small population of the *Z* component the upfield resonance is not well resolved. Table 5.1 lists all the ligands with the *E,Z* isomer populations as determined by digital integration of the N-H singlet resonances. The table shows that the relative percentage of *E* is much higher than that of *Z* for all the ligands under investigation. What is more, the relative distribution of the *E* isomer is increased even further from methyl to isopropyl to cyclohexyl to pentyl and is almost the exclusive isomer present (98%) in the ligands with a cyclohexyl or pentyl group.

Table 5.1 Relative distributions of the *E,Z* configurational isomers of three different types of *N*-alkyl-*N*-(*para*-X-phenyl)-*N-2,2*-dimethylpropanoylthioureas as determined from digital integration of the N-H singlet resonances in the ^{1}H NMR spectra measured at 243 K. The reported percentage distributions are estimated to have an error of ± 1%.

Ligand	*N*-(*para*-X-phenyl)	*N*-alkyl	*Z*-isomer (%)	*E*-isomer (%)
[a]HL^{1A}	*N*-(4-Methoxy-Ph)	*N*-CH_3	13	87
HL^{1B}		*N*-$CH(CH_3)_2$	3	97
HL^{1C}		*N*-cyclo(C_6H_{11})	2	98
HL^{1D}		*N*-$(CH_2)_4CH_3$	2	98
[a]HL^{2A}	*N*-(Ph)	*N*-CH_3	10	90
HL^{2B}		*N*-$CH(CH_3)_2$	7	93
HL^{2C}		*N*-cyclo(C_6H_{11})	2	98
HL^{2D}		*N*-$(CH_2)_4CH_3$	2	98
[a], [b]HL^{3A}	*N*-(4-Nitro-Ph)	*N*-CH_3	-	-
[b]HL^{3D}		*N*-$(CH_2)_4CH_3$	-	-

[a] These ligands were already discussed in the previous chapter and are included in this series for the sake of comparison and the *E,Z* isomer distributions of these were obtained by deconvolution analysis of the *N*-CH_3 proton resonances. These resonances were singlets and readily to integrated.

[b] The *E,Z* isomer distribution of these ligands could not be determined since the C-N bond rotation is not sufficiently slow on the NMR time scale even at 198 K in dichloromethane.

In Table 5.1 it can be seen that for bulkier *N*-alkyl groups the population is skewed even more towards the *E* isomer. Similarly to the ligands HL^{1A} and HL^{2A}, discussed in the previous chapter the observed *E/Z* ratios seem to fall in the same general range of N-alkylacetanilides, which exist predominantly as the exo isomer,[5-8] for which the introduction of bulkier alkyl substituents, the *E* isomer is also found to dominate even further.

In the new series of ligands discussed in this chapter two crystal structures were determined for both *N*-cyclohexyl- and *N*-pentyl-*N*-(4-methoxy-phenyl)-*N'-2,2*-dimethylpropanoylthiourea, HL^{1C} and HL^{1D}. For both ligands only the *E* isomer was isolated in solid state, which is not surprising since the *E* components were in large excess over the *Z* components for both ligands in solution (Table 5.1). Both ligands have a C-N bond of the (S)C-N(alkyl)(*para*-X-Ph) moiety that is significantly shorter than a C-N single bond of 1.472(5) Å with HL^{1C} C-N bond length being 1.338(3) Å and that of HL^{1D} being 1.332(3) Å. These are comparable to bond lengths of HL^{1A} [1.343(3) Å] and HL^{2A} [1.340(4) Å] discussed in the previous chapter. It could therefore be anticipated that these ligands display *E,Z* isomerism due to the restricted rotation about this C-N bond.

5.3.2 Platinum(II) chelates derived from asymmetrically disubstituted N-alkyl-N-(phenyl)-N'-acylthioureas, $HL^{2A,2B,2C,2D}$.

On coordination to the Pt(II) metal centre, all the asymmetrically disubstituted ligands pass on their *E,Z* configurational isomerism and form *ZZ*, *EZ* and *EE* platinum(II) chelates similar to molecules previously shown in **chapter 4**. Again it is easy to see the presence of these isomers by observing the ^{195}Pt NMR spectra of these complexes as they show three well-resolved resonances at 303 K in chloroform. Since some of the new complexes, which will be encountered later are in fast exchange at ambient temperature, all the spectra reported in Figure 5.2 and the data in Table 2 were recorded at a common temperature of 243 K.

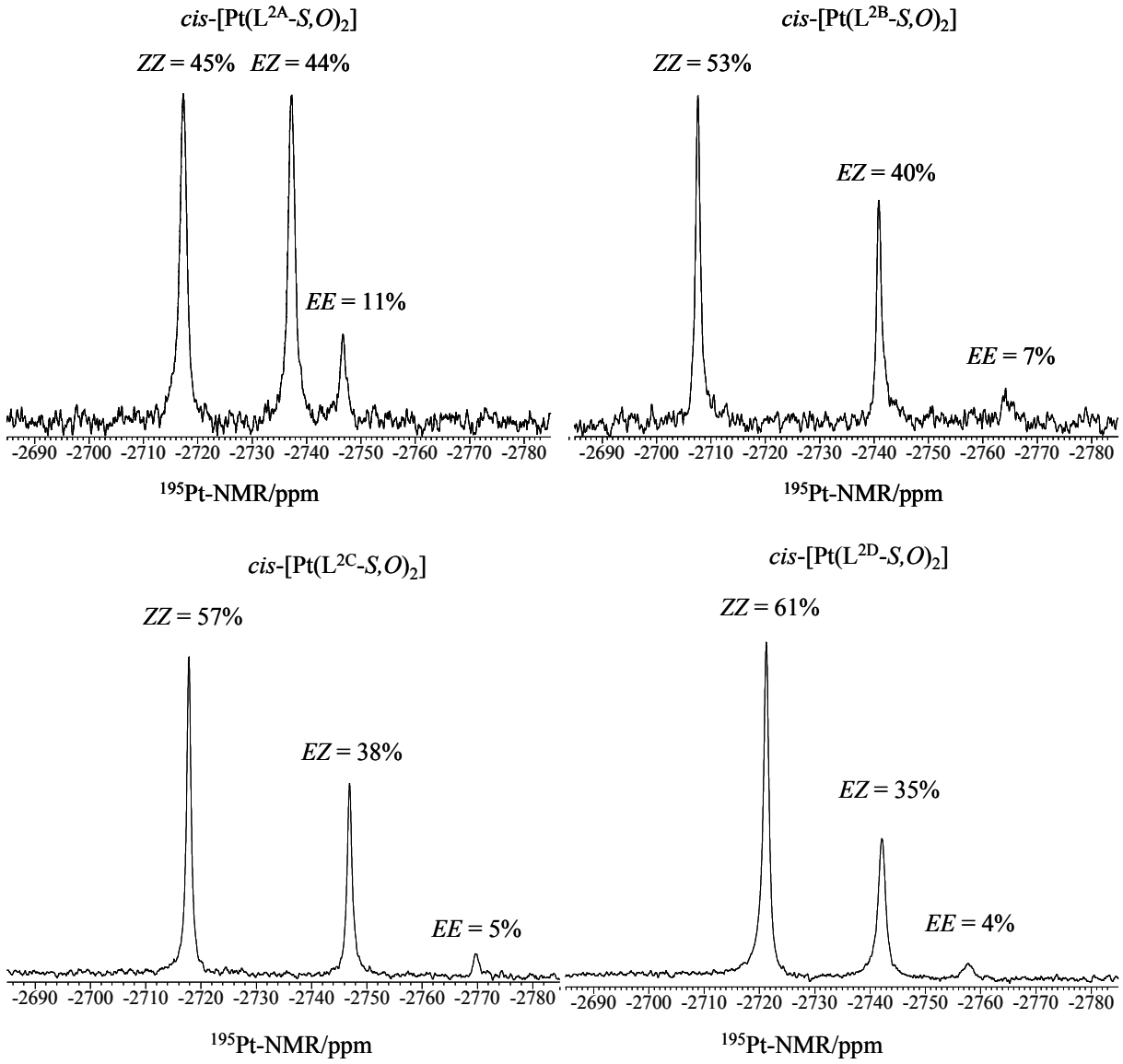

Figure 5.2 The 86 MHz ^{195}Pt NMR spectra of ***cis*-[Pt($L^{2A,2B,2C,2D}$-*S,O*)$_2$]** complexes showing their *ZZ*, *EZ* and *EE* isomer distributions. All the measurements were carried out in deuterated chloroform at 243 K.

Table 5.2 Assignments of δ(^{195}Pt) (ppm) and the relative *ZZ*, *EZ* and *EE* isomer distributions (taken from ^{195}Pt NMR deconvolution analysis) of configurational isomers of ***cis*-[Pt(L^{2A,2B,2C,2D}-*S,O*)$_2$]** complexes. All the spectra were measured in $CDCl_3$ at 243 K.

N-alkyl substituent, R	Complex	*ZZ*	*EZ*	*EE*
methyl	δ(^{195}Pt) ***cis*-[Pt(L^{2A}-*S,O*)$_2$]**	-2717	-2737	-2746
	[a] Statistical (%)	5	10	85
	[b] Relative integrals (%)	45	44	11
*iso*propyl	δ(^{195}Pt) ***cis*-[Pt(L^{2B}-*S,O*)$_2$]**	-2708	-2743	-2765
	[a]Statistical (%)	3.5	7	89.5
	[b] Relative integrals (%)	53	40	7
*cyclo*hexyl	δ(^{195}Pt) ***cis*-[Pt(L^{2C}-*S,O*)$_2$]**	-2718	-2748	-2770
	[a]Statistical (%)	1	2	97
	[b] Relative integrals (%)	57	38	5
n-pentyl	δ(^{195}Pt) ***cis*-[Pt(L^{2D}-*S,O*)$_2$]**	-2721	-2743	-2758
	[a]Statistical (%)	1	2	97
	[b] Relative integrals (%)	61	35	4

[a] Based on the *E,Z* isomer distributions assuming no inter-conversion during and after complexation to the Pt(II) centre.

[b] The observed relative integrals of the ^{195}Pt NMR spectra measured at 243 K. These values are estimated to have an error of ± 1%.

At 243 K both the ^{1}H and the ^{13}C NMR spectra of all the complexes studied can be used to confirm the presence of the three configurational isomers. Similar to the unbound ligands these spectra tend to be more complex and not so easy to integrate reliably as shown by the ^{1}H NMR section of a complex resulting from HL^{2B}, ***cis*-[Pt(L^{2B}-*S,O*)$_2$]** in Figure 5.3. The assignment of this spectrum is therefore based on the relative populations of the *ZZ*, *EZ* and *EE* isomers obtained from the ^{195}Pt NMR spectra.

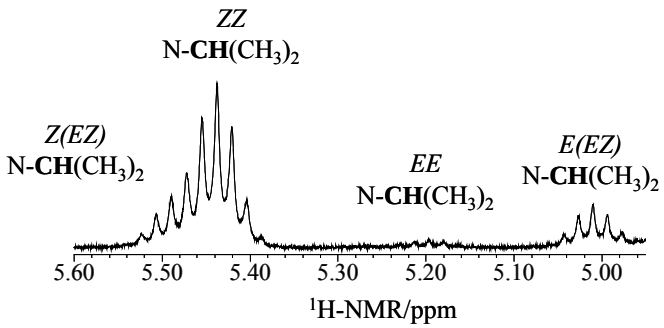

Figure 5.3 Low temperature (243 K) ^{1}H NMR spectrum section of ***cis*-[Pt(L^{2B}-*S,O*)$_2$]** showing the presence of three configurational isomers. The *EZ* isomer has two magnetically non-equivalent *N*-CH- protons hence there are four resonances for the three isomers.

Similar to the *N*-**CH**$(CH_3)_2$ proton region of the unbound ligand (Figure 5.1), the *N*-**CH**$(CH_3)_2$ proton region (Figure 5.3) of the complex is a lot more complicated to integrate and determine the *ZZ*, *EZ* and *EE* configurational isomer than integrating singlet resonances in the ^{195}Pt NMR spectrum. We demonstrated in the previous chapter that the ^{1}H and ^{195}Pt NMR spectra at the same temperature are complimentary within experimental error when comparing the isomer distributions. Therefore, it suffices to exclusively use the ^{195}Pt NMR spectra deconvolution analysis for comparing the isomer distributions when we evaluate the influence of the change of the *N*-alkyl group has on the isomer distributions.

It is clear from Figure 5.2 and Table 5.2 that the concentration of the *ZZ* isomer progressively grows at the expense of the *EZ* and *EE* isomers as the *N*-alkyl group is altered in the sequence: methyl < isopropyl < cyclohexyl < pentyl. As found in the previous chapter the *ZZ* isomer was observed to be favoured more if the energy of the C-N bond rotation barrier is increased. Even though the C-N rotation barriers in the set of complexes (***cis*-[Pt(L^{2B,2C,2D}-*S,O*)$_2$]**) could not be quantitatively determined, it has been noted that the configurational isomers of the new complexes are observable at room temperature in the ^{1}H NMR spectra. This is unlike the complexes ***cis*-[Pt(L^{1A,2A,3A}-*S,O*)$_2$]**, studied in chapter 4, whose configurational isomers were only observable at low temperatures from their ^{1}H NMR spectra. What this means in principle is that the complexes where the *N*-alkyl group is other than methyl, have a relatively higher rotation barrier than the *N*-methyl derivatives discussed in the previous chapter. It can be argued that in terms of the *N*-alkyl substituent sequence in which the *ZZ* isomer is favoured that the C-N bond rotational barrier in these complexes also follow this sequence i.e. $\Delta G^{\neq}$ increases in the order of alkyl substituent: methyl < isopropyl < cyclohexyl < pentyl. It is not likely that the rise in rotation barrier is due to increasing steric factors since it has been shown crystal structures that bulkier groups produce increasing non-planar distortions in substituted amides (*N*-ethyl-*N*-*4*-nitrophenylcarbamoyl chloride and *N*-phenylurethane) by twisting about the C-N bond.[9] The overall effect of introducing bulkier alkyl substituent in these substituted amides gave rise to relatively longer C-N bond. This in turn should lead to a lower rotation barrier. In support of this observation Isbrandt *et al.*[10] who studied unsymmetrically disubstituted *N,N*-disubstituted amides $CH_3C(O)N(CH_3)R'$ found that $\Delta G^{\neq}$ (kcal/mol) decreases in the sequence 18.1 R' = methyl, 18.0 R' = 18.0 ethyl, 17.9 R' = n-butyl, 17.1 R' = cyclohexyl and 17.0 R' = isopropyl.

Contrary to these two systems we have noted that on introducing bulkier *N*-alkyl substituents in our ligands has lead to a relatively shorter C-N bond length. Ligand HL^{1C} with a cyclohexyl group has a C-N bond length of 1.338(3) Å and that of HL^{1D} with a pentyl group has a C-N bond length of 1.332(3) Å while HL^{1A} with a methyl group has a C-N bond length of 1.343(3) Å. Intuitively, HL^{1C} and HL^{1D} should have a relatively higher C-N rotation barrier than HL^{1A} and that seems to be the case when comparing the isomer distributions in Figure 5.4 which we shall discuss shortly. A possible explanation for the increase in the double bond character of the C-N bond upon bulkier *N*-alkyl substitution could be due to relatively higher inductive effect of bulkier alky groups.

5.3.3 Platinum(II) chelates derived from asymmetrically disubstituted N-alkyl-N-(4-methoxy-phenyl)-N'-acylthioureas, $HL^{1A,1B,1C,1D}$ and N-alkyl-N-(4-nitro-phenyl)-N'-acylthioureas, $HL^{3A,3D}$

To establish the findings observed in the previous section regarding the influence of the bulkiness of the *N*-alkyl chain on the distribution of configurational isomers the same series of *N*-alkyl substituent (methyl, *iso*-propyl, cyclohexyl and *n*-pentyl) was used to make a new series of related ligands and Pt(II) complexes. In the first series the aryl group of the ligand is substituted at the *para* position with a methoxy substituent. In the second series the N-aryl group of the ligand is substituted at the *para* position with a nitro substituent (see Scheme 1). All ligands in the methoxy series display *E,Z* isomerism, and on coordination to Pt(II) metal centre, they pass on this configurational isomerism to result in *ZZ, EZ* and *EE* Pt(II) chelates.

The summary of the results that show the *N*-alkyl influence on the Pt(II) chelates isomer distributions in the methoxy series are shown in Figure 5.4 and Table 5.3. As the *N*-alkyl group is altered the *ZZ* isomer progressively grows at the expense of the *EZ* and *EE* isomers as was found in the previous series of Pt complexes of the unsubstituted phenyl, $HL^{2A,2B,2C,2D}$ ligands: methyl < isopropyl < cyclohexyl < pentyl. The *E,Z* isomers of both the *N*-methyl- and *N*-pentyl-(4-nitro-phenyl)-*N'-2,2*-dimethylpropanoylthioureas, HL^{3A} and HL^{3D} are in fast exchange on the NMR time scale to be observed as separate resonances. However upon coordination to Pt(II) metal centre these ligands display *E,Z* isomerism upon. The summary of the results for the incomplete series of the nitro-substituted ligands is shown in Table 5.4., showing similar trends as for the 4-methoxy substituted phenyl series and the unsubstituted phenyl series ligands. The consistency of the effect of the *N*-alkyl substituent change in different electronic environments (X = H in Section 5.3.2, X = O-CH_3 and X = NO_2 in Section 5.3.3) means that we are indeed making accurate assessments of the effect of these alkyl groups on the isomer distributions we observe.

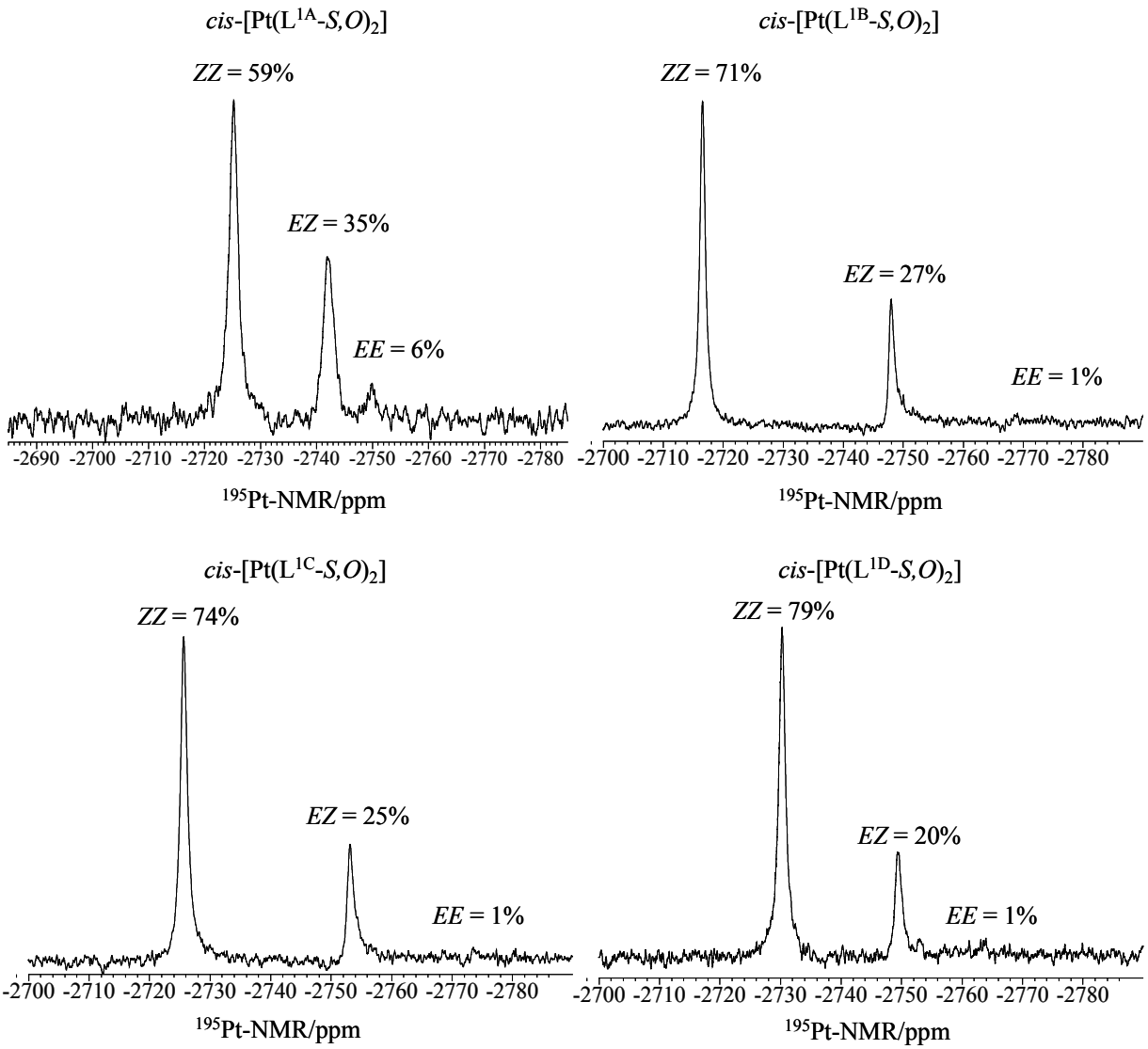

Figure 5.4 The 86 MHz ^{195}Pt NMR spectra of ***cis*-[Pt(L^{1A,1B,1C,1D}-*S,O*)$_2$]** complexes showing their *ZZ*, *EZ* and *EE* isomer distributions. All the measurements were carried out in deuterated chloroform at 243 K.

Table 5.3 Assignments of δ(^{195}Pt) (ppm) and the relative *ZZ*, *EZ* and *EE* isomer distributions (taken from ^{195}Pt NMR deconvolution analysis) of configurational isomers of ***cis*-[Pt(L^{1A,1B,1C,1D}-*S,O*)$_2$]** complexes. All the spectra were measured in $CDCl_3$ at 243 K.

N-alkyl substituent, R	Complex	*ZZ*	*EZ*	*EE*
methyl	δ(^{195}Pt) ***cis*-[Pt(L^{1A}-*S,O*)$_2$]**	-2725	-2742	-2750
	[a] Statistical (%)	6.5	13	80.5
	[b] Relative integrals (%)	59	35	6
*iso*propyl	δ(^{195}Pt) ***cis*-[Pt(L^{1B}-*S,O*)$_2$]**	-2717	-2748	-2767
	[a] Statistical (%)	1.5	3	95.5
	[b] Relative integrals (%)	72	28	< 1
*cyclo*hexyl	δ(^{195}Pt) ***cis*-[Pt(L^{1C}-*S,O*)$_2$]**	-2726	-2756	-2773
	[a] Statistical (%)	1	2	97
	[b] Relative integrals (%)	75	25	< 1
n-pentyl	δ(^{195}Pt) ***cis*-[Pt(L^{1D}-*S,O*)$_2$]**	-2730	-2748	-2765
	[a] Statistical (%)	1	2	97
	[b] Relative integrals (%)	76	24	< 1

[a] Based on the *E,Z* isomer distributions assuming no inter-conversion during and after complexation to the Pt(II) centre.

[b] The observed relative integrals of the ^{195}Pt NMR spectra measured at 243 K. These values are estimated to have an error of ± 1%.

Table 5.4 Assignments of δ(^{195}Pt) (ppm) and the relative *ZZ, EZ* and *EE* isomer distributions taken from ^{195}Pt NMR deconvolution analysis of configurational isomers of ***cis*-[Pt(L^{3D}-*S,O*)$_2$]** complex were measured in $CDCl_3$ at 243 K. The relative isomer distributions of ***cis*-[Pt(L^{3A}-*S,O*)$_2$]** complex were taken from ^{1}H NMR deconvolution analysis which was measured in CD_2Cl_2 at 198 K.

N-alkyl substituent, R	Complex	*ZZ*	*EZ*	*EE*
methyl	δ(^{195}Pt) ***cis*-[Pt(L^{3A}-*S,O*)$_2$]**	-	-	-
	[a]Statistical	-	-	-
	[b] Relative integrals (CD_2Cl_2)	27	46	27
n-pentyl	δ(^{195}Pt) ***cis*-[Pt(L^{3D}-*S,O*)$_2$]**	-2710	-2723	-2734
	[a]Statistical	-	-	-
	[c] Relative integrals ($CDCl_3$)	47	42	11

[a] Since *E,Z* isomers of HL^{3A} and HL^{3D} could not be observed as separate signals (*i.e.* their distribution is unknown) therefore the distribution of resultant complexes could not be predicted.

[b] The ^{1}H NMR resonances in which the deconvolution analysis was carried out were very sharp and these values are estimated to have an error of no more than 1%.

[c] The observed relative integrals of the ^{195}Pt NMR spectra measured at 243 K. These values are estimated to have a much bigger error than complexes discussed above due to broad line widths of the ^{195}Pt NMR peaks.

In the previous chapter it was argued that the ligand with the highest rotation barrier stabilises the *ZZ* isomer, and an electron-donating methoxy group on the *N*-aryl group should do this better than a hydrogen atom, which in turn is better than the nitro group. In this chapter we observed that bulkier alkyl groups lead to even higher C-N bond rotation barriers, so that the combined effect of electron donating group on the aryl moiety and bulkier *N*-alkyl substituent are expected lead to more stabilisation of the *ZZ* isomer and that is observed to be so. The highest *ZZ* population (76%) is observed is in complexes with *N*-pentyl-*N*-(4-methoxy-phenyl)- groups, complex ***cis*-[Pt(L^{1D}-*S,O*)$_2$]**, while the smallest *ZZ* population (27%) is when the ligands have *N*-methyl-(4-nitro-phenyl)- groups, complex ***cis*-[Pt(L^{3A}-*S,O*)$_2$]**.

Another important observation is that when comparing all pairs of complexes with the same *N*-alkyl substituent the *ZZ* isomer is always present at higher concentration for complexes derived from methoxy-substituted phenyl ring type ligands and at lowest concentration complexes derived from nitro-substituted phenyl ring type ligands. The complexes derived from the unsubstituted phenyl ring type ligands always fall between these extremes. This is consistent with the conclusions that we arrived at regarding the trends of electronic effects discussed in the previous chapter.

5.3.4 Evidence that the barrier to rotation around the (S)C-N(alkyl)(para-X-Ph) bond is higher with bulkier N-alkyl substituent

The ^{1}H NMR spectra of both the nitro-substituted ligands HL^{3A} and HL^{3D} do not display *E,Z* isomerism even at 198 K in deuterated dichloromethane. As mentioned before this is caused by the low rotation barrier of these compound, which is the direct consequence of the strongly electron-withdrawing nitro group. In solution both these ligands are cleaved exactly at this bond and this can be monitored by means of ^{1}H or ^{13}C NMR spectroscopy. Their respective complexes however, remain stable in solution. This is an indication that the C-N bond strengthens upon ligand complexation to the Pt(II) metal centre despite the contradictory lengthening of this bond in the solid-state structure reported for HL^{1D} vs ***cis*-[Pt(L^{1D}-*S,O*)$_2$]** in Section 5.3.5. These two complexes were suitable candidates for monitoring their rotational barriers. Figure 5.5 shows the ^{195}Pt NMR temperature array spectra of both complexes, ***cis*-[Pt(L^{3A}-*S,O*)$_2$]** and ***cis*-[Pt(L^{3D}-*S,O*)$_2$]**. This analysis unfortunately is not quantitative as in the manner with which the barrier to rotational around the (S)C-N(methyl)(*para*-X-Ph) bond for ***cis*-[Pt(L^{1A}-*S,O*)$_2$]**, ***cis*-[Pt(L^{2A}-*S,O*)$_2$]** and ***cis*-[Pt(L^{3A}-*S,O*)$_2$]** was carried out with ^{1}H NMR spectroscopy where coalescence temperatures were measured and $\Delta G^{\neq}_{c}$ values were estimated. From Figure 5.5 it is clear that at 243 K the complex with an *N*-pentyl group ***cis*-[Pt(L^{3D}-*S,O*)$_2$]** all the three isomers are observable while for ***cis*-[Pt(L^{3A}-*S,O*)$_2$]**, the complex with *N*-methyl group it would be necessary to lower the temperature even further to 'freeze' all the isomers. This means that the coalescence temperature for ***cis*-[Pt(L^{3D}-*S,O*)$_2$]** is higher than that of ***cis*-[Pt(L^{3A}-*S,O*)$_2$]** and therefore it should follow that its C-N bond rotation barrier is also higher. This higher C-N bond rotation barrier for ***cis*-[Pt(L^{3D}-*S,O*)$_2$]** over ***cis*-[Pt(L^{3A}-*S,O*)$_2$]** can only be attributed to the change from *N*-methyl group to *N*-pentyl group. Comparison of the isomer distributions between these two complexes in Table 5.4 shows that the *ZZ* isomer is stabilised more with *N*-pentyl

group. This in a qualitative way allows us to rank the effect of the *N*-alkyl substituent on the C-N rotation barrier by simply observing the population of the *ZZ* isomer.

Attempts of measuring higher coalescence temperatures and therefore determination of the rotational barriers quantitatively in other complexes were not possible. The reason being the lack of suitable solvent with a high boiling point in which the complexes are reasonably soluble. For example, in deuterated benzene (a solvent with a boiling point of 80 ºC) a ^{1}H NMR temperature array spectrum of the complex ***cis*-[Pt(L^{1C}-*S,O*)$_2$]** was carried out without reaching the coalescence temperature at 70 ºC. Qualitatively it can be deduced that this complex with a cyclohexyl group has a much higher rotation barrier than ***cis*-[Pt(L^{1A}-*S,O*)$_2$]** with a methyl substituent. The coalescence temperature of ***cis*-[Pt(L^{1A}-*S,O*)$_2$]** was measured in chloroform and dichloromethane and was fond to be 34 ±1 ºC.

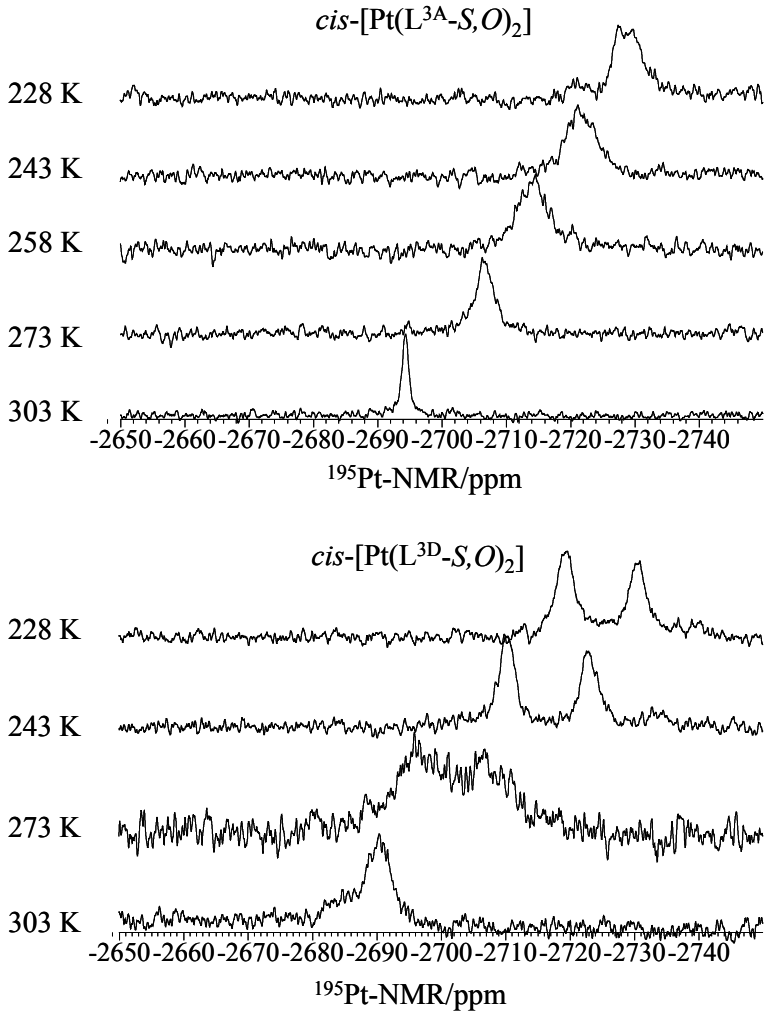

Figure 5.5 ^{195}Pt NMR spectra of ***cis*-[Pt(L^{3A}-*S,O*)$_2$]** and ***cis*-[Pt(L^{3D}-*S,O*)$_2$]** measured in $CDCl_3$ as the temperature is lowered from 303 K to 228 K. For both compounds at 303 K their *ZZ*, *EZ* and *EE* isomers have coalesced into one resonance. At 243 K ***cis*-[Pt(L^{3D}-*S,O*)$_2$]** is resolved into three resonances while ***cis*-[Pt(L^{3A}-*S,O*)$_2$]** is not even at lower temperature.

From both temperature arrays ^{195}Pt NMR spectra displayed in Figure 5.5 an upfield shift as the temperature is lowered is observed. The temperature effect on the ^{195}Pt chemical shift has already been observed in the Pt complexes ***cis*-[Pt(L^{1A}-*S,O*)$_2$]** and ***cis*-[Pt(L^{2A}-*S,O*)$_2$]** discussed in chapter 4. These observations are consistent with Cohen and Brown[11] studies of various platinum(II) complexes at various temperatures who observed a similar δ(^{195}Pt) chemical shift dependence on temperature. Since all the ^{195}Pt NMR spectra of all the new complexes were ran at intervals of 30 degrees we also compared their δ(^{195}Pt) chemical shift dependence as a function of temperature for the complexes that had well resolved isomer distributions at these temperatures. Again it was shown that for all these complexes the same chemical shift dependence with remarkable correlation coefficients, R^2 = ranging from 0.99 to 1.00 and all the plots are shown in Figure 5.6.

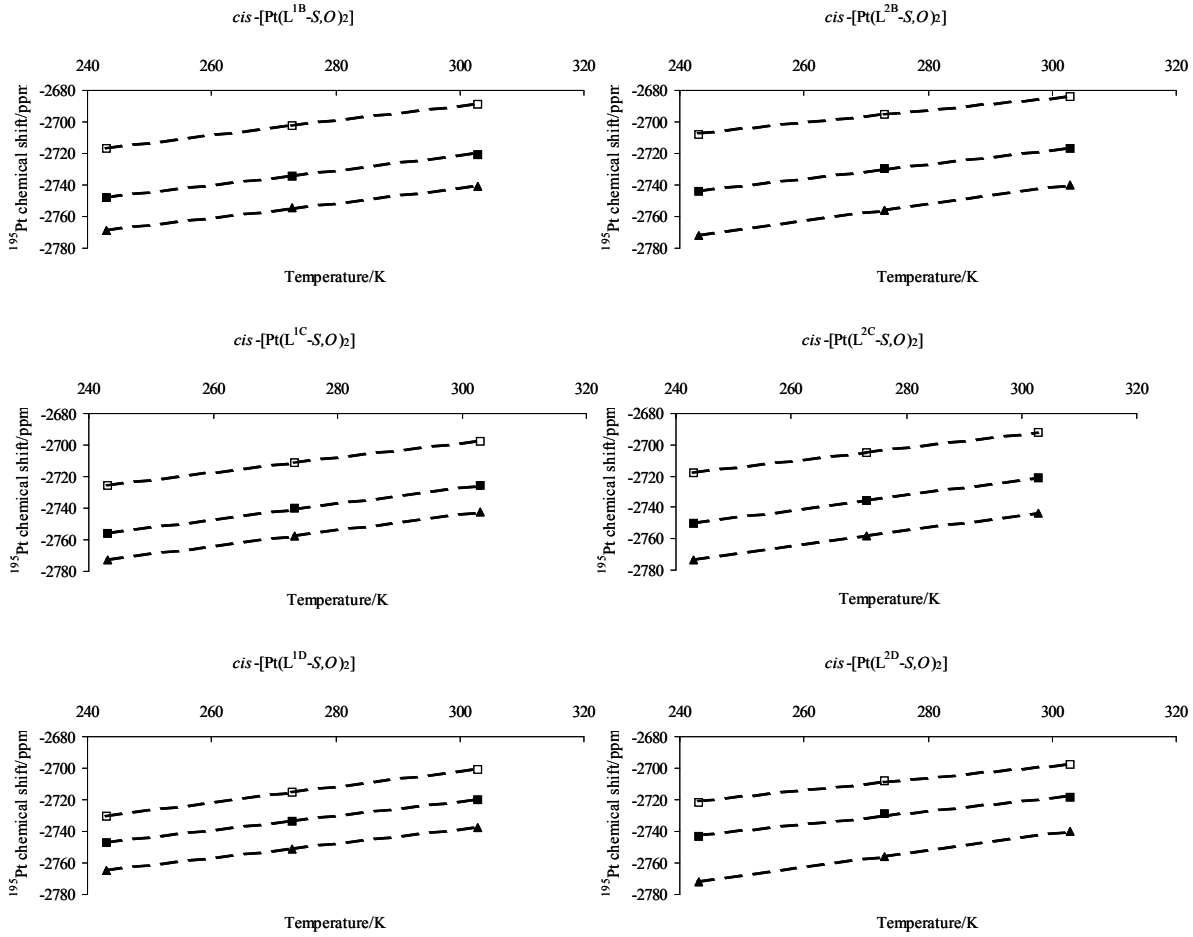

Figure 5.6 Temperature dependence of δ(^{195}Pt) chemical shifts of ***cis*-[Pt(L^{2B,2C,2D}-*S,O*)$_2$]** and ***cis*-[Pt(L^{1B,1C,1D}-*S,O*)$_2$]** complexes with □ *ZZ* ■ *EZ* and ▲ *EE* configurational isomer respectively.

5.3.5 Molecular structure of cis-bis*(N-pentyl-N-(4-methoxy-phenyl)-N'-2,2-dimethylpropanoylthioureato)platinum(II),* ***cis*-[Pt(*ZZ*-L^{1D}-*S,O*)$_2$]**

This compound *cis*-bis(*N*-pentyl-*N*-(4-methoxy-phenyl)-*N'-2,2*-dimethylpropanoylthioureato)platinum(II), ***cis*-[Pt(*ZZ*-L^{1D}-S,O)$_2$]** crystallised in chloroform at low temperature. All the relevant crystallographic data is shown in Table 5.5. The molecular structure of ***cis*-[Pt(*ZZ*-L^{1D}-*S,O*)$_2$]**, showing the atomic numbering scheme, is given in Figure 5.7 and the relevant bond lengths and angles are summarised in Table 5.6 together with those of the unbound ligand and a related complex.

Table 5.5 Crystallographic data for ***cis*-[Pt(*ZZ*-L^{1D}-*S,O*)$_2$]**.

Compound	***cis*-[Pt(L^{1D}-*S,O*)$_2$]**
Molecular formula	$C_{36}H_{54}ClN_4O_4PtS_2$
Formula weight/g.mol^{-1}	901.49
Crystal system	Triclinic
Space group	P-1
a/Å	11.223(2)
b/Å	13.696(3)
c/Å	14.452(3)
α/°	90.00
β/°	90.00
γ/°	107.785(3)
V/Å^3	2115.2(8)
Z	2
T/K	100(2)
Calculated density/g.cm^{-3}	1.415
μ/mm^{-1}	3.517
F(000)	914
θ Range scanned/°	1.41 – 28.28
No. Reflections collected/unique	13325/9299
Goodness of fit on F^2	1.596
Final R indices [I > 2σI]	R1 = 0.0746
R indices [all data]	wR2 = 0.0829
Largest difference peak and hole/e Å^{-3}	5.825/-1.930

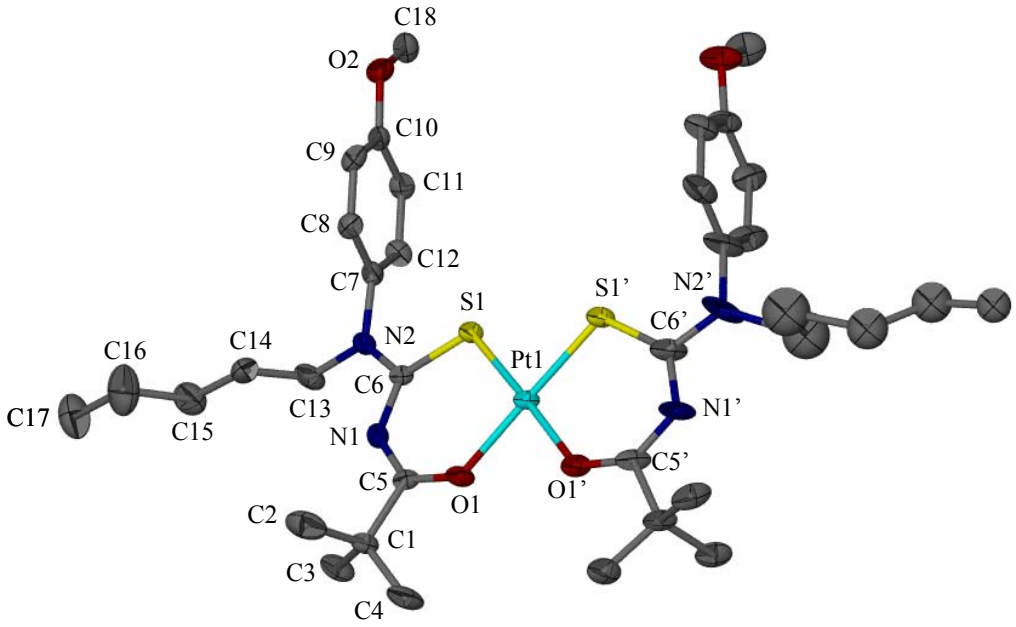

Figure 5.7 The *ZZ* stereochemistry of the complex is clearly depicted by the molecular structure of ***cis*-[Pt(*ZZ*-L^{1D}-*S,O*)$_2$]** with atomic numbering scheme. Displacement ellipsoids are drawn at the 50% probability level. One of the *N*-pentyl groups is highly disordered. For clarity the hydrogen atoms have been omitted

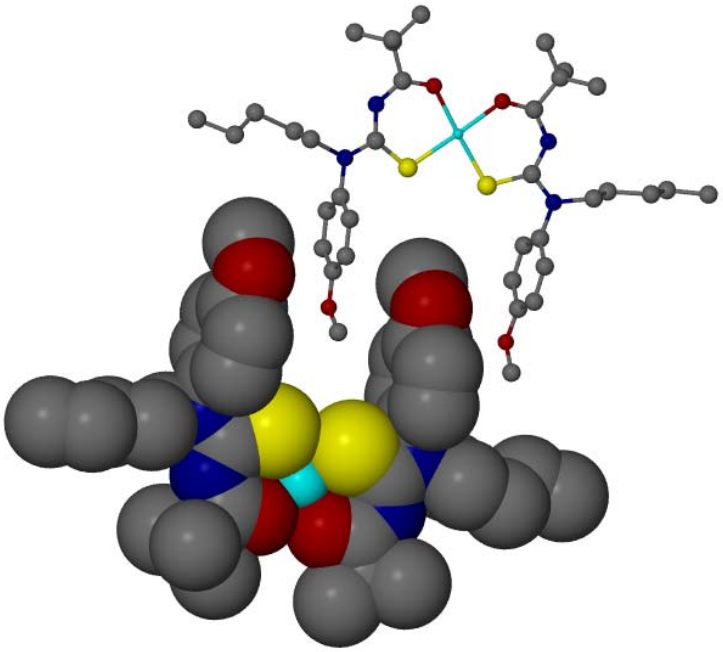

Figure 5.8 Packing diagram of the ***cis*-[Pt(*ZZ*-L^{1D}-*S,O*)$_2$]** complex, specifically showing the interaction of the phenyl region. The hydrogen atoms have been omitted for clarity.

Table 5.6 Selected bond lengths (Å) and angles (°) for the unbound ligand, HL^{1D} and the Pt(II) complex derived from this ligand, ***cis*-[Pt(*ZZ*-L^{1D}-*S,O*)$_2$]**.

	Unbound ligand, HL^{1D}	Bound ligand without disorder	Bound ligand with disorder	Bound ligand average	*cis*-[PtL_2] average[lit][a]
Pt1-O1/Pt1-O1'		2.032(6)	2.030(6)	2.031	2.021
Pt1-S1/Pt1-S1'		2.233(2)	2.238(2)	2.236	2.232
C5-O1/C5'-O1'	1.213(3)	1.257(11)	1.272(12)	1.264	1.267
C6-S1/C6'-S1'	1.678(2)	1.714(9)	1.714(11)	1.714	1.727
N1-C5/N1'-C5'	1.367(3)	1.320(11)	1.324(14)	1.322	1.316
N1-C6/N1'-C6'	1.404(3)	1.365(12)	1.359(13)	1.362	1.346
N2-C6/N2'-C6'	1.332(3)	1.341(11)	1.350(15)	1.346	1.343
O1-Pt1-S1/O1'-Pt1-S1'		95.34(18)	95.6(2)	95.47	94.6
O1-Pt1-O1'		82.3(3)			82.7(2)
S1-Pt1-S1'		86.87(8)			88.10(7)
C6-N2-C7/C6'-N2'-C7'	122.85(19)	122.2(7)	120.7(10)	121.5	123.3
C6-N2-C13/C6'-N2'-C13'	120.9(2)	122.1(8)	115.3(12)	118.7	121.7
C7-N2-C13/C7'-N2'-C13'	115.24(19)	115.6(7)	112.7(12)	114.2	115.1

[a] Data from the molecular structure of *cis*-bis(*N,N*-diethyl-*N'*-benzoylthioureato)platinum(II), *cis*-[PtL_2].[12]

The overall structure is consistent with many other related Pt(II) complexes of this type found in the literature[12-14] in that the ligands are coordinated in a *cis* chelating fashion. This structure serves as the very first example of a Pt(II) chelate with asymmetrically disubstituted thioureas that we have managed to isolate to date. Even though one of the *N*-pentyl groups is highly disordered and could not be modelled sufficiently enough to be shown, the stereochemistry of this complex is clearly the *ZZ* configuration in that both the aromatic groups of the coordinated ligands are on the same side as the sulphur atom. This *ZZ* stereochemistry strongly supports the solution NMR assignments of the complexes. Moreover, this structure also supports the idea of inversion of the stereochemistry of the ligand (which was predominantly the *E* configuration) upon complexation to the metal centre, which consistently results in statistically unexpected isomer distribution of the complexes in these systems. We assume that the majority 76% *ZZ* isomer is more likely to crystallise over the less than 1% *EE* isomer. The aromatic groups lie nearly perpendicular to the chelate ring and are 'face-to-face' with each other such that in the packing diagram of the complex there is enough space to partially fit another aromatic group of an adjacent molecule.

The bond lengths and angles of the coordinated ligand compare very well with those reported for *cis*-bis(*N,N*-diethyl-*N'*-benzoylthioureato)platinum(II).[12] In the complex the bond lengths of the carbonyl [C5-O1 = 1.257(11), C5'-O1' = 1.272(12) Å] and the thiocarbonyl [C6-S1 = 1.714(9), C6'-S1' = 1.714(11) Å] bonds are longer than the carbonyl C=O = 1.213(3) Å bond and thiocarbonyl C=S = 1.678(2) Å bond of the unbound ligand. All the C-N bonds in the

chelate ring are in the range [1.320(11) to 1.369(12) Å] which is shorter than an average C-N single bond 1.472(5) Å. These features are indicative extensive delocalisation of electrons within the chelate ring of the complex, which is expected upon ligand complexation. The Pt-O and Pt-S bonds shown in Table 5.6 also compare very well with the literature.[12-14] The C6-N2 bond of interest that gives rise to the configurational isomerism in discussion interestingly lengthens upon ligand complexation to the Pt(II) centre. This is interesting in the sense that this C-N bond length is suppose to be the most structural feature that can be linked to rotation barrier discussed in the previous chapter. In the previous chapter we have observed that complexes have a higher rotation barrier that unbound ligands and that is consistent with the work of Behrendt *et al*.,[15] on Ni(II) complexes of various *N,N*-dialkyl-*N'*-benzoylthioureas. Intuitively it would be expected that this C-N bond shortens upon ligand complexation. Lengthening of this C-N bond upon ligand complexation has also been observed by Miller[16] who worked with many examples of *N,N*-dialkyl-*N'*-benzoylthioureas and their Pt(II) complexes. The bond angles around the nitrogen atom of the (S)C-N(Pentyl)(OMe-Phenyl) moiety are comparable to those of the unbound ligand *ca* 120°. It seems that there are no major electronic changes on this nitrogen atom upon coordination as it adopts an sp^2 hybridisation in both cases.

5.4 Concluding remarks

Low temperature NMR proved to be a very useful tool in establishing *E,Z* isomerism in the new set of ligands of the type R"C(O)NHC(S)N(alkyl)(*para*-X-phenyl), (X = O-CH_3, H and NO_2) which was not possible at room temperature 298 K. In the unbound ligands the *E* configuration was found to be dominant, ranging from 87% up to as high as 98%, which his consistent with the literature on related N-alkylacetanilides. The *E* isomer was found to be most dominant with bulkier *N*-alkyl substituents. On coordination to Pt(II) metal centre the *E,Z* isomerism in the unbound ligand was carried through resulting in *ZZ*, *EZ* and *EE* Pt(II) chelates, which is easily observable by means of ^{195}Pt NMR spectroscopy. The ^{195}Pt NMR spectra allowed us to compare these isomer distributions as the *N*-alkyl group is altered. The *ZZ* isomer is observed to be most favoured followed by the *EZ* isomer and the *EE* isomer being the least favoured isomer. As the *N*-alkyl groups are changed these isomer distributions are noticed to change. The established trend was that the *ZZ* isomer grows at the expense of both the *EZ* and *EE* isomers as the alkyl group is changed in the order: methyl < isopropyl < cyclohexyl < pentyl. This same trend was established in all three series of complexes *viz*: *N*-phenyl system, *N*-(4-methoxy-phenyl) system and *N*-(4-nitro-phenyl) system. The latter system was not complete and only two *N*-alkyl groups were compared, the *N*-methyl and *N*-pentyl group. In this *N*-(4-nitro-phenyl) system we were able to establish by means of temperature array of ^{195}Pt NMR spectra that a pentyl group give rise to higher C-N bond rotation barrier than the methyl group. The complex with a higher rotation barrier in turn is associated with more *ZZ* isomer. We can therefore use the *ZZ* population as a qualitative measure of the C-N bond rotation barriers and these follow the same trend of *N*-alkyl substitution as the *ZZ* isomer grows.

References

1 K. R. Koch, C. Sacht, T. Grimmbacher, and S. Bourne, *S. Afr. J. Chem.*, **1995**, *48*, 71.
2 G. M. Sheldrick, *SHELXS-97 and SHELXL-97, Programs for the Solution and Refinement of Crystal Structures, University of Göttingen, Germany*, **1997**.
3 L. J. Barbour, *J. Supramol. Chem.*, **2003**, *1*, 189.
4 A. Liden and J. Sandstrom, *Acta. Chem. Scand.*, **1973**, *27*, 2567.
5 B. F. Pedersen and B. Pedersen, *Tetrahedron Lett.*, **1965**, 2995.
6 J. A. Weil, A. Blum, A. H. Heiss, and J. K. Kinnaird, *J. Chem. Phys.*, **1967**, *46*, 3132.
7 R. E. Carter, *Acta Chem. Scand.*, **1967**, *21*, 75.
8 J. P. Chupp and J. F. Olin, *J. Org. Chem.*, **1967**, *32*, 2297.
9 M. Goodman, P. Ganis, G. Avitabile, and S. Migdal, *J. Am. Chem. Soc.*, **1971**, *93*, 3328.
10 L. Isbrandt, W. C. T. Tung, and M. T. Rogers, *J. Magn. Reson.*, **1973**, *9*, 461.
11 S. M. Cohen and T. H. Brown, *J. Chem. Phys.*, **1974**, *61*, 2985.
12 C. Sacht, M. S. Datt, S. Otto, and A. Roodt, *J. Chem. Soc., Dalton Trans.*, **2000**, 727.
13 A. Irving, K. R. Koch, and M. Matoetoe, *Inorg. Chim. Acta*, **1993**, *206*, 193.
14 K. R. Koch, C. Sacht, and S. Bourne, *Inorg. Chim. Acta*, **1995**, *232*, 109.
15 S. Behrendt, L. Beyer, F. Dietze, E. Kleinpeter, E. Hoyer, E. Ludwig, and E. Uhlemann, *Inorg. Chim. Acta*, **1980**, *43*, 141.
16 J. D. S. Miller, *PhD Thesis, University of Cape Town*, **2000**.

Chapter 6: Concluding remarks and recommendations

6.1 Concluding remarks

A series of unsymmetrically disubstituted *N*-alkyl-*N*-alkyl(aryl)-*N'*-acylthioureas of the type, R"C(O)NH(S)CNRR' have been synthesised by a well established synthetic route. All these ligands display *E/Z* configurational isomerism in solution. This isomerism is displayed by duplication of peaks in the ^{1}H and ^{13}C NMR spectra of these ligands and it is the manifestation of the restricted rotation around the (S)C-NRR' bond. In solid state all the isomers that have been isolated, were in an *E* configuration. The (S)C-NRR' bond length fell in the range [1.343(3)-1.329(3) Å], which is significantly shorter than the average C-N single bond of 1.472(5) Å, hence resulting in configurational isomers. The magnetic anisotropy of the thiocarbonyl group is thought to deshield the *N*-alkyl group co-planar to it and thereby the proton resonances of this *N*-alkyl group appear at a relatively downfield chemical shift to those pointing away from the thiocarbonyl group. This was consistently used as a means of assigning all these *E/Z* configurational isomers. It has been demonstrated that low temperature NMR is a valuable tool in revealing the *E/Z* configurational isomers which are in fast exchange at ambient temperature. The *E* to *Z* isomer ratio has been shown to be dependent on the R and R' substituents of the (S)C-NRR' moiety. In one class the *Z* isomer was noted to be the favoured isomer while in the other class the *E* isomer was favoured.

In both classes of ligands, it was easily illustrated by ^{1}H and ^{195}Pt NMR spectroscopy that the isomerism in the unbound ligands is passed on to the resultant platinum(II) chelates derived from them, resulting in ***cis*-[Pt(*ZZ*-L-*S,O*)$_2$]**, ***cis*-[Pt(*EZ*-L-*S,O*)$_2$]** and ***cis*-[Pt(*EE*-L-*S,O*)$_2$]** configurational isomers. The *ZZ* configurational isomer was found to be favoured in all the complexes and even in those complexes that start with the *E* unbound ligand as a favoured isomer. The complexes ***cis*-[Pt(L^{5,6,7}-*S,O*)$_2$]** were used as examples for illustrating how these types of isomers could be assigned. Low magnetic field ^{13}C NMR spectroscopy revealed long-range ^{4}J(^{195}Pt-^{13}C) couplings only between the ^{195}Pt nucleus and *N*-alkyl carbons that are orientated in a **W** pathway to the ^{195}Pt nucleus. This spatial relation of the ^{195}Pt nucleus with the *N*-CH_3 and the *N*-CH_2- carbons, together with the good dispersion of the *N*-CH_3 and the *N*-CH_2- protons in 1H NMR spectra of the complexes allowed for an indirect link of the ^{195}Pt resonances with the *N*-alkyl protons via 2D gHSQC (^{1}H/^{13}C) experiments. This was sufficient for the assignment of the ***cis*-[Pt(*ZZ*-L^{5,6,7}-*S,O*)$_2$]**, ***cis*-[Pt(*EZ*-L^{5,6,7}-*S,O*)$_2$]** and ***cis*-[Pt(*EE*-L^{5,6,7}-*S,O*)$_2$]** configurational isomers in all of the ^{1}H, ^{13}C and ^{195}Pt NMR spectra. Having achieved the assignment of these configurational isomers, it was observed

that the *E,Z* isomer distributions of the unbound ligands may not necessarily be the factor that determines the *ZZ*, *EZ* and *EE* isomer distributions of the resultant complexes.

To determine the factors that influence the isomer distribution, a new series of ligands with a general motif *N*-methyl-*N*-(*para*-X-phenyl)-*N'*-acylthioureas, (X = O-CH_3, H and NO_2) together with their Pt(II) chelates was synthesised. The influence that the remote substituent, X, has on the partial double bond character of the (S)C-N(Me)(*para*-X-Ph) bond in the resultant Pt(II) complexes was shown to impact on the *ZZ*, *EZ and EE* configurational isomer distributions. The *ZZ* isomer was noted to be stabilised by a high barrier to rotation around this C-N bond, which was the case when X was the methoxy substituent which is electron releasing. In the case where X was the nitro subtituent, the least concentration of the *ZZ* isomer was observed. We therefore concluded that electronic effects play a crucial role in the distribution of configurational isomers of platinum complexes derived from these ligands. The solution ^{1}H NMR calculations of the barrier to rotation around the (S)C-N(Me)(*para*-X-Ph) bond followed the order viz: NO_2 < H < O-CH_3, in the strengthening of this partial double (S)C-NR(*para*-X-Ph) bond. In addition to electronic effects of the substituent, X, the influence of the solvent polarity as well as the temperature at which the isomer distributions are determined proved to be quite significant in the rotational barrier of thiocarbonyl C-N bond and subsequently the isomer distribution. It is therefore essential to measure and quote the distributions in identical conditions. The solution ^{1}H NMR results for the determination of the barrier to rotation around the (S)C-N(Me)(*para*-X-Ph) bond as a function of the *para*-substituent in these complexes were also complimented by DFT theoretical calculations. The trends that are obtained theoretically in this study were in good agreement with our experimental data as well as theoretical studies of other similar compounds by other workers.

Lastly, how the change of the *N*-alkyl group in *N*-alkyl-*N*-(*para*-X-phenyl)-*N'*-acylthiourea ligands influences the isomer distribution in the complexes was investigated. The established trend was that the *ZZ* isomer grows at the expense of both the *EZ* and *EE* isomers as the alkyl group is changed in the order: methyl < isopropyl < cyclohexyl < pentyl. This same trend was established in all three series of complexes *viz*: *N*-phenyl system, *N*-(4-methoxy-phenyl) system and *N*-(4-nitro-phenyl) system. In the *N*-(4-nitro-phenyl) system was established by means of temperature array study of ^{195}Pt NMR spectra that a pentyl group gives rise to higher barrier to rotation around the C-N bond than the methyl group. The complex with a higher C-N bond rotation barrier in turn is associated with more *ZZ* isomer. We can therefore use the *ZZ* population as a qualitative measure of the barriers to rotation around the C-N bond and these follow the same trend of *N*-alkyl substitution as the *ZZ* isomer grows. Isolation of the *cis*-bis(*N*-pentyl-*N*-(4-methoxy-phenyl)-*N'*-*2,2*-dimethylpropanoylthioureato)platinum(II), ***cis*-[Pt(*ZZ*-L^{1D}-*S,O*)$_2$]** complex, which is present in solution as a 76% component (while the *EZ* and *EE* isomers are *ca* 24% and *ca* <1% components, respectively), strongly supports the NMR assignments. The complex ***cis*-[Pt(*ZZ*-L^{1D}-*S,O*)$_2$]** is the first example of a platinum(II) chelate with asymmetrically substituted ligands to be isolated to date.

6.2 Recommendations

6.2.1 A direct NMR assignment of the ZZ, EZ and EE isomers of the Pt(II) chelates derived from N-alkyl-N-(para-X-phenyl)-N'-acylthioureas using ^{13}C NMR experiment

Since the *ZZ*, *EZ* and *EE* isomers of the Pt(II) complexes ^{195}Pt NMR spectra of in chapters 4 and 5 were not explicitly assigned but relied on the assignments of related complexes discussed in chapter 3, a simple ^{13}C NMR spectrum of these complexes is proposed to resolve any uncertainty. This experiment requires ^{13}C enrichment of the primary carbon of the *N*-alkyl group. For an example, the complexes *cis*-bis(*N*-methyl-*N*-(*para*-X-phenyl)-*N'-2,2*-dimethylpropanoylthioureato)platinum(II), (X = O-CH_3, H and NO_2) could be ^{13}C labelled at the *N*-methyl carbon. This means that this should be carried out during the synthesis of the secondary amine that is used for the synthesis of the unbound ligand. The motivation behind such an experiment is that the low temperature ^{13}C NMR spectra of these complexes show well-resolved *N*-CH_3 resonances for the four different environments in which they are (Figure 6.1 and 6.2).

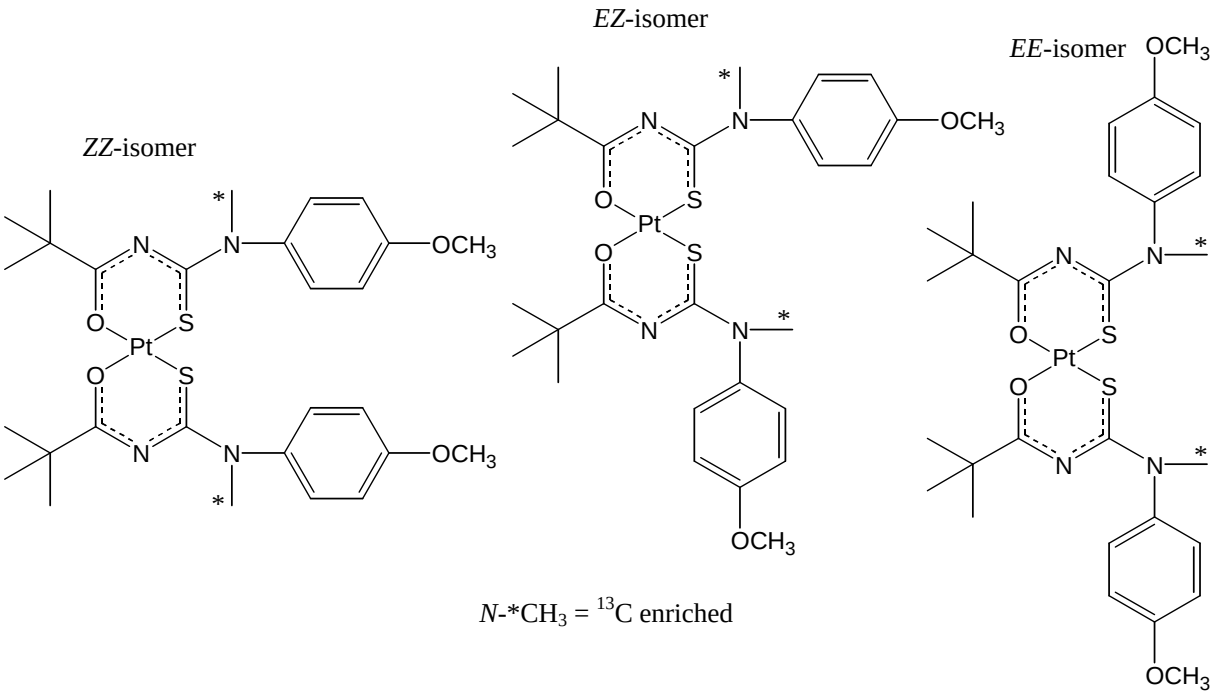

Figure 6.1 *ZZ*, *EZ* and *EE* isomers of *cis*-bis(*N*-methyl-*N*-(4-methoxy-phenyl)-*N'-2,2*-dimethylpropanoylthioureato)platinum(II), ***cis*-[Pt(L^{1A}-*S,O*)$_2$]**, showing the four different environments of the *N*-CH_3 groups.

Choosing ***cis*-[Pt(L^{1A}-*S,O*)$_2$]** as an example here illustrates the different concentrations of *ZZ* and *EE* isomers much easier in the ^{13}C NMR spectrum (Figure 6.2), otherwise this applies to all the three *para*-substituted complexes.

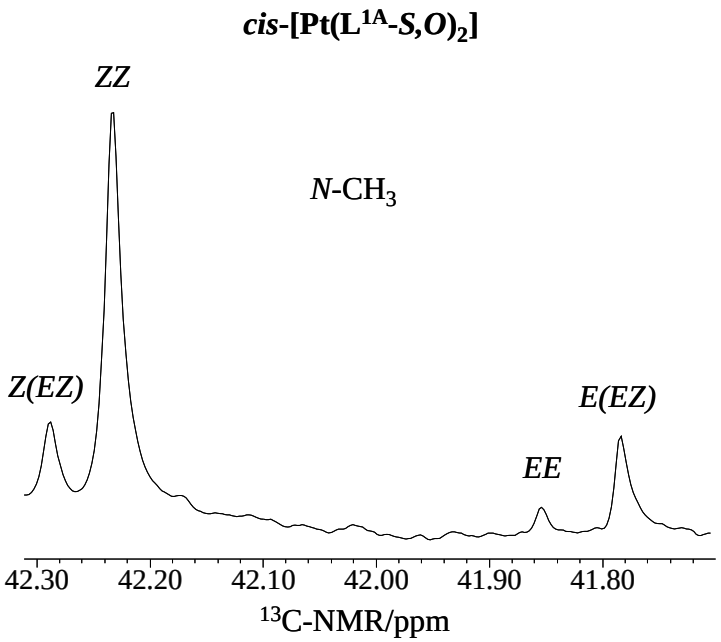

Figure 6.2 A low temperature (243 K) ^{13}C NMR section of ***cis*-[Pt(L^{1A}-*S,O*)$_2$]**, showing the *N*-CH_3 resonances of all the different environments in which they appear.

Now, if the *N*-CH_3 carbons are labelled with ^{13}C isotope then it will be easy to observe the $^4J(^{195}Pt\text{-}^{13}C)$ coupling satellites. The key in resolving the assignment in this way is that only the *ZZ* and the *Z(EZ)* *N*-$^{13}CH_3$ carbon resonances are expected to have the associated $^4J(^{195}Pt\text{-}^{13}C)$ coupling satellites since they are in a favourable **W** coupling pathway to the ^{195}Pt isotope. Firstly, the $^4J(^{195}Pt\text{-}^{13}C)$ coupling satellites establish the spatial relationship of the *N*-CH_3 carbons with the ^{195}Pt nucleus. Secondly the concentration of the *ZZ, EZ* and *EE* isomers from the ^{13}C NMR spectrum can be directly correlated to the ^{195}Pt NMR spectrum. This experiment will then settle any ambiguity of assigning the *ZZ* and *EE* isomers.

Alternatively, if the ^{13}C enrichment of the *N*-CH_3 group is expensive, a similar experiment (^{31}P NMR instead of ^{13}C NMR experiment) can be conducted by substituting the -CH_3 group with a phosphine, PR_3 ligand with the view that phosphorus has 100% abundant nuclear active isotope ^{31}P. But one would need to be careful in making any generalisation since this would be a different class of ligands.

6.2.2 The influence of the solvent polarity on the configurational isomer

In chapter 4, it was observed that dissolving the complexes in $CDCl_3$ and CD_2Cl_2 gave rise to different isomer distributions. The slight difference in the polarity of these solvents was speculated to be the reason why they gave different isomer distributions. It is therefore worthwhile to study this phenomenon systematically with solvents of varying polarity.

6.2.3 Preliminary Reverse Phase High Performance Liquid chromatography(RP-HPLC) results

The success of Mautjana[1] in separating Pt(II), Pd(II) and Rh(III) chelates of hydrophilic *N,N*-dialkyl-*N'*-acylthioureas together with the recent separation of *cis/trans*-Pd(II) chelates of aroylthioureas[2] by means of RP-HPLC encouraged us to attempt to separate the *ZZ*, *EZ* and *EE* configurational isomers by the same technique. The desired results were unfortunately unsuccessful using either 90% acetonitrile: 10% acetate buffer or pure acetonitrile. With the latter mobile phase a solitary peak with retention time of *ca* 21 minutes was detected while a solitary peak appeared after 70 minutes with the 90% acetonitrile : 10% acetate buffer mobile phase. With less encouraging results and time limitations we could not explore other conditions. Clearly RP-HPLC separation of these configurational isomers as a second handle besides multinuclear NMR spectroscopy has desirable spin offs. RP-HPLC coupled to electron spray mass spectrometry could be used to confirm the configurational isomers as they would have the same m/z values. Using a preparative column would allow isolation of the individual isomers and it may be much easier to crystallise them if they are not in a mixture. For any progress to be made though using this line of analysis it would depend on whether the configurational isomerism is a dynamic or static phenomenon in solution.

References

1 A. N. Mautjana, J. D. S. Miller, A. Gie, S. A. Bourne, and K. R. Koch, *J. Chem. Soc., Dalton Trans.*, **2003**, 1952.
2 D. Hanekom, J. M. McKenzie, N. M. Derix, and K. R. Koch, *Chem. Commun.*, **2005**, 767